LANGLEY RESEARCH CENTER
3 1176 00500 3109

NASA CR-156879
N81-32581

Aerospace Report No.
ATR-81(7805)-1

NASA-CR-156879
19810024038

MILLIMETER-WAVE SENSING OF THE ENVIRONMENT: A BIBLIOGRAPHIC SURVEY

Prepared by

E. Schneider
and
E. E. Epstein
Electronics Research Laboratory

LIBRARY COPY

JAN 27 1982

LANGLEY RESEARCH CENTER
LIBRARY, NASA
HAMPTON, VIRGINIA

29 May 1981

Laboratory Operations
THE AEROSPACE CORPORATION
El Segundo, California 90245

Prepared for

National Aeronautics and Space Administration
Wallops Flight Center
Wallops Island, Virginia

Contract No. NAS6-2960

Report No.
ATR-81(7805)-1

MILLIMETER-WAVE SENSING OF THE ENVIRONMENT:
A BIBLIOGRAPHIC SURVEY

Prepared by

E. Schneider

E. E. Epstein

Approved by

H. E. King, Head
Antennas and Propagation
Department

D. H. Phillips, Director
Electronics Research Laboratory

ABSTRACT

This literature survey was conducted to examine the field of millimeter-wave remote sensing of the environment and collect all relevant observations made in the atmospheric windows near 90, 140, and 230 GHz of ocean, terrain, man-made features, and the atmosphere. Over 170 articles and reports have been examined; bibliographic references are provided for all and abstracts are quoted when available. Selected highlights have been extracted from the pertinent articles.

CONTENTS

ABSTRACT..... v

INTRODUCTION..... 1

ARRANGEMENT OF BIBLIOGRAPHIC ENTRIES..... 2

Altshuler and Ebeoglu: Second DOD Workshop on Millimeter Wave Terminal Guidance Systems..... 3

Apletalin, Kraftmacher, Meriakri, Ushatkin, and Chigriai: Material Research at Submillimeter Wavelengths with the Help of Beam Waveguide Spectroscopy Methods..... 4

ARPA: Report of the ARPA/Tri-Service Millimeter Wave Workshop..... 5

Au, Kenney, and Kerr: Microwave Radiometric Temperatures of Aircraft..... 6

Aumiller: An Airborne 90-GHz Radiometer..... 7

Baird: Millimeter and Infrared Image Scans of Reentry Vehicle Targets..... 8

Basharinov, Borodin, Egorov, and Shutko: Microwave Radiation Characteristics of Dry and Moist Ground Covers..... 9

Bauerle: Near Earth Radiometric Measurements at 2.17 Millimeters..... 10

Bechis: Atmospheric Influences on Passive Millimeter-Wave Seekers..... 11

Beebe and Salsman: 94-GHz Sensor Tower Test Program..... 12

Blue: Permitivity of Sea Water at Millimeter Wavelengths..... 13

Blue and Perkowitz: Reflectivity of Common Materials in the Submillimeter Region..... 14

Bommarito, Stogryn, Poe, Dickey, and Olson: Microwave Imager Sensor Study..... 15

Border: Millimeter Wave Radiometric Target Acquisition System..... 16

Chantry: Dielectric Measurements in the Submillimeter Region and a Suggested Interpretation of the Poley Absorption..... 17

Ciotti, Solimini, and Basili: Spectra of Atmospheric Variables as Deduced From Ground-Based Radiometry..... 18

Coffrin: Millimeter Radio Transmission for Intra-Base Communications..... 19

CONTENTS (Continued)

Concoran: Far-Infrared-Submillimeter Phased Arrays and Applications..... 20

Corsi, Dall'Oglio, Fonti, Guidi, Melchiorri, Melchiorri, and Natale: Atmospheric Noise in the Far Infrared..... 21

Crane: Attenuation Due to Rain..... 22

Crane: Rain Effects in the 10 to 100 GHz Frequency Range..... 23

Currie, Dyer, and Ewell: Characteristics of Snow at Millimeter Wavelengths..... 24

Currie, Dyer, and Hayes: Radar Land Clutter Measurements at Frequencies of 9.5, 16, 35, and 95 GHz..... 25

Currie, Hayes, Bomar, Applegate, Hoover, and Dyer: Radar Millimeter Backscatter Measurements..... 26

Currie, Hayes, and Warner: Millimeter Target Signature Measurements..... 27

Currie, Hoover, Bomar, and Warner: Radar Millimeter Backscatter Measurements on Hard Targets..... 28

Currie, Martin, and Dyer: Radar Foliage Penetration Measurements at Millimeter Wavelengths..... 29

DARPA: Proceedings of the Eighth DARPA/Tri-Service Millimeter Wave Conference..... 30

DARPA: Proceedings of the Sixth DARPA/Tri-Service Millimeter Wave Conference..... 31

Davies, Pardoe, Chamberlain, and Gebbie: Submillimetre- and Millimetre-Wave Absorptions of Some Polar and Non-Polar Liquids Measured by Fourier Transform Spectroscopy..... 32

Deirmendjian: Far Infrared and Submillimeter Wave Attenuation by Clouds and Rain..... 35

Digest of Literature on Dielectrics..... 36

Downs: A Review of Atmospheric Transmission Information in the Optical and Microwave Spectral Regions..... 37

Dudzinsky: Atmospheric Effects on Terrestrial Millimeter Wave Communications..... 38

Dyer: Radar Clutter at Millimeter Wave Frequencies..... 39

CONTENTS (Continued)

Emery: Atmospheric Absorption Measurements in the Region of 1 mm Wavelength..... 40

Emery, Moffat, Bohlander, and Gebbie: Measurements of Anomalous Atmospheric Absorption in the Wave Number Range 4 cm^{-1} to 15 cm^{-1}..... 41

Essenwanger and Stewart: Proceedings of the Workshop on Millimeter and Submillimeter Atmospheric Propagation Applicable to Radar and Missile Systems..... 42

Essig: A Sampling of Millimeter Wave Technology in Europe-Fall 1977.... 43

Foral: Millimeter Radar Investigation..... 44

Gallagher, McMillan, Rogers, and Snider: Measurements of Attenuation Due to Simulated Battlefield Dust at 94 and 140 GHz..... 45

Gamble and Hodgens: Propagation of Millimeter and Submillimeter Waves..... 46

Gaut and Reifenstein: Interaction Model of Microwave Energy and Atmospheric Variables..... 50

General Precision: Final Report on a Millimeter Wave Radiometer Guidance Measurement Program..... 51

Geophysics: Handbook of Geophysics..... 52

Gibbins, Wrench, and Croom: Atmospheric Emission Measurements Between 22 and 150 GHz..... 53

Gniss and Magura: Millimeter Wave Imaging of Ground Based Objects..... 54

Goldhirsch: Prediction Methods for Rain Attenuation Statistics at Variable Path Angles and Carrier..... 55

Goldsmith, Plambeck, and Chiao: Measurement of Atmospheric Attenuation at 1.3 and 0.87 mm with an Harmonic Mixing Radiometer..... 56

Gordon: Detection of Strategic Targets with a NMMW Satellite Radiometer..... 57

Gordon: Detection of Strategic Targets with a NMMW Satellite Radiometer..... 58

CONTENTS (Continued)

Greenebaum and Koppel: A Study of Millimeter and Submillimeter Wave Attenuation and Dispersion in the Earth's Atmosphere..... 59

Gruener: Simultaneous Radiometric Measurements at 32 GHz and 90 GHz.... 60

Guenther: Index of 3.2-mm and 10.6-μm Image Data Tapes..... 61

Guenther: Submillimeter Research, Preliminary Report on Millimeter and Infrared Images of Military Vehicles..... 62

Guenther, Bennett, Gamble, and Hartman: Submillimeter Research; A Propagation Bibliography..... 63

Hayes, Lammers, Marr, and McNally: Millimeter Wave Propagation Measurements Over Snow..... 64

Hayes, Lammers, Marr, and McNally: Scattering Measurements at 35, 94, and 140 GHz from Metamorphic Snow..... 65

Hayes, Scheer, and Lane: Reflectivity and Emissivity Characteristics of Snow, Ice, and Wet Ground at Millimeter Wave Frequencies..... 66

Hills, Webster, Alston, Morse, Zammit, Martin, Rice, and Robson: Absolute Measurements of Atmospheric Emission and Absorption in the Range 100-1000 GHz..... 67

Ho, Mavrokoukoulakis, and Cole: Rain-Induced Attenuation at 36 and 110 GHz..... 68

Hofer and Schanda: Emission Properties of Water Surfaces at 3 mm Wavelength (URSI Meeting)..... 69

Hofer and Schanda: Emission Properties of Water Surfaces at 3 mm Wavelength (ERI Meeting)..... 70

Hofer and Schanda: Signatures of Snow in the 5 to 94 GHz Range..... 71

Hogg: Millimeter-Wave Communication Through the Atmosphere..... 72

Hollinger: Passive Microwave Measurements of the Sea Surface..... 73

Hollinger: Passive Microwave Measurements of Sea Surface Roughness..... 74

Hollinger: Remote Passive Microwave Sensing of the Ocean Surface..... 75

Hollinger, Kenney, and Troy: A Versatile Millimeter-Wave Imaging System..... 76

CONTENTS (Continued)

Ishakov, Sokolov, Sukhonin, and Cheryshov: Attenuation of Radio Waves at Wavelengths from 0.45 to 4.0 mm in the Earth's Surface Through the Slant Paths..... 77

Johansen and Maffett: Near Field Target Measurements..... 78

Kammerer and Richer: Cross Section Measurements of US Army Targets by 140 GHz Radar..... 79

Kammerer and Richer: 140 GHz Millimetric Bistatic Continuous Wave Measurements Radar..... 80

Keelty and Crane: Millimeter Investigations..... 81

Keizer, Snieder, and de Haan: Rain Attenuation Measurements at 94 GHz; Comparison of Theory and Experiment..... 82

King, White, Wilson, Mori, Hollinger, Troy, Kenney, and McGoogan: 90 GHz Radiometric Imaging..... 84

Knox: Effects of Smoke Obscurants on Millimeter Waves..... 93

Knox: Millimeter Wave Propagation in Smoke..... 94

Kondrat'yev, Rabinovich, Timofeyev, and Shul'gina: Microwave Remote Environment Sounding..... 97

Kritikos and Shiue: Microwave Sensing from Orbit..... 98

Kukin, Nozdrin, Ryadov, Fedoseyev, and Furashov: Determination of the Contribution of Water Vapor Monomers and Dimers to Atmospheric Absorption from Measurement Data in the 1.15-1.55 mm Wavelength Band..... 99

Kulpa and Brown: Absorption of Near-Millimeter Radiation by Liquid Fogs..... 100

Kulpa and Brown: Near-Millimeter Wave Technology Base Study..... 101

Kunzi, Wuthrich, and Schanda: A mm-Wave Scanning Radiometer For Terrain Mapping..... 117

Lawrence, Clifford, and Ochs: The Distribution of Turbulent Fluctuations of Refractive Index in the Atmosphere..... 118

Lerner and Hollinger: Analysis of 1.4 GHz Radiometric Measurements From Skylab..... 119

Liebe: Millimeter Wave Attenuation in Moist Air--A Review..... 120

CONTENTS (Continued)

Litvak, Weiss, and Dionne: Submillimeter-Wave Properties of Thermospheric Rocket Plumes..... 125

Lo, Fannin, and Straiton: Attenuation of 8.6 and 3.2 mm Radiowaves by Clouds..... 126

Lukes: Penetrability of Haze, Fog, Clouds and Precipitation by Radiant Energy Over the Spectral Range 0.1 Micron to 10 Centimeters..... 127

McGee: Millimeter Wave Radiometric Detection of Targets Obscured by Foliage..... 130

McGee: 140 and 220 GHz Development Work at BRL..... 131

McGee and Loomis: Radar Tracking of an M-48 Tank at 94 and 140 GHz..... 132

McMillan, Gallagher, and Cook: Calculations of Antenna Temperature, Horizontal Path Attenuation, and Zenith Attenuation Due to Water Vapor in the Frequency Band 150-700 GHz..... 133

McMillan, Rogers, Platt, Guillory, and Gallagher: Millimeter Wave Propagation Through Battlefield Dust..... 134

McMillan and Snider: Atmospheric Turbulence Effects on Infrared and Near-Millimeter Wave Propagation..... 135

McMillan, Wiltse, and Snider: Atmospheric Turbulence Effects on Millimeter Wave Propagation..... 136

McSweeney and Sheppard: Millimeter and Submillimeter Wave Dielectric Measurements with an Interference Spectrometer..... 137

Malyshenko and Vakser: Measurement of the Attenuation Coefficient of 1.2 and 0.86 mm Radio Waves in Rain..... 138

Mayer: Target Contrast Considerations in Millimeter Wave Radiometry for Airborne Navigation..... 139

Medhurst: Rainfall Attenuation of Centimeter Waves; Comparison of Theory and Measurement..... 140

Mink: Rain Attenuation and Side-Scatter Measurements of Millimeter Waves Over Short Paths..... 141

Moore and Vitale: MICRAD Ship Classification..... 142

Morgan, Stettler, and Tanton: Results of MIRADCOM Workshop on Millimeter and Submillimeter Atmospheric Propagation Applied to Radar and Missile Systems..... 143

CONTENTS (Continued)

Mundie: Passive Millimeter-Wave Radiometry and Some Possible Applications..... 144

Nelson: Millimeter Target Measurements and Seeker Effort..... 146

Ogrodnik: Covert Sensing From Orbit..... 147

Olsen, Rogers, and Hodge: The aR^b Relation in the Calculation of Rain Attenuation..... 148

Parker and Johnson: Millimeter-Wave High Resolution Plan Position Indicator and Azimuth-Elevation Imagery for Surveillance and Classification..... 149

Pascalar: Investigation of Passive Microwave Sensing from Satellites..... 150

Patton, Petrovic, and Teti: Propagation Effects for mm Wave Fire Control System..... 151

Perry: Parameters Affecting the Propagation of 15, 35, and 95 GHz Radio Signals in Cold Regions..... 152

Petito and Harris: Millimeter Wave Radar Transmission Through High Explosive Artillery Barrages..... 153

Plambeck: Measurements of Atmospheric Attenuation Near 225 GHz, Correlation with Surface Water Density..... 154

Polge and Sinh: Reduction and Analysis of Cross Section Measurement Data at 35 GHz and 94 GHz..... 156

Polge and Sinh: Two-Dimensional Processing Along Lines of Minimum Variance for rf Seeker Applications..... 157

Porter: Microwave Radiometric Field Measurement Program Final Report..... 158

Preissner: The Influence of the Atmosphere on Passive Radiometric Measurements..... 168

Rainwater, Gallagher, and Reinhart: Seasonal Atmospheric Emission at 94 GHz..... 170

Rice and Ade: Absolute Measurements of the Atmospheric Transparency at Short Millimeter Wavelengths..... 175

Richard: Millimeter Wave Radar Applications to Weapons Systems..... 176

CONTENTS (Continued)

Richard and Kammerer: Millimeter Wave Rain Backscatter Measurements..... 177

Richard and Kammerer: Rain Backscatter Measurements and Theory at Millimeter Wavelengths..... 181

Richard, Kammerer, and Reitz: 140-GHz Attenuation and Optical Visibility Measurements of Fog, Rain and Snow..... 182

Richer and Bauerle: Near-Earth Millimeter Wave Radiometer Measurements..... 195

Richer, Bauerle, and Knox: 94 GHz Radar Cross Section of Vehicles..... 196

Roeder, Day, Conners, Milstead, and Hoffman: Millimeter-Wave Semiactive Guidance System Concept Investigation..... 197

Roeder, Wilt, and Milstead: Target Detection by Millimeter Wave Radiometry..... 199

Sander: Rain Attenuation of Millimeter Waves at Wavelengths of 5.77, 3.3, and 2 mm..... 201

Schaerer: A Comparison of Thermal Imaging at Microwave and Infrared Wavelengths..... 203

Schaerer: Terrestrial Radiometry at 3-mm Wavelength..... 204

Schaerer and Schanda: Deteriorating Effects on 3-mm Wave Passive Imagery..... 206

Schanda: Microwave Radiometry Applications to Remote Sensing..... 214

Schanda, Fulde, and Kunzi: Microwave Limb Sounding of Strato- and Mesosphere..... 215

Schanda and Hofer: Emissivities and Forward Scattering of Natural and Man-Made Material at 3-mm Wavelength..... 216

Schanda and Hofer: Scattering, Emission, and Penetration of 3-mm Waves in Soil..... 221

Schanda, Schaerer, and Wuthrich: Radiometric Terrain Mapping at 3-mm Wavelength..... 222

Scheer, Odom, and Haraway: Reflectivity Characteristics of Clutter at 35 and 95 GHz..... 223

CONTENTS (Continued)

Schmugge, Wilheit, Webster, Jr., and Gloersen: Remote Sensing of Soil Moisture with Microwave Radiometers-II..... 224

Seashore, Miley, and Kearns: mm-Wave Radar and Radiometer Sensors for Guidance Systems..... 225

Shcherbov, Kuleshov, and Goroshko: Measuring the Dielectric Constant of Materials in the Millimeter Wave Range..... 226

Shimabukuro and Epstein: Attenuation and Emission of the Atmosphere at 3.3 mm..... 227

Simonis: Optical Material Literature Index for the Near-Millimeter Wave Spectral Region..... 228

Snider, McMillan, and Gallagher: Measured Effects of Battlefield Dust and Smoke on Visible, Infrared, and Millimeter Wavelength Propagation; A Preliminary Report on Dusty Infrared Test-I..... 229

Sokolov and Sukhonin: Attenuation of Submillimeter Radio Waves in Rain..... 232

Sperry Microwave Electronics: Radiometric Detection and Tracking Flight Test Program (RADAT)..... 233

Stewart: Infrared and Submillimeter Extinction by Fog..... 234

Straiton: The Absorption and Reradiation of Radio Waves by Oxygen and Water Vapor in the Atmosphere..... 235

Straiton: Cloud Attenuation at 35 and 95 GHz and Attenuation Diversity Measurements at 30 GHz..... 236

Straiton, Fannin, et al.: Atmospheric Limitations on the Use of Radio Waves with Frequencies of 15, 35, and 95 GHz..... 237

Suits and Guenther: Targets and Background..... 238

Tanton, Stettler, Morgan, Osmundsen, Mitra, and Castle, Jr.: Near-Ground Atmospheric Attenuation of 0.89-mm Radiation..... 239

Target Signature Analysis Center: Data Compilation..... 240

Target Signature Analysis Center: Data Compilation Eleventh Supplement..... 241

Thompson: Dust Clouds - Models and Propagation Events..... 242

CONTENTS (Continued)

Thompson and Haroules: A Review of Radiometric Measurements of Atmospheric Attenuation at Wavelengths from 75 Centimeters to 2 Millimeters..... 243

Tomiyasu: Remote Sensing of the Earth by Microwaves..... 245

Trebits, Currie, Dyer, and Teti: Multifrequency Millimeter Radar Sea Clutter Measurements..... 246

Trebits, Hayes, and Bomar: mm-Wave Reflectivity of Land and Sea..... 247

Trerise: 94-GHz Radiometric Sensor..... 248

Ulaby: Absorption in the 220-GHz Atmospheric Window..... 249

Ulaby and Straiton: Atmospheric Absorption of Radio Waves Between 150 and 350 GHz..... 250

Vakser, Malyshenko, and Kopolovich: The Effect of Rain on the Millimeter and Submillimeter Radiowave Distribution..... 251

Vardanyan, Iskhakov, Sokolov, and Sukhonin: Measurements of the 980-1600 Micrometer Atmospheric Absorption by Radioastronomical Means..... 252

Vogel: Scattering Intensity Plots and Transmission Coefficients for Millimeter-Wave Propagation Through Rain..... 253

Vote: Tactical Target/Clutter Signature Studies at K_u/K_a Band..... 254

Wallace: 35-GHz Radiometric Signatures of Artillery Pieces and Their Applications to HOWLS..... 255

West and Ashwell: Passive Radiometer Performance in Foul Weather..... 256

Wilt: 94-GHz Radiometer..... 257

Wisler and Hollinger: Estimation of Marine Environmental Parameters Using Microwave Radiometric Remote Sensing Systems..... 258

Wrixon: Measurements of Atmospheric Attenuation on an Earth-Space Path at 90 GHz Using a Sun Tracker..... 259

Wrixon and McMillan: Measurements of Earth-Space Attenuation at 30 GHz..... 262

Yaplee, Hollinger, and Troy: Millimeter Wave Measurements of Targets and Clutter..... 263

CONTENTS (Continued)

Zabolotniy, Iskhakov, Sokolov, and Sukhonin: Attenuation of Radiation at Wavelengths of 1.25 and 2.0 mm..... 264

Zrazhevskiy: Method of Calculating the Atmospheric Water Vapor Absorption of Millimeter and Submillimeter Waves..... 265

APPENDIX..... 267

Gruner: Simultaneous Radiometric Measurements at 32 GHz and 90 GHz..... 269

Hofer and Schanda: Emission Properties of Water Surfaces at 3 mm Wavelength..... 276

Kulpa and Brown: Absorption of Near-Millimeter Radiation by Liquid Fogs..... 283

Schanda and Hofer: Scattering, Emission and Penetration of Three Millimeter Waves in Soil..... 286

INTRODUCTION

Interest in the millimeter-wave region has been increasing because of potential applications in secure communications links, high-resolution radar, tactical target detection, and surveillance systems, and because of developments in millimeter-wave system components. Compared to use of the microwave spectrum, use of the millimeter-wave spectrum permits antennas to be of smaller size and permits wider information bandwidths to be incorporated. Millimeter waves also propagate under a wider variety of environmental conditions, relative to optical wavelengths.

The purpose of this literature survey was to examine the field of millimeter-wave remote sensing of the environment and to collect all relevant available observations made in the atmospheric windows near 90, 140, and 230 GHz of ocean, terrain, man-made features, and the atmosphere. We have emphasized measurements rather than theory and passive rather than radar studies. Although we strove for completeness in this survey, there are undoubtedly some reports that have escaped our attention.

A supplementary classified document contains entries in which the extracts or the author's abstract is classified.

ARRANGEMENT OF BIBLIOGRAPHIC ENTRIES

Every article examined has an entry in this report. Entries are listed alphabetically by author's last name and include the following information:

1. An asterisk (*) in the upper corner of the page indicates that the article deals principally with theoretical studies, radar work, or frequencies other than 90, 140, and 230 GHz.

2. The title.

3. The author's name and address.

4. The bibliographic reference.

5. The DTIC number, followed in parentheses by The Aerospace Corporation library access number.

6. If the referenced document is classified, the level of classification is indicated below the DTIC number. If the extracts or the author's abstract is classified, an additional entry is included in the supplementary classified document. (There are five classified entries.)

7. The author's abstract.

8. Selected highlights (not meant to be exhaustive) appear under EXTRACTS. For four very pertinent entries, the entire article is reproduced in the Appendix.

SECOND DOD WORKSHOP ON MILLIMETER WAVE TERMINAL GUIDANCE SYSTEMS (ADVERSE WEATHER EFFECTS)

Edward E. Altshuler
Deputy for Electronic Technology
Hanscom AFB, MA 01731

David B. Ebeoglu
Air Force Armament Laboratory
Eglin AFB, FL 32542

Report No. RADC-TM-76-9, May 1976
ADA-026 270 (A76 5072)

A one-day workshop was held at the Air Force Cambridge Research Laboratories (AFCRL) on 28 January 1976, on the subject of Millimeter-Wave Measurements in Adverse Weather. This workshop was organized by the Air Force Armament Laboratory (AFATL), Eglin AFB, Florida in conjunction with AFCRL, Hanscom AFB, Massachusetts, and was a part of the DOD Joint Technical Coordinating Group (JTCG), and Sensors and Seekers Subgroup, coordination activities.

The objective of this workshop was to extend the level of understanding of the adverse weather problem within the DOD, so that millimeter-wave systems can be designed and tested effectively. The key frequencies of interest are 35 and 95 GHz. Invited papers were presented by nationally recognized researchers from laboratories that had investigated the effects of adverse weather on the point-to-point propagation of microwaves. These papers reviewed measurements, described measurement techniques, and reviewed and recommended instrumentation. It was concluded that a broad program of controlled experiments to measure the effects that precipitation and wet background would have on system performance should be conducted. In addition, it was recommended that flight tests of millimeter-wave systems under actual adverse weather conditions be carried out. (Authors)

EXTRACTS:

This document contains brief summaries of the 9 papers given at the workshop.

The following relevant paper from this workshop has a separate entry in this survey:

Cloud Attenuation at 35 and 95 GHz and Attenuation Diversity Measurements at 30 GHz, by A. W. Straiton, University of Texas, Austin, TX 78731.

APLETALIN, KRAFTMACHER, MERIAKRI,
USHATKIN, AND CHIGRIAI

MATERIAL RESEARCH AT SUBMILLIMETER WAVELENGTHS WITH THE HELP OF BEAM WAVEGUIDE SPECTROSCOPY METHODS

S. N. Apletalin, G. A. Kraftmacher, V. V. Meriakri, E. F. Ushatkin, and E. E. Chigriai
Institute of Radioengineering and Electronics
Academy of Sciences of the USSR, Moscow

Anglo-Soviet Seminar on Atmospheric Propagation at Millimeter and Submillimeter Wavelengths, Nov. 28-Dec. 3, 1977, G1-G9, Institute of Radioengineering and Electronics, Moscow.

The determination of dielectric properties of water and other materials at submillimeter wavelengths is very important for propagation problems as well as for some other applications. We have investigated at submillimeter wavelengths some materials - liquids, low loss solid materials, and ferrites. (Authors)

EXTRACTS:

Primarily submillimeter data. The only millimeter data are:

Dielectric constant = E' + iE"

Compound	E'	E"	Frequency (GHz)
propane iodide	47	428	230
iso-propyl iodide	44	552	230
benzyl chloride	46	220	140
benzyl iodide	57	115	140
mixture of benzyl bromide and chloride	51	161	140
water	73	89	140

NOTE: All values measured at 20°C.

REPORT OF THE ARPA/TRI-SERVICE MILLIMETER WAVE WORKSHOP

APL/JHU QM-75-009, ARPA TIO-75-3, January 1975
Naval Electronics Laboratory Center
Compiled by: Applied Physics Laboratory, The Johns Hopkins University,
8621 Georgia Avenue, Silver Spring, MD 20920
ADA 089 512 (A79 06241 V1)

An ARPA/Tri-Service Workshop to define an integrated program for the development and military utilization of the millimeter (1 mm to 1 cm) portion of the electromagnetic spectrum was held at the Applied Physics Laboratory on December 16-18, 1974. (L. D. Strom, DARPA)

EXTRACTS:

The following pertinent article is entered separately in this document:

F. B. Dyer, Radar Clutter at Millimeter Wave Frequencies.

AU, KENNEY, AND KERR*

MICROWAVE RADIOMETRIC TEMPERATURES OF AIRCRAFT

Benjamin D. Au, James E. Kenney, and David W. Kerr
Airborne Radar Branch, Radar Division
Naval Research Laboratory
Washington, DC 20375

NRL Memorandum Report 2801, May 1974
AD-530 342L (A78 0528)

CONFIDENTIAL

Microwave radiometry was investigated as a possible sensor technique for detecting low-flying aircraft from shipboard. If feasible, it would have the advantage of being all weather, day-night, and passive. Radiometric target size of B-727, B-737, and DC-9 commercial jets, a P-3 turbo-prop military aircraft, and A6 and F4 jet fighters were measured using a ground-based X-band radiometer. Radiometric target sizes of the attack-sized aircraft were so small that it was judged unlikely that microwave radiometry could form the basis of a practical passive system for detecting aircraft attacking an EMCOM ship. (Authors)

AN AIRBORNE 90-GHz RADIOMETER

B. Aumiller
Deutsche Forchungs- und Versuchsanstalt fuer Luft- und Raumfahrt
Institut fuer Flugfunk und Mikrowellen
Oberpfaffenhofen, West Germany

Translation of DLR-Mitt 74-05, 1974 (European Space Research Organization)
(A76 02054)

This report describes the development, construction, and performance tests of an airborne 90-GHz radiometry receiver for thermal millimeter wave radiation measurement. A modified Dicke principal having 2 reference noise sources is used in the receiver, thus ensuring reproducible absolute calibration. The design of the circuit is dealt with hereinafter, with the exception of the theory of the thermal millimeterwave radiation and antenna problems. The description of the individual units is intended to explain their mode of operation and to make signal tracing possible. The chapters on alignment, performance test, and calibration give instructions for operating the radiometer and for quantitative analysis of the measurement results. (Author)

BAIRD

MILLIMETER AND INFRARED IMAGE SCANS OF REENTRY VEHICLE TARGETS

J. M. Baird
Hughes Research Laboratories
3011 Malibu Canyon Road
Malibu, CA 90265

Technical Report Calspan 23963, September 1976
(A80 01114)

This report describes the methods and equipment used to take image data on reentry vehicle targets at 3.2-mm and 10.6-μm wavelengths. The work was sponsored by the Calspan Corporation of Buffalo, N. Y., within the framework of programs originating with Ballistic Missile Defense Advanced Technology Center (BMDATC), Huntsville, Alabama. The measurements were made using Hughes image scanning equipment. (Author)

EXTRACTS:

This report describes data tapes; no sample data were presented.

MICROWAVE RADIATION CHARACTERISTICS OF DRY AND MOIST GROUND COVERS

A. E. Basharinov, L. F. Borodin, S. T. Egorov, and A. M. Shutko
Institute of Space Research
Academy of Sciences, Moscow

Meeting of the Soviet-American Working Group on Remote Sensing of Natural Environment from Space, Feb. 12-17, 1973

NASA Technical Translation F-14975
N73-26153 (A79 06610)

Microwave measurements from space can be used to detect fires, measure soil moisture and temperature, measure sub-ice soil temperatures and the thickness of ice cover, as well as in the search for subsurface water. (Authors)

EXTRACTS:

1) Observations made above dry, uniform cover devoid of dense vegetation permit measurement of the monthly mean ground temperatures from radio-brightness measurements in a single centimeter-wave channel. Thus, latitudinal changes in temperature of the surfaces of Australia and North Africa were established from measurements made by radiometers aboard satellites. The findings were in agreement with the monthly mean air temperatures in these regions.

The latitude trend of the temperature is less well-expressed for the Sahara; this is completely in accord with the known picture of the temperature regime in this region. Spectral contrast measurements show that the diurnal thermal trend has a marked effect on the brightness temperature as measured in the short-wave region of the centimeter band.

2) Pronounced contrast characteristics are to be expected in the presence of fires. Observations of radio-brightness contrast in areas of burning peatbogs and forest fires yielded abrupt increases of 100°-300° above the background temperature at 8 mm wavelength.

3) Measurements of the radio brightness characteristics of moist surfaces in the Soviet Union (cm-band) and in the United States (cm- and dm-bands) have shown that the brightness temperature and the moisture content of the soil are correlated.

Measurements above salt-marshes showed considerable variation in brightness--by as much as tens of degrees Kelvin--in the absence of patches of open water on the surface. Estimates show that such variations in brightness correspond to fluctuations in moisture content of 7-10%. The accuracy of the ground moisture estimate made from microwave radiometer data was 3-5% for surfaces lacking vegetation cover. The influence of vegetation was significant in the centimeter range and was at times evident in the decimeter range.

4) Satellite measurements made over Antarctica revealed a correlation between the monthly mean glacier temperatures and the radiometric temperatures.

Due to the weak absorption of microwaves in snow cover, brightness temperature observations can be used to estimate ground temperature.

5) The authors recommend using centimeter wavelengths to determine the temperature of the ground cover in the absence of a vegetative cover. However, with a vegetative cover, or for measurements on snow-covered ground, they recommend wavelengths of 10 - 30 cm.

BAUERLE

NEAR EARTH RADIOMETRIC MEASUREMENTS AT 2.17 MILLIMETERS (138 GHz)

D. G. Bauerle
Ballistic Research Laboratories
Aberdeen Proving Ground, MD 21005

BRL Memorandum Report No. 1658, June 1965
AD-366 497(A66 00668)

CONFIDENTIAL

Radiometric characteristics of ground targets and near-earth millimeter wave propagation in the 138 GHz "atmospheric window" are examined. A Dicke type radiometer is used to measure the radiometric temperature difference between certain ground based targets and their natural background. The variations in radiometric temperature contrasts are noted for gross changes in atmospheric weather. (Author)

EXTRACTS:

1. Dry snowfall does not change the target-to-background temperature contrast, but heavy wet snow can eliminate all temperature contrasts.
2. Any amount of rainfall, from a light drizzle to a heavy thunderstorm, will completely eliminate all target-to-background contrast.
3. Ground fog and light cloud cover will reduce only slightly the target-to-background contrast.
4. Heavy rain clouds can raise the apparent sky temperature to the ambient background temperature, eliminating target-to-background contrast.

ATMOSPHERIC INFLUENCES ON PASSIVE MILLIMETER-WAVE SEEKERS: MEASUREMENTS, MODELING, AND SYSTEMS APPLICATIONS

K. P. Bechis
The Analytic Sciences Corporation
Reading, MA 01867

Proceedings of the Workshop on Millimeter and Submillimeter Atmospheric Propagation Applicable to Radar and Missile Systems
Technical Report RR-80-3, 143-148, February 1980

The overall effectiveness of millimeter wave radiometry in passive missile guidance and target detection systems is influenced principally by atmospheric effects on signal propagation and on the contrast brightness temperatures between targets and their surroundings. The attenuating effects of clouds, rain, and other aerosols, along with atmospheric molecular resonant absorption lines, must be considered in predicting the effectiveness of both up- or down-looking mm-wave radiometric systems. This paper presents measurements of various sky brightness temperatures and attenuations through clear sky, various cloud overs, and precipitation (made with the University of Massachusetts 13.7-m mm-wave radio telescope). This paper also describes a very flexible mathematical model and FORTRAN program (at the Analytic Sciences Corporation (TASC)) capable of predicting the performance of a passive up- or down-looking radiometer at any altitude, zenith or nadir angle, in any weather environment, and for any postulated target. (Author)

BEEBE *et al.**

94-GHz SENSOR TOWER TEST PROGRAM: FINAL REPORT

M. E. Beebe, J. Salsman, *et al.*
Missile Systems Group
Hughes Aircraft Co.
Canoga Park, CA
(213) 883-2400, Ext. 1053

Report No. MSG 6507R, February 1976

Done for MOMT at Eglin AFB. Comments by Beebe on September 12, 1979: "An old report with very limited data. Georgia Tech now has far better data." Report not obtained.

PERMITIVITY OF SEA WATER AT MILLIMETER WAVELENGTHS

M. D. Blue
Georgia Institute of Technology
Atlanta, GA 30332

Project #A-1784, August 1976
NASA-CR-148719
N76 30911 (A79 06609)

Measurements of reflectivity of sea water and ice at 100, 140 and 180 GHz are reported. Measurements on water covered the temperature range 0 to 50°C. No anomalies in the dielectric properties of water due to the presence of either salts or organic matter were found. The reflectivity of water and its temperature dependence are consistent with recent dielectric properties models derived from data at other wavelengths. The index of refraction of ice is constant at 1.78 throughout this region. (Author)

EXTRACTS:

	Sea Water	Tap Water	Tap Water	Tap Water
Temperature	-5 to -20°C	20°C	20°C	-10°C
Frequency (GHz)	99	103.8	135.6	135.6
Reflectivity	0.0785 ± 0.0112	0.392 ± 0.014	0.341 ± 0.002	---
Change in reflectivity with temperature near 20°C	---	0.0036/°C	0.0042/°C	---
Index of refraction	†1.78 ± 0.08	3.24 - i 1.825	2.94 - i 1.52	1.78 ± 0.02
Dielectric constant	†3.17 ± 0.27	7.16 - i 11.825	6.33 - i 8.96	---

The 103.8-GHz reflectivities at 20°C of Gulf of Mexico sea water and tap water are not measurably different.

†Imaginary component has not been determined.

BLUE AND PERKOWITZ*

REFLECTIVITY OF COMMON MATERIALS IN THE SUBMILLIMETER REGION

M. D. Blue
Georgia Institute of Technology
Atlanta, GA 30332

S. Perkowitz
Emory University
Atlanta, GA 30332

IEEE Transactions MTT-25, No. 6, June 1977, 491-493.

The appearance of an illuminated scene at submillimeter wavelengths is determined by surface reflectivity. Reflectivities of some man-made and natural materials have been measured. The results provide some insight for evaluating possible applications of submillimeter radiation. (Authors)

EXTRACTS:

Natural and man-made samples' reflectivities were measured at 20 to 200 cm^{-1} (600 to 6000 GHz, or 0.5 to 0.05 mm).

MICROWAVE IMAGER SENSOR STUDY

J. J. Bommarito, A. P. Stogryn, G. A. Poe, R. D. Dickey, and B. C. Olson
Aerojet ElectroSystems Co.
1100 West Hollyvale Street
Azusa, CA 91702

Volume I - Executive Summary, Volume II - Final Report
June 1976
ADB-012 514L (A78 05315)

This final report details the work performed on a study to develop an approach to the detection and quantification of precipitation over land and water backgrounds and to determine the accuracy to which sea surface winds could be measured utilizing satellite-borne passive microwave radiometry.

Prior work had indicated that detection of precipital activity might be restricted to ocean surface backgrounds. A major breakthrough in the modeling of precipitation signatures was realized by the incorporation of the scattering effects from rain particles into the analytical model which previously considered only absorption and reradiation effects. It was determined that precipitation can be effectively detected over both land and ocean backgrounds and classified into light (2 mm/hr), medium (2-10 mm/hr) and heavy (10 mm/hr) rainfall rates with a combined 37- and 94-GHz imaging microwave radiometer. The results of the theoretical model were verified at 37 GHz using data obtained from the Electronically Scanned Microwave Radiometer on Nimbus 6 and extensive ground truth data.

It was determined by theoretical analysis that sea surface wind speed may be inferred from microwave data over a large range of conditions with an accuracy of better than 2 meters per second with a combined 19.35- and 37-GHz sensor.

A hardware study was performed and a preliminary design of a dual-polarized mechanically scanned system operating at 19.35, 37 and 94 GHz was generated. This design is compatible with the measurement accuracy requirement for precipitation detection and quantification, sea surface measurement, and sea ice mapping. The system is also compatible with the physical constraints imposed by the DMSP Block 5D-2 vehicle and utilizes near term (1976-1980) hardware technology. Concepts for next generation systems utilizing far term technology (mid 1980's) were also investigated. (Authors)

BORDER*

MILLIMETER WAVE RADIOMETRIC TARGET ACQUISITION SYSTEM

Robert L. Border
Aerojet-General Corporation
9200 East Flair Drive
El Monte, CA 91734

AFAL-TR-70-31, March 1970
AD 512 228 (A70 06022)

CONFIDENTIAL

Description of a 19.35-GHz passive radiometer.

DIELECTRIC MEASUREMENTS IN THE SUBMILLIMETER REGION AND A SUGGESTED INTERPRETATION OF THE POLEY ABSORPTION

G. W. Chantry
Division of Electrical Science
National Physical Laboratory
Teddington, Middlesex, England

IEEE MTT-25, No. 6, 496-500, June 1977

Modern activity in the field of extra-high-frequency dielectric measurements on polar liquids is briefly reviewed and the means for carrying them out briefly described. It is now possible to determine the complex permittivity (and hence the complex refractive index) over the range 10^8 - 10^{13} Hz to an absolute precision of 1 percent and it is therefore worthwhile to reexamine the "liquid-lattice" theory which was put forward some time ago as an explanation for the additional Poley absorption. This theory is found to give a good account of the absorption spectrum of liquid chlorobenzene in the microwave, millimeter, and submillimeter regions. (Author)

CIOTTI, SOLIMINI & BASILI*

SPECTRA OF ATMOSPHERIC VARIABLES AS DEDUCED FROM GROUND-BASED RADIOMETRY

P. Ciotti, D. Solimini, and P. Basili
Istituto di Elettronica
Facolta di Ingegneria
Universita di Roma
Via Eudossiana 18
00184 Rome, Italy

1978 International IEEE/AP-S Symposium and USNC/URSI Spring Meeting,
Washington, D.C., May 1978

Ground-based radiometric observations have proven to be effective means for remotely determining both the static and the dynamic thermal vertical structure of the lower troposhere. Since the meteorological parameters are random fields, the atmospheric radiance measured by a ground-based radiometer fluctuates randomly in time, and, under suitable conditions, these fluctuations result essentially from atmospheric temperature fluctuations. A relationship between the spectral density of the output of the radiometer and the spectrum of the atmospheric temperature is obtained, and in particular the special case of frozen turbulence is investigated.

In the experiment which is reported the downgoing radiance has been measured in several bands of the infrared in which the atmosphere exhibits different absorptions. The low-frequency spectral density of the fluctuating radiance has been computed both by a suitably windowed fast Fourier transform and by the maximum-entropy method. The latter technique is shown to yield either high spectral resolution or enhanced smoothing according to the order of the prediction filter which controlled the spectral estimation procedure. Data are presented on two classes of spectra corresponding to different stability conditions of the atmospheric boundary-layer. (Authors)

EXTRACTS:

Atmospheric modeling and comparison with data taken around the absorption peaks of CO_2 (4.5 micrometers) and H_2O (6.4 micrometers).

MILLIMETER RADIO TRANSMISSION FOR INTRA-BASE COMMUNICATIONS

W. E. Coffrin
Raytheon Company
Communications Systems Laboratory
141 Spring Street
Lexington, MA 02173

CR-13, 15 July 1971
AD-901 371

The multiple pair cable used in current intra-base communications tends to complicate system installation, operation, and maintenance. An exchange area radio net using a low cost and lightweight transceiver would be a major improvement. This study investigates the suitability of digital transmission on millimeter radio for the intra-base system.

A base communication model is derived to illustrate the telephone transmission requirement and the physical characteristics of the intra-base system. A radio system concept is developed and evaluated. Background studies cover design questions in the areas of propagation, system installation, system self-interference and radio design. A cost analysis indicates the economic practicality of the system by comparison to multiple pair cable system costs. (Author)

CONCORAN*

FAR-INFRARED-SUBMILLIMETER PHASED ARRAYS AND APPLICATIONS

W. J. Concoran
Institute for Defense Analyses
Arlington, VA 22202

IEEE MTT-22, 1103-1107, Dec. 1974

The concept of a phased array of far-infrared (FIR) or submillimeter (SMM) waveguide lasers that can be scanned electronically is presented. Grating lobe reduction by computer analysis is shown. Possible applications of SMM arrays are considered. (Author)

ATMOSPHERIC NOISE IN THE FAR INFRARED (300-3000 MICROMETERS)

S. Corsi, G. Dall'Oglio, S. Fonti, I. Guidi, B. Melchiorri, F. Melchiorri, and V. Natale
Infrared Section of Florence TESRE Laboratory
Consiglio Nazionale delle Ricerche
Florence, Italy

F. Mencaraglia
Cattedra di Fisica dello Spazio
University of Florence
Florence, Italy

P. Lombardini and P. Trivero
Laboratorio di Cosmogeofisica
Consiglio Nazionale delle Ricerche
Torino, Italy

S. Sivertsen
Auroral Observatory
Tromsoe, Norway

IEEE MTT-22, No. 12, 1036-1041, December 1974

Noise measurements in the frequency regions 5-200 Hz and 5.2×10^{-4} to 8.3×10^{-3} Hz have been performed in the wavelength region between 300 and 3000 micrometers from the high altitude observatory of Testa Griga, Italy (3,500 m). In the high frequency region a specially designed Ge bolometer operating in background-limited-infrared-photoconductor conditions matched to a 1.5-m telescope has been used, while at low frequencies a radiometer designed for atmospheric transmittance measurements was employed. In both regions no excess noise with respect to the photon noise relative to 300° K blackbody has been detected. (Authors)

CRANE*

ATTENUATION DUE TO RAIN—A MINI-REVIEW

Robert K. Crane
Lincoln Laboratory
Massachusetts Institute of Technology
Lexington, MA 02173

IEEE AP-23, 750-752, September 1975.

This is a brief review paper on rain-caused attenuation. The paper is a mini-review sponsored by the Wave Propagation Standards Committee of the IEEE. The paper reviews progress on the development and verification of a theory of rain-caused attenuation. The paper also considers the statistical models required to predict attenuation. (Author)

RAIN EFFECTS IN THE 10 TO 100 GHz FREQUENCY RANGE

R. K. Crane
Environmental Research and Technology, Inc.
696 Virginia Road
Concord, MA 01742

Proceedings of the Workshop on Millimeter and Submillimeter Atmospheric Propagation Applicable to Radar and Missile Systems, Redstone Arsenal, AL 38509, O. M. Essenwanger and D. A. Stewart (editors)
Technical Report RR-80-3, 24-31, February 1980

Rain can significantly affect the operation of active or passive sensor systems operating with 10 to 100 GHz or higher frequencies. Reasonable models are available for the estimation of the magnitude of the specific attenuation and backscatter cross section per unit volume produced by rain of known intensity. Occurrence prediction models are also available. Model calculations are presented and combined with observations. (Author)

CURRIE, DYER, AND EWELL*

CHARACTERISTICS OF SNOW AT MILLIMETER WAVELENGTHS

N. C. Currie, F. B. Dyer, and G. W. Ewell
Engineering Experiment Station
Georgia Institute of Technology
Atlanta, GA 30332

AP-S Digest, October 1976

A series of radar measurements were performed at 35 and 95 GHz in order to determine the penetration and backscatter properties of snow. The radars utilized for these measurements were relatively short pulse (approximately 50 ns) systems employing relatively narrow antenna beamwidths (approximately 1 degree). Both of the systems were dual polarized, that is, either horizontal or vertical polarization could be transmitted, and the parallel and cross-polarized component received. Both of the radar systems were triggered simultaneously, and the antennas could be accurately aimed using boresighted riflescopes; these features permitted truly simultaneous pulse-by-pulse data to be obtained. Both of the systems employed logarithmic receivers and suitable sample-and-hold circuits so that true pulse-by-pulse data were recorded. The systems were installed in a truck-mounted instrumentation van with a temporary shelter erected on top for protection of exposed equipment from the environment; mylar windows were provided for each of the systems to view the measurement area. (Authors)

RADAR LAND CLUTTER MEASUREMENTS AT FREQUENCIES OF 9.5, 16, 35, AND 95 GHz

N. C. Currie, F. B. Dyer, and R. D. Hayes
Engineering Experiment Station
Georgia Institute of Technology
Atlanta, GA 30332

Contract DAAA-25-73-C-0256, 2 April 1975
AD-A012 709 (A76 01485)

A series of measurements of radar backscatter from foliage and other natural objects have been made at frequencies of 9.5, 16.5, 35, and 95 GHz. The geometry of the experiments and the equipment were chosen so as to provide data useful to the equipment designer in the choice of operating frequency for his particular mission. Amplitude statistics for both horizontal and vertical polarizations were obtained. Noncoherent spectral measurements and correlation properties were investigated in detail as functions of frequency, incident angle, and windspeed. Limited comparisons are made between previous measurements and analyses and the current experimental results, and certain properties of the results are discussed in relation to the phenomenology of land clutter. Extensive summaries of the data obtained are included as a part of the report. (Authors)

CURRIE, HAYES, BOMAR, APPLEGATE,
HOOVER, AND DYER

RADAR MILLIMETER BACKSCATTER MEASUREMENTS, VOLUME II, TARGET SIGNATURES

Nicholas C. Currie, Robert D. Hayes, Lucien C. Bomar, Marshall S. Applegate,
Ralph A. Hoover, and Frederick B. Dyer
Engineering Experiment Station
Georgia Institute of Technology
Atlanta, GA 30332

Report No. AFAL-TR-77-92, Vol. 2, July 1977
ADC 015 118 (A79 07104 V2)

CONFIDENTIAL

A series of radar backscatter measurements of the reflectivity properties of snow, wet/dry foliage, and man-made targets have been made at K-band (35 GHz) and M-band (94 GHz) in support of the Millimeter-wave Contrast Guidance (MCG) Seeker program. The results are presented in two volumes: Volume I gives the snow and wet/dry foliage reflectivity results and Volume II, presented here, summarizes the signature measurements on man-made targets. The measurements of the radar and radiometric signatures of man-made targets were conducted at 35 GHz and 93 GHz. Radar cross-section azimuth cuts were performed for depression angles of 20 degrees, 29 degrees, 40 degrees, and 49 degrees, for horizontal and vertical polarization. Passive radiometric cuts were also performed but for a limited subset of the targets. The results of these tests are discussed along with descriptions of the test site, measurement procedures, and the targets on which the measurements were performed. The results include comparisons of the data for similar targets, distributions of the cross-section values, polar presentation of the target responses, spectral properties, and a description of a brief target modeling effort for one target. Recommendations are made as to further testing and analysis which are needed to fully characterize the target signatures. (Authors)

See also the extract in the supplementary classified document.

MILLIMETER TARGET SIGNATURE MEASUREMENTS

N. C. Currie and R. D. Hayes
Engineering Experiment Station
Georgia Institute of Technology
Atlanta, GA 30332

C. L. Warner
Air Force Armament Laboratory
Eglin Air Force Base, FL 32542

Proceedings of the Sixth DARPA/Tri-Service Millimeter Wave Conference
Tactical Technology Office (Editors), Defense Advanced Research Projects Agency, 1400 Wilson Blvd., Arlington, VA 22209, p. 225-237, November 1977
(A78 01438)

SECRET

Previous programs aimed at determining the military usefulness of passive millimeter-wave radiometric guidance techniques have concluded that a severe range limitation exists due to the small target-to-background contrast. Various signal processing techniques have been explored to enhance the probability of detection; however, it presently appears that the active radar mode of operation is necessary to achieve adequate detection ranges with the limited apertures available in small missile airframes. Design for operation in this mode requires a thorough evaluation of target and background signatures for the frequency regions of interest. These signature measurements are necessary to generate target detection algorithms, evaluate effects of target scintillation on guidance aimpoint accuracy, determine the minimum dynamic receiver signal range necessary for proper performance, and predict probable target-to-background signal ratios. (Authors)

See also the extract in the supplementary classified document.

CURRIE, HOOVER, BOMAR, AND WARNER*

RADAR MILLIMETER BACKSCATTER MEASUREMENTS ON HARD TARGETS

N. C. Currie, R. A. Hoover, L. C. Bomar, and C. L. Warner, II
Engineering Experiment Station
Georgia Institute of Technology
Atlanta, GA 30332

AFAL-TR-77-13
AD-C01 261L (A78 00461)

CONFIDENTIAL

A series of measurements on the active cross-section of armored targets has been made at 35 and 93 GHz. Radar cross-section and passive radiometric contrast azimuthal cuts have been performed for depression angles of 20, 29, 40 and 49° for horizontal and vertical polarizations. These data are discussed in the report along with descriptions of the test site, the measurements procedure, and the targets on which the measurements are performed. Data analysis includes comparison of the results of similar targets and preliminary distributions of the cross-section values. Recommendations are made as to further data analysis which should be performed on the data collected during the tests. (Authors)

See also the extract in the supplementary classified document.

RADAR FOLIAGE PENETRATION MEASUREMENTS AT MILLIMETER WAVELENGTHS

N. C. Currie, E. E. Martin and F. B. Dyer
Engineering Experiment Station
Georgia Institute of Technology
Atlanta, GA 30332

Georgia Institute of Technology Project No. A-1485-100, 31 December 1975
AD-A023 838 (A79 06021)

A series of radar measurements on the penetration of foliage has been made at frequencies of 9.4, 16.2, 35, and 95 GHz. Comparison measurements were made using both one-way and two-way techniques at 9.4 and 16.4 GHz, and two-way techniques only at 35 and 95 GHz for similar foliage areas. The bulk of the measurements were made at depression angles below 3°, although a few one-way measurements were made at 9.4 and 16.2 GHz for depression angles near 30°. Attenuation properties, polarization ratios, and noncoherent spectral and correlation properties were investigated as a function of frequency, polarization, depth of foliage, and wind speed. Limited comparisons are made with published data for the lower frequencies. (Authors)

EXTRACTS:

95-GHz experimental measurements of radar foliage penetration:

1. Attenuation varies as a function of foliage depth. Maximum depth of radar penetration was about 4 meters at 95 GHz.

For a single oak tree the average dry attenuation was 4.5 (±1.6) dB/m and the average wet attenuation was 12.2 dB/m.

2. Dry measurements indicate that the attenuation constant varies directly with the log of the frequency, and is essentially independent of polarization.

The foliage examined was deciduous: oak, dogwood, hickory, maple and sweetgum.

DARPA

PROCEEDINGS OF THE EIGHTH DARPA/TRI-SERVICE MILLIMETER WAVE CONFERENCE

System Planning Corporation
1500 Wilson Boulevard
Arlington, VA 22209

August 1979
(A80 00326)

SECRET

These Proceedings contain papers presented at the Eighth DARPA/Tri-Service Millimeter Wave Symposium, held on 3 to 5 April 1979, at Eglin Air Force Base, Florida. Papers were presented on millimeter wave guidance, surveillance, target acquisition, and fire control systems, and on components, phenomenology, simulation, and modeling.

The following pertinent articles have separate entries in this survey:

1. Reflectivity Characteristics of Clutter and Targets at 35 and 95 GHz by J. A. Scheer, D. L. Odom, and R. C. Haraway.

2. Millimeter Wave Propagation Measurements Over Snow by D. T. Hayes et al.

3. Reflectivity and Emissivity Characteristics of Snow, Ice and Wet Ground at Millimeter Wave Frequencies by R. D. Hayes, J. A. Scheer, and R. Lane.

4. Multifrequency Millimeter Radar Sea Clutter Measurements by R. N. Trebits, N. C. Currie, F. B. Dyer, and J. J. Teti.

5. Results of MIRADCOM Workshop on Millimeter and Submillimeter Atmospheric Propagation Applied to Radar and Missile Systems by R. L. Morgan, J. D. Stettler, and G. A. Tanton.

6. Effects of Smoke Obscurants on Millimeter Waves by J. E. Knox.

7. Millimeter Wave Radar Transmission Through High Explosive Artillery Barrages by F. C. Petitio and R. Harris.

8. Near-Field Target Measurement by E. L. Johansen and A. Moffet.

9. Millimeter-Wave High-Resolution Plan Position Indicator and Azimuth-Elevation Imagery for Surveillance and Classification by J. H. Parker and L. P. Johnson.

10. Covert Sensing From Space by R. F. Ogrodnik.

11. Millimeter Wave Measurements of Targets and Clutter by B. S. Yaplee, J. P. Hollinger and B. E. Troy.

12. 140 and 220 GHz Development Work at BRL by R. A. McGee.

PROCEEDINGS OF THE SIXTH DARPA/TRI-SERVICE MILLIMETER WAVE CONFERENCE

Tactical Technology Office
Defense Advanced Research Projects Agency
1400 Wilson Boulevard
Arlington, VA 22209

November 1977
(A78 01438)

SECRET

These Proceedings contain papers presented at the Sixth DARPA/Tri-Service Millimeter Wave Symposium, held on 29 and 30 November 1977, at Harry Diamond Laboratories, Adelphi, Maryland. Papers were presented in four sessions: Tactical Systems, Strategic Systems, Phenomenology, and Components.

The following pertinent articles have separate entries in this survey:

1. Detection of Strategic Targets with a NMMW Satellite by G. A. Gordon.

2. Radar Tracking of an M-48 Tank at 94 and 140 GHz by R. A. McGee and J. M. Loomis.

3. Target Detection by Millimeter Wave Radiometry by R. S. Roeder, R. E. Wilt, and M. M. Milstead.

4. Propagation Effects for Millimeter Wave Fire Control System by T. N. Patton, J. J. Petrovic, and J. Teti.

5. Scattering Measurements at 35, 94, and 140 GHz From Metamorphic Snow by D. T. Hayes et al.

6. Millimeter Target Signature Measurements by N. C. Currie, R. D. Hayes, and C. L. Warner.

7. Passive Radiometer Performance in Foul Weather by M. West, Jr. and J. R. Ashwell.

DAVIES, PARDOE, CHAMBERLAIN, AND GEBBIE

SUBMILLIMETRE- AND MILLIMETRE-WAVE ABSORPTIONS OF SOME POLAR AND NON-POLAR LIQUIDS MEASURED BY FOURIER TRANSFORM SPECTROSCOPY

M. Davies and G. W. F. Pardoe
Edward Davies Chemical Laboratory
University College of Wales
Aberystwyth, Cardiganshire, England

John Chamberlain
Division of Electrical Science
National Physical Laboratory
Teddington, Middlesex, England

H. A. Gebbie
National Bureau of Standards
Boulder, CO 80302

Transactions of the Faraday Society 66, 273, 1970

An assessment of the Fourier transform spectrometer indicates the advantages to be gained from its application to the millimetre-wave region (10 to 2 cm^{-1}). The attainable resolving power is adequate for the study of broad absorptions which occur in liquids below 100 cm^{-1}. With a mercury arc source, appropriate beam dividers, and an indium antimonide detector at 1 K continuous refraction and absorption spectra have been obtained below 50 cm^{-1} (to 2 cm^{-1}) for some typical polar and non-polar liquids.

Results for water, aniline, 1,4-dioan, cyclohexane, decahydronapthalene, dimethyl acetylene (2-butyne) and 1-octyne are reported and considered in relation to earlier microwave dielectric data and far infra-red measurements. Water and aniline show strong, almost featureless, absorptions which are probably due to the superposition of three or four processes. The non-polar and weakly polar liquids show much smaller absorptions: 1,4-dioxan has a profile consistent with a zero permanent electric dipole moment; 2-butyne and 1-octyne show α rising linearly with $\tilde{\nu}$ over the range 5-50 cm^{-1}. The origin of the absorption in non-polar liquids is different from the dominant mechanism in polar liquids although the peak values for both lie in the submillimetre-wave regions. The non-polar absorption peaks occur at frequencies which correlate with those calculated for molecular collisions in the liquids using the formulations of Mie and Bradley. (Authors)

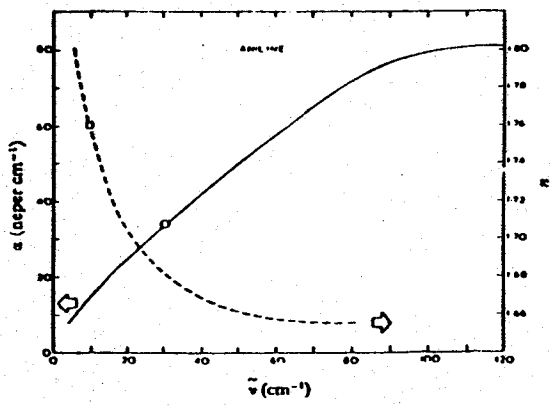

FIG. 6.—Absorption coefficient (α) and refractive index n of liquid aniline at 22±2°C. ——, observed values of α; - - - - -, observed values of n; O, 337 μm maser value of α; □, extrapolated from data of Garg and Smyth.[20]

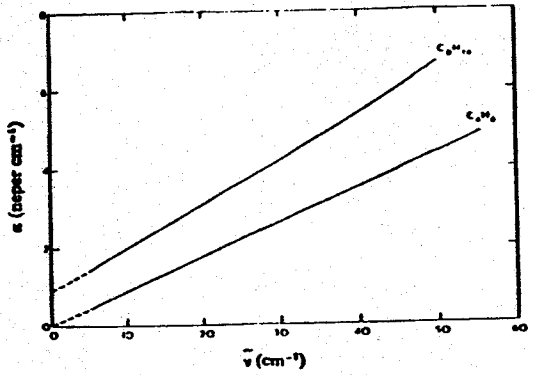

FIG. 11.—Observed absorption coefficient (α) of (*a*) liquid 2-butyne (C_4H_6) and (*b*) 1-octyne (C_8H_{14}) at 24°C; - - - - -, linear extrapolation to $\tilde{\nu} = 0$.

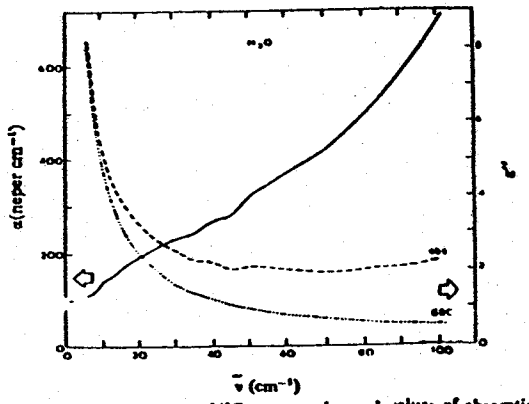

FIG. 5.—Attenuation of liquid water at 24°C. ——, observed values of absorption coefficient α (average of several scans [5]); - - - - -, α(obs) converted to ϵ''(obs); . . . . ., ϵ''(calc) from GBC parameters.[20]

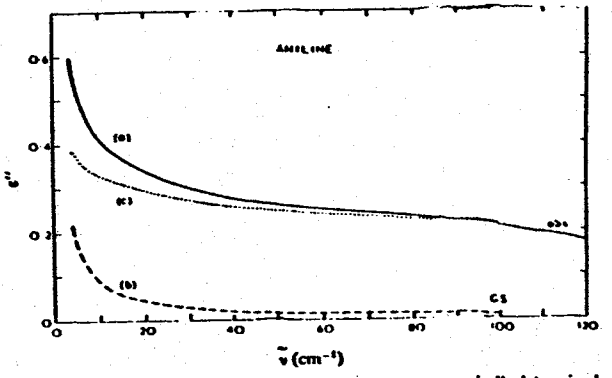

FIG. 7.—Dielectric loss factor ϵ'' of liquid aniline. (*a*) ——, spectroscopically determined values from data of fig. 6; (*b*) - - - - -, ϵ'' values of Garg and Smyth [20] extrapolated from Debye absorption; (*c*) . . . . ., the difference (*a*) − (*b*) = ϵ''(*c*).

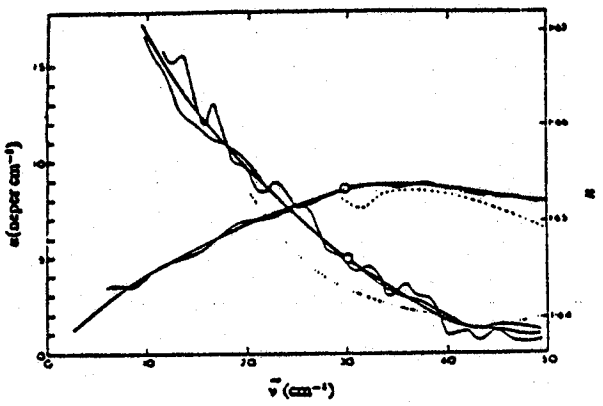

FIG. 4.—Absorption (α) and refraction (n) spectra of liquid tetra-bromoethane at 22°C. The thin full lines represent separate determinations of the spectra while the thick full lines indicates a smoothed average value. The open circles are values measured using a 337 μm maser [12]; the broken line represents values reduced from the transmission values of G. W. Chantry, H. A. Gebbie, P. R. Griffiths and R. F. Lake, *Spectrochim. Acta*, 1966, 22, 125; the dotted line shows an earlier measurement on the liquid.[9] α was measured with the specimen at A; n was measured with the specimen at R (fig. 4). The absolute value of n was fixed by the maser measurement.

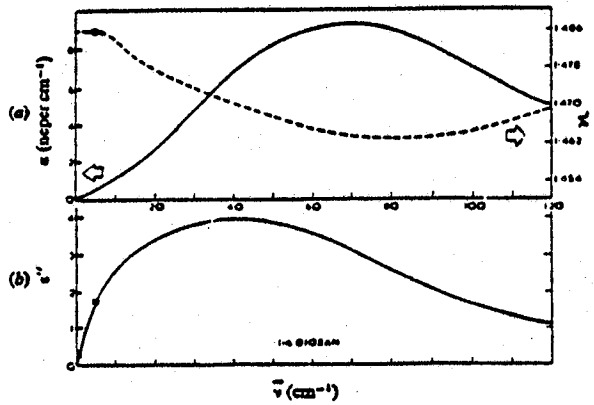

FIG. 9.—The attenuation and refractive index for liquid 1,4-dioxan at 22±2°C. (*a*) ——, observed absorption coefficient (α) and - - - - -, observed refractive index (n); ⊡, ref. (43). (*b*) ——, dielectric loss factor deduced from n and α; ▲, ref. (42); ⊡, ref. (43).

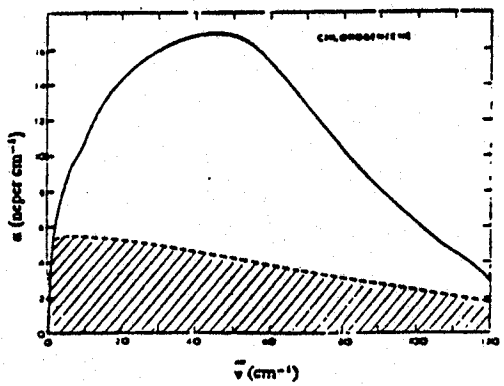

FIG. 12.—Experimentally determined plot of α against $\bar{\nu}$ for liquid chlorobenzene.[17] In eqn (10), σ is proportional to α and ν to $\bar{\nu}$. The shaded area represents the contribution of the Debye dipolar absorption to the area A beneath the curve. It is 35 % of the total area.

FAR INFRARED AND SUBMILLIMETER WAVE ATTENUATION BY CLOUDS AND RAIN

D. Deirmendjian
The Rand Corporation
Santa Monica, CA 90406

April 1975
ADA-021 942 (A76 00650)

Newly determined optical constants for water at far infrared and submillimeter wavelengths, as revealed by a recent survey, are used to estimate water cloud and rain attenuation over the wavelength range between 12 μm and 2 cm. For this purpose new analytic dropsize distribution models simulating fog, nimbostratus clouds, and rain corresponding to rainfall rates of 10 and 50 mm/hr, are set up. The corresponding volume extinction and absorption coefficients are computed according to polydisperse Mie scattering theory at specific wavelengths and presented in tables and graphically in plots for purposes of interpolation.

It is found that cloud extinction may exceed 50 nepers per kilometer in the $\lambda < 100$ μm region whereas for wavelengths longer than 200 μm, under near saturation conditions, water vapor absorption should be the dominant attenuator. The greatest attenuation by heavy rain may be expected around 5 mm with a value of about 5 nepers per kilometer. The results also suggest that, in the presence of non-precipitating water clouds or fog there may be a relative transmission "window" centered around 1.3 mm. (Author)

EXTRACTS:

Complex indices of refraction of water = 2.50 - 1.09i at 1 mm
= 2.5604 - 0.8947i at 2 mm

DIGEST*

DIGEST OF LITERATURE ON DIELECTRICS, VOLS. 36 & 37 (1972-3)

Library of Congress 45-33864
45-33582B
45-335818

EXTRACTS:

Frequencies of measurement were rarely indicated, but when specified they were 0.1 or 10 GHz.

A REVIEW OF ATMOSPHERIC TRANSMISSION INFORMATION IN THE OPTICAL AND MICROWAVE SPECTRAL REGIONS

A. R. Downs
Ballistics Research Laboratory
Aberdeen Proving Ground, MD 21005

BRL Memorandum Report No. 2710, December 1976
ADA 035 059 (A79 06032)

Much information has been generated over a long period of time on the transmission through the atmosphere of radiation of various wavelengths. This report represents an attempt to consolidate some of the available information into a single report. This report addresses five wavelengths each in the optical and microwave regions. Attenuation mechanisms considered are Rayleigh and Mie scattering and absorption by both water vapor and water drops. Atmospheres characterized by visibilities between 0.1 km (fog) and 325 km (clear air) and by rainfalls at rates up to 64 mm/hr are considered. Pertinent formulations and tables are provided to assist in calculating attenuation coefficients characteristic of a wide variety of atmospheres, and the adequacy of the data bases upon which such calculations rest is assessed. A limited amount of information is also provided on the attenuation characteristics of smoke and dust. (Author)

EXTRACTS:

The wavelengths of 0.55, 1.06, 2., 3.8, and 10.6 micrometers are examined. Computed rain absorption and transmission coefficients for frequencies of 9.375, 35, 94, 140, and 240 GHz are tabulated.

DUDZINSKY*

ATMOSPHERIC EFFECTS ON TERRESTRIAL MILLIMETER WAVE COMMUNICATIONS

S. J. Dudzinsky
Rand Corporation
Santa Monica, CA 90606

Report No. R-1335-ARPA, March 1974
AD-780 602 (A74 05916)

This report, prepared as a contribution to the Defense Advanced Research Projects Agency's study on Millimeter Wave Technology, combines the most current information on the transmission properties of millimeter waves with currently available meteorological data to derive a methodology that may be used by the design engineer in estimating the performance of millimeter-wave systems in the atmosphere and in the presence of rainfall. An understanding of atmospheric transmission losses, especially losses due to rainfall attenuation, is required to properly design reliable millimeter-wave communication links and other millimeter-wave systems that rely on propagation through the atmosphere. The emphasis here is on high-reliability communications in which outages are 0.1 percent (530 min of outage per year) or less, but the methodology described applied to higher outage systems as well. (Author)

RADAR CLUTTER AT MILLIMETER WAVE FREQUENCIES

F. B. Dyer
Sensor Systems Division
Engineering Experiment Station
Georgia Institute of Technology
Atlanta, GA 30332

Report of the ARPA/Tri-Service Millimeter Wave Workshop
APL/JHU QM-75-009, ARPA TIO-75-3, January 1975
Compiled by Applied Physics Laboratory, The Johns Hopkins University,
Silver Spring, MD 20920

The purpose of the discussions presented here is to provide an overview of the current status of clutter measurements at millimeter wavelengths and to suggest some areas where additional measurements might be fruitful. Backscatter from rain, land clutter, and sea clutter at the principal millimeter radar bands is reviewed and related to benchmark data obtained at X band. Although only data obtained by Georgia Tech investigators are presented, it is believed that they represent an important area of current interest. Because the investigations are actually still being actively pursued, many of the results reported are preliminary in nature and should be considered as subject to change. (Author)

EMERY

ATMOSPHERIC ABSORPTION MEASUREMENTS IN THE REGION OF 1 mm WAVELENGTH

R. Emery
Goddard Institute for Space Studies
New York, NY 10025

Infrared Physics 12, 65-79, March 1972.

Using a Froome-type plasma-metal junction harmonic generator, high resolution transmission measurements have been made on the atmosphere in the wavelength range 0.5-3.0 mm. Theoretical spectra have been computed for submillimetre-millimetre wavelength atmospheric absorption due to water vapor using the kinetic equation form for the line shape.

Measurements were made on the basic parameters of the main water vapor absorption lines occurring in the wavelength range 0.65-3.0 mm. The pure water vapor line width parameters are found to be constant for the three main absorption lines in this range and equal to 0.55 ± 0.05 cm^{-1}. The water vapor-nitrogen line width parameter for the 1.64-mm wavelength line is measured to be 16 per cent larger than theory, having a value of 0.111 ± 0.005 cm^{-1}, and is constant over a range of pressures.

Comparison between theory and observation for the absorption in two submillimeter wavelength windows strongly favors the kinetic equation form of the line shape rather than the more usual Lorentz shape. (Author)

MEASUREMENTS OF ANOMALOUS ATMOSPHERIC ABSORPTION IN THE WAVE NUMBER RANGE 4 cm^{-1} TO 15 cm^{-1}

R. J. Emery, P. Moffat, R. A. Bohlander, and H. A. Gebbie
Appleton Laboratory
Ditton Park
Slough S13 9JX, England

Journal of Atmospheric and Terrestrial Physics 37, No. 4, 587-594, April 1975

Field measurements have been made of atmospheric absorption in the wavenumber range 4 cm^{-1} to 15 cm^{-1} [2.5 mm to 0.7 mm], using a 200-meter horizontal transmission path and at a resolution of 0.2 cm^{-1}. The results are compared with theoretical spectra based on water vapor monomer absorption, and anomalous absorption spectra are presented. There is support from some preliminary laboratory work. A binding energy of between 0.4 and 0.8 electron volts per molecule is derived for the water vapor complex responsible for the absorption. (Author)

PROCEEDINGS OF THE WORKSHOP ON MILLIMETER AND SUBMILLIMETER ATMOSPHERIC PROPAGATION APPLICABLE TO RADAR AND MISSILE SYSTEMS, Redstone Arsenal, 20-22 March 1979

O. M. Essenwanger and D. A. Stewart, editors
Research Directorate
U.S. Army Missile Laboratory
Redstone Arsenal, AL 35809

Technical Report RR-80-3, February 1980

A workshop on millimeter and submillimeter wave propagation through the atmosphere was held on 20-22 March 1979 at Redstone Arsenal, Alabama. This workshop served as a forum where scientists in diversified fields exchanged information on the latest results and discussed controversial issues and unresolved problems.

The first few papers were concerned with MICOM needs. They specified the operating regions of interest for tactical applications and explained the rationale for the selection of these regions. The Terminal Homing Measurements Program was described.

Several papers discussed absorption by water vapor. Classical theories do not adequately describe the measured absorption in window regions between strong absorption lines. Alternate methods of explaining the discrepancies are to introduce reasonable modifications to existing models of line shapes or to consider the effect of water vapor dimers.

Other effects on atmospheric propagation and instrumentation for measuring these effects were also discussed. Absorption and scattering by hydrometeors, dust and smoke were considered. Additional papers were concerned with terrain effects, turbulence, natural atmospheric emissions, refractivity gradients, and the relatively new method of pulse generation by swept-gain superradiance. (Authors)

EXTRACTS:

Pertinent articles have been entered separately in this document:

1. Rain Effects in the 10 to 100 GHz Frequency Range, R. K. Crane.
2. Seasonal Atmospheric Emission at 94 GHz, J. H. Rainwater, J. J. Gallagher, and P. B. Reinhart.
3. Measurements of Attenuation Due to Simulated Battlefield Dust at 94 and 140 GHz, J. J. Gallagher, R. W. McMillan, R. C. Rogers, and D. E. Snider.
4. Atmospheric Influences on Passive Millimeter-Wave Seekers: Measurements, Modeling, and Systems Applications, K. P. Bechis.
5. Millimeter Wave Attenuation in Moist Air--A Review, H. J. Liebe.
6. Dust Clouds--Models and Propagation Effects, J. H. Thompson.

A SAMPLING OF MILLIMETER WAVE TECHNOLOGY IN EUROPE--FALL 1977

F. C. Essig
Physics Division
Naval Weapons Center, China Lake

ADB 026 692L

EXTRACTS:

A survey of experimental European research sites in the millimeter-wave region.

FORAL*

MILLIMETER RADAR INVESTIGATION

Marvin J. Foral
Aero-electronic Technology Department
Naval Air Development Center
Warminster, PA 18974

Airtask No. A370370E/0018/3F34371709, 26 March 1973
AD-910 157L (A79 06629)

The first effective radar system operating at 95 GHz was constructed and tested at NAVAIRDEVCEN, Hanover, New Hampshire, Boca Raton, Florida, and Montauk Point, Long Island. The tests were conducted with various targets over land, snow and water. These results and possible applications of the radar system are discussed. (Author)

MEASUREMENTS OF ATTENUATION DUE TO SIMULATED BATTLEFIELD DUST AT 94 AND 140 GHz

J. J. Gallagher, R. W. McMillan, and R. C. Rogers
Georgia Institute of Technology
Engineering Experiment Station
Atlanta, GA 30332

D. E. Snider
U. S. Army Atmospheric Sciences Laboratory
White Sands Missile Range, NM 88002

Proceedings of the Workshop on Millimeter and Submillimeter Atmospheric Propagation Applicable to Radar and Missile Systems, Redstone Arsenal, AL 35809
O. M. Essenwanger and D. A. Stewart (editors)
Technical Report RR-80-3, 100-108, February 1980

During the fall of 1978, a series of measurements, called DIRT I, of electro-magnetic wave propagation through simulated battlefield dust were conducted at White Sands Missile Range. This paper gives an overview of the entire DIRT I test as well as detailed results of those tests for millimeter wave (94 and 140 GHz) frequencies.

Attenuation measurements were made over an instrumented 2 km range. In the center of the range, explosive charges of different sizes were detonated, and the resulting signal level was compared to that existing before the explosive event. Measurements were also made of attenuation caused by artillery shells fired into the center of the range, and of that caused by burning diesel oil and rubber.

Both magnitude and duration of attenuation were found to vary with the amount of the explosive, sometimes reaching 30 dB and 20 seconds respectively. Copies of chart recorder tracings showing attenuation of both explosion products and oil smoke are presented. Oil smoke propagation measurements show scintillations of 3 to 5 dB. (Authors)

EXTRACTS:

Additional reports on the DIRT I measurements are:

1) Measured Effects of Battlefield Dust and Smoke on Visible, Infrared, and Millimeter Wavelength Propagation compiled by J. D. Lindberg. An entry for this report is under Snider, McMillan and Gallagher.

2) Millimeter Wave Propagation Through Battlefield Dust by R. W. McMillan, R. Rogers, R. Platt, D. Guillory, J. J. Gallagher and D. E. Snider. This report is entered under McMillan et al.

PROPAGATION OF MILLIMETER AND SUBMILLIMETER WAVES

William L. Gamble and Tony D. Hodgens
U.S. Army Missile Research and Development Command
Redstone Arsenal, AL 36809

U.S. Army Missile Research and Development Command Report No. TE-77-14
22 June 1977
AD-023 662L (A79 06507)

This report presents the results of a literature survey of the effects of the atmosphere on millimeter and submillimeter wave propagation. The regions investigated were confined to a range of 35 to 408 GHz (8.570 to 0.835 mm). A summary of existing theoretical and experimental data is presented for various atmospheric conditions. Meteorological uncertainties and their effects on attenuation measurements are described. Areas where supplemental data are required for an understanding sufficient to the needs of systems designers are presented. (Authors)

EXTRACTS:

Clear air: Considerable differences exist in experimental (and theoretical) data.

Inclement weather: Attenuation through standard atmospheres with fog (visibility = 100 m, T = 18-24°C) and with rain (T = 23°C) are compared with theoretical values.

Rain: Almost no experimental data exist on the volume reflectivity of rain above 100 GHz. Graphs of average backscatter and measured attenuation vs. rain rate.

Fog and haze: Characteristics of advection and radiation fog vs. liquid water content.

Smoke, dust, plumes: Experimental data virtually non-existent. BRL made 94- and 140-GHz measurements through fog, oil, and hexachloroethane smoke dust from 155-mm howitzer white phosphorus rounds and a moving vehicle. No measurable attenuation recorded.

Snow and hail: Experimental data practically non-existent (some work performed in USSR). Attenuation of wet snow was 2.5 times greater than that of an equivalent rainfall (wet snow has 30-40% greater water content than dry snow). Overall, propagation through snow is expected to be excellent unless heavy wet snows are encountered.

Weather conditions: Weather conditions are divided and averaged, separating the four seasons. Charts for W. Germany and central NATO of rainfall rate, temperature, frequency and duration of fog, and average cloud ceilings.

Several of the authors' figures follow.

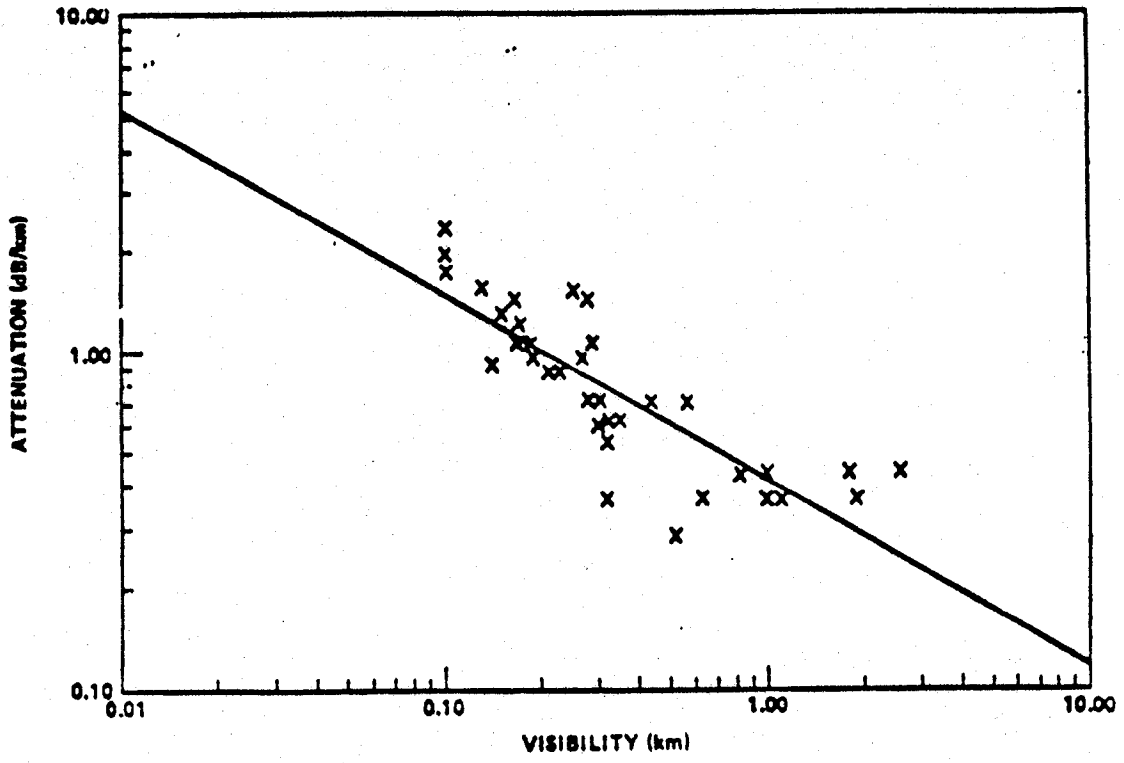

Figure 27. 140-GHz one-way attenuation in fog versus visibility [38]. (140-GHz attenuation may be correlated with liquid water vapor content with the aid of Fig. 23.)

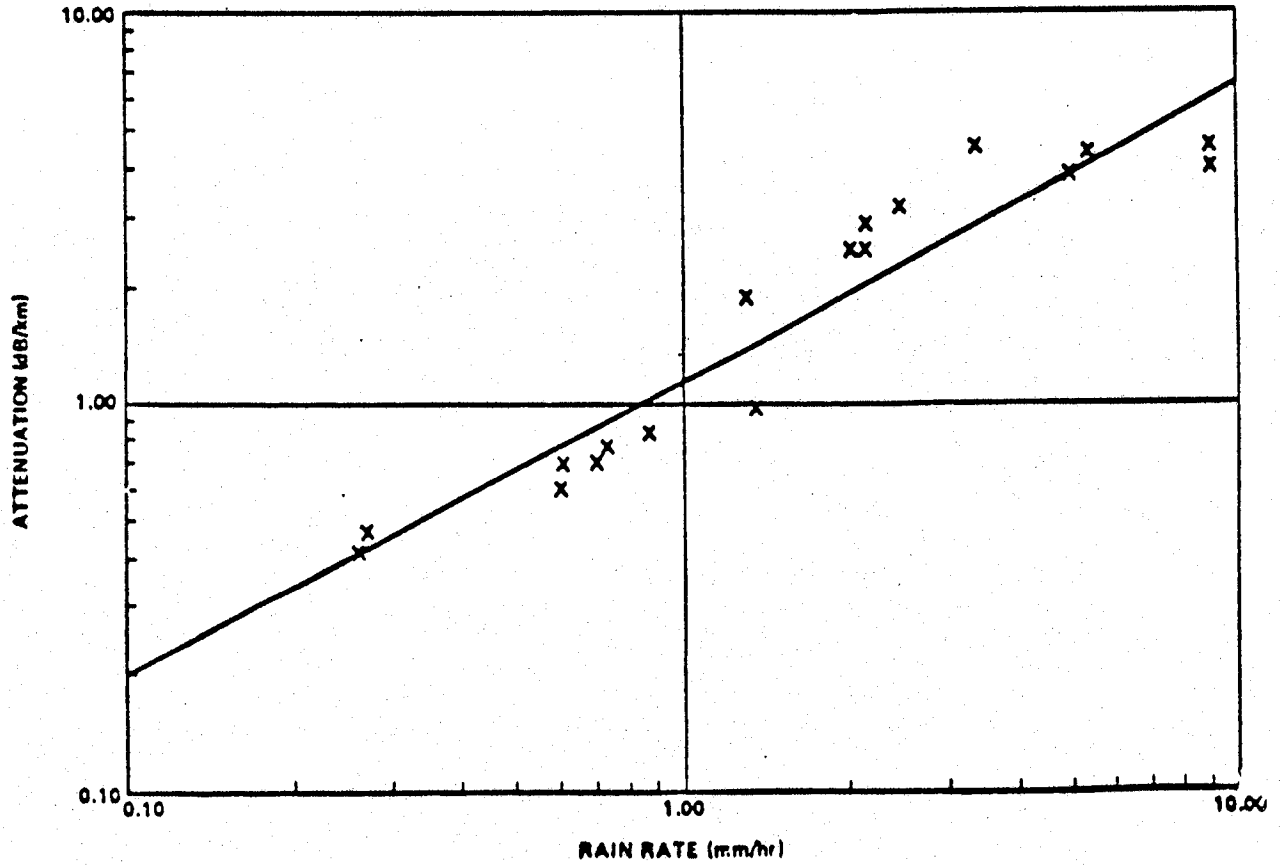

Figure 21. 140-GHz rain attenuation versus rate [38].

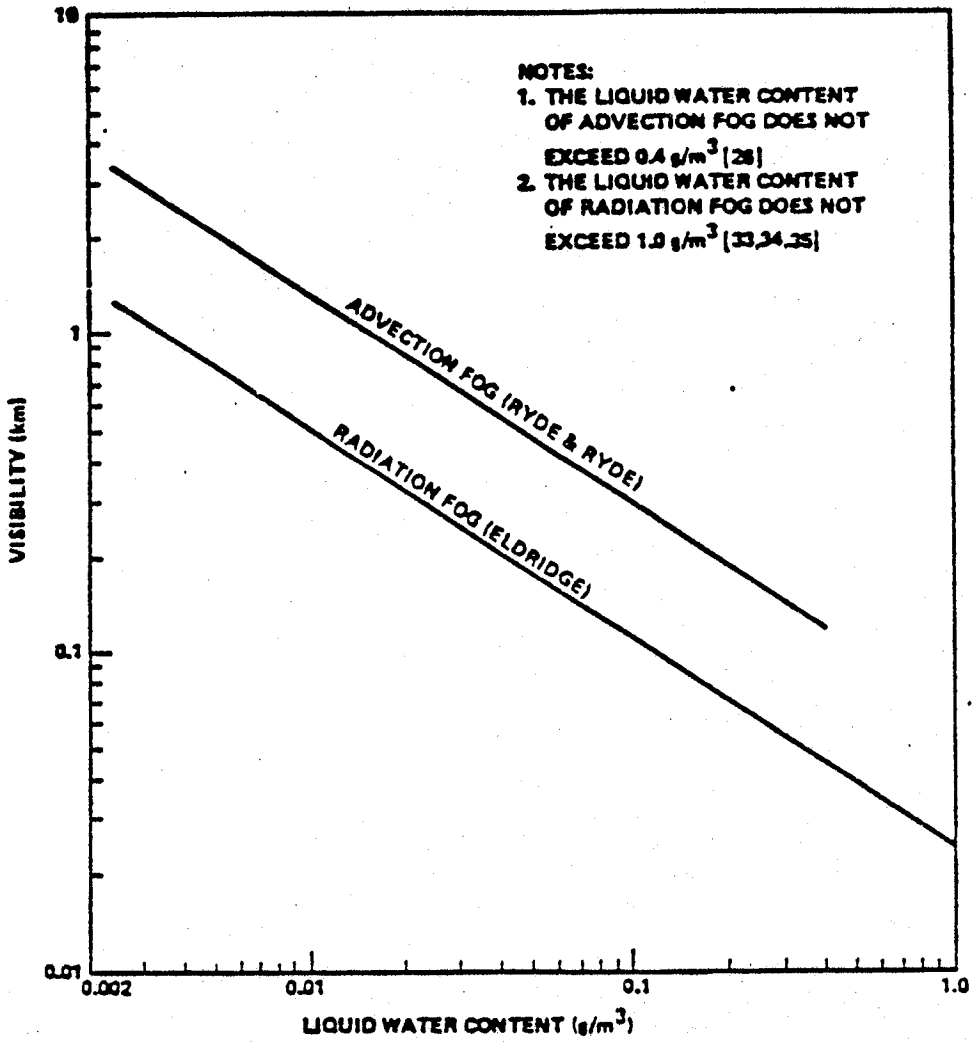

Figure 23. Correlation of visibility in fog to liquid water content [3].

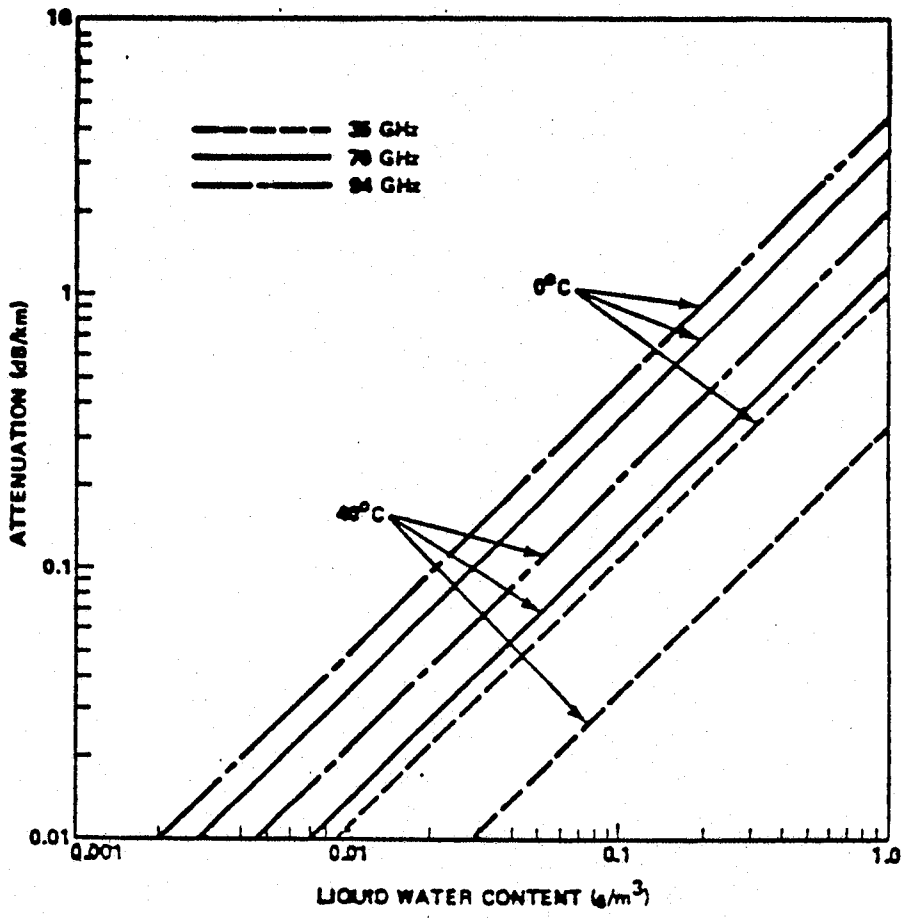

Figure 24. One-way attenuation in fog as a function of liquid water content [32].

GAUT AND REIFENSTEIN*

INTERACTION MODEL OF MICROWAVE ENERGY AND ATMOSPHERIC VARIABLES

Norman E. Gaut and Edward C. Reifenstein, III
Environmental Research and Technology, Inc.
58 Guinan Street
Waltham, MA 02154

NASA CR-61348, April 20, 1971
N71-25079 (A79 03037)

Results are presented for a study of the effects of water vapor, liquid water and ice upon radiative transfer processes at microwave frequencies and in the far infrared. The fundamental processes by which these species interact with microwave energy are discussed, and their statistics analyzed in terms of their application to a range of remote sensing problems.

Theoretical expressions for the water vapor absorption coefficent at microwave frequencies are reviewed, and an efficient computer oriented algorithm is presented for its computation. The Mie theory is reviewed, and the unit volume effects of typical liquid water and ice cloud distributions of the spectral region from 10 cm to 10 microns are examined. Characteristics of the two dimensional distributions of water vapor, liquid water, and ice in the atmosphere have been collected on planetary, synoptic, meso and microscales, and are examined in terms of remote sensing applications. Extreme values of each are established as a function of scale size and related to the attenuation and noise energy produced and their fluctuations in time.

The information content of radiosonde and cloud data has been used in the 4-D Atmospheric Model and Cloud Statistics Program. This model is examined for its utility in simulating and predicting the influence of the atmosphere on surface observations from a space observer. (Authors)

FINAL REPORT ON A MILLIMETER WAVE RADIOMETER GUIDANCE MEASUREMENT PROGRAM

Systems Division
General Precision, Inc.
Aerospace Group
Wayne, NJ 07470

Contract No. DA-30-069-AMC-621(R), October 1964
K2091014 (A65 05284)

CONFIDENTIAL

A field measurements program was conducted to evaluate the performance of a closed-loop 35-gc passive radiometer system. This work, under the sponsorship of Ballistic Research Laboratories, Aberdeen, Maryland, was performed using an experimental radiometer guidance system developed by Aerospace Systems Division, General Precision, Inc.

This report correlates actual data with system performance predicted by a theoretical model. The data supports the theoretical model, within the constraints imposed by characteristics of the experimental equipment and the test sites.

This measurements program has resulted in several significant accomplishments:

- Effective passive tracking of stationary and moving targets in their natural environment have been demonstrated.
- Tracking ranges and angular rates approaching predicted values were achieved.
- Specific improvements in equipment parameters to improve system performance have been identified. These parameter improvements are well within the state-of-the-art.
- Successful semi-active tracking was also demonstrated.

Recommendations are made for additional effort which will demonstrate the full potential of passive millimeter-wave tracking. Such an effort would require the use of improved equipment in a test site affording visibility from an elevated vantage point. (Author)

GEOPHYSICS*

HANDBOOK OF GEOPHYSICS

Revised Edition, 1960
United States Air Force
Air Research and Development Command
Air Force Research Division
Geophysics Research Directorate

ATMOSPHERIC EMISSION MEASUREMENTS BETWEEN 22 AND 150 GHz

C. J. Gibbins, C. L. Wrench, and D. L. Croom
Science Research Council
Appleton Laboratory
Slough, Great Britain

Anglo-Soviet Seminar on Atmospheric Propagation at Millimeter and Submillimeter Wavelengths, Nov. 28 - Dec. 3, 1977, K1-K5
Institute of Radioengineering and Electronics, Moscow

Atmospheric emission measurements have been made under clear sky conditions at frequencies between 22 and 150 GHz. These measurements have been used to determine the total one-way atmospheric attenuation at the zenith. Comparison between experimental results and theoretical calculations indicate that at the higher frequencies, the attenuation due to water vapor is in excess of that predicted by up to about 60%. (Authors)

EXTRACTS:

95 GHz: Zenith attenuation versus total precipitable water (W, in cm):

$$A\ (dB) = 0.41\ (\pm 0.04) + 0.35\ (\pm 0.02)\ W$$

Compared to the 90-GHz measurements of Shimabukuro and Epstein:

$$A\ (dB) = 0.16 + 0.40\ W\ [\text{Std. Dev.} = 0.18]$$

150 GHz: Zenith attenuation versus total precipitable water (W):

$$A\ (dB) = 0.28\ (\pm 0.25) + 1.19\ (\pm 0.14)\ W$$

GNISS AND MAGURA*

MILLIMETER WAVE IMAGING OF GROUND BASED OBJECTS

H. Gniss and K. Magura
Forschungsinstitut fuer Hochfrequenzphysik
Forschungsgesellschaft fuer Angewandte Naturwissenschaften e. V.

Forshungsbericht Nr. 1-78
Lfd. Nr. 153
Wachtberg-Werthoven, January 1978
(A80 00444)

This report deals with the problems concerning the recognizability of millimeter wave images, which were obtained from various targets (models of ground based objects) at 36 GHz in laboratory experiments. Of special interest is the dependence of the image fidelity on lateral resolution of the mapping aperture and the form, orientation and depolarization properties of the target. Because of the spatial distribution of only a limited number of scattering centers on the object, which depend on aspect angle and polarization generally, the image fidelity is affected strongly. Smoothing of the resulting image intensity fluctuations is obtained through incoherent superposition of independent partial images. Finally, the image disturbances resulting from ground and environment clutter are investigated. (Authors)

PREDICTION METHODS FOR RAIN ATTENUATION STATISTICS AT VARIABLE PATH ANGLES AND CARRIER

Julius Goldhirsch
Applied Physics Laboratory
Johns Hopkins University
Laurel, MD 20810

IEEE AP-23, No. 6, 786-791, November 1975

Fade depth and space diversity statistics of propagation along earth-satellite paths have been calculated from radar reflectivity data of rain using modeling procedures. The reflectivity data base was obtained during the summer of 1973 at Wallops Island, VA, using a high resolution S-band radar interfaced with a computer and digital processing system. Fade statistics have been calculated at various path angles at several frequencies between 13 and 100 GHz. Subsequent analysis has demonstrated the ability to predict the following: 1) fade statistics at other path elevation angles given similar type statistics at a particular path angle, 2) space diversity statistics at other frequencies, given similar type statistics at a particular frequency, and 3) fade statistics at a third frequency given similar type statistics at two other frequencies. Although a specific data base was used pertaining to the climatology at Wallops Island, the techniques developed are general and may be applied to existing or future "fade measurements" at other climatological locations. (Author)

GOLDSMITH, PLAMBECK, AND CHIAO

MEASUREMENT OF ATMOSPHERIC ATTENUATION AT 1.3 AND 0.87 mm WITH AN HARMONIC MIXING RADIOMETER

P. F. Goldsmith, R. L. Plambeck, and R. Y. Chiao
Department of Physics
University of California
Berkeley, CA 94720

IEEE MTT-22, 1115-1116, December 1974

The atmospheric attenuation at 1.3 and 0.87 mm was measured above Mount Hamilton, California in the period December 5 to December 9, 1973. The total beamwidth of the 120" Lick Observatory telescope used in the Coude configuration was measured to be 3' at 1.3 mm. (Authors)

EXTRACTS:

The attenuation at 1.3 and 0.87 mm is due primarily to water vapor absorption lines at 2.25 mm (183.3 GHz), 0.926 mm (323.8 GHz), and 0.795 mm (377.4 GHz). The authors state "the present measurements confirm the expectation of Ulaby and Straiton that their predicted attenuation between the lines [i.e., at 230 GHz] is too low compared to the attenuation near the line centers," but give no predicted attenuation values to compare with their measurements.

Calibration measurements were taken as the temperature difference between an absorber (Eccosorb AN-72) at liquid nitrogen temperature and at ambient temperature.

DETECTION OF STRATEGIC TARGETS WITH A NMMW SATELLITE RADIOMETER

G. A. Gordon
R & D Associates
Post Office Box 9695
Marina del Rey, CA 90291

August 1977
(A77 05360)

SECRET

New analyses of aircraft and ship detection performance of a passive radiometer operating in the NMMW region.

EXTRACTS:

This document is a rough draft of the article which appears in Proceedings of the Sixth DARPA/Tri-Service Millimeter Wave Conference by the same author and title.

At 1.3 mm wavelength, even a cloud with extreme ice density (0.3 g/m^3) and maximum thickness (7 km) has negligible effect on target visibility. For 0.1 g/m^3 ice crystal density the attenuation rate is estimated at 0.04 dB/km at 1.3-mm wavelength.

GORDON*

DETECTION OF STRATEGIC TARGETS WITH A NMMW SATELLITE RADIOMETER

G. A. Gordon
R & D Associates
Post Office Box 9695
Marina del Rey, CA 90291

Proceedings of the Sixth DARPA/Tri-Service Millimeter Wave Conference
Tactical Technology Office (editor), Defensed Advanced Research Projects
Agency, 1400 Wilson Blvd., Arlington, VA 22209, p. 63-71, November 1977
(A78 01438)

SECRET

This paper considers the performance of a satellite-based radiometer operating at near-millimeter wavelengths for detecting strategic targets such as large aircraft. (Author)

Extracts are in the supplementary classified document.

A STUDY OF MILLIMETER AND SUBMILLIMETER WAVE ATTENUATION AND DISPERSION IN THE EARTH'S ATMOSPHERE

M. Greenebaum and D. Koppel
Riverside Research Institute
80 West End Avenue
New York, NY 10023

ADA-015 544 (A79 07630)

A summary is presented of new calculations of atmospheric absorption line parameters and of a slant-path absorption line model intended for use in the millimeter and submillimeter wave spectral regions. Results of a literature survey concerning altitude-dependent attenuation and dispersion in this spectral region, as well as weather-dependent scattering and fading strengths, are also summarized. Recommendations are given for improving the data base and for reducing the uncertainties in the model predictions.

A list of the 318 absorption lines of the molecular oxygen isotopes of principal concern in atmospheric transmission below 300 cm^{-1} is included, together with their integrated strengths at 296 K, line widths, lower-state energies, and identifying quantum numbers, in the format of the AFCRL Atmospheric Absorption Line Parameters Compilation. Reference is made to a series of Technical Reports which give complete documentation of the calculations leading to these values and to similar calculations for carbon monoxide, as well as of a detailed description of the SLAM program. (Authors)

GRUENER

SIMULTANEOUS RADIOMETRIC MEASUREMENTS AT 32 GHz AND 90 GHz

K. Gruener
Deutsche Forschungs- und Versuchsanstalt fuer Luft- und Raumfahrt
D 8031 Oberpfaffenhoffen, Federal Republic of Germany

Proceedings of the 9th International Symposium on Remote Sensing of the Environment, 15-19 April 1974, 151-157, Environmental Research Institute, University of Michigan, Ann Arbor, MI 48104

ADA 008 469 (A77 00616)

The paper gives an insight upon a part of the present experimental activities in the area of microwave radiometry. A preliminary selection of measurements which were made from a stationary platform 21 meters above ground is discussed. (Authors)

The entire article has been reproduced in the Appendix.

INDEX OF 3.2-mm AND 10.6-μm IMAGE DATA TAPES

B. D. Guenther
Physical Sciences Directorate
Technology Laboratory
U.S. Army Missile Research and Development Command
Redstone Arsenal, AL 35809

Technical Report TR-77-2, 1 February 1977

This report describes radar image data of military vehicles at wavelengths of 3.2 mm and 10.6 μm available on magnetic tape from the Physical Sciences Directorate. This report is to provide an index of the available images for prospective users. Additional study of the images and methods of processing them will be carried out at Hughes Research Laboratories and the U.S. Army Missile Research and Development Command. (Author)

GUENTHER*

SUBMILLIMETER RESEARCH: PRELIMINARY REPORT ON MILLIMETER AND INFRARED IMAGES OF MILITARY VEHICLES

B. D. Guenther
Physical Sciences Directorate
U.S. Army Missile Research, Development and Engineering Laboratory
U.S. Army Missile Command
Redstone Arsenal, AL 35809

Technical Report RR-77-4, 10 November 1976

A summary of the types of radar images obtained at 3.2 mm and 10.6 μm are presented along with samples of some of the images. (Author)

SUBMILLIMETER RESEARCH: A PROPAGATION BIBLIOGRAPHY

B. D. Guenther, J. S. Bennett, W. L. Gamble, and R. L. Hartman
Physical Sciences Directorate
U.S. Army Missile Research, Development and Engineering Laboratory
U.S. Army Missile Command
Redstone Arsenal, AL 35809

Technical Report RR-77-3, November 1976

This report is an annotated bibliography given on the subject of submillimeter propagation. Several articles are recommended as a good starting point for reviewing the current state-of-the-art. (Authors)

HAYES, LAMMERS, MARR, AND McNALLY

MILLIMETER WAVE PROPAGATION MEASUREMENTS OVER SNOW

D. T. Hayes, U. H. W. Lammers, R. A Marr, and 1st Lt. J. J. McNally
Rome Air Development Center
Hanscom AFB, MA 01731

Proceedings of the Eighth DARPA/Tri-Service Millimeter Wave Conference
System Planning Corporation (editor), 1500 Wilson Blvd., Arlington, VA 22209,
p. 91-100, April 1979
(A80 00206)

SECRET

Data are presented showing the scattering properties of snow as a function of frequency (35, 98, and 140 GHz), incident angle, polarization, snow type and free water content. Data are also included to demonstrate the effect of snow cover on multipath propagation at the same frequencies. (Authors)

SCATTERING MEASUREMENTS AT 35, 94 AND 140 GHz FROM METAMORPHIC SNOW

D. T. Hayes, U. H. W. Lammers, R. A. Marr, and J. J. McNally
Rome Air Development Center
Electromagnetic Sciences Division
Hanscom AFB, MA 01731

Proceedings of the Sixth DARPA/Tri-Service Millimeter Wave Conference
Tactical Technology Office (editors) Defense Advanced Research Projects Agency, 1400 Wilson Blvd., Arlington, VA 22209, p. 216-224, November 1977
(A78 01438)

SECRET

The normalized backscatter coefficient from metamorphic snow has been measured as a function of incidence angle. Measurements were also made for various bistatic angles. Among other factors the effect on the normalized backscatter coefficient of free water in the snow was determined. (Authors)

HAYES, SCHEER, AND LANE

REFLECTIVITY AND EMISSIVITY CHARACTERISTICS OF SNOW, ICE AND WET GROUND AT MILLIMETER WAVE FREQUENCIES

R. D. Hayes and J. A. Scheer
Engineering Experiment Station
Georgia Institute of Technology
Atlanta, GA 30332

Captain T. Lane
Air Force Armament Technology Laboratory
Eglin AFB, FL 32542

Proceedings of the Eighth DARPA/Tri-Service Millimeter Wave Conference
System Planning Corporation (editor), 1500 Wilson Blvd., Arlington, VA 22209,
p. 101-108, April 1979
(A80 00206)

SECRET

The data presented in this paper will assist in determining the potential for the capability of processing techniques to enhance the target in the clutter background. (Authors)

EXTRACTS:

Emissivity Calculated from Radiometric Data

	94 GHz Vertical Polarization	94 GHz Horizontal Polarization
2' tall grass (water on the ground)	0.86	0.78
4" grass (75% soil moisture)	0.98	0.96
Snow falling (1"/hour)	—	0.73

ABSOLUTE MEASUREMENTS OF ATMOSPHERIC EMISSION AND ABSORPTION IN THE RANGE 100-1000 GHz

Infrared Physics 18, 819-825, September 1978

R. E. Hills and A. S. Webster
Cavendish Laboratory
Madingley Road
Cambridge CB3 OHE, U.K.

D. A. Alston, P. L. R. Morse and C. C. Zammit
Polytechnic of Central London
115 New Cavendish St.
London W1M 8JS, U.K.

D. H. Martin and D. P. Rice
Queen Mary College
Mile End Road
London E1 4NS, U.K.

E. I. Robson
Preston Polytechnic
Corporation Street
Preston, PR1 2TQ, U.K.

A spectrometer has been constructed which consists of a polarizing Michelson interferometer with a cooled detector, hot and cold reference bodies, a tilting mirror and a computerized control and data handling system. It has been used to obtain well-calibrated spectra of atmospheric emission as a function of water vapor content and zenith angle. Preliminary analysis of spectra taken at 2400 m on Tenerife shows that the opacity in the millimeter wavelength windows is low, is proportional to the secant of the zenith angle under stable conditions, and is well correlated with the readings of near-IR hygrometers. (Authors)

EXTRACTS:

Preliminary results only.
No reduced data for a frequency near 230 GHz were presented.

HO, MAVROKOUKOULAKIS, AND COLE*

RAIN-INDUCED ATTENUATION AT 36 AND 110 GHz

K. L. Ho
Department of Electronic Engineering
Hong Kong Polytechnic, Hong Kong

N. D. Mavrokoukoulakis and R. S. Cole
Department of Electronic and Electrical Engineering
University College London, London WC1E 7JE

Results are presented of the ratios of the rainfall attenuation measured simultaneously along a common path at 36 GHz and 110 GHz. These ratios agree well with the theoretically derived ratios assuming the Laws-Parsons distribution. (Authors)

EMISSION PROPERTIES OF WATER SURFACES AT 3 mm WAVELENGTH

R. Hofer and E. Schanda
Institute of Applied Physics
University of Berne
3000 Berne, Switzerland

Proceedings of the URSI Commission II, Specialist Meeting on Microwave Scattering and Emmission from the Earth, 23-26 September 1974, 17-23
(QC 809, M6 I61)

Antenna temperature and forward scattering measurements at 94 GHz on water surfaces in a temperature range between 7 and 45°C are compared and discussed. The angular dependence of the considerable atmospheric contribution in this frequency region according to the secant-law is verified and taken into account for all measurements. Oil-polluted water and surface waves are studied. (Authors)

EXTRACTS:

Dielectric constant ($\varepsilon = E' - iE''$) measurements:

	E'	E"	emissivity
Water T = 9°C	9.4	8.6	0.66
15	7.3	10.6	0.63
20	—	—	0.62
23	8.0	13.2	0.60
Oil film	2.5	7.6	0.67

HOFER AND SCHANDA

EMISSION PROPERTIES OF WATER SURFACES AT 3 mm WAVELENGTH

R. Hofer and E. Schanda
Institute of Applied Physics
University of Berne
3000 Berne, Switzerland

Proceedings of the 9th International Symposium on Remote Sensing of the Environment, 15-19 April 1974, 17-23, Environmental Research Institute, University of Michigan, Ann Arbor, MI 48104

ADA 008 469(A77 00616)

Antenna temperature- and forward-scattering measurements at 94 GHz on water surfaces in a temperature range between 7 and 43 °C are compared and discussed. The angular dependence of the considerable contribution of the atmosphere in this frequency region according to the secant-law is verified and taken into account for all measurements. An oil-polluted water surface and surface waves are studied. (Authors)

The entire article has been reproduced in the Appendix.

SIGNATURES OF SNOW IN THE 5 TO 94 GHz RANGE

R. Hofer and E. Schanda
Institute of Applied Physics
University of Berne
Sidlestrasse 5
CH-3012 Berne, Switzerland

Radio Science 13, No. 2, 365-369, March-April 1978

A long-term observational study of the microwave emission and scattering behavior of snow under quasi-controlled conditions was started recently on a high-altitude Alpine test site. Results of the first set of measurements, carried out with five radiometers at frequencies of 4.9, 10.5, 21, 36, and 94 GHz, are reported and preliminary interpretations are given. The spectral reversal of the brightness temperature and its dependence on look angle and polarization provided a means to distinguish between different snow states and to estimate the wetness factors of the surface layer of the snow pack. From an electromagnetic scattering standpoint snow cover is an excellent medium to use for studying volume scattering. (Authors)

EXTRACTS:

Snow characterized according to wetness:

a) dry--no liquid water content.
b) wet--more than 1% liquid water content. Causes a blackbody behavior at 36 and 21 GHz: shows no angular variation and the brightness temperature is nearly identical to its physical temperature.
c) humid--lies between dry and wet. Brightness temperature at higher microwave frequencies may change 50 K or more due to changing humidity within less than a half hour.

At 94 GHz the snow surface acted almost like a diffuse scatterer with only slight variations due to look angle and polarization.

HOGG*

MILLIMETER-WAVE COMMUNICATION THROUGH THE ATMOSPHERE

D. C. Hogg
Bell Telephone Labs
Crawford Hill Laboratory
Holmdel, NJ 07733

Science 159, Number 3810, 39-46, 5 January 1968

The known and unknown features of short radio wave propagation are discussed.

PASSIVE MICROWAVE MEASUREMENTS OF THE SEA SURFACE

James P. Hollinger
E. O. Hulbert Center for Space Research
Naval Research Laboratory
Washington, D. C. 20390

Journal of Geophysical Research 75, No. 27, 5209-5213, Sept. 20, 1970

Passive measurements of the sea surface were made in March and April 1969 from the Argus Island tower at 8.36 and 19.34 GHz over a range in wind speeds of from calm to 10 m/sec. These measurements show a definite dependence of microwave brightness temperature on wind speed and on sea foam. This dependence is the same at the two observational frequencies within the error of measurement. (Author)

HOLLINGER*

PASSIVE MICROWAVE MEASUREMENTS OF SEA SURFACE ROUGHNESS

James P. Hollinger
E. O. Hulbert Center for Space Research
Naval Research Laboratory
Washington, D.C. 20390

IEEE GE-9, 165-169, July 1971

Passive microwave measurements of the sea surface were made from Argus Island tower at 1.41, 8.36, and 19.34 GHz over a range in wind speeds from calm to 15 m/s. These measurements show a definite frequency-dependent correlation between the microwave brightness temperature and wind speed. This dependence results from roughness effects of the compact sea surface associated with wind-driven waves. (Author)

REMOTE PASSIVE MICROWAVE SENSING OF THE OCEAN SURFACE

J. P. Hollinger
E. O. Hulbert Center for Space Research
Naval Research Laboratory
Washington, D.C. 20390

Preprint, 1970

The important potential of all-weather determination of ocean surface wind fields by means of remote passive microwave sensing is discussed. The wind speed dependence of the microwave brightness temperature of the sea is interpreted as resulting from small-scale wave structure at wind speeds below about 15 to 20 m/sec and from the increasing coverage of sea foam at higher wind speeds. Measurements of these two effects are combined to estimate the total microwave brightness temperature dependence of a wind driven sea as viewed from a satellite. Taken together the two effects allow the determination of ocean surface wind fields over the entire range of wind speeds. The sensitivity to wind speeds increases with observational frequency and is most pronounced from horizontal polarization at larger incidence angle. (Author)

EXTRACTS:

Frequencies of 1.41, 8.36, and 19.34 GHz are explored.

HOLLINGER, KENNEY, AND TROY*

A VERSATILE MILLIMETER-WAVE IMAGING SYSTEM

James P. Hollinger, James E. Kenney, and Ballard E. Troy, Jr.
Space Science Division
Naval Research Laboratory
Washington, D.C. 20375

IEEE MTT-24, No. 11, 786-793, November 1976

A new millimeter-wave imaging system has been assembled at the Naval Research Laboratory and flight-tested using the NASA/Wallops C-54 aircraft. The system incorporates an oscillating mirror and interchangeable radiometer units making it particularly adaptable to variations in the operational frequency, polarization, and the angular resolution. Flight tests of the system have been conducted at 90 GHz and simultaneously at 22 and 31 GHz using a dual frequency radiometer. The imaging system and data processing are described and some of the initial flight test results at 90 GHz are presented. (Authors)

ATTENUATION OF RADIO WAVES AT WAVELENGTHS FROM 0.45 TO 4.0 mm IN THE EARTH'S ATMOSPHERE THROUGH THE SLANT PATHS

I. A. Ishakov, A. V. Sokolov, W. V. Sukhonin, and V. I. Cheryshov
Institute of Radioengineering and Elecronics
Academy of Sciences of the USSR, Moscow

Anglo-Soviet Seminar on Atmospheric Propagation at Millimeter and Submillimeter Wavelengths, Nov. 28 - Dec. 3, 1977, J1-J6
Institute of Radioengineering and Electronics, Moscow

1.5 to 0.4 mm wavelength measurements of the total zenith absorption (cloudless atmosphere), and attenuation from clouds have been made near Moscow and in Armenian SSR at an elevation of 3250 m. 4 mm measurements of cloud and rain attenuation have been taken at Gorky. (Authors)

EXTRACTS:

Zenith attenuation in clouds at wavelength of 1.26 mm:

altocumulus	0.16 dB
stratus	0.16
cumulus	1.75
congested cumulus	8.7

JOHANSEN AND MAFFETT*

NEAR-FIELD TARGET MEASUREMENTS

E. L. Johansen and A. Maffett
Environmental Research Institute of Michigan
University of Michigan
Ann Arbor, MI 48104

Proceedings of the Eighth DARPA/Tri-Service Millimeter Wave Conference
System Planning Corporation (editor), 1500 Wilson Blvd., Arlington, VA 22209,
p. 57-66, April 1979
(A80 00206)

SECRET

During the program, ERIM made high resolution radar images at 34.1 GHz, analyzed the images and made radar maps of three armored targets to support seeker modeling and analysis. (Authors)

CROSS SECTION MEASUREMENTS OF US ARMY TARGETS BY 140 GHz RADAR

J. E. Kammerer and K. A. Richer
Ballistic Research Labs
Aberdeen Proving Ground, MD

BRL Report No. 1785, August 1966
AD 378 097 (A73 03226)

CONFIDENTIAL

Some backscatter data needed in the solution of the near-earth missile guidance problem have been taken at a radio frequency of 140 GHz (2.1 millimeters wavelength). Measurements to determine the characteristics of radar cross section versus target azimuth angle were made for military targets having maximum dimensions between 800 and 5300 radar wavelengths. These targets were an M67A tank, a 2 1/2 ton Shop Van, an M116 Personnel Carrier, a UH-1B Helicopter and a man carrying small arms. The measurements were made with linearly polarized signals and are compared with cross section data reported in the literature for similar military targets measured by lower frequency radar. Observations on clutter and target obscuration by foliage and rainfall are included. (Authors)

KAMMERER AND RICHER*

140 GHz MILLIMETRIC BISTATIC CONTINUOUS WAVE MEASUREMENTS RADAR

J. E. Kammerer and K. A. Richer
Ballistic Research Labs
Aberdeen Proving Ground, MD 21005
(301) 278-4289

BRL Memo Report Number 1730, January 1966
AD-484 693 (A66 07916)

A laboratory model continuous wave bistatic radar operating at heretofore unmeasured millimetric wavelengths is being used in a field measurements program to explore the effects of the near-earth environment. Operational at a radio frequency of 140 GHz (2.1 millimeters wavelength), the radar frequency generating and receiving equipment are described and measured sensitivities are listed. The radar is adaptable to field measurements programs that cover a range of operational frequencies extending into the submillimeter wavelength region of the spectrum. (Authors)

MILLIMETER INVESTIGATIONS, VOLUME 5

J. M. Keelty and R. A. Crane
Research Laboratories
RCA Limited
1001 Lenoir St.
Montreal 207, Canada

RCA Report No. 3576-B/96690-3, January 1969
AD-857 436L (A71 00667)

Volume 5 contains samples of the computer analysis of various parameters salient to the description of system performance. Printouts detailing precipitation-rates, error-run data, and signal strength variations for various meteorological conditions and a section discussing the results of a helicopter interference test are included. (Authors)

EXTRACTS:

Frequencies of 15 and 35 GHz are explored.

KEIZER, SNIEDER, AND DE HAAN

RAIN ATTENUATION MEASUREMENTS AT 94 GHz: COMPARISON OF THEORY AND EXPERIMENT

W. P. M. N. Keizer, J. Snieder and C. D. de Haan
Physics Laboratory TNO
P.O. Box 96864
2509 JG The Hague
The Netherlands

AGARD Conference Proceedings No. 245, February 1979
Millimeter and Submillimeter Wave Propagation and Circuits
Edited by E. Spitz and G. Cachier

Since October 1977, measurements have been made of attenuation at 94 GHz caused by rain on a 935-meter terrestrial path. Simultaneously, the raindrop size distribution has been measured with a distrometer, together with the rainfall intensity recorded with three rapid-response rain gauges spaced about 500 m apart along the propagation path.

Using the actually measured raindrop size distribution and assuming spherical raindrops, the attenuation caused by rain has been calculated with the aid of Mie's scattering theory for water spheres. The result is compared with the measured data. In the case of uniform rainfall along the path, good agreement has been observed between the measured and the calculated attenuation.

This paper deals with the description of the propagation link, the experimental results, and the comparison between theory and measurement. The paper describes also the decrease of antenna gain at 94 GHz due to water on a 1.2-m Cassegrain antenna. For accurate propagation measurements it is absolutely necessary to equip the antennas with protective shelters. (Authors)

EXTRACTS:

Two of the authors' figures are shown.

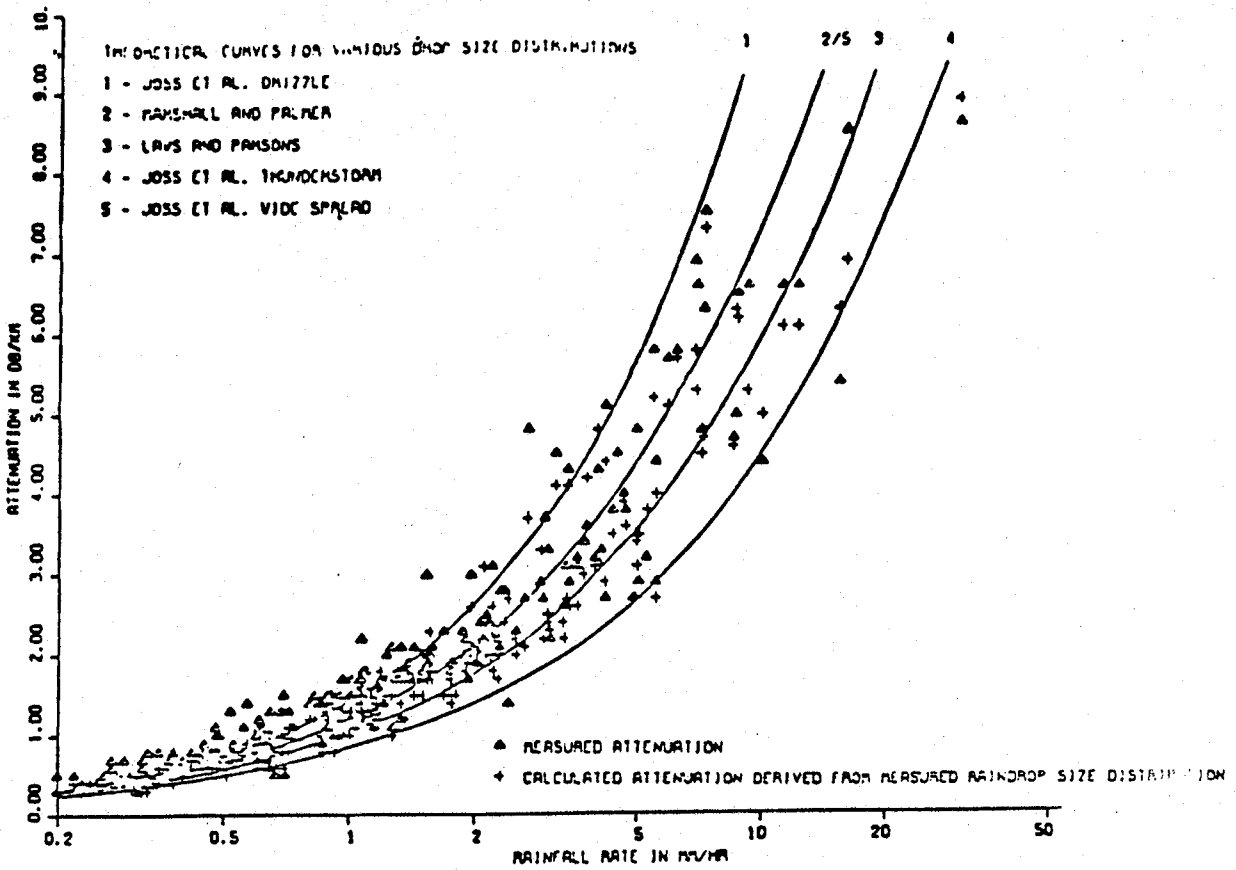

MEASURED AND CALCULATED ATTENUATION VERSUS RAINFALL RATE AT 94 GHZ

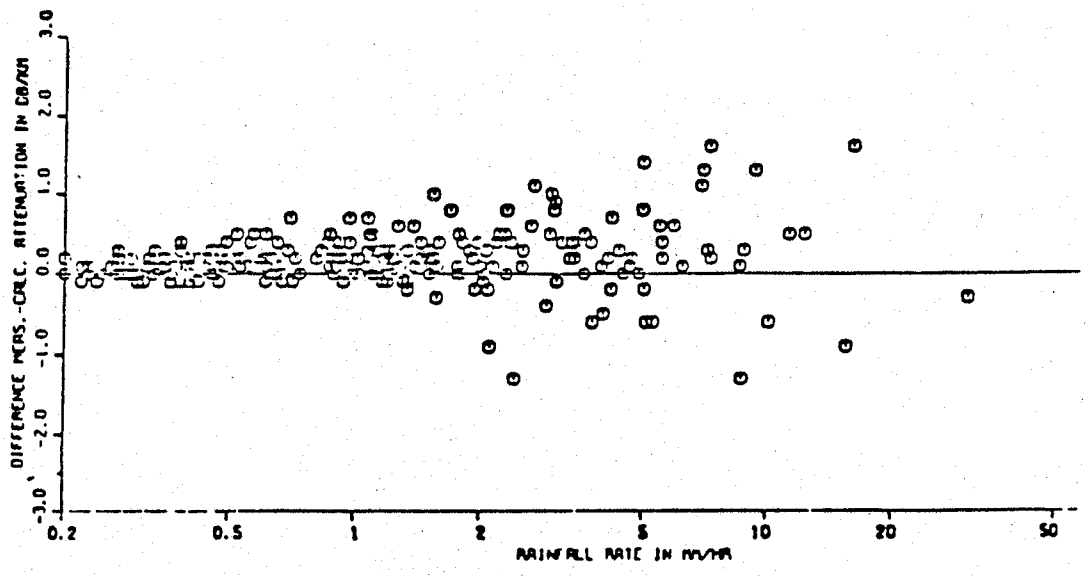

DIFFERENCE OF MEASURED AND CALCULATED ATTENUATION

KING, WHITE, WILSON, MORI, HOLLINGER, TROY,
KENNEY, AND McGOOGAN

90 GHz RADIOMETRIC IMAGING

H. E. King, J. D. White, W. J. Wilson, and T. T. Mori
Electronics Research Laboratory
The Aerospace Corporation
El Segundo, CA 90245

J. P. Hollinger, B. E. Troy, and J. E. Kenney
Space Sciences Division
Naval Research Laboratory
Washington, D.C. 20390

J. T. McGoogan
Applied Sciences Directorate
Wallops Island, VA 23337

SAMSO Report No. TR-76-37, 19 February 1976

A 90-GHz (3-mm wavelength) radiometer with a noise output fluctuation of 0.22 °K (RMS), with a scanning antenna beam mirror, and the data processing system are described. Real-time radiometric imaging of terrain and man-made objects are shown. Flying at an altitude of 1500 feet a radiometer antenna with a 2° halfpower beamwidth can distinguish landforms, waterways, roads, runways, bridges, ships at sea and their wakes, aircraft on runways, and athletic fields. A flight taken at an altitude of 3000 feet with approximately 2000 feet of clouds below the radiometer demonstrates the ability to distinguish bridges, rivers, marshland and other landforms even though the clouds are optically opaque. The radiometric images of a few representative scenes along with photographs of the corresponding scenes are presented to demonstrate the resolution of the imager system. Antenna temperature distributions of a variety of land targets are tabulated and the complexity of deriving target brightness temperatures from the measured antenna temperatures are discussed. Applications of millimeter-wave radiometric images for civil and military systems are described. (Authors)

EXTRACTS:

Several 90-GHz radiometric images and a tabulation of antenna temperatures of selected targets are shown.

KING, WHITE, WILSON, MORI, HOLLINGER, TROY, KENNEY, AND McGOOGAN

ANTENNA TEMPERATURES OF SELECTED TARGETS

Targets	Temperature, °K — Frequency		
	14 GHz	19 GHz	90 GHz
Vegetation	237 ± 16 N = 12	239 ± 11 N = 12	279.5 ± 3.5 N = 396
Concrete (Runway)	———	———	266 ± 4 N = 288
Docks	190 ± 11 N = 4	189 ± 5 N = 4	259 ± 7 N = 303
Ocean Water	105 ± 6 N = 14	114 ± 3 N = 16	207 ± 6 N = 242
Ships at Sea	———	———	159 ± 13 * N = 255
Ships at Dock	80 N = 1	< 100 N = 1	168 ± 12 ** N = 168
C-54 Aircraft (on Runway)	———	———	225 ± 9 N = 18

N = number of samples
1σ = ± values

* 4 ships, 425 ft to 708 ft lengths
** 5 ships, 250 ft to 750 ft lengths

KING, WHITE, WILSON, MORI, HOLLINGER, TROY,
KENNEY, AND McGOOGAN

90 GHz Radiometric Image*

ASSATEAGUE ISLAND THROUGH CLOUD COVER **

RADIOMETRIC IMAGE

Image width compressed by a factor of 2:1

GEOLOGICAL SURVEY MAP

**Flight Altitude - 3000 ft
Clouds Broken - 800 ft - 1100 ft
Clouds Solid - 1100 ft - 2800 ft

*Flight Support: J. T. McGoogan, NASA Wallops
Data Processing and Support Equipment: J.P. Hollinger, NRL
Radiometer: The Aerospace Corporation, Electronics Research Laboratory

90 GHz Radiometric Image*

CHINCOTEAGUE ISLAND THROUGH CLOUD COVER**

RADIOMETRIC IMAGE

Image width compressed by a factor of 2:1

GEOLOGICAL SURVEY MAP

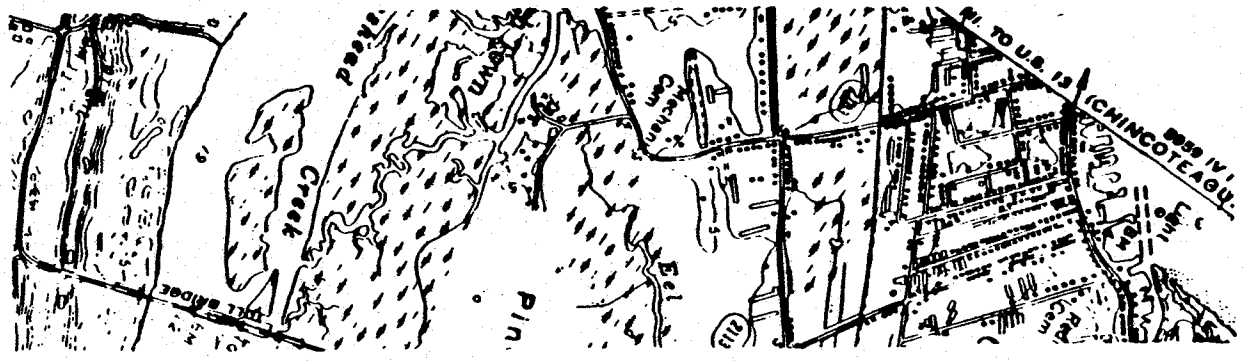

**Flight Altitude - 3000 ft
Clouds Broken - 800 ft - 1100 ft
Clouds Solid - 1100 ft - 2800 ft

*Flight Support: J. T. McGoogan, NASA Wallops
Data Processing and Support Equipment: J.P. Hollinger, NRL
Radiometer: The A

KING, WHITE, WILSON, MORI, HOLLINGER, TROY, KENNEY, AND McGOOGAN

KING, WHITE, WILSON, MORI, HOLLINGER, TROY,
KENNEY, AND McGOOGAN

90 GHz Radiometric Image*

RADIOMETRIC IMAGE

PHOTOGRAPH

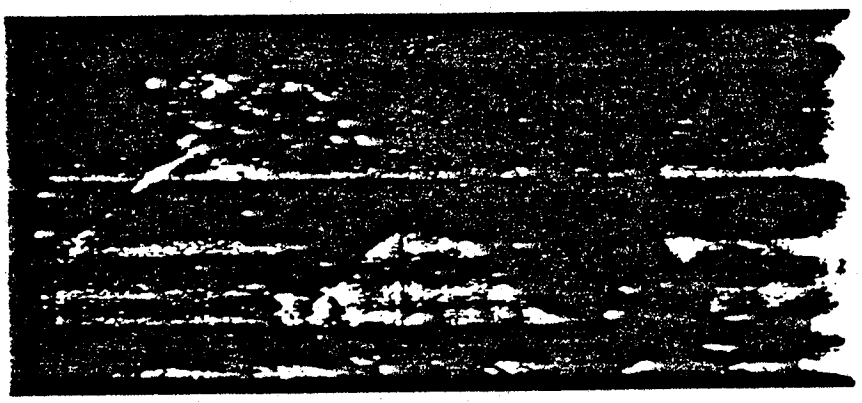

* Flight Support: J.T. McGoogan, NASA Wallops
Data Processing and Support Equipment: J.P. Hollinger, NRL
Radiometer: The Aerospace Corporation, Electronics Research Laboratory

KING, WHITE, WILSON, MORI, HOLLINGER, TROY,
KENNEY, AND McGOOGAN

90 GHz Radiometric Image*
SHIP AND WAKE

RADIOMETRIC IMAGE

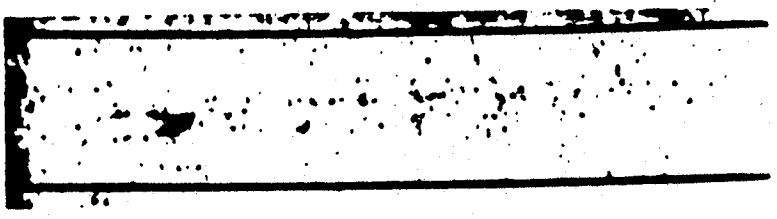

PHOTOGRAPH

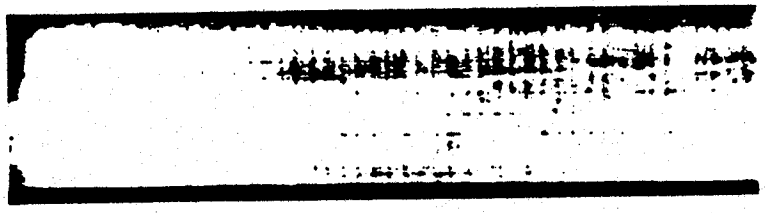

*Flight Support: J.T. McGoogan, NASA Wallops
Data Processing and Support Equipment: J.P. Hollinger, NRL
Radiometer: The Aerospace Corporation, Electronics Research Laboratory

KING, WHITE, WILSON, MORI, HOLLINGER, TROY,
KENNEY, AND McGOOGAN

90 GHz Radiometric Image *

CHINCOTEAGUE ISLAND

RADIOMETRIC IMAGE

PHOTOGRAPH

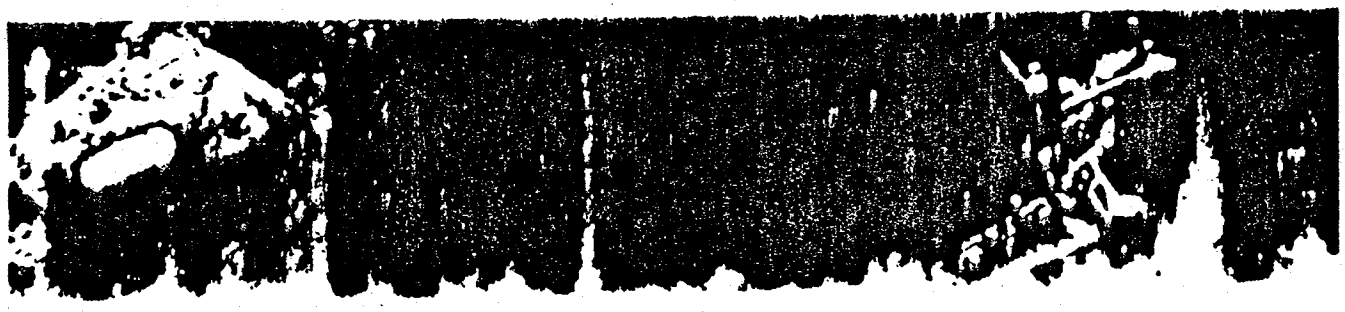

* Flight Support: J.T. McGoogan, NASA Wallops
Data Processing and Support Equipment: J.P. Hollinger, NRL
Radiometer: The Aerospace Corporation, Electronics Research Laboratory

90 GHz Radiometric Image

RUNWAY - NASA-WALLOPS STATION, VA

RADIOMETRIC IMAGE

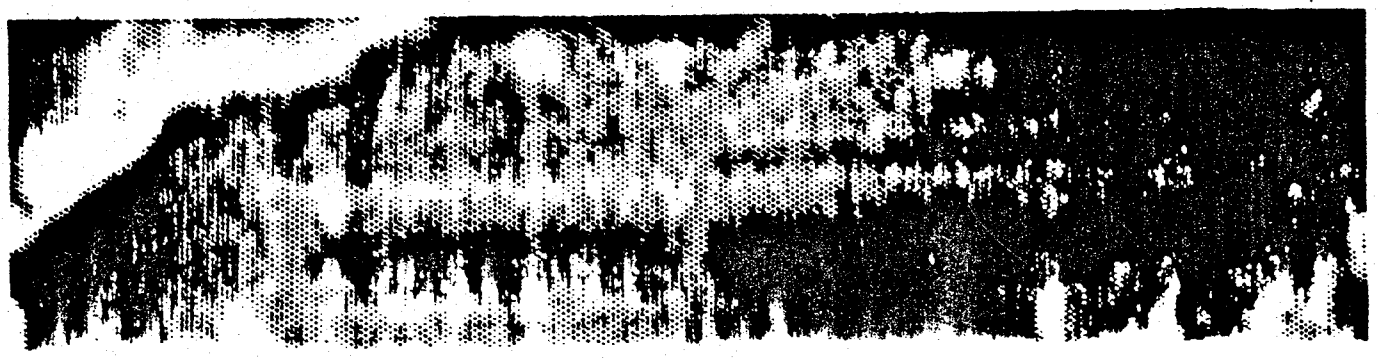

PHOTOGRAPH

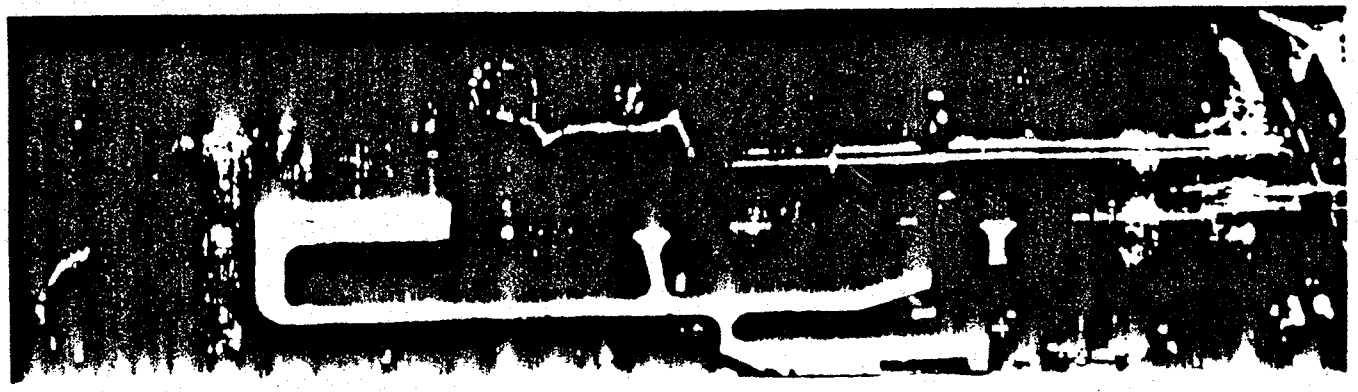

* Flight Support: J. T. McGoogan, NASA Wallops
  Data Processing and Support Equipment: J. P. Hollinger, NRL
  Pulsar ... The Aerospace Corporation, Electronics Research Laboratory

KING, WHITE, WILSON, MORI, HOLLINGER, TROY, KENNEY, AND McGOOGAN

KING, WHITE, WILSON, MORI, HOLLINGER, TROY,
KENNEY, AND McGOOGAN

TEMPERATURE DISTRIBUTION OF VARIOUS TARGETS.

94 GHz

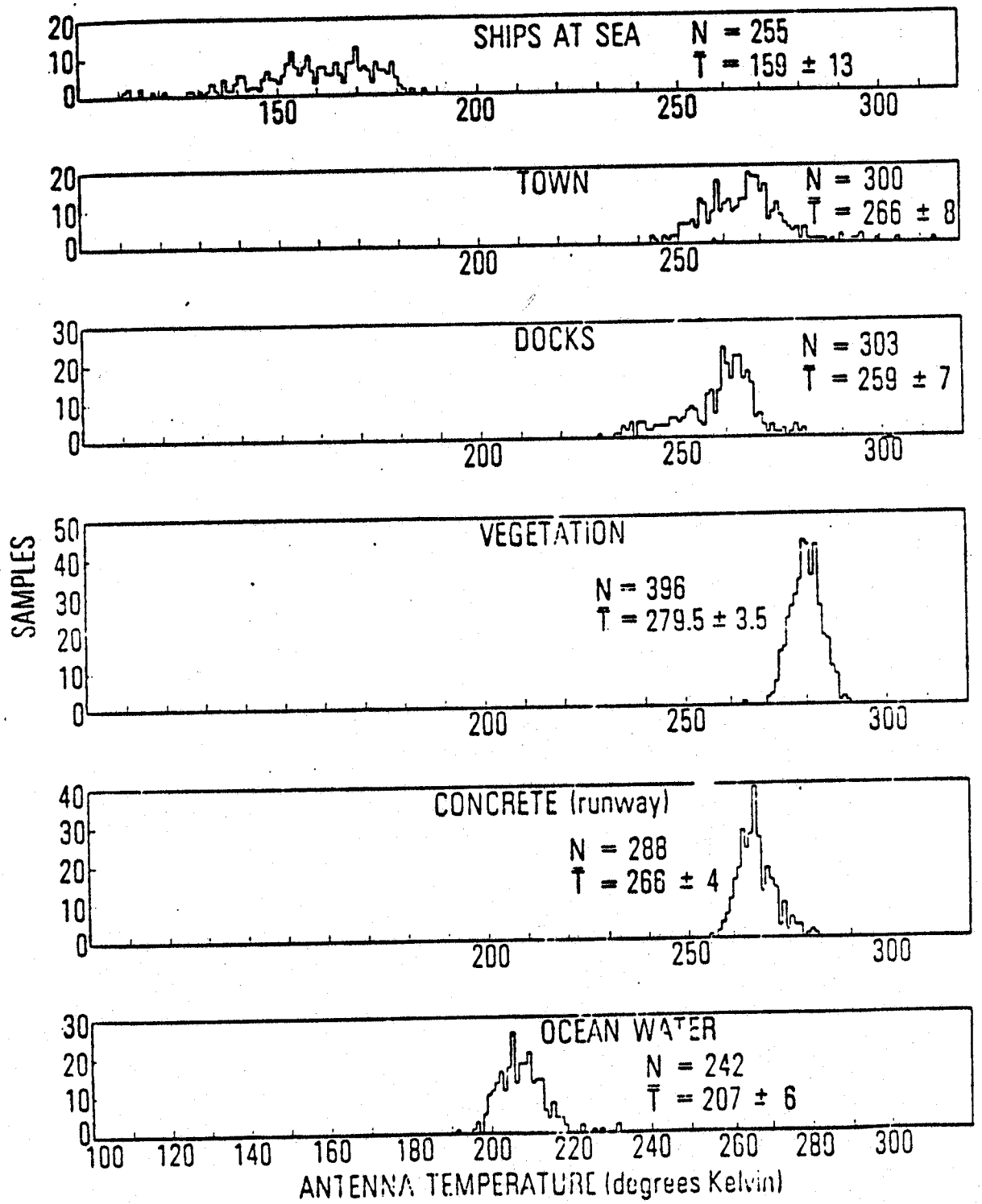

EFFECTS OE SMOKE OBSCURANTS ON MILLIMETER WAVES

J. E. Knox
U.S. Army Armament Research and Development Command
Ballistic Research Laboratory
Aberdeen Proving Ground, MD 21005

Proceedings of the Eighth DARPA/Tri-Service Millimeter Wave Conference
System Planning Corporation (editor), 1500 Wilson Blvd., Arlington, VA 22209,
p. 127-134, April 1979
(A80 00206)

SECRET

In November 1978, BRL measured attenuation through obscurant clouds at 35, 94 and 140 GHz. The obscurants included fog, oil, white and red phosphorus, CS, and some foreign and experimental materials. The sensors used for the attenuation measurements were low-power, pulse radar, range-gated onto a corner cube reflector at a range of 600 meters. The reflected radar power was recorded during each obscurant test.

Dust was found to be the only obscurant to affect transmissivity. The maximum attenuation observed during the tests was 0.4 dB. Therefore it is concluded that none of the obscurants would have adversely affected a system which depended upon a millimeter wave sensor to track a target. (Author)

KNOX

MILLIMETER WAVE PROPAGATION IN SMOKE

Joseph E. Knox
U.S. Army Armament Research and Development Command
Ballistic Research Laboratory
Aberdeen Proving Ground, MD 21005

Electronics and Aerospace Systems Conference (EASCON)
Volume II, Conference Record 79CH1476, Oct. 9-11, 1979
Arlington, VA 22209

The transmission of millimeter waves was measured through clouds of typical battlefield smokes and obscurants at 35, 94, and 140 GHz. Dust dispersed by a high explosive detonation was the only obscurant to affect transmissivity. The smallest transmissivity observed in that case was 91%. It is concluded that none of the materials dispersed would have prevented a millimeter wave sensor from performing its mission. (Author)

EXTRACTS:

Data have been taken by radar with a one-way path length of 800 meters. The author's discussion and data are attached.

DISCUSSION

The test results for the smokes were not unexpected. The sizes of the smoke particles generated during Smoke Week II were 0.5 to 20 microns in diameter, or less than 0.01 times the wavelength. Furthermore, the materials were nonconductive. For these reasons, one would not expect interaction between the radar signals and the smoke.

The radars did see the dust clouds, however. Since range data could not be correlated with radar signal attenuation, we must look to other sources of information for an explanation.

The largest sized particle which could be measured by the range instrumentation was 13 microns. One of the participants was operating a particle counter with a particle size window around 50 microns, and it detected a "significant" number of particles. Calculations show that particles larger than 100 microns could still have been falling through the radar line-of-sight during the time of maximum attenuation, approximately 20 seconds after firing time. It is likely, then, that the attenuation was a result of blockage by larger particles than were sampled by the range instrumentation.

There were no obscurants at Smoke Week II which would have prevented a millimetre wave sensor from operating. There still exists a need to demonstrate the transparency of these obscurants to millimetre waves under other operating conditions, however. For example, phosphorous is anhydrous, and will absorb moisture in amounts which are very sensitive to the relative humidity in the air. It would be worth-while, therefore, to conduct a series of tests under conditions of very high humidity.

BRL plans to continue measuring attenuation through obscurants, especially any which are new or experimental. With this in mind, BRL is presently assembling a set of radars (at 35, 94, and 140 GHz) which will be used solely for propagation measurements, both chamber tests and open air tests.

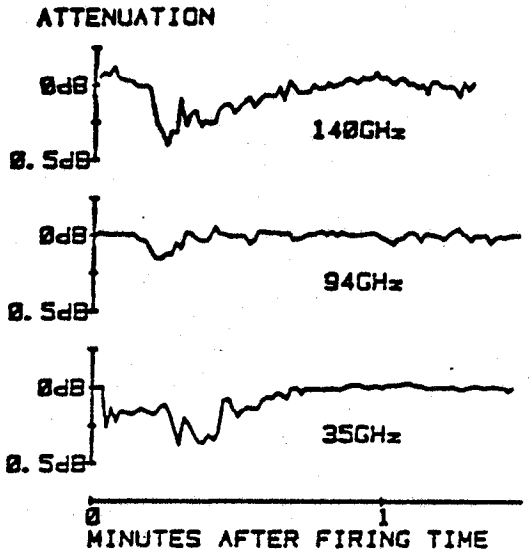

FIGURE 4. ATTENUATION DUE TO H.E. DUST.

Table II. Maximum Attenuation During H.E. Dust Trials.

TRIAL NUMBER	AMOUNT OF H. E.	MAXIMUM ATTENUATION 35 GHz	94 GHz	140 GHz
23	6ea. 5lb. C4	0 dB	0 dB	0 dB
23R	6ea. 5lb. C4	0	0.3	0.2
26	6ea. 15lb. C4	0.3	0.2	0.4
29	6ea. 15lb. C4	0	0	0
30	6ea. 5lb. C4	0.3	0	0.3

H.E. Dust is dust dispersed by detonating high explosives.

KONDRAT'YEV, RABINOVICH, TIMOFEYEV,
AND SHUL'GINA *

MICROWAVE REMOTE ENVIRONMENT SOUNDING

K. Ya. Kondrat'yev, Yu. I. Rabinovich, Yu. M. Timofeyev, and Ye. M. Shul'gina
Main Department of Hydrometeorological Service
USSR Council of Ministers
All-Union Scientific Research Institute of Hydrometeorological Information
World Data Center, Information Center, Obninsk

Prepared at the A. I. Voyeykov Main Geophysical Observatory
NASA TT F-16930, July 1976
N76-27449 (A79 06608)

Microwave remote sounding has two principally important advantages: 1) a multipurpose nature in the sense that the measurement data of outgoing microwave radiation can be used for remote indication of the parameters of the atmosphere, the underlying surface and the upper soil layer (depending on the sounding frequencies selected), and 2) all-weather applications which make it possible, for example, to perform thermal sounding in the atmosphere, regardless of cloud conditions. It is these circumstances that attract great attention to the development and application of microwave remote sounding methods. Despite the great potential of microwave remote sounding, there is no doubt that the further development in the remote indication of environmental parameters will proceed (as is the case at present) along the lines of combining different spectral ranges. Specific capabilities of microwave remote sounding are considered, beginning with an examination of the physical basis of the method. (Authors)

KRITIKOS AND SHIUE*

MICROWAVE SENSING FROM ORBIT

H. N. Kritikos
Moore School of Electrical Engineering
University of Pennsylvania
Philadelphia, PA 19104

J. Shiue
NASA Goddard Space Flight Center
Greenbelt, MD 20771

IEEE Spectrum 17, 34-41, August 1979

Enhanced devices penetrate cloud cover to provide data for weather prediction and terrain analysis. (Authors)

EXTRACTS:

Microwaves can detect soil moisture because the soil dielectric constant changes in the presence of water. Moisture increases the reflection coefficient, causing a decrease in emissivity ($\varepsilon = 1 - R$).

Reflection and emissivity are dependent upon frequency, polarization, angle of incidence, material inhomogeniety, and surface roughness (emissivity is less sensitive to the latter).

A difference in brightness temperature can reach 70 - 80 K between wet soil (emissivity = 0.6 - 0.7) and dry land (emissivity = 0.8 - 0.9), with dry land having a higher brightness temperature than the wet soil.

A sharp contrast in emissivity exists between water (ε = 0.3 - 0.4) which is highly polarized and exhibits a large dielectric constant, and sea ice (ε = 0.8 - 0.9). Water has a lower brightness temperature (lower dielectric constant) than sea ice.

DETERMINATION OF THE CONTRIBUTION OF WATER VAPOR MONOMERS AND DIMERS TO ATMOSPHERIC ABSORPTION FROM MEASUREMENT DATA IN THE 1.15-1.55 mm WAVELENGTH BAND

L. M. Kukin, Yu. N. Nozdrin, V. Ya. Ryadov, L. I. Fedoseyev,
and N. I. Furashov

Radio Engineering and Electronic Physics 20, No. 10, 7-13, October 1975

The components of the water vapor absorption coefficient that are linearly and quadratically dependent on the absolute humidity of the air are determined from measurements of the dependence of the received radiation intensity on humidity. The linear component, together with a certain portion of the quadratic component, takes into consideration the self-broadening of the H_2O monomer lines, and identifies the dimer absorption coefficient. It is noted that experiments lead to values of monomer absorption coefficients that are about 30% larger than those obtained from theoretical calculations, and they give a value for the dimer absorption that is about 2.5 times smaller than that calculated in (1). (Authors)

(1) A. A. Viktotova and S. A. Zhevakin, Dokl. Akad. Nauk SSSR 194, No. 3, 540, 1970.

KULPA AND BROWN

ABSORPTION OF NEAR-MILLIMETER RADIATION BY LIQUID FOGS

S. M. Kulpa and E. A. Brown
U.S. Army Electronics Research and Development Command
Harry Diamond Laboratories
2800 Powder Mill Road
Adelphi, MD 20783

Fourth International Conference on Infrared and Millimeter Waves and Their Applications
IEEE Cat. No. 79 CH 1384-7 MTT, December 10-15, 1979
Post-Deadline Digest Contributions, 30-32

Interest in the near-millimeter wave portion of the spectrum stems principally from the fact that in limited visibility situations such radiation offers a compromise between the high-resolution capabilities of infrared and low-loss propagation characteristics of microwaves. Since fog penetration is a central concern, numerous estimates have been made in attempts to quantify near-millimeter wave attenuation effects in such environments. In this paper we compare various calculations of absorption effects based on limited theoretical and experimental data for the temperature and frequency dependence of the near-millimeter wave dielectric constants of water. (Authors)

The entire article appears in the Appendix.

NEAR-MILLIMETER WAVE TECHNOLOGY BASE STUDY

Stanley M. Kulpa and Edward A. Brown
U.S. Army Electronics Research & Development Command
Harry Diamond Laboratories
2800 Powder Hill Hoad
Adelphi, MD 20783

November 1979
Volume I: Propagation and Target/Background Characteristics
HDL-SR-79-8

This document is a comprehensive summary of the Near-Millimeter Wave (100-1000 GHz) technology base and its potential applications. The state of the art is reviewed, and technology gaps are identified. Volume I contains the analysis of various factors influencing atmospheric propagation and target/background signatures. Comparisons are made between theoretical predictions and limited experimental data in several key areas. Topics discussed include clear air absorption, the effects of atmospheric particulates (rain, fog, clouds, etc.), turbulence, measurement techniques, and the signature characteristics of a variety of targets and backgrounds at near millimeter (NMM) wavelengths. A summary is given of research thrusts which would be useful in establishing a more reliable data base for evaluating near-millimeter wave systems applications. Also included is a list of facilities and organizations actively involved in this technology, plus a comprehensive reference list of current and historical literature pertinent to the material in this volume. (Authors)

EXTRACTS:

Chapter 1:

Gebbie et al. reported horizontal path measurements of absorption which 1) is variable in both strength and spectral distribution; 2) does not appear to depend in any simple way on the standard meteorological variables of temperature or water vapor density; 3) is strongest at high levels of saturation, and appears to be particularly so when liquid water or ice is present along with vapor in or near the absorbing path; 4) for a given amount of water, increases rapidly with decreasing temperature; 5) generally shows greater anomalous absorption than laboratory measurements. Absorption is in the range of 4 - 15 cm^{-1}.

Plambeck's 225-GHz measurements from a 1-km elevation site yield a zenith absorption dependent upon the surface water vapor density, $Q(g/m^3)$:

$$A(dB) = 0.50\ Q,$$ valid for clear sky only.

Wrixon and McMillan have found that the absorption at 230 GHz in clear sky at Holmdel, New Jersey, is

$$A(dB) = 0.35\ Q.$$

Shimabukuro and Epstein measured the zenith opacity at 90 GHz as a function of the surface water vapor density and found

$$A(dB) = 0.17 + 0.06\ Q.$$

Sokolov, Sukhonin, and Ishakov report measured 238-GHz zenith attenuation (dB) in clouds: altocumulus, 0.16; stratus, 0.16; cumulus, 1.75; and cumulus congestus, 8.7.

Detailed studies (vertical polarization) of rain attenuation at 94 GHz on a 1000-m terrestrial path have been made by Keizer, Sneider, and de Haan. Figure I-19 shows the measured attenuation versus rainfall rate for a 1-km path length.

Richard et al. show measured attenuation at 140 GHz (700-m path length) versus rate in Figure I-22.

Chapter 3:

Bauer et al. (BRL Report #538) published a plot of experimental 140-GHz one-way attenuation in fog versus visibility (Figure III-11). BRL has also shown that at 140 GHz no measurable attenuation is observed due to dust caused by vehicular traffic. This dust is sufficient to severely attenuate near-infrared and optical links. Figure III-13 displays experimental 140-GHz rain attenuation versus rain rate.

Attenuation (dB/km)

	100 GHz	140 GHz	220 GHz
Fog (T = 10°C, visibility = 10 m, w = 0.3 g/m^3)	1.4	2.25	3
vehicular dust	negligible	negligible	negligible
rain (10 mm/hr)	8.7	8.7	8.3
snow (10 mm H_2O/hr)			
dry	~4.4	~4.4	~4.1
wet	~8.7	~8.7	~8.3

Table III-5 also presents the attenuation (dB/km) due to liquid water in a radiation fog at 24°C, for wavelengths 1.2, 2.3, and 3.19 mm.

We include here the authors' extensive list of references.

Volume IV contains classified information of interest.

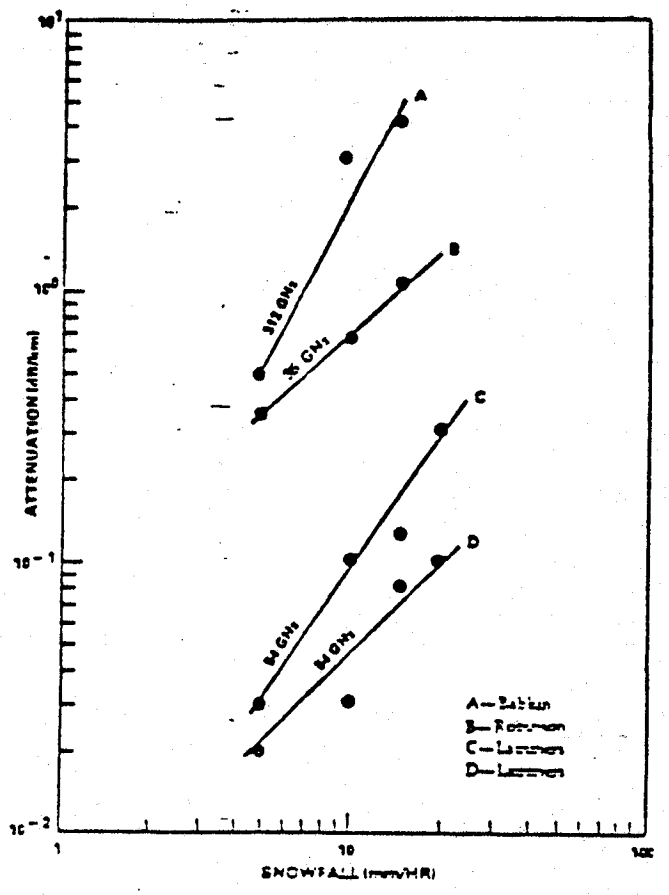

Figure III-15. Measured attenuation in snow versus snowfall rate. V. W. Richard, *TTCP Ad-Hoc Study Group 102 Electro-Optical Low Angle Tracking (December 1976).*

ATTENUATION (dB/km) DUE TO LIQUID WATER

IN A RADIATION FOG AT 24 C

V† (m)	W (g/m³)	Wavelength 1.3 mm	2.3 mm	3.19 mm
1000	0.0032	0.039	0.018	0.011
900	0.0038	0.047	0.022	0.013
800	0.0045	0.055	0.026	0.015
700	0.0056	0.069	0.032	0.020
600	0.0071	0.090	0.040	0.025
500	0.0094	0.120	0.054	0.033
400	0.013	0.160	0.074	0.046
300	0.020	0.246	0.11	0.070
200	0.036	0.467	0.22	0.13
100	0.111	1.36	0.63	0.39
90	0.131	1.61	0.75	0.46
80	0.157	1.93	0.89	0.55
70	0.193	2.37	1.10	0.68
60	0.244	3.00	1.39	0.85
50	0.323	3.97	1.84	1.13
40	0.456	5.61	2.59	1.60
30	0.710	8.73	4.05	2.49

†V is the visibility.

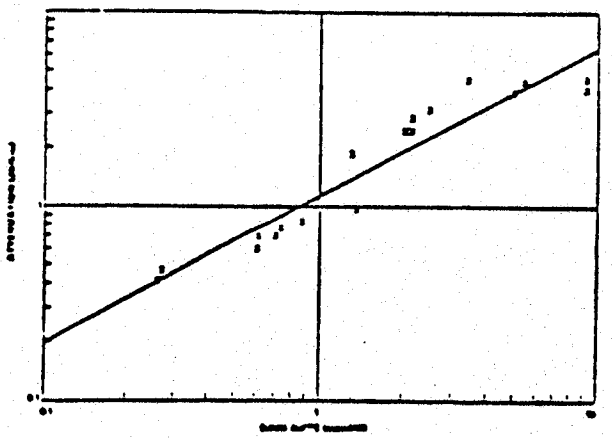

Figure III-13. 140-GHz rain attenuation versus rain rate. D. G. Bauer et al, *Ballistic Research Laboratories, Interim Memorandum Report 538 (January 1977).*

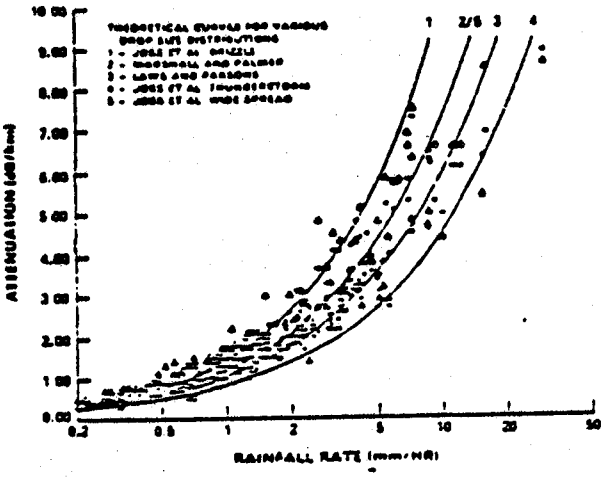

Figure I-19. Measured (Δ) and calculated (+) 94-GHz attenuation versus rainfall rate. *Calculated values derived from measured rain drop size distribution. Path length, 1 km.*

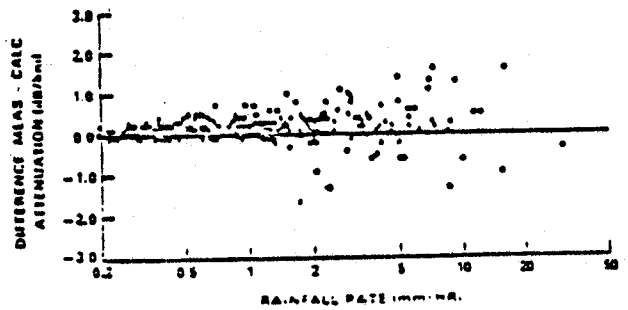

Figure I-20. Difference between measured and calculated rain attenuation at 94 GHz.

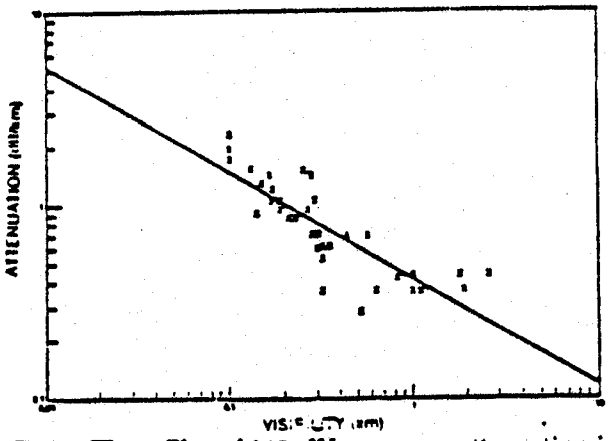

Figure III-11. Plot of 140-GHz one-way attenuation in fog versus visibility. *D. G. Bauer et al. Ballistic Research Laboratories. Interim Memorandum Report 538 (January 1977).*

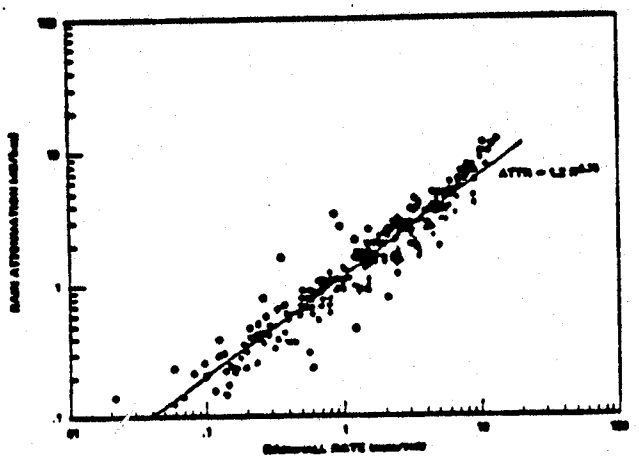

Figure I-22. Measured attenuation at 140-GHz versus rainfall rate.

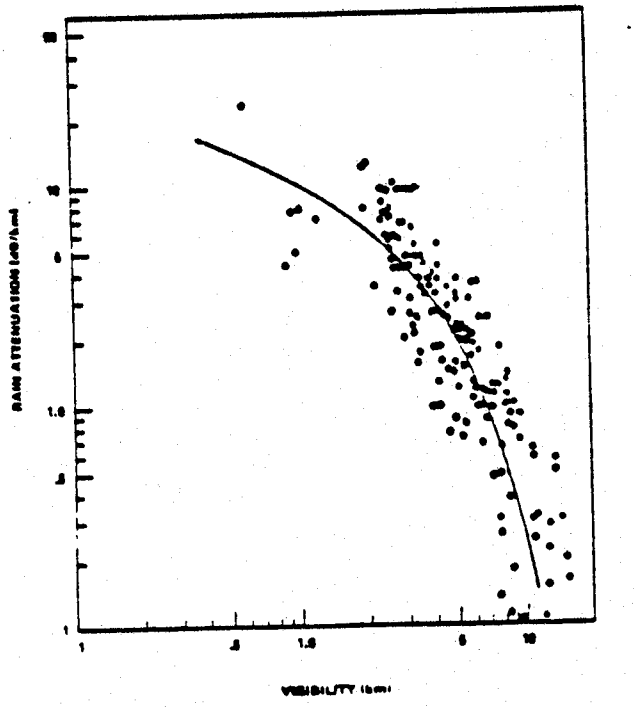

Figure I-23. Measured attenuation at 140 GHz versus visibility.

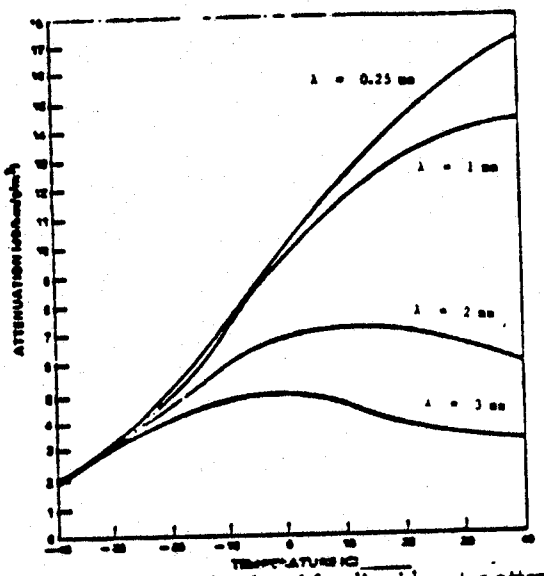

Figure III-19. Plot of cloud and fog liquid water attenuation versus temperature for the indicated wavelength.

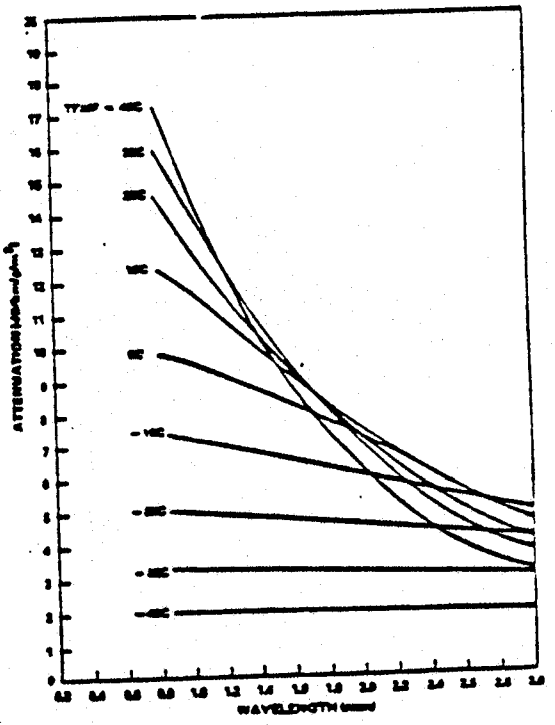

Figure III-20. Plot of cloud and fog liquid water attenuation versus wavelength.

Richard et al[11] have measured rain attenuation at 140 GHz together with rainfall rate and optical visibility. Interestingly, even over their relatively short path length (700 m), the three distributed rain gauges often showed differences of up to four to one. Their attenuation measurements were performed when all three gauges gave close agreement, thus somewhat assuring a uniform rain rate. Figure I-22 shows their measurements correlated with rate. The scatter observed is roughly consistent with values spanning the various types of distributions, as shown in figure I-19. Figure I-23 shows the correlation of the 140-GHz attenuation and rain visibility measurements. The large scatter of the data indicates a weak relationship. As discussed earlier, this stems from the fact that the water droplets as a function of temperature renders data such as that from Diermendjian uncertain by as much as a factor of 2. This is especially true for wavelengths less than 2 mm where both Rozenberg and Ray agree that the imaginary part of the refractive index drops significantly as the temperature drops.

Since fog is by far the most frequent condition causing severely restricted visibility in Europe, it is worthwhile to estimate the total attenuation of NMMW radiation during fog (including absorption due to water vapor and oxygen). Water vapor will be near saturation during fog so that a knowledge of the temperatures at which fogs occur is sufficient for such an estimation. Essenwanger[9] has determined that 80 percent of fogs in Western Europe occur with an absolute humidity less than 7.5 g/m³ and that only 7 percent of such fogs occur when the relative humidity is greater than 9.4 g/m³.

[11] V. W. Richard, J. E. Kammerer, and R. G. Reitz, 140-GHz Attenuation and Optical Visibility Measurements of Fog, Rain, and Snow, U.S. Army Ballistic Research Laboratories Memorandum Report, ARBRL-MR-2800 (December 1977).

[9] O. M. Essenwanger, Estimation of the Temperature During Fog in Europe, Missile Research and Development Command (in press).

III-4. DUST

Naturally occurring dust storms are not a problem in Europe in the sense of causing attenuation of NMMW radiation. According to Hinds and Hordale[17] visibility is reduced to less than a kilometer only once every 10 years. BRL[12] has shown that at 2.1 mm (140 GHz), sufficient dust to severely attenuate near-infrared and optical links caused no measurable attenuation at NMM wavelengths. This dust was generated by vehicular traffic.

[12] D. G. Bauer, R. A. McGee, J. E. Knox, and H. B. Wallace, 140-GHz Brassmidder Feasibility Experiment, Ballistic Research Laboratories, Interim Memorandum Report No. 536 (January 1977).

[17] B. D. Hinds and G. D. Hordale, Boundary Layer Dust: Occurrence IV. Atmospheric Dust Over Selected Geographic Areas, USA Electronics Command ECOM-DR-77-3 (June 1977).

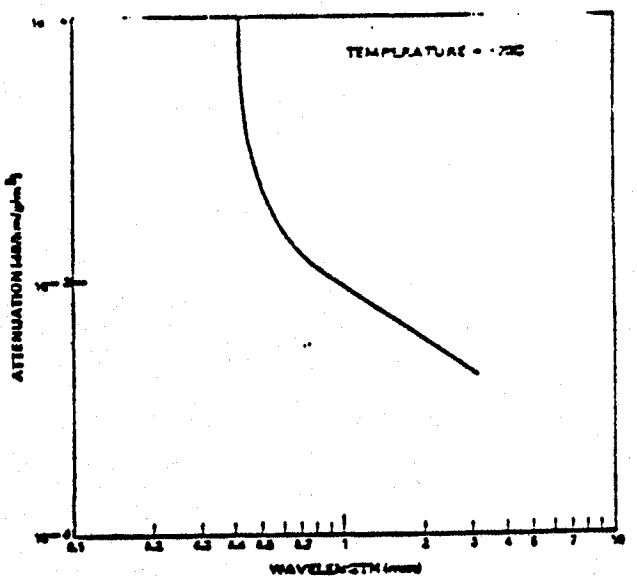

Figure III-21. Plot of ice cloud or ice fog attenuation versus wavelength.

CHAPTER I.—LITERATURE CITED

1. J. W. Waters, Absorption and Emission by Atmospheric Gases, Methods of Experimental Physics, vol. 12, Part B, Ch 2.3, M. L. Meeks, Ed., Academic Press (1976).

   N. E. Gaut and E. C. Reifenstein, III, Environmental Research and Technology Report 13, Lexington, MA (1971).

3. H. R. Carlon, Phase Transition Changes in the Molecular Absorption Coefficient of Water in the Infrared: Evidence for Clusters, Applied Optics, vol. 17, no. 20 (15 October 1978), 3192-3193.

4. H. R. Carlon, Molecular Interpretation of the IR Water Vapour Continuum: Comments, Applied Optics, vol. 17, no. 20 (15 October 1978), 3193-3195.

5. A. Ben-Reuven, Advances in Atomic and Molecular Physics, vol. 5 (1969), 201.

6. D. T. Llewellyn-Jones, R. J. Knight, and H. A. Gebbie, Absorption by Water Vapour at 7.1 cm^{-1} and its Temperature Dependence, Nature, vol. 274 (August 1978), 876-878.

7. E. R. Westwater and D. C. Hogg, Evidence for the Quadratic Dependence on Water Vapor of the Microwave Absorption Coefficient of Moist Air, presented at the URSI-National Radio Science Meeting, Boulder, CO (January 1978).

8. D. C. Hogg, Measurements of 70- and 80-GHz Attenuation by Water Vapor on a Terrestrial Path, presented at the URSI-National Radio Science Meeting, Boulder, CO (January 1978).

9. R. J. Emery, P. Moffat, R. A. Bohlander, and H. A. Gebbie, Measurements of Anomalous Absorption in the Wavenumber Range 4 cm^{-1} – 15 cm^{-1}, Journal of Atmospheric and Terrestrial Physics vol. 37 (1975), 587-594.

10. R. J. Emery, A. Zavody, and H. A. Gebbie, Further Measurements of Anomalous Atmospheric Absorption in the Range 4 cm^{-1} - 15 cm^{-1}, Journal of Atmospheric and Terrestrial Physics (submitted for publication).

11. P. H. Moffat, R. A. Bohlander, W. R. Macrae, and H. A. Gebbie, Atmospheric Absorption between 4 and 30 cm^{-1} Measured Above Mauna Kea, Nature, vol. 269 (October 1977), 676-677.

    R. E. Hills, A. S. Webster, D. A. Alston, P. L. R. Morse, C. C. Zammit, D. H. Martin, D. P. Rice, and E. I. Robson, Absolute Measurements of Atmospheric Emission and Absorption in the Range 100 – 1000 GHz, reported at the Third International Conference on SMM Waves (April 1978); published in Infrared Physics, vol. 18, no. 5/6 (1978), 819-825.

    R. L. Plambeck, Measurements of Atmospheric Attenuation near 225 GHz: Correlation with Surface Water Vapor Density, IEEE Transactions on Antennas and Propagation, vol. AP-26 (September 1978), 737-738.

    G. T. Wrixon and R. W. McMillan, Measurements of Earth-Space Attenuation at 230 GHz, IEEE Transactions on Microwave Theory and Techniques, vol. MTT-26, no. 6 (June 1978), 434-439.

CHAPTER I.—LITERATURE CITED (Cont'd)

F. I. Shimabukuro and E. E. Epstein, Attenuation and Emission of the Atmosphere at 3.3 mm, IEEE Transactions on Antennas and Propagation, vol. AP-18 (1970), 485.

16. A. V. Sokolov, E. V. Sukhonin, and I. A. Iakhakov, Attenuation of Radio Waves at Wavelengths from 0.45 to 4.0 mm in the Earth's Atmosphere through the Slant Paths, presented at the Second International Conference on SMM Waves, San Juan (December 1976).

V. W. Richard, J. E. Kammerer, and R. G. Reitz, 140-GHz Attenuation and Optical Visibility Measurements of Fog, Rain, and Snow, U.S. Army Ballistic Research Laboratories Memorandum Report, ARBRL-MR-2800 (December 1977).

18. N. P. Robinson, Measurements of the Effect of Rain, Snow, and Fogs on 8.6-mm Radar Echoes, Proc. IEE, London, vol. 203B (September 1955), 709-714.

19. L. I. Fidoseev, SMM Atmospheric Research in the USSR, presented at the Third International Conference on SMM Waves, Guildford, England (April 1978).

R. L. Olsen and D. V. Rogers, The aR^b Relation in the Calculation of Rain Attenuation, IEEE Transaction on Antennas and Propagation, vol. AP-26, no. 2 (March 1978), 318-329.

21. D. T. Llewellyn-Jones and A. M. Zavody, Rainfall Attenuation at 110 and 890 GHz, Electronics Letters, vol. 7, no. 12 (1971), 321-322.

22. A. M. Zavody and B. N. Harden, Attenuation/Rain Rate Relationships at 36 and 110 GHz, Electronics Letters, vol. 12 (1976), 422-424.

K. L. Ho, N. D. Mavrokoukoulakis, and R. S. Cole, Rain Induced Attenuation at 36 GHz and 110 GHz, IEEE Transactions on Antennas and Propagation, vol. AP-26 (November 1978), 873-875.

24. W. P. M. N. Keizer, J. Snieder, and C. D. de Haan, Rain Attenuation Measurements at 94 GHz: Comparison of Theory and Experiment, NATO AGARD Conference Proceedings no. 245 (February 1979).

25. M. M. Kharadly, J. D. McNichol, and J. B. Peters, Measurement of Attenuation Due to Rain at 74 GHz, NATO AGARD Conference Proceedings no. 245 (February 1979).

V. W. Richard and J. E. Kammerer, Rain Backscatter Measurements and Theory at Millimeter Wavelengths, U.S. Army Ballistic Research Laboratory Report no. 1838 (October 1975).

27. U. Lammers, Investigations of the Effects of Precipitation on MM-Wave Propagation, Doctoral-Engineering Dissertation, Technik Universitat Berlin, D 83 (1965), Translation by U.S. Army FSTC-HT-23-0298-75, Defense Intelligence Agency Task No. T741301 (1975).

28. K. A. Aganbekyan, V. P. Bisyarin, A. Yu. Zrazhevsky, A. O. Izyumov, A. V. Sokolov, and E. V. Sukhonin, The Propagation of Submillimeter, Infrared, and Visible Waves in the Earth's Atmosphere, Rasprostraneniye Radiovoln, Institut Radiotekhniki i Electroniki, published by Nauka (1975), 187-227.

29. R. L. Fante, Electromagnetic Beam Propagation in a Turbulent Media, Proc. IEEE, vol. 63, no. 12 (1975), 1669-1692.

CHAPTER I.—LITERATURE CITED (Cont'd)

30. J. I. Davis, Consideration of Atmospheric Turbulence in Laser Systems Design, Applied Optics, vol. 5, no. 1 (January 1966), 139-147.

31. R. S. Lawrence, A Review of the Optical Effects of Clear Turbulent Atmosphere, SPIE, vol. 75 (1976), 2-8.

32. H. T. Yura, An Elementary Derivation of Phase Fluctuations of an Optical Wave in the Atmosphere, SPIE, vol. 75 (1976), 9-15.

33. V. I. Tatarski, Wave Propagation in a Turbulent Medium (Translated from the Russian by R. A. Silverman), McGraw-Hill Book Co., Inc., New York (1961).

34. R. S. Lawrence and J. W. Strohbehn, A Survey of Clear-Air Propagation Effects Relevant to Optical Communications, Proceedings of IEEE, vol. 58, no. 10 (October 1970), 1523-1545.

35. F. F. Hall, Jr., Index of Refraction Structure Parameter in the Real Atmosphere—An Overview, OSA Topical Meeting on Propagation through Turbulence, Rain and Fog, Paper TuC1 (9 to 11 August 1977).

36. J. J. Gallagher et al, Application of Submillimeter Wave Gigawatt Sources, Georgia Institute of Technology, Final Report GT/EES, Project No. A-1717 (1975).

37. W. D. Brown, A Model for the Refractive Index Structure Constant at Microwave Frequencies, Sandia Laboratories Report SAND 76-0593 (February 1977).

38. N. A. Armand, A. O. Izyumov, and A. V. Sokolov, Fluctuations of Submillimeter Waves in a Turbulent Atmosphere, Radic Engineering and Electronic Physics, vol. 14, no. 10 (1971), 1259-1266.

39. M. D. Kanevskii, The Problem of the Influence of Absorption on Amplitude Fluctuations of Submillimeter Radio Waves in the Atmosphere, Izvestiya Vysshikh Uchebnykh Zav. Radiofizika, vol. 15, no. 12 (December 1972), 1939-1940.

40. K. L. Ho, N. D. Mavrokoukoulakis, and R. S. Cole, Wavelength Dependence of Scintillation Fading at 110 and 36 GHz, Electronics Letters, vol. 13, no. 7 (31 March 1977), 181-183.

K. L. Ho, R. S. Cole, and N. D. Mavrokoukoulakis, The Effect of Wind Velocity on the Amplitude Scintillations of Millimetre Radio Waves, Journal of Atmospheric and Terrestrial Physics, vol. 40 (1978), 443-448.

42. R. S. Cole, K. L. Ho, and N. D. Mavrokoukoulakis, The Effect of the Outer Scale Turbulence and Wavelength on Scintillation Fading at Millimeter Wavelengths, IEEE Transactions on Antennas and Propagation, vol. AP-26 (September 1978), 712-715.

43. K. L. Ho, N. D. Mavrokoukoulakis, and R. S. Cole, Determination of the Atmospheric Refractive Index Structure Parameter from Refractivity Measurements and Amplitude Scintillation Measurements at 36 GHz, Journal of Atmospheric and Terrestrial Physics, vol. 40 (1978), 745-747.

44. N. D. Mavrokoukoulakis, K. L. Ho, and R. S. Cole, Temporal Spectra of Atmospheric Amplitude Scintillations at 110 GHz and 36 GHz, IEEE Transactions on Antennas and Propagation, vol. AP-26 (November 1978), 875-877.

CHAPTER I.—LITERATURE CITED (Cont'd)

45. D. T. Gjessing, A. G. Kjelaas, and E. Golton, Small Scale Atmospheric Structure Deduced from Measurements of Temperature, Humidity, and Refractive Index, Boundary-Layer Meterol (1972), 475.

46. D. E. Snider, J. C. Wiltse, and R. W. McMillan, The Effects of Atmospheric Turbulence and Adverse Weather on Near Ground 94- and 140-GHz Systems, MIRADCOM Workshop on Millimeter and Submillimeter Atmospheric Propagation Applicable to Radar and Missile Systems (March 1979).

47. A. Ishimaru, Temporal Frequency Spectra of Multi-Frequency Waves in a Turbulent Atmosphere, IEEE Transactions on Antennas and Propagation, vol. AP-20 (1972), 10-19.

48. D. P. Haworth, N. J. McEwan, and P. A. Watson, Effect of Rain in the Near Field of an Antenna, Electronics Letters, vol. 14, no. 4 (16 February 1978), 94-96.

49. vW. Wiesbeck, Regenechos bei Nahbereichsimpulsradaranlagen, A.E.U. band 30, heft II, (1976), 429.

CHAPTER II.—LITERATURE CITED

(1) R. A. McClatchey, W. S. Benedict, S. A. Clough, D. E. Burch, R. F. Calfee, K. Fox, L. A. Rothman, and J. S. Garing, AFCRL Atmospheric Absorption Line Parameters Compilation, Air Force Geophysical Laboratories AFCRL-TR-73-0096 (January 1973).

(2) D. E. Burch, Absorption of Infrared Radiant Energy by CO_2 and H_2O. III. Absorption by H_2O between 0.5 and 36 cm^{-1} (278 μm to 2 cm), Journal of the Optical Society of America, vol. 58 (1968), 1383-1394.

(3) S. L. Valley, Handbook of Geophysics and Space Environments, Air Force Cambridge Research Laboratory (AFCRL) (1965).

(4) R. A. McClatchey, R. W. Fenn, J. E. A. Selby, F. E. Volz, and J. S. Garing, Optical Properties of the Atmosphere (Revised), AFCRL-71-0279, Environmental Research Papers, No. 354 (10 May 1971).

(5) N. Sissenwine, D. D. Grantham, and H. A. Salemla, Humidity Up to the Mesopause, AFCRL-68-0550 (1968).

(6) Ya. V. Ryadov and N. I. Furashov, Investigation of the Spectrum of Radiowave Absorption by Atmospheric Water Vapor in the 1.15 to 1.5-mm Range, Radio Physics and Quantum Electronics, vol. 15, no. 10 (October 1974), 1124-1128.

(7) L. Frenkel and D. Woods, The Microwave Absorption by H_2O Vapor and Its Mixtures with Other Gases Between 100 and 300 GHz, Proceedings of the IEEE, vol. 54 (1966), 498-505.

(8) A. W. Straiton and C. W. Tolbert, Anomalies in the Absorption of Radio Waves by Atmospheric Gases, Proceedings of the IRE, vol. 48 (1960), 898.

CHAPTER II.—LITERATURE CITED (Cont'd)

(9) Yu. A. Dryagin, A. G. Kislyakov, L. M. Kukin, A. I. Naumov, and L. I. Fedoseyev, Measurements of Atmospheric Absorption of Radiowaves in 1.36- to 3.0-mm Range, Izvestiya VUZ Radiophysica, vol. 9, no. 6 (1966), 624-627.

(10) B. D. Guenther, J. S. Bennett, W. L. Gamble, and R. L. Hartman, Submillimeter Research: A Propagation Bibliography, U.S. Army Missile Command, Technical Report RR-77-3 (November 1976).

(11) D. E. Burch, Semi-Annual Technical Report: Investigation of the Absorption of Infrared Radiation by Atmospheric Gases, Contract No. F19628-69-C-0263, Aeronutronic-Ford Publication U-4784 (January 1970).

(12) R. E. Roberts, J. E. Selby, and L. M. Biberman, Infrared Continuum Absorption by Atmospheric Water Vapor in 8-12-μm Window, Applied Optics, vol 15, no. 9 (September 1976), 2085-2090.

(13) R. W. Watkins and K. O. White, Water-Vapor-Continuum Absorption Measurements (3.5-4.0-μm) Using HDO-Depleted Water, Optics Letters, vol. 1, no. 1 (July 1977). 31-32.

(14) D. E. Burch, D. A. Gryvnak, and G. H. Piper, Infrared Absorption by H_2O and N_2O, AFCRL-TR-73-0530 (July 1973).

R. W. McMillan, J. J. Gallagher, and A. M. Cook, Calculations of Antenna Temperature, Horizontal Path Attenuation, and Zenith Attenuation Due to Water Vapor in the Frequency Band 150-700 GHz, IEEE Trans. Microwave Theory and Techniques, vol. MTT-25, no. 6 (June 1977), 484-488.

(16) R. J. Emery, P. Moffat, R. A. Bohlander, and H. A. Gebbie, Measurements of Anomalous Atmospheric Absorption in the Wavenumber Range 4 cm^{-1} - 15 cm^{-1}, Journal of Atmospheric and Terrestrial Physics, vol. 37 (1975), 587-594.

(17) D. E. Burch, D. A. Gryvnak, R. R. Patty, and C. E. Bartky, Absorption of Infrared Radiant Energy by CO_2 and H_2O. IV. Shapes of Collision-Broadened CO_2 Lines, Journal of the Optical Society of America, vol. 59, (1969), 267-280.

(18) H. J. Liebe and T. A. Dillon, Journal of Chemical Physics, Accurate Foreign-Gas-Broadening Parameters of the 22-GHz H_2O Line from Refraction Spectroscopy, vol. 50 (1969), 727-732.

CHAPTER III.—LITERATURE CITED

1. J. A. Stratton, Electromagnetic Theory, McGraw-Hill Book Company, New York (1941), 554-573.

2. H. C. Van de Hulst, Light Scattering by Small Particles, John Wiley and Sons, New York (1957).

3. D. E. Kerr, ed., Propagation of Short Radio Waves, McGraw-Hill Book Company, New York, Ch 7-8 (1951).

4. D. Diermendjian, Far Infrared and Submillimeter Wave Attenuation by Clouds and Rain, Rand Corporation Report AD-A021-947 (April 1975).

5. V. L. Rozenberg, Scattering and Attenuation of Electromagnetic Radiation by Atmospheric Particles, Hydrometeorological Press, Leningrad, USSR (1972).

6. G. D. Lukes, Penetrability of Haze, Fog, Clouds, and Precipitation by Radiant Energy over the Spectral Range 0.1 Micron to 10 Centimeters, The Center for Naval Analyses of the University of Rochester, Report No. 61 (May 1968).

7. P. S. Ray, Broadband Complex Refractive Indices of Ice and Water, Applied Optics, vol. 11 (1972), 1839.

8. M. Davies, G. W. F. Pardoe, J. Chamberlain, and H. A. Gebbie, Submillimeter- and Millimeter-wave Absorption of Some Polar and Non-polar Liquids Measured by Fourier Transform Spectroscopy, Transactions of the Faraday Society, vol. 66 (1970), 273.

9. B. J. Mason, Cloud Physics, 2nd edition, Claredon Press (1971).

10. W. E. K. Middleton, Vision Through the Atmosphere, University of Toronto Press (1963).

11. R. G. Eldridge, Haze and Fog Aerosol Distributions, Journal of Atmospheric Science, vol. 23 (1966), 608.

12. O. Essenwanger, On the Duration of Widespread Fog and Low Ceiling in Central Europe and Some Aspects of Predictability, Missile Research and Development Command TR-RR-73-9 (1 August 1973).

13. D. G. Bauer, R. A. McGee, J. E. Know, and H. B. Wallace, 140-GHz Beamrider Feasibility Experiment, Ballistic Research Laboratories, Interim Memorandum Report No. 538 (January 1977).

14. A. V. Sokolov and Ye. V. Sukhonin, Attenuation of Submillimeter Radio Waves in Rain, Radio Engineering and Electronic Physics, vol. 15, no. 12 (1970), 2167.

15. V. W. Richard, Low Angle Tracking at Millimeter Wavelengths, TTCP Ad-Hoc Study Group 102, Electro-Optical Low Angle Tracking (December 1976).

16. V. W. Richard, Millimeter Wave Radar Applications to Weapon Systems, Memorandum Report No. 2631, Ballistic Research Laboratories (June 1976).

17. B. D. Hinds and G. D. Hordale, Boundary Layer Dust Occurrence IV, Atmospheric Dust Over Selected Geographic Areas, USA Electronics Command, ECOM-DR-77-3 (June 1977).

18. E. Bauer, The Scattering of Infrared Radiation from Clouds, Applied Optics, vol. 3 (1964), 197.

19. L. W. Carrier, G. A. Cato and K. J. von Essen, The Backscattering and Extinction of Visible and Infrared Radiation by Selected Major Cloud Models, Applied Optics, vol. 6 (1967), 1209-1216.

CHAPTER VI.—LITERATURE CITED

1. J. R. Maxwell, Environmental Research Institute of Michigan, ERIM 123800-2-L (18 November 1976). (CONFIDENTIAL)

2. M. W. Long, Radar Reflectivity of Land and Sea, Lexington Books, Lexington, MA (1975).

3. S. L. Johnston, Submillimeter Wave Radar Technology (U), 22nd Annual Tri-Service Radar Symposium, Colorado Springs, CO (6-8 July 1976). (CONFIDENTIAL)

4. M. E. Beebe, J. Salzman, et al. 94 GHz Sensor Tower Test Program: Final Report, No. MSG 65075, Missile Systems Group, Hughes Aircraft Company (February 1976).

K. A. Richer, D. G. Bauerle, and J. E. Knox, 94 GHz Radar Cross Section of Vehicles (U), Ballistic Research Laboratories BRL-MR-2491 (June 1975), AD C002 505L. (CONFIDENTIAL)

6. B. D. Guenther, Submillimeter Wave Research: Index of 3.2 mm and 10.6 μm Image Data Tapes, U.S. Army Missile Research and Development Command TR-77-2 (1 February 1977).

7. J. M. Bair, Millimeter and Infrared Image Scans of Reentry Vehicle Targets, Technical Report Calspan 23963, Hughes Research Laboratories (September 1976).

8. P. S. Ray, Applied Optics, vol. 11, no. 8 (August 1972), 1836-1844.

9. Manual of Remote Sensing, vol. I, American Society of Photogrammetry (1975).

H. E. King and C. J. Zamites, Terrain Backscatter Measurements at 40 to 90 GHz, Aerospace Corporation, SAMSO-TR-70-220 and TR-0066 (5816-41)-1 (June 1970).

11. L. D. Strom, Application for Millimeter Radars (U), Report No. 108, System Planning Corporation (December 1973), AD 529 566. (CONFIDENTIAL)

J. E. Kammerer and K. A. Richer, Cross Section Measurements of U.S. Army Targets by 140 GHz Radar (U), Ballistic Research Laboratories BRL-MR-1785 (August 1966), AD 378 097. (CONFIDENTIAL)

13. W. H. Peake and T. L. Oliver, The Response of Terrestrial Surfaces at Microwave Frequencies, Ohio State University AFAL-TR-70-301 and ESL-2440-7 (May 1971), AD 884 106.

14. L. Chanzit, L. Kosowsky, K. Koester, and I. Goldmacher, Study of Airborne Millimeter Radar Techniques, United Aircraft Corporation ECOM-02125-F (June 1970), AD 373 641.

15. L. J. Greenstein et al. A Comprehensive Ground Clutter Model for Airborne Radars, IIT Research Institute, Chicago, IL (September 1969), AD 861 913L.

16. F. Nathanson, Radar Design Principles, McGraw-Hill, New York (1969), 264.

CHAPTER VI.—LITERATURE CITED (Cont'd)

17. N. C. Currie et al, Radar Land Clutter Measurement at Frequencies of 9.5, 16, 35, and 94 GHz, Georgia Institute of Technology (April 1975).

18. M. E. Beebe et al, 94 GHz Sensor Tower Test Program, Hughes Report No. MSG 65075R (February 1976).

19. Manual of Remote Sensing, vol. II, American Society of Photogrammetry (1975).

20. R. L. Cosgriff et al, Terrain Scattering Properties for Sensor System Design, Engineering Experiment Station Bulletin, Ohio State University, Columbus, OH (May 1960).

21. K. A. Richer, 4.4 mm Wavelength Near Earth Propagation Measurements, Ballistic Research Laboratories BRL-MR-1403 (May 1962), AD 331 098.

22. B. J. Starkey, Bi-Static Ground Scatter Measurements in X-Band and the Ground Scatter Jammer Parameters (U), Directorate of Electronic Warfare S957-104-3 (DEW), Air Force Headquarters, Ottawa, Canada (September 1963). (SECRET)

23. S. T. Cost, Measurements of the Bistatic Echo Area of Terrain at X-Band, Ohio State University Report No. 1822-2 (May 1965).

24. J. A. Rupke and G. S. Rasswelier, Investigation of Ground Illumination at Radar Frequencies (U), AFAL-TR-65-204 and 6148-17-F, The University of Michigan, Willow Run Laboratories (September 1965), AD 366 232. (SECRET)

25. R. W. Larson et al, Measurements of Bistatic Scattering Coefficients Using Air-Ground Coherent Instrumentation, Environmental Research Institute of Michigan Report 118200-14-F (April 1977).

26. R. A. McGee, Millimeter Wave Radiometric Detection of Targets Obscured by Foliage, Ballistic Research Laboratories BRL-MR-1901 (January 1968), AD 667 962.

27. J. R. Houck et al, The Far Infrared and Submillimeter Background, Cornell University (1 September 1972), AD 763 139.

28. J. A. Stratton, Electromagnetic Theory, McGraw-Hill Book Company (1941).

29. M. D. Blue and S. Perkowitz, Reflectivity of Common Materials in the Submillimeter Region, IEEE Trans. on Microwave Theory and Tech., vol. MTT-25 (1977), 491-493.

30. S. Perkowitz and B. L. Bean, Far Infrared Absorption of Chlorophyll in Solution, Journal of Chemical Physics, vol. 66 (1977), 2231-2232.

31. K. D. Möller and W. G. Rothchild, Far-Infrared Spectroscopy, Wiley-Interscience (1971).

32. W. Wolfe (ed.), Handbook of Military Infrared Technology, Office of Naval Research (1965), 797.

33. Charles Kittel, Introduction to Solid State Physics, John Wiley and Sons (1956).

CHAPTER VII.— LITERATURE CITED

1. A. B. Crawford and D. C. Hogg, Measurement of Atmospheric Attenuation at Millimeter Wavelengths, Bell System Technical Journal, vol. 35 (July 1956), 907-16.

2. D. E. Burch, Absorption of Infrared Radiant Energy CO_2 and H_2O. III. Absorption between 0.5 and 36 cm^{-1} (278 μm - 2 cm), Journal of the Optical Society of America, vol. 58, 10 (1968), 1383-1394.

3. D. C. Hogg and T. S. Chu, The Role of Rain in Satellite Communications, IEEE Proceedings, vol. 63, 9 (September 1975), 1308-1331.

4. M. T. Decker, E. R.Westwater, and F. O. Guiraud, Microwave Sensing of Atmospheric Temperature and Water, Navy Workshop on Remote Sensing of the Marine Boundary Layer, Vail, CO (9-11 August 1976).

5. B. J. Mason, The Physics of Clouds, Clarendon Press, Oxford (1957).

6. P. Spyers-Duran, Measuring the Size, Concentration, and Structural Properties of Hydrometeors in Clouds with Impactor and Replicating Devices, Atmospheric Technology 8, NCAR (1976), 3-9.

7. R. G. Knollenberg, The Optical Array: An Alternative to Scattering or Extinction for Airborne Particle Size Determination, Journal of Applied Meteorology, vol. 9 (1970), 86-103.

8. C. B. Neel, A Heated-Wire Liquid-Water Content Instrument and Results of Initial Flight Tests In Icing Conditions, NASA Research Memorandum RM 454123 (1955).

9. A. Wexler and R. E. Ruskin, Humidity and Moisture, vol. I, Principles and Methods of Measuring Humidity in Gases, Reinhold Publishing Corporation, New York (1965).

10. R. E. Ruskin, Liquid Water Content Devices, Atmospheric Technology, 8 (1976), 38-42.

11. E. A. Mueller and A. L. Sims, The Influence of Sampling Volume on Raindrop-Size Spectra, Proceedings of the 12th Conference on Radar Meteorology (October 1966), 135.

12. Ting-i Wang and S. F. Clifford, Use of Rainfall-Induced Optical Scintillations to Measure Path-Averaged Rain Parameters, Journal of the Optical Society of America, vol. 65, 8 (August 1975), 927-37.

13. D. H. Ring, Bell Telephone Laboratories, Final Report AF-19-(122)-458 to Lincoln Laboratories (released 1962).

14. H. J. Liebe, Studies of Oxygen and Water Vapor Microwave Spectra under Simulated Atmospheric Conditions, Office of Telecommunications Report OT 75-65 (June 1975); available from U.S. Government Printing Office, Washington, DC 20402.

CHAPTER VIII.—LITERATURE CITED

1. Summary Technical Report of Division 14—National Defense Research Committee. Volume 1—Radar, Washington, DC (1946).

2. H. E. Guerlac, Radar in World War II, available from Library of Congress Photoduplication Service, PB 93618 through PB 93621 (May 1947).

3. J. W. Waters, Absorption and Emission by Atmospheric Gases, Methods of Experimental Physics, Vol. 12, Part B, Chapter 2.3, Academic Press (1976).

4. D. T. Llewellyn-Jones et al, Absorption by Water Vapour at 7.1 cm^{-1} and its Temperature Dependence, Nature, Vol. 274 (August 1978), 876-878.

5. R. J. Emery et al, Measurements of Anomalous Absorption in the Wave Number Range 4 cm^{-1} - 15 cm^{-1}, Journal of Atmospheric and Terrestrial Physics, Vol. 37 (1975), 587-594.

6. V. I. Rozenberg, Scattering and Attenuation of Electromagnetic Radiation by Atmospheric Particles, Hydrometeorological Press, Leningrad, USSR (1972).

7. M. N. Afsar and J. B. Hasted, Submillimeter Wave Measurements of Optical Constants of Water at Various Temperatures, Infrared Physics, Vol. 18 (1978), 835-841.

8. J. Sander, Rain Attenuation of Millimeter Waves at λ = 5.77, 3.3, and 2 mm, IEEE Transactions on Antennas and Propagation, Vol. AP-23, No. 2 (March 1975), 213-220.

9. V. W. Richard, J. E. Kammerer, and R. G. Reitz, 140 GHz Attenuation and Optical Visibility Measurements of Fog, Rain, and Snow, U.S. Army Ballistic Research Laboratories Memorandum Report ARBRL-MR-2800 (December 1977).

10. D. T. Llewellyn-Jones and A. M. Zavody, Rainfall Attenuation at 110 and 890 GHz, Electronics Letters, Vol. 7, No. 12 (1971), 321-322.

11. W. P. M. N. Keizer, J. Shields, and C. D. de Haan, Rain Attenuation Measurements at 94 GHz: Comparison of Theory and Experiment, NATO AGARD Conference Proceedings No. 245 (February 1979).

A mm-WAVE SCANNING RADIOMETER FOR TERRAIN MAPPING

K. Kunzi, M. Wuthrich, and E. Schanda
Institute for Applied Physics
University of Berne
3000 Berne, Switzerland

Seventh International Symposium on the Remote Sensing of the Environment
J. J. Cook, et al. (editors), Environmental Research Institute of Michigan,
Center for Remote Sensing, University of Michigan, Ann Arbor, MI 48104,
1971

A narrow-beam, microwave radiometer working at 94 GHz with a real-time TV display for terrain mapping is described. The research areas for this instrument are mentioned. Further, a survey of the mathematical analysis of the blurring of contours or measured objects through the antenna pattern and the output integration are given. This effect is demonstrated by scanning a point source. (Authors)

LAWRENCE, CLIFFORD, AND OCHS*

THE DISTRIBUTION OF TURBULENT FLUCTUATIONS OF REFRACTIVE INDEX IN THE ATMOSPHERE

R. S. Lawrence, S. F. Clifford and G. R. Ochs
NOAA Research Laboratories
Boulder, CO 80302

The turbulent fluctuations of temperature that are responsible for scintillation and image distortion of light waves and for most of the troposheric forward scatter and scintillation of radio waves occur irregularly throughout the atmosphere. The refractive-index structure parameter C_n^2 is distributed irregularly in space so that a given volume often contains one hundred times the magnitude of an adjacent volume the same size. Measurements made with high-speed temperature probes reveal a number of interesting features of the distribution of C_n^2, and some of these will be discussed. However, an understanding of the climatology of refractive-index fluctuations will require continuous measurements from ground-based sensors. We describe a technique, already in use, for using scintillations of starlight to measure the smoothed vertical profile of C_n^2 throughout the atmosphere. We are presently developing methods for profiling C_n^2 along ground-to-ground line-of-sight paths. (Authors)

ANALYSIS OF 1.4 GHz RADIOMETRIC MEASUREMENTS FROM SKYLAB

Robert M. Lerner and James P. Hollinger
Advanced Spaced Sensing Applications Branch
Space Science Division
Naval Research Laboratory
Washington, DC 20375

Remote Sensing of the Environment 6, 251-269, 1977

Results from the 1.4 GHz, S-194, microwave radiometer located on the SKYLAB satellite are presented. The objective of the investigation is to establish the degree to which quantitative measurements of sea surface temperature, salinity and related marine wind fields can be made using the S-194 radiometer. The analysis of the S-194 data demonstrates that it is possible to make measurements of the brightness temperature of open ocean areas with an RMS absolute accuracy of 1.3 K over a wide range of environmental conditions. The S-194 is relatively insensitive to sea surface temperature changes and, even though measurements are available over a range in sea surface temperature of 30°C, no significant change in the measured antenna temperature was detected. However, S-194 is relatively sensitive to changes in surface salinity and the analysis of data taken over the open ocean shows that salinity can be determined to an accuracy of 2 parts per thousand. Further, it is shown that it is possible to accurately model complex regions such as lakes and bays, where a significant portion of the antenna beam is filled by land, and obtain excellent agreement between calculated and measured antenna temperatures. Open ocean measurements, obtained over the wide range in winds speeds of 0 to 48 knots, show the antenna temperature to be weakly, but unambiguously, correlated to the wind speed. The wind speed dependence determined, of 0.16°K/knot, indicates that surface wind speed can be measured to an accuracy of 8 knots using the S-194. (Authors)

LIEBE

MILLIMETER WAVE ATTENUATION IN MOIST AIR--A REVIEW

H. J. Liebe
National Telecommunications and Information Administration
Institute for Telecommunication Sciences
Boulder, CO 80303

Proceedings of the Workshop on Millimeter and Submillimeter Atmospheric Propagation Applicable to Radar and Missile Systems, Redstone Arsenal, AL 38509, O. M. Essenwanger and D. A. Stewart (editors)
Technical Report RR-80-3, 118-128, February 1980

Considerable attention is currently being given to EHF (30-300 GHz) systems, in part due to their ability to penetrate most adverse atmospheric conditions (dust, smoke, clouds, fog, light rain). To assess the "all-weather" capabilities of such systems requires accurate predictions of the propagation effects under varying conditions of weather, height, location, etc. This complex task involves molecular absorption from oxygen, water vapor, and several trace gases (O_3, CO, etc.) and absorption and scattering loss from particulates. Most applications will operate in the four spectral windows of the EHF region. Observations in clear air by laboratory and field experiments have found in these windows the existence of anomalous water vapor absorption (AWA). Anomalous implies that no reliable model exists to predict the effects of AWA. In particular, it was found that AWA increases in a complicated manner with humidity.

This paper reviews the AWA problem before the background of the known molecular absorption characteristics and discusses possibilities to gain a better understanding of the underlying physical phenomena. (Author)

EXTRACTS:

We include the author's list of references and several graphs of attenuation versus water vapor.

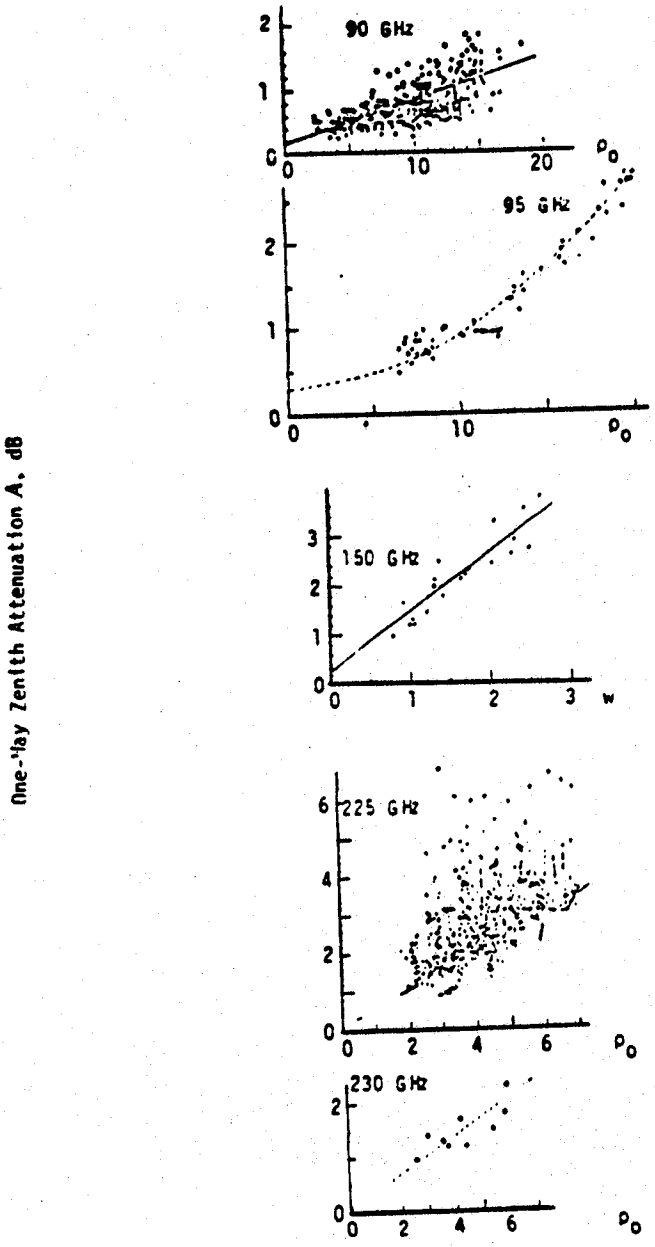

Reported zenith attenuation in clear air as a function of water vapor density at 90 GHz[32], 95 GHz [29], 110 GHz[24], 150 GHz[25], 225 GHz[33], 230 GHz[31].

REFERENCES

(* indicates a representative review of sub-heading topic)

a) Laboratory Measurements

1. Becker, E. G. and S. H. Autler, 1946: Water vapor absorption of EM radiation in the cm range. Phys. Rev., 70 (5,6), 300-307.

2. Bignell, K. J., 1970: The water-vapour infra-red continuum. Quart. J. Royal Meteor. Soc., 96, 390-403.

*3. Boudouris, G., 1963: On the index of refraction of air, the absorption and dispersion of centimeter waves by gases. J. Res. NBS, 67D (6), 631-684 (and 183 references therein).

4. Bryant, D. L. and J. J. Auchterlonie, 1979: Measurement of the extinction cross-sections of dry and wet ice spheres at 35 GHz. Electron. Lett., 15 (2), 52-53.

5. Burch, D., D. Gryvnak, and J. Pembrook, Jr., 1971: Continuous Absorption in the 8-14 μm Range by Atmospheric Gases. Philco-Ford Report F19 628-69-C-0263.

6. Carlon, H. R., 1979: Variations in emission spectra from warm water fogs: Evidence for clusters in the vapor phase. Infrared Phys., 19, 49-64.

7. Dillon, T. A. and H. J. Liebe, 1971: Dispersion studies of the 22 GHz water vapor line shape. J. Quant. Spectrosc. Radiat. Transfer, 11, 1803-1817.

8. Frenkel, L. and D. Woods, 1966: The microwave absorption of H_2O vapor and its mixtures with other gases between 100 and 300 GHz. Proc. IEEE, 54 (4), 498-505.

9. Harries, J. E., W. J. Burrougns, and H. A. Gebbie, 1969: MM wavelength spectroscopic observations of water dimer in the vapour phase. J. Quant. Spectrosc. Radiat. Transfer, 9, 799-807.

10. Hemmi, C. O. and A. W. Straiton, 1969: Pressure broadening of the 1.63 mm water vapor absorption line. Radio Sci., 4 (1), 9-15.

11. Liebe, H. J., 1966: Untersuchungen an Gasmischungen, Wasserdampf-Luft, mit einem digitalen Mikrowellen-Refraktometer. Ph.D. Thesis, Techn. University, W-Berlin, Electr. Eng. Dept. (D 83), 1964; also NTZ Communications J. 19, 79-83.

12. Liebe, H. J., 1975: Studies of Oxygen and Water Vapor Microwave Spectra under Simulated Atmospheric Conditions. OT Rpt. 75-65, June 1975, (U. S. Government Printing Office).

13. Llewellyn-Jones, D. T., R. J. Knight, and H. A. Gebbie, 1978: Absorption by water vapour at 7.1 cm-1 and its temperature dependence. Nature, 274 (5674), 876-878.

14. Mrowinski, D., 1970: Refraktion und Absorption in atmosphaerischen Gasen in der Umgebung der 22 GHz H_2O Linie. Ph.D. Thesis, Techn. University, W-Berlin, Electr. Eng. Dept., 1969; also Z. Angew. Phys., 29 (5), 323-330, 1970.

15. Sheppard, A. P., K. H. Breeden, and A. McSweeney, 1970: High resolution sub-mm measurements of atmospheric water vapor absorption. Proc. Sym. on Sub-mm Waves, Polytechn. Inst. Brooklyn, 445-453.

16. Straiton, A. W., B. M. Fannin, and J. W. Perry, 1974: Measurements of index of refraction and signal loss due to an ice fog medium at 97 GHz using a Fabry-Perot reasonator. IEEE Trans., AP-22 (4), 613-616.

17. White, K. O., W. R. Watkins, and L. R. Bruce, 1978: Water Vapor Continuum Absorption in the 3.5 to 4 μm Region. U.S. Army Atm. Sciences Laboratory Report ASL-TR-0004, March 1978; and Report ASL-TR-0017, September 1978.

b) Field Measurements

18. Altshuler, E. E., M. A. Gallop, and L. E. Telford, 1978: Atmospheric attenuation statistics at 15 and 35 GHz for very low elevation angles. Radio Sci., 13 (5), 839-852.

19. Crawford, A. B. and D. C. Hogg, 1971: Measurement of atmospheric attenuation at mm. Bell Sys. Tech. J., 35 (6), 907-916, 1956, also D. Hogg, Progress in Radio Science 1966-69, Vol. 2, URSI 1971.

20. Emery, R. J., P. Moffat, R. Bohlander, H.G. Gebbie, 1975: Measurement of anomalous atmospheric absorption in the 4 to 15 cm-1 range. J. Atmos. Terrestr. Phys., 37, 587-594.

21. Emery, R. J., A. M. Zavody and H. A. Gebbie, 1979: Measurements of atmospheric absorption in the range 4-17 cm-1 and its temperature dependence. J. Atmos. Terr. Phys., 1979.

22. Fogarty, W. G., 1975: Total atmospheric absorption at 22.2 GHz. IEEE Trans., AP-23 (3) 441-444.

23. Gibbins, C. J., A. C. Gordon-Smith, and H. A. Gebbie, 1973: Anomalous absorption in the atmosphere for 2.7 mm radiation. Nature, 243, 397.

24. Gibbins, C. J., A. C. Gordon-Smith, and D.L. Croom, 1975: Atmospheric emission measurements at 85 to 118 GHz. Planet. Space Sci., 23, 61-73.

25. Gibbins, C. J., C. L. Wrench, and D. L. Croom, 1976: Atmospheric emission measurements between 22 and 150 GHz. Proc. URSI Comm. F. Sym., Labaule, France, 19-21.

26. Gimmestad, G. G. and H. A. Gebbie, 1976: Atmospheric absorption in the range 12 to 31 cm-1 measures in a horizontal path. J. Atmos. Terr. Phys., 38, 325-328.

27. Gimmestad, G. G., R. H. Ware, R. A. Bohlander, and H. A. Gebbie, 1977: Observations of anomalous submillimeter atmospheric spectra. Astroph. J., 218, 311-313.

28. Goldsmith, P. F., R. L. Plambeck, and R. Y. Chiao, 1974: Measurements of atmospheric attenuation at 1.3 and 0.87 mm. IEEE Trans., MTT 22 (12), 1115-1116.

29. Lo, L. I., B. M. Fannin, and A. W. Straiton, 1975: Attenuation of 8.6 and 3.2 mm radio waves by clouds. IEEE Trans., AP-23 (6), 782-786.

30. Malyshenko, Y. I., 1969: Measurement of absorption coefficient of water vapor in the transparency window at 1.3 mm. Rad. Eng. & Electr. Phys., 14 (3), 447-448, (Engl. Transl.).

31. Mather, J. C., M. W. Werner, and P. L. Richards, 1971: A search for spectral features in the sub-mm background radiation. Astrophys. J., 170, L59-65.

32. Moffat, P. H., R. A. Bohlander, W. R. Macrae, H. A. Gebbie, 1977: Atmospheric absorption between 4 and 30 cm-1 measured above Mauna Kea. Nature, 269, 676-677.

33. Plambeck, R. L., 1978: Measurements of atmospheric attenuation near 225 GHz: Correlation with surface water vapor density. IEEE Trans., AP-26, 737-738.

34. Ryadov, V. Y., N. I. Furashov, and G. A. Sharonov, 1964: Measurement of atmospheric transparency to 0.87 mm waves. Rad. Eng. & Electr. Phys., 11, 773-778.

*35. Thompson, III, W. I., 1971: Atmospheric Transmission Handbook. NASA Tech. Rept. No. DOT-TSC-NASA-71-6 (Chapter 9 and 140 references therein).

36. Tolbert, C. W., L. C. Krause, and A. W. Straiton, 1964: Attenuation of the earth's atmosphere between 100 and 140 GHz. J. Geophys. Res., 69 (7), 1349-1357.

37. Ulaby, F. T. and A. W. Straiton, 1969: Atmospheric attenuation studies in the 183-325 GHz region. IEEE Trans., AP-17 (3), 337-342.

38. Ulaby, F. T., 1973: Absorption in the 220 GHz atmospheric window. IEEE Trans., AP-21 (2), 266-269.

39. Whaley, T. W., 1969: Characterization of free space propagation near the 183 GHz H_2O line. Ph.D. Thesis, U. of Texas, Electr. Eng. Dept., 1968, also IEEE Trans., AP-17 (5), 682-684, 1969.

40. Wrixon, G. T., 1971: Measurements of atmospheric attenuation on an earth-space path at 90 GHz using a sun tracker. Bell Sys. Tech. J., 50 (1), 103-114.

41. Wrixon, G. T. and R. W. McMillan, 1978: Measurements of earth-space attenuation at 230 GHz. IEEE Trans., MTT-26 (6), 434-439.

c) Theory, Predictions, Modelling

*42. Carlon, H. R., 1979: Infrared Absorption by Water Clusters. U.S. Army Armament Research and Development Command, Aberdeen P.G., MA 21010, Technical Report ARCSL-TR-79013, March 1979 (and 33 references therein).

43. Deirmendjian, D., 1975: Far infrared and sub-mm scattering, II: Attenuation by clouds and rain. The Rand Corp., Rept R-1718-PR, Feb. 1975; also J. Appl. Meteor., 14 (8), 1584-1593.

44. Derr, V. E., and R. F. Calfee, 1977: Spectral Transmission of Water Vapor from 1 to 1200 cm-1 at Low Concentration and Low Pressure. NOAA Tech. Memo ERL WPL-24, July 1977.

45. Hall, J. T.., 1970: Atmospheric effects on sub-mm radiation. Proc. Sym. on Sub-mm Waves, Polytechn. Inst., Brooklyn, 455-465.

*46. Lam, K. S., 1977: Application of pressure-broadening theory to the calculation of atmospheric oxygen and water vapor microwave absorption. J. Quant. Spectrosc. Radiat. Transfer, 17, 351-383 (and 68 references therein).

47. Liebe, H. J. and G. G. Gimmestad, 1978: Calculation of clear air EHF refractivity, Radio Sci., 13 (2), 245-251.

48. Liebe, H. J. and R. K. Rosich, 1978: Modelling of EHF propagation in clear air. Proc. IEEE Conf. Space Instrum. for Atm. Observation, El Paso, 4/1-15, April 1979; also AGARD CP 236-II, 45/1-18, 1978

49. McClatchey, R. A., W. S. Benedict, S. A. Clough, D. E. Burch, R. F. Calfee, K. Fox, L. S. Rothman, and J. S. Garing, 1978: AFCRL Atmospheric absorption line parameters compilation, AFCRL Environm. Research Paper No. 434, 1973; Appl. Optics, 15, 2616-2617, 1976; 17, 507, 1978.

50. McMillan, R. W., J. J. Gallagher, and A.M. Cook, 1977: Calculation of antenna temperature, horizontal path attenuation, and zenith attenuation due to water vapor in the band 150-700 GHz. IEEE Trans., MTT-25 (6), 484-488.

51. Ulaby, F. T. and A. W. Straiton, 1970: Atmospheric absorption of radio waves between 150 and 350 GHz. IEEE Trans., AP-18 (4), 479-48[illegible]

52. Waters, J. R., 1976: Absorption and emission by atmospheric gases. (Chapter 2.3 in Methods of Experimental Physics, Vol. 12B; editor, M. L. Meeks), N.Y., Academic Press.

d) Atmospheric Water Vapor Properties

53. Bohlander, R. A. and H. A. Gebbie, 1975: Molecular complexity of water vapour and the speed of sound. Nature, 253 (5492), 523-525.

54. Hall, M. P., 1977: Variability of atmospheric water-vapor concentration and its implications for microwave-radio-link planning. Electron. Lett., 13 (21), 650-652.

*55. Haenel, G., 1976: The properties of atmospheric aerosol particles as a function of the relative humidity. Advances in Geophysics, Vol. 19, Academic Press, 74-189.

56. Harries, J. E., 1977: The distribution of water vapor in the stratosphere. Rev. Geophys. & Space Phys., 14 (4), 465-475.

*57. Pruppacher, H. R. and J. D. Klett, 1978: Microphysics of clouds and precipitation. D. Reidel Publ. Comp., Dordrecht, Boston, London, 1978 (and about 1350 references therein).

SUBMILLIMETER-WAVE PROPERTIES OF THERMOSPHERIC ROCKET PLUMES

M. M. Litvak
Jet Propulsion Laboratory
California Institute of Technology
Pasadena, CA 91103

J. A. Weiss and G. F. Dionne
Massachusetts Institute of Technology
Lexington, MA 92173

Fourth International Conference on Infrared and Millimeter Waves and Their Applications
IEEE Cat. No. 79 CH 1384-7 MTT, 139-140, December 10-15, 1979

Observability of rocket plumes at thermospheric altitudes using high-resolution submillimeter-wave spectral line radiometry has been investigated. Calculations that include collisional, radiative, and flow effects indicate that low-lying rotational transitions of plume species, particularly water vapor, have sufficient optical depth and spatial extent for satellite applications. (Authors)

LO, FANNIN, AND STRAITON

ATTENUATION OF 8.6 AND 3.2 mm RADIOWAVES BY CLOUDS

L. I. Lo
Sperry Support Services
Sperry Rand Corporation
Huntsville, AL 35809

B. M. Fannin and A. W. Straiton
Electrical Engineering Research Laboratory
University of Texas
Austin, TX 78757

IEEE AP-23, No. 6, 782-786, November 1975

Measured attenuations associated with a variety of cloud conditions at wavelengths near 8.6 and 3.2 mm are reported. Two specific events, during which heavy rain clouds covered the sky, are examined and statistical data collected over a 6-month period on a variety of cloud types are presented. The number of observations of some cloud types was not large and it was not possible to account for the gaseous attenuation with sufficient accuracy to get reliable values for the attenuation by the cloud droplets from a number of cloud types. The clouds causing the largest attenuations were the rain-bearing cumulonimbus. Of the non-rain clouds, the two types for which the sample sizes are adequate and attenuations are sufficient for meaningful conclusions are stratocumulus and cumulus, their 35 GHz/95 GHz mean attenuation values being 0.18/0.61 and 0.12/0.34, respectively. (Authors)

EXTRACTS:

The following 95-GHz cloud attenuation data has been corrected by accounting for zenith angle and then subtracting attenuation of clear sky data:

Cloud Type	Ground Level Water Vapor Density (g/m^3)	Measured Cloud Attenuation and Standard Deviation (dB)
altocumulus	16.8 ± 1.43	-0.23 ± 0.30
altostratus	14.7 ± 1.53	0.30 ± 0.05
stratocumulus	18.9 ± 1.68	0.61 ± 0.41
stratus	19.1 ± 2.30	0.12 ± 0.24
nimbostratus	20.8 ± 0.31	0.11 ± 0.24
cumulus	18.7 ± 1.81	0.34 ± 0.36
cumulonimbus	18.1 ± 2.39	2.36 ± 1.86

The authors note that "the cloud attenuation values have been 'normalized' by dividing by the secant of the zenith angle, which can be misleading for localized clouds with pronounced vertical development."

PENETRABILITY OF HAZE, FOG, CLOUDS AND PRECIPITATION BY RADIANT ENERGY OVER THE SPECTRAL RANGE 0.1 MICRON TO 10 CENTIMETERS

G. D. Lukes
Center for Naval Analyses
Rochester, NY

Naval Warfare Analysis Group, Study 61
AD 847 658L (A70 1692)

To determine attenuation values over a wide range of wavelengths, an analytical methodology is developed to accommodate the population of droplets according to size in unit volume of several models of water-occluded atmospheres. The etent of penetrability of cloudy and rainy atmospheres is then demonstrated analytically as a function of wavelength. Unique phenomena appear at wavelengths from about 100 microns to 2 millimeters, in part due to the population of droplets by size in clouds and rain, but also due to the strong wavelength dependence of the complex index of refraction of liquid water. The submillimeter band is accordingly given special emphasis. Most layer-type clouds, especially if of maritime origin, are readily penetrable at these wavelengths. Attenuation due to rain of moderate intensity is found to decrease slowly with decreasing wavelength below 2 millimeters. Further, pronounced forward scatter in moderate rain, adding to the forward transmission, first begins to appear at a wavelength of 2 millimeters and becomes increasingly more pronounced the shorter the wavelength. None of these trends would be predicted by simple extrapolation of experience at microwave frequencies. The analysis of attenuation by water droplet atmospheres draws on the Mie theory of absorption and scatter by spherical droplets. It is shown that the essential condition of incoherent scattering is satisfied by haze, fog, clouds, and rain. Multiple scatter in clouds for radiation at submillimeter wavelengths and longer is found to be exceedingly weak and may be ignored. The question of possible effects of multiple scatter in rain is not settled analytically, but if such scatter cannot be ignored, it is unquestionably multiple incoherent scatter. This suggests the application of radiative transfer theory to elucidate more definitively the effects of scatter in rain.

The absorption profile arising from atmospheric gases is structured in fine detail from 0.4 micron to 3.2 centimeters by extensive search of the literature. Gaseous absorption along a zenith path through a cloudless maritime polar atmosphere is computed for wavelengths from 164 microns to 3.2 centimeters. Seventeen windows of elevated transparency in this profile are identified. A stratocumulus cloud and rain are then induced by turbulence in this model atmosphere, and comparative and composite values of attenuation due to clouds, rain, and gases are derived. From 345 microns to 3 millimeters, the contribution by cloudy and rainy atmospheres to total atmospheric attenuation is found to be relatively minor, even at the wavelengths of gaseous windows.

Because of requirements forged by its scope, the study provides an extensive data base on the population of droplets by size in various water-occluded atmospheres. The exremes are remarkable: thick fog ms, have over 100 billion droplets per cubic meter of 0.4 micron droplet-radius peak population compared to a mere 200 in mist of 75 micron peak population. The chemical properties of liquid water are drawn from some 80 sources in order to structure the real and imaginary parts of te complex index of refraction over the spectral range of 0.1 micron to 10 centimeters, essential to the application of the Mie theory. (Author)

EXTRACTS:

Tabular and graphical data follow.

SUMMARY OF GASEOUS ABSORPTION AT SELECTED WAVELENGTHS ALONG A ZENITH PATH THROUGH A CLOUDLESS MARITIME POLAR ATMOSPHERE

Wavelength λ	Characteristic in absorption spectra	Absorption due to water vapor: γ_o (db per km)	Absorption due to water vapor: Γ (in db over height interval 0-8.4 km)	Absorption due to water vapor: $R = \frac{\Gamma}{\gamma_o}$	Absorption due to oxygen: γ_o (db per km)	Absorption due to oxygen: Γ (db over height interval 0-8.4 km	Absorption due to oxygen: $R' = \frac{\Gamma}{\gamma_o}$	Absorption due to oxygen: Γ' (db) over height interval 0-19.3km	Absorption due to oxygen: $R'' = \frac{\Gamma'}{\gamma_o}$	Gaseous absorption (in decibels) along zenith path due to water vapor and oxygen distribution in a maritime polar atmosphere: Water vapor	Oxygen	Combined absorption
1.0mm	Slope - H_2O	2.65	6.48	1.69	5.7×10^{-2}					6.48	0.57	5.05
1.1mm	Slope - O_2	1.9	(2.17)	(1.63)	1.1×10^{-2}	6.33×10^{-2}	5.76	9.02×10^{-2}	8.19	2.17	0.11	2.28
1.3mm	Valley - H_2O	1.13	1.91	1.73	1.3×10^{-2}					1.91	0.13	2.04
1.5mm	Slope - H_2O	1.75	3.00	1.69	1.6×10^{-2}					3.00	0.16	3.16
1.63mm	Peak - H_2O	3.00×10	7.66×10	2.56	1.7×10^{-2}					76.65	0.17	76.77
2.15mm	Slope - O_2	2.8×10^{-1}	(5.04×10^{-1})	(1.8)	3.0×10^{-2}	1.72×10^{-1}	5.73	2.44×10^{-1}	8.13	0.50	0.30	0.80
2.4mm	Slope - O_2	2.0×10^{-1}	(1.60×10^{-1})	(1.8)	6.0×10^{-2}	1.51×10^{-1}	5.55	4.99×10^{-1}	8.31	0.36	0.60	0.96
2.53mm	Peak - O_2	1.9×10^{-1}	(3.42×10^{-1})	(1.9)	1.0	1.72×10	5.73	2.44×10	8.15	0.34	30.00	30.34
2.7mm	Valley - O_2	1.5×10^{-1}	(2.85×10^{-1})	(1.9)	6.6×10^{-2}	3.77×10^{-1}	5.72	5.36×10^{-1}	8.13	0.28	0.66	0.94
3.9mm	Slope - O_2	6.3×10^{-2}	(1.20×10^{-1})	(1.9)	3.0×10^{-1}	1.72	5.73	2.44	8.15	0.12	3.00	3.12

Index of Refraction ($\nu + i\kappa$) of Liquid Water

Wavelength	ν	κ
1.0 mm	2.48	0.96
2.1 mm	2.77	1.33
3.3 mm	3.10	1.67

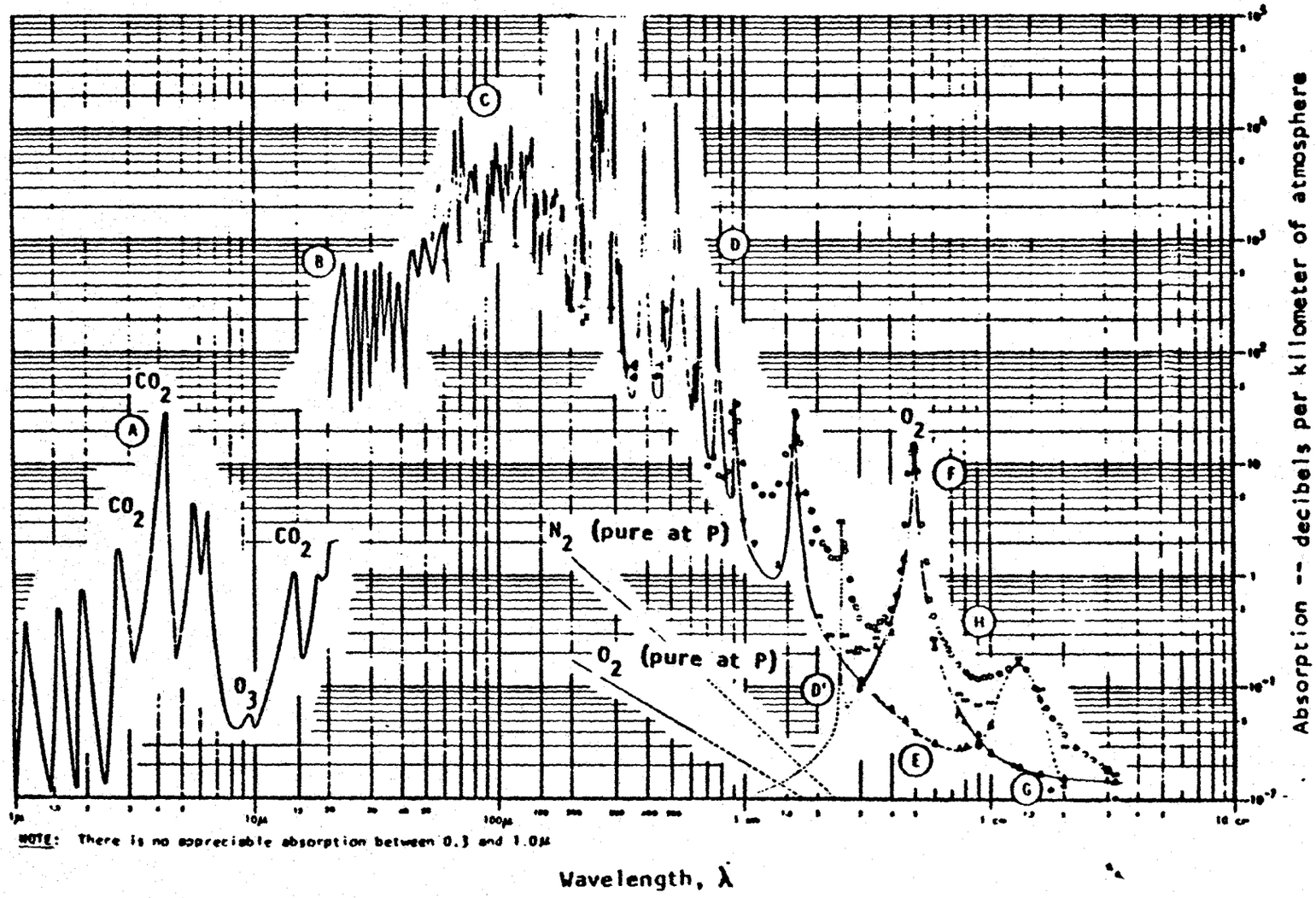

FIG. 1: ABSORPTION COEFFICIENTS DUE TO ATMOSPHERIC GASES AT SEA LEVEL CONDITIONS FOR THE SPECTRAL RANGE 0.3u TO 3.2 cm

McGEE*

MILLIMETER WAVE RADIOMETRIC DETECTION OF TARGETS OBSCURED BY FOLIAGE

Richard A. McGee
Ballistic Research Laboratories
Aberdeen Proving Ground, MD 21005

BRL MR No. 1901, January 1968
AD 667 962 (A79 07150)

The problem of passive detection by millimeter wave [35 GHz] radiometry of metallic targets obscured by foliage and other vegetation is defined and discussed. A model of the foliage obscuration situation is presented and evaluated on the basis of data collected in a field measurement program. Results obtained show the millimeter wave radiometric obscuration; hence, the maximum range of a radiometric system will be reduced linearly with optical obscuration instead of theoretically with a square root relationship. Further refinements of the model are discussed and are to be included in a general foliage penetration model to be evaluated at a later date. (Author)

140 AND 220 GHz DEVELOPMENT WORK AT BRL

R. A. McGee
BRL/ARRADCOM
Aberdeen Proving Ground, MD 21005

Proceedings of the Eighth DARPA/Tri-Service Millimeter Wave Conference System Planning Corporation (editor), 1500 Wilson Blvd., Arlington, VA 22209, p. 243-248, April 1979
(A80 00206)

SECRET

The Ballistic Research Laboratory (U.S. Army Armament Research and Development Command) at Aberdeen Proving Ground, Maryland, is carrying out experimental programs with 140 and 220 GHz radars. These radars use solid state sources and are primarily used for near earth propagation and target tracking experiments. (Author)

McGEE AND LOOMIS*

RADAR TRACKING OF AN M-48 TANK AT 94 AND 140 GHz

R. A. McGee
U.S. Army Armament Research and Development Command
Aberdeen Proving Ground, MD 21005

J. M. Loomis
U.S. Army Missile Research and Development Command
Huntsville, AL 35809

Proceedings of the 6th DARPA/Tri-Service Millimeter Wave Conference
Tactical Technology Office (editors), Defense Advanced Research Projects
Agency, 1400 Wilson Blvd., Arlington, VA 22209, 123-128, November 1977
(A78 01438)

SECRET

This report provides a description of the 94-GHz and 140-GHz radar systems used in the ground-based tracking of M-48 tanks. (Authors)

CALCULATIONS OF ANTENNA TEMPERATURE, HORIZONTAL PATH ATTENUATION, AND ZENITH ATTENUATION DUE TO WATER VAPOR IN THE FREQUENCY BAND 150-700 GHz

R. W. McMillan, J. J. Gallagher, and A. M. Cook
Engineering Experiment Station
Georgia Institute of Technology
Atlanta, GA 30332

IEEE MTT-25, No. 6, 484-488, June 1977

The results of calculations of antenna temperature at zenith, both with and without the sun viewed as a source, are given. Horizontal path and total zenith attenuation are also calculated. Each of these calculations was made over the frequency band 150-700 GHz, using data from the 24 water-absorption lines between 150 and 1000 GHz. (Authors)

McMILLAN, ROGERS, PLATT, GUILLORY,
AND GALLAGHER

MILLIMETER WAVE PROPAGATION THROUGH BATTLEFIELD DUST

R. W. McMillan, R. Rogers, R. Platt, D. Guillory, and J. J. Gallagher
Georgia Institute of Technology
Engineering Experiment Station
Atlanta, GA 30332

Donald E. Snider
Atmospheric Sciences Laboratory
White Sands Missile Range, NM 88002

Report Number ASL-CR-0026-1

In order to assess battlefield obscuration at visible, infrared, and millimeter wavelengths, the Dusty Infrared Test I (DIRT-I) was conducted between 2 and 14 October 1978 at White Sands Missile Range. As part of this test, millimeter transmissometers at 94 GHz and 140 GHz were operated by personnel of the Georgia Institute of Technology.

Preliminary conclusions are: tactical size explosions can produce large attenuation (up to 30 dB) at millimeter wavelengths for short periods of time (1 to 2 seconds). Total attenuation was measured—it is not possible to separate absorption and scattering. (Author)

EXTRACTS:

Additional reports on the DIRT I measurements are:

1. Measured Effects of Battlefield Dust and Smoke on Visible, Infrared, and Millimeter Wavelength Propagation compiled by J. D. Lindberg. An Entry for this report is under Snider, McMillan and Gallagher.

2. Measurements of Attenuation Due to Simulated Battlefield Dust at 94 and 140 GHz by J. J. Gallagher, R. W. McMillan, R. C. Rogers, and D. E. Snider.

ATMOSPHERIC TURBULENCE EFFECTS ON INFRARED AND NEAR-MILLIMETER WAVE PROPAGATION

R. W. McMillan
Georgia Institute of Technoloy
Engineering Experiment Station
Atlanta, GA 30332

D. E. Snider
Atmospheric Sciences Laboratory
White Sands Missile Range, NM 88002

Fourth International Conference on Infrared and Millimeter Waves and Their Applications
IEEE Cat. No. 79 CH 1384-7 MTT, 119-120, December 10-15, 1979

Scintillation of electromagnetic energy traversing the turbulent atmosphere is caused by refractive index inhomogeneities in the path that cause phase shifts, giving rise to selective reinforcement or degradation of the energy across the beam. The resulting energy distribution is log normal, characterized by a variance that is a function of the degree of atmospheric turbulence. These inhomogeneities also cause angle of arrival fluctuations, depolarization, frequency shift, and thermal blooming; although the latter three effects are thought to be of minor importance in the NMMW spatial region.

Most of the original work on atmospheric turbulence was done in Russia by Chernov and Tatarshi, who treated mainly optical fluctuations and neglected the effects of absorption on the fluctuation intensity. This approach has worked well for optical wavelengths, as attested by the large number of turbulence papers which show reasonable agreement between theory and experiment. More recently, several other Russian workers have examined the problem of millimeter and submillimeter wave fluctuations; which requires [sic] that absorption by atmospheric constituents, mainly water vapor, be considered. This approach was apparently first taken by Izyumov who solved the wave equation using a complex index of refraction to account for absorption and thus obtained expressions for amplitudes and phase fluctuations valid for NMMW propagation. This work was refined by Gurvich and by Armand, Izyumov and Sokolov, who obtained the reasonably tractable expressions used for calculations in this paper. (Authors)

McMILLAN, WILTSE, AND SNIDER*

ATMOSPHERIC TURBULENCE EFFECTS ON MILLIMETER WAVE PROPAGATION

R. W. McMillan and J. C. Wiltse
Engineering Experiment Station
Georgia Institute of Technology
Atlanta, GA 30332

D. E. Snider
Atmospheric Science Laboratory
White Sands Missile Range
White Sands, NM 88002

EASCON 1979 Conference Record, Electronics and Aerospace Systems Conference,
October 9-11, 1979
IEEE Publication 79 CH 1476-1 AES

The effects of atmospheric turbulence on the propagation of optical signals have been thoroughly analyzed by other workers; in the case of millimeter microwave radiation less work has been done, and theory predicts a strong dependence of the scintillation amplitude and angle of arrival variations on the humidity structure parameter C_Q in addition to the temperature structure parameter C_T. This paper extends the work of several Russian authors to the point of calculating both intensity and angle of arrival fluctuations in the atmospheric windows at 94 and 140 GHz. The calculated results are compared to experiment for both frequencies, and reasonably good agreement is obtained in both cases. (Authors)

MILLIMETER AND SUBMILLIMETER WAVE DIELECTRIC MEASUREMENTS WITH AN INTERFERENCE SPECTROMETER

A. McSweeney and A. P. Sheppard
Engineering Experiment Station
Georgia Institute of Technology
Atlanta, GA 30332

Georgia Tech Final Report No. A-934, 14 April 1970
AD 709 893 (A79 06024)

Dielectric constants, loss tangents, and transmission coefficients for a large number of materials have been measured in the millimeter and submillimeter-wave part of the electromagnetic spectrum. Instrumentation and measurement techniques for obtaining these data are described in detail. These include interference spectroscopy using a black body source with appropriately designed filters, and coherent techniques using a Fabry-Perot interferometer or a short-circuited waveguide filled with powdered samples. The measurements show that many materials commonly employed in the microwave spectrum tend to be very lossy as a function of increasing frequencies toward 2000 GHz ($67\ cm^{-1}$). Some materials, such as Teflon, polyethylene, Rexolite, and slip-cast fused silica, were observed to have relatively low dissipation factors so as to represent excellent candidates for component and electromagnetic window applications throughout the millimeter and submillimeter wave part of the spectrum. (Authors)

EXTRACTS:

Dielectric constants measured at 139 GHz:

plexiglass	2.61
teflon	2.07
polystyrene	2.53

MEASUREMENT OF THE ATTENUATION COEFFICIENT OF 1.2 AND 0.86 mm RADIO WAVES IN RAIN

Yu. I. Malyshenko and I. Kh. Vakser
Institute of Radio Physics and Electronics
Academy of Sciences of the Ukranian SSR

Izvestiya Vysshikh Uchebnykh Zavedenii, Radio Fizika 14, No. 6, 958-960, June 1971

Attenuation coefficient measurements were taken during rains of vertically polarized radio waves. The regions of experimentation were the short-wave portion of the millimeter range and a long wave portion of the sub-millimeter range. Measurements were made on a short (120 meter) route along the earth's surface. (Authors)

EXTRACTS:

Measured attenuation coefficients during a rain at 1.3-mm wavelength (I is the rainfall rate in mm/hr):

$$A(\text{dB/km}) = 0.76I \quad (I < 10 \text{ mm/hr})$$

$$= 3.2 + 0.33I \quad (10 < I < 50 \text{ mm/hr})$$

TARGET CONTRAST CONSIDERATIONS IN MILLIMETER WAVE RADIOMETRY FOR AIRBORNE NAVIGATION

A. Mayer
NASA/Ames Research Center
Moffett Field, CA 94035

NASA-TM-X-62082, August 1971
N72 10539 (A79 02091)

This report describes target signal requirements for aircraft navigation systems that use radiometric receivers which "map" thermally emitted power radiated by terrain or power radiated by ground-based beacons. For selected mm-wavelength bands, microwaves suffer relatively little degradation by absorption or scattering on passage through the atmosphere, despite extreme weather changes. Interest centers on 8-mm waves because of component availability, portability (small size), high image resolution, and all-weather capability at this wavelength.

Section 1 briefly introduces the idea of radiometric airborne navigation. In Section 2, elements of radiometry, terrain radiation, and atmospheric transmission characteristics are reviewed, and data pertaining to them at 8-mm wavelength are collected. In Section 3, calculation of radiometric contrasts is discussed for some simple models of terrain targets. (Author)

EXTRACTS:

Brightness temperature measurements of beach sand, emissivity = 0.8, incidence angle unspecified, University of Texas data 70 GHz, horizontal polarization:

	T_B =
clear day	318 K
cloudy day	285 K
typical day	309 K
typical night	282.6 K

MEDHURST*

RAINFALL ATTENUATION OF CENTIMETER WAVES: COMPARISON OF THEORY AND MEASUREMENT

Richard G. Medhurst
Telecommunications Research Laboratory
Hirst Research Centre
General Electric Company, Ltd.
Wembly, England

IEEE Trans. AP-13, 550-564, July 1965

Numerical results for attenuation of centimeter waves by rainfall have been computed from J. W. Ryde's formula. These correct, and considerably extend, the previously published Ryde results. Comparison with available measurements suggests that the agreement is not entirely satisfactory; there is a tendency for measured attenuations to exceed the maximum possible levels predicted by the theory. (Author)

RAIN ATTENUATION AND SIDE-SCATTER MEASUREMENTS OF MILLIMETER WAVES OVER SHORT PATHS

James W. Mink
Communications/Automatic Data Processing Laboratory
AMSEL-NL-RH
Fort Manmouth, NJ 07703

Final Report #CY 73 and 74, June 1975
ADA 012 167 (A76 02037)

Results of rain-attenuation and side-scatter measurements at millimeter waves are presented that have been obtained with a shuttle-pulse technique. This technique requires a path length through rain of only a few meters, so that rainfall rate and drop-size distribution can be considered uniform along this path. (Author)

EXTRACTS:

Measurements of rainfall variations were made. Drop-size distribution, index of refraction, and terminal velocity for the same rainfall rate vary substantially from shower to shower.

Wavelengths were not indicated for the sparse radar data.

MOORE AND VITALE*

MICRAD SHIP CLASSIFICATION

R. P. Moore and E. Vitale
Naval Weapons Center
China Lake, CA 93555

DOC MO 35-935, June 1976
(A78 04832)

SECRET

The work reported here was supported by NAVAIR 370F under AirTask A370370F/008B/5F12-100-700. The objective of this effort was to establish the characteristics and uniqueness of MICRAD (microwave radiometric) ship signatures and determine the method by which such signatures could be used in an ocean surveillance system. The investigations consisted of laboratory, computer, and theoretical analysis of MICRAD ship data. Data collected on previous programs and data collected specifically for this program were used in the analysis. All data were collected with Naval Weapons Center K-band mapping systems. Successful development of the MICRAD ship classification system would provide the fleet with a passive, adverse weather, 24-hour capability for detection and classification of ships, as well as the capability for monitoring their movements. This report discusses the results of this investigation and defines further development required to attain an operational capability. (Authors)

See also the extract in the classified supplement.

MORGAN, STETTLER, AND TANTON

RESULTS OF MIRADCOM WORKSHOP ON MILLIMETER AND SUBMILLIMETER ATMOSPHERIC PROPAGATION APPLIED TO RADAR AND MISSILE SYSTEMS

R. L. Morgan, J. D. Stettler, and G. A. Tanton
U.S. Army Missile Research and Development Command
Redstone Arsenal, AL 35809

Proceedings of the Eighth DARPA/Tri-Service Millimeter Wave Conference, System Planning Corporation (editor), 1500 Wilson Blvd., Arlington, VA 22209, p. 119-126, April 1979
(A80 00206)

SECRET

This paper presents a summary of the results of a workshop on millimeter and submillimeter wave propagation under various atmospheric conditions held at the U.S. Army Missile Research and Development Command, Redstone Arsenal, Alabama, on 20-22 March 1979. (Authors)

MUNDIE

PASSIVE MILLIMETER-WAVE RADIOMETRY AND SOME POSSIBLE APPLICATIONS

L. G. Mundie
The Rand Corporation
Santa Monica, CA 90406

R-1175-ARPA, April 1973
(A73 02251)

CONFIDENTIAL

The overall objectives of Rand's study of millimeter-wave technology for the Defense Advanced Research Projects Agency are to determine the near-term applicability of millimeter waves to tactical military requirements, to identify appropriate systems for which millimeter wavelengths offer significant advantages, and to recommend research and development programs for advancement of the operational capability of these systems. Systematic investigation of millimeter-wave potential is particularly appropriate at this time in view of recent progress in the technological state of the art and knowledge of the phenomenology.

A survey was made of the technology and phenomenology to establish state of the art equipment and environmental constraints. On the basis of a preliminary investigation of potential systems applications, it was concluded that military applications of interest fall broadly into three categories: communications, radar, and radiometry (passive sensing). This report examines passive millimeter-wave radiometry. The other two categories are under study at Rand and will be reported on in the near future.

The several advantages (better resolution and less susceptibility to jamming) of millimeter-wave radiometers over those operating at longer wavelengths are weighed against such disadvantages as susceptibility to degradation in poor weather. (Author)

EXTRACTS:

		Visibility	Attenuation Rate At Sea Level (dB/km)	
			94 GHz	140 GHz
Clear Air				
Humidity	7.5 g H_2O/m^3	20 mi	0.4	1.6
Rain				
Drizzle	0.25 mm/hr	14 mi	0.17	0.2
Light	1.0 mm/hr	6 mi	0.6	0.7
Moderate	4.0 mm/hr	2.5 mi	3.0	3.2
Heavy	16.0 mm/hr	1 mi	8.0	9.0
Fog				
Light	0.01 g/m^3	0.5 mi	0.035	0.07
Thick	0.1 g/m^3	600 ft	0.35	0.7
Dense	1.0 g/m^3	100 ft	3.5	7.0

Atmospheric Attenuation Constants

	94 GHz	140 GHz
Attenuation due to oxygen (ground level)	0.11 dB/km	0.06 dB/km
Attenuation due to water vapor (ground level)	0.04 $\frac{dB/km}{g/m^3}$	0.17 $\frac{dB/km}{g/m^3}$
Scale height for oxygen	4 km	4 km
Scale height for water vapor	2 km	2 km
Attenuation coefficient of cumulus cloud	3.5 dB/km	10 dB/km
Attenuation coefficient of rain (4 mm/hr)	3 dB/km	3.2 dB/km

Apparent Sky Temperatures (°K)

	94 GHz	140 GHz
Clear	50	81
Moderate Overcast	120	200
Rain	220	250

Emissivities of Various Materials in the Microwave Region

Material	Emissivity
Grass	1
Dry Soil	0.93
Moist Soil	0.68
Concrete	0.85
Water	0.45
Metal	≈0

NELSON*

MILLIMETER TARGET MEASUREMENTS AND SEEKER EFFORT

Ralph W. Nelson
Advanced Sensors Directorate
U.S. Army Missile Research, Development and Engineering Laboratory
U.S. Army Missile Command
Redstone Arsenal, AL 35809

Army Missile Command Technical Report RE-76-23, January 1976
AD-C005 528 (A78 04876)

This report addresses the Advanced Sensors Directorate, U.S. Army Missile Command, involvement in land combat target and background signatures as measured by millimeter wavelength sensors, and the application of this data to the design and development of millimeter seekers. The data were collected over a three-year period using pulsed and FM/CW modulated sensors operating at 35 GHz. The data were collected from static test towers at Eglin Air Force Base, Florida, and from the U.S. Army Missile Command Airborne Measurement System helicopter at Redstone Arsenal, Alabama. The data confirm that clutter and false target return as seen by land combat oriented seekers present a difficult target/clutter discrimination problem. (Author)

VERT SENSING FROM ORBIT

F. Ogrodnik
me Air Development Center
iffiss AFB, NY 13441

roceedings of the Eighth DARPA/Tri-Service Millimeter Wave Conference
ystem Planning Corporation (editor), 1500 Wilson Blvd., Arlington, VA 22209,
p. 179-188, April 1979
A80 00206)

ECRET

Passive surveillance from space at weather penetrating frequencies in the illimeter wave spectrum offers the inherent advantages of covert detection, ecognition/identification, and surveillance of military activities and force rectoring without interruptions or limitations due to political restraints or conditions of weather. This paper assesses both the potential capabilities and technology development requirements for such a sensor. (Author)

OLSEN, ROGERS, AND HODGE*

THE aR^b RELATION IN THE CALCULATION OF RAIN ATTENUATION

R. L. Olsen
Department of Communications
Communications Research Center
Ottawa, ON K2H 8S2, Canada

D. V. Rogers
Operations Research, Inc.
Silver Spring, MD 20910

D. B. Hodge
ElectroScience Laboratory
Department of Electrical Engineering
Ohio State University
Columbus, OH 43212

IEEE AP-26, No. 2, 318-329, March 1978

Because of its simplicity, the empirical relation $A = aR^b$ between the specific attenuation A and the rainrate R is often used in the calculation of rain attenuation statistics. Values for the frequency dependent parameters a and b are available, however, for only a limited number of frequencies. Some of these values, furthermore, were obtained experimentally, and may contain errors due to limitations in the experimental techniques employed. The aR^b relation is shown to be an approximation to a more general relation, except in the low-frequency and optical limits. Because the approximation is a good one, however, a comprehensive and self-consistent set of values for a and b is presented in both tabular and graphical for the frequency range 1-1000 GHz. These values were computed by applying logarithmic regression to Mie scattering calculations. The dropsize distributions of Laws and Parsons, Marshall and Palmer, and Joss et al., were employed to provide calculations applicable to "widespread" and "convective" rain. Empirical equations for some of the curves of a(f) and b(f) are presented for use in systems studies requiring calculations at many frequencies. Some comparisons are also made with experimental results, and suggestions are given regarding application of the various calculations. (Authors)

MILLIMETER-WAVE HIGH-RESOLUTION PLAN POSITION INDICATOR AND AZIMUTH-ELEVATION IMAGERY FOR SURVEILLANCE AND CLASSIFICATION

J. H. Parker, Jr. and L. P. Johnson
Goodyear Aerospace Corporation
Litchfield, AZ 85340

Proceedings of the Eighth DARPA/Tri-Service Millimeter Wave Conference
System Planning Corporation (editor), 1500 Wilson Blvd., Arlington, VA 22209,
p. 67-76, April 1979
(A80 00206)

SECRET

Noncoherent 95-GHz radar imagery is shown to exhibit significant potential for battlefield surveillance and correlation guidance. Tank trails, bunkers, and natural terrain features are recognizable. Also, large targets such as ships may be classified. (Authors)

PASCALAR

INVESTIGATION OF PASSIVE MICROWAVE SENSING FROM SATELLITES—INTERIM REPORT

Herb Pascalar
Aerojet ElectroSystems Company
1100 West Hollyvale Street
Azusa, CA 91702

MIRADCOM Contract No. DAAK40-78-C-0175, 31 October 1978
ARPA Order No. 3536

A quantitative evaluation of the opportunities for enhanced satellite surveillance afforded by the cloud and weather penetration capabilities of microwave/millimeter-wave sensors constitute the overall objective for this DARPA/STO-sponsored study. (Author)

EXTRACTS:

The analysis considers three frequency bands centered at 140 GHz, 95 GHz, and 35 GHz.

PROPAGATION EFFECTS FOR mm WAVE FIRE CONTROL SYSTEM

T. N. Patton and J. J. Petrovic
IIT Research Institute
Chicago, IL 60690

J. Teti
Naval Surface Weapons Center
Dahlgren, VA 22448

Proceedings of the 6th DARPA/Tri-Service Millimeter Wave Conference
Tactical Technology Office (editor), Defense Advanced Research Projects Agency, 1400 Wilson Blvd., Arlington, VA 22209, p. 170-178, November 1977
(A78 01438)

SECRET

This paper presents the results of a survey of propagation effects of the atmosphere on a millimeter wave signal used by a sea based fire control radar for use against short range, low altitude, targets. Factors which influence detection range and tracking accuracies are considered. Primary goal was to determine whether normal low altitude conditions of over [sic] sea refractivity will seriously degrade the performance of a pencil beam mm wave radar. It is concluded that the literature is inconclusive on the matter and that experimental work is required. (Author)

PERRY

PARAMETERS AFFECTING THE PROPAGATION OF 15, 35, AND 95 GHz RADIO SIGNALS IN COLD REGIONS

John W. Perry
Millimeter Wave Sciences Group
Electrical Engineering Research Laboratory
University of Texas
Austin, TX 78712

AFAL-TR-71-147
Technical Report No. 71-1, 30 April 1971

A literature survey of parameters affecting the propagation of 15-, 35-, and 95-GHz radio signals in cold regions is presented. Theoretical calculations and experimental measurements in the following areas were examined: attenuation of millimeter-wave signals by falling snow, ground snow, and ice fogs; the measurement of the electrical properties of ice and snow as they effect the millimeter-wave propagation at low temperatures by calibrated millimeter-wave signal attenuation over a known path. This report is a detailed review of the measurements on the properties as available in the published literature. (Author)

EXTRACTS:

The salinity of sea ice varies randomly with age.
This report contains very few measurements.

MILLIMETER WAVE RADAR TRANSMISSION THROUGH HIGH EXPLOSIVE ARTILLERY BARRAGES

F. C. Petito
U.S. Army Night Vision and Electro-Optics Laboratory
Fort Belvoir, VA 22060

R. Harris
System Planning Corporation
Arlington, VA 22209

Proceedings of the Eighth DARPA/Tri-Service Millimeter Wave Conference
System Planning Corporation (editor), 1500 Wilson Blvd., Arlington, VA 22209,
p. 135-146, April 1979
(A80 00326)

SECRET

The Night Vision and Electro-Optics Laboratory conducted a multispectral Dirty Battlefield Sensors Test (Graff II) at the Seventh Army Training Center, Grafenwhor, West Germany, from 9-21 November 1978. One of the objectives of this test was to measure the transmissive properties of 95-GHz millimeter wave radar through typical intensities of 155-mm-high explosive artillery barrages. A brief description of the test and instrumentation are given. The data along with some preliminary conclusions are presented below. (Authors)

PLAMBECK

MEASUREMENTS OF ATMOSPHERIC ATTENUATION NEAR 225 GHz: CORRELATION WITH SURFACE WATER DENSITY

R. L. Plambeck
Radio Astronomy Laboratory
University of California
Berkeley, CA 94720

IEEE AP-26, No. 5, 737-738, September 1978

The total attenuation through the earth's atmosphere for radio waves at frequencies near 225 GHz have been monitored for several weeks from a 1-km elevation site. The zenith attenuation at these frequencies was found to be correlated with the ground level water vapor content of the atmosphere; the correlation is consistent with the relation A (dB) = 0.50 ρ (g/m^3 of water) predicted for clear sky conditions by theory, assuming a 2-km scale height for water in the atmosphere. (Author)

EXTRACTS:

Surface water density versus zenith attenuation (experimental and theoretical data) are plotted.

A(dB) = 0.50 ρ, where ρ is the density of water in g/m^3.

Wrixon and McMillan measured, at 230 GHz, A(dB) = 0.35 ρ at sea level.

A plot of 225-GHz zenith attenuation versus surface water vapor density follows.

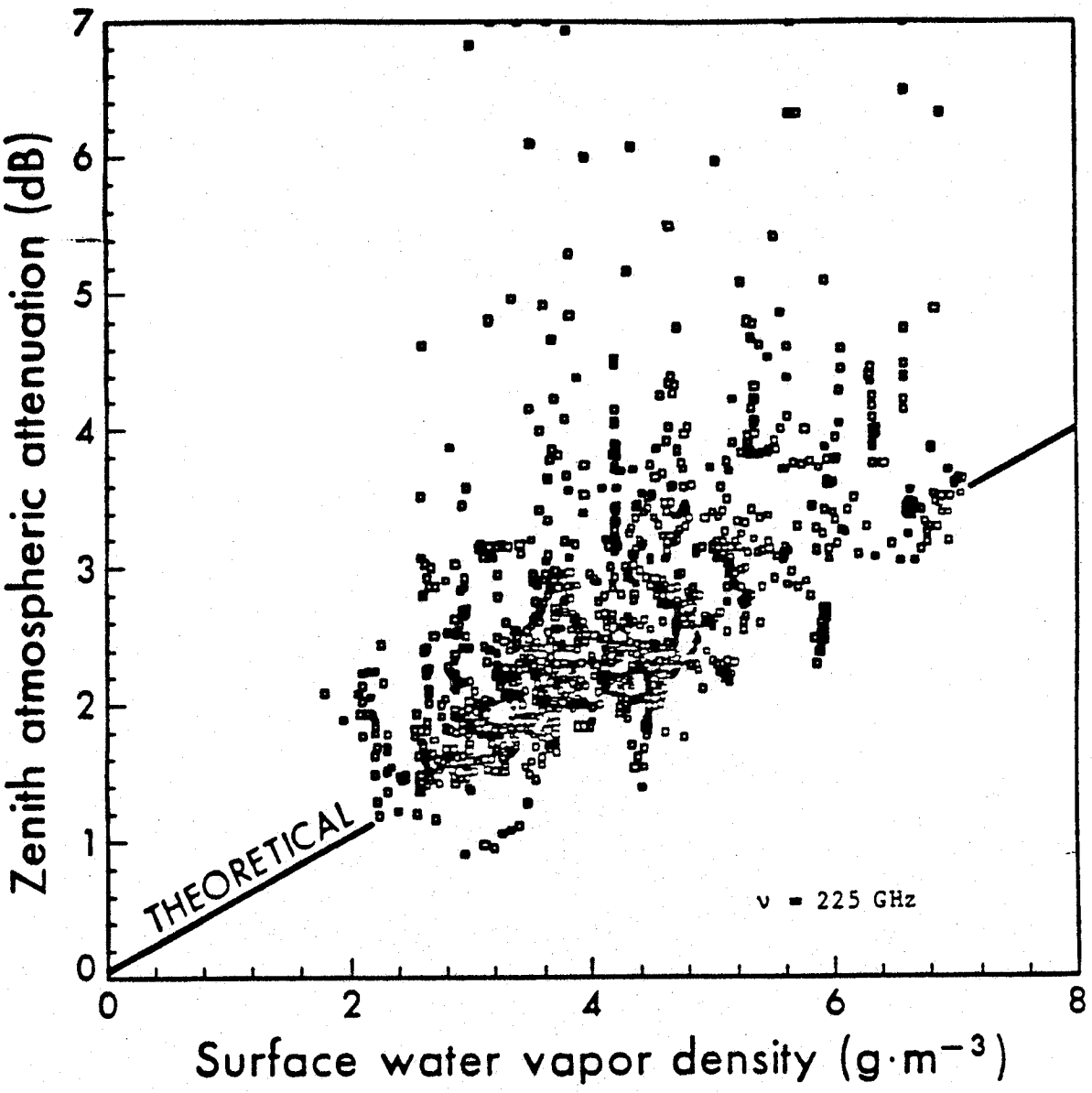
Zenith atmospheric attenuation (dB)
Surface water vapor density (g·m⁻³)
THEORETICAL
ν = 225 GHz
0
1
2
3
4
5
6
7
0
2
4
6
8

POLGE AND SINH*

REDUCTION AND ANALYSIS OF CROSS SECTION MEASUREMENT DATA AT 35 GHz AND 94 GHz

R. J. Polge and A. Sinh
The University of Alabama in Huntsville
P.O. Box 1247
Huntsville, AL 35809

Volumes I, II and III, July 1978
ADC 015 411 (A79 07601)

CONFIDENTIAL

Radar measurements.

TWO-DIMENSIONAL PROCESSING ALONG LINES OF MINIMUM VARIANCE FOR RF SEEKER APPLICATIONS

R. J. Polge and A. Sinh
University of Alabama in Huntsville
P.O. Box 1247
Huntsville, AL 35809
(205) 895-6096

Final Report (Volume IV), September 1978
UAH Research Report No. 216
ADC 015 411 (A79 07601)

The detection of a target using the video return of an RF seeker is very difficult in the presence of nonhomogeneous clutter such as a road. This report presents a new processing technique where the video return is displayed as a donut-shaped map and processed along lines parallel to the direction of minimum variance. Computer programs were developed to estimate the direction of minimum variance and to process the map. The difficult case of a target on a low reflectivity road is used as an example. After processing, the road has been cancelled and the target has become highly visible. (Authors)

PORTER

MICROWAVE RADIOMETRIC FIELD MEASUREMENT PROGRAM FINAL REPORT

R. A. Porter
GCA Corporation
GCA Technology Division
Bedford, MA 01730

GCA-TR-67-10-G(I), July 1967

A large amount of useful measured data were accumulated at three frequencies--94, 16.5, and 9.5 GHz. This data [sic] includes information on the absolute and contrasting apparent temperatures of the following combinations of target materials: bare aluminum vs. asphalt, vs. concrete, vs. wood on aluminum, vs. foliage on aluminum, vs. foliage on asphalt, vs. painted aluminum, vs. grass; and asphalt vs. grass. Specular emissivities of the above materials were also determined during data reduction. (Author)

EXTRACTS:

The glossary of symbols used in the following presentation of their measurements is:

$T_{s\Phi}$	Apparent sky temperature at zenith angle Φ
AL	Aluminum (bare)
B-AL	Bare aluminum (on Figures 43 and 52)
P-AL	Painted aluminum
F	Foliage (tree branches)
T_{AL}, T_C, etc.	Surface temperature of aluminum, concrete, etc.
C	Concrete
AS	Asphalt
G	Grass
W	Wood (1.5 inches of plywood)

1. Bare Aluminum vs Asphalt

Dry - Figures 32, 33, 18
Wet - Figures 34, 35, 20

a. Dry Condition

At 16.5 GHz and an incidence angle of 45 degrees, the contrasts between aluminum and asphalt are 192°K and 217°K for horizontal and vertical polarizations, respectively. As indicated in Section V-A, this is to be expected due to the shape of the asphalt emissivity curves. In addition, metal does not demonstrate any significant polarization dependence. Figure 32 shows this rather clearly. Other plots, discussed in the sections to follow, substantiate this observation.

Referring to Figure 33, the contrast between asphalt and aluminum is smaller at 94 GHz than at 16.5 GHz. This is principally due to the higher apparent sky temperatures ($T_{s\phi}$) recorded at 94 GHz, which raise the apparent temperatures of the aluminum to a greater extent than those of asphalt.

b. Wet Condition

At 16.5 GHz and an incidence angle of 45 degrees, the wet surface coupled with the intervening spray, has reduced the asphalt-aluminum contrast to 63°K at horizontal polarization. This represents a contrast reduction by a factor of three. The vertical component is reduced by a factor of 1.6

At 94 GHz, the contrast is reduced to 73°K, for horizontal polarization. This represents a factor of 1.8 in contrast reduction from dry to wet. The vertical component contrast is reduced by a factor of 1.9. An unusual feature, in Figure 35, is the peak in the asphalt curve at 45 degrees. This is probably due to nonuniformity of the water spray during measurements at different antenna nadir angles.

2. Bare Aluminum vs Concrete

Dry - Figures 36, 37, 13
Wet - Figures 38 and 39

a. Dry Condition

At 16.5 GHz and $\phi = 45°$, the concrete-aluminum contrasts are 174°K and 173°K at horizontal (H) and vertical (V) polarizations, respectively, which is 18°K and 44°K smaller, respectively, than the asphalt-aluminum contrast. This is understandable, since the theoretical emissivity of concrete is, in general, lower than asphalt at a given polarization.

As expected from the asphalt measurements, the concrete-aluminum contrast is lower at 94 GHz, being 152°K and 156°K for H and V polarizations, respectively. Again, this is due to the influence of higher values of $T_{s\phi}$ on the apparent temperatures of the aluminum.

b. Wet Condition

At 16.5 GHz, the H and V polarization contrasts are reduced by a factor of 2.4 and 1.8, respectively, from dry to wet.

At 94 GHz, the contrast practically disappears, being approximately 8°K for both polarizations. The resultant contrast reductions, from the dry state, are 19 and 20, respectively. It appears, however, that a calibration error has forced the apparent temperature of the aluminum above that of the concrete in the H polarization plot. It is likely, from the V polarization data, that the apparent temperature of the aluminum should be approximately 10°K below that of concrete. A second run would have resolved this uncertainty.

3. Bare Aluminum vs Wood on Aluminum

Dry - Figures 40, 41, 19
Wet - Figures 42, 43, 44, 20

a. Dry Condition

At 16.5 GHz, $\phi = 45°$ and H polarization, the addition of 1.5 in. of plywood to the aluminum has raised the apparent temperature of the target from 62°K to 270°K. Since only 23°K remains before the apparent temperature reaches blackbody temperature, i.e., the temperature of the surface, the plywood almost completely obscures the aluminum. If the apparent temperatures of the two targets are normalized, by referring them to their surface temperatures, the result would be 0.21 and 0.92 for aluminum and wood on aluminum, respectively. Thus, the detectability of the aluminum has been reduced by a factor of 4.4 by the 1.5 inches of plywood. At V polarization, the effect is slightly less pronounced.

At 94 GHz, the normalized apparent temperatures of aluminum and wood on aluminum are 0.29 and 0.82, respectively, for H polarization. Thus, the detectability of aluminum has been reduced by a factor of 2.8. This is difficult to understand, since transmission through the plywood appears to be better at 94 GHz than at 16.5 GHz. For V polarization, the normalized apparent temperatures are 0.28 and 0.94 for aluminum and wood on aluminum, respectively. The reduction in detectability is, therefore, 3.4 which is slightly greater than for the other polarization. This is somewhat more understandable since the emissivity of an infinitely thick layer of wood is expected to be higher for V polarization than for H polarization.

b. Wet Condition

At 16.5 GHz and $\phi = 45^{\circ}$, the contrast essentially disappears between aluminum and wood on aluminum, for both polarizations. In addition, the apparent temperature of the aluminum rises very rapidly from $\phi = 30^{\circ}$ to $\phi = 45^{\circ}$. Finally, the polarization effects of wood on aluminum are quite pronounced.

Unfortunately, wet bare aluminum data were not taken at 94 GHz; only wet wood on aluminum measurements were made. Thus, nothing can be said about contrasts between bare aluminum and wood on aluminum in the wet state. However, as in the case of the 16.5 GHz data, the H polarization wood on aluminum apparent temperatures are relatively low and the polarization effects are also quite pronounced.

4. Bare Aluminum vs Aluminum through Foliage

Figures 45, 46, 47, 22, 23, 24

These measurements were made at all three frequencies; however, the foliage used in the 9.5 GHz measurements was considerably thicker and more dense than that used for the 16.5 and 94 GHz observations. Thus, the frequency dependence of attenuation by foliage can only be determined with the latter two frequencies. The analysis for all three frequencies will be for an incidence angle of 30 degrees.

a. 9.5 GHz Data

As shown in Figure 45, the contrast between aluminum and aluminum through foliage is quite large, being 201°K and 208°K for H and V polarizations, respectively. Attenuation by the foliage has been determined by means of the familiar expression

$$T_A = T_S \left(\frac{1}{L}\right) + T_o \left(1 - \frac{1}{L}\right), \ ^{\circ}K$$

where T_A = apparent temperature of the foliage and aluminum combination, °K

T_S = apparent temperature of the aluminum, °K

L = attenuation by foliage

and T_o = thermodynamic temperature of foliage (taken to be equal to the measured air temperature), °K

The above expression can be written in somewhat simpler form as follows:

$$T_A = T_o + (T_S - T_o) \frac{1}{L}, \ ^{\circ}K$$

Referring to Run Nos. 59 and 60 in Volume II of this report, the air temperature was 285°K at the time of the 9.5 GHz measurements. Using data from Run 60, the foliage attenuation can be determined by solving for L in the above equation. Thus,

$$249 = 285 + (47 - 285)\,\frac{1}{L}\ ,\ ^{o}K$$

From which L = 6.6, or 8.2 dB. Since the foliage was approximately 3 feet thick, the attenuation was approximately 2.7 dB/ft. For the vertical component, the attenuation is 2.8 dB/ft at an incidence angle of 30 degrees. Although these are rather heavy attenuations, it should be recalled that the foliage model was quite dense in the 9.5 GHz measurements.

b. 16.5 GHz Data

The data shown in Figure 46 is rather interesting in that the increase in apparent temperature, caused by the foliage on the aluminum is relatively small at $\phi = 30^{o}$. The data at V polarization is rather similar. The calculated attenuation by this foliage model is 0.34 dB/ft and 0.63 dB/ft for H and V polarizations, respectively.

c. 94 GHz Data

At this frequency, attenuation by the foliage model used in the 16.5 GHz measurements is approximately three times as great as at 16.5 GHz. Calculated values show attenuations of 0.94 dB/ft and 1.57 dB/ft for H and V polarizations, respectively. As in the case of the lower frequency measurements, the polarization dependence is not significant.

5. Asphalt vs Asphalt through Foliage

Figures 46 and 47

These measurements were performed on the lighter foliage model at 16.5 and 94 GHz. Data was not taken at 9.5 GHz due to the inoperative state of this channel at the time of measurements at Camp San Luis Obispo. For some unknown reason, measurements were not taken at an incidence angle of 30 degrees. However, the data at $\phi = 45^{o}$ is perhaps indicative. Since measurements on asphalt alone were not made, calculations of foliage attenuation are not possible for this target model.

a. 16.5 GHz Data

As shown in Figure 46, H polarization, there is a small increase in the apparent temperature of asphalt through foliage over aluminum through foliage. Referring to Figure 32, H polarization, asphalt alone has an apparent temperature approximately equal to that of the combination of foliage and asphalt in this run. However, since these runs were separated in time by several days, it is inadvisable to attempt to make precise comparisons on an absolute basis.

At V polarization, the increase in apparent temperature of asphalt through foliage, over that of aluminum through foliage, is somewhat greater than for H polarization. It is difficult to draw any significant conclusions from this comparison since only a single run is involved in each case.

b. 94 GHz Data

Referring to Figure 47, the increase in apparent temperature of asphalt through foliage, over that of aluminum through foliage is similar to the 16.5 GHz case for both polarizations. However, the absolute levels of all of the data shown in this plot are higher than those at the lower frequency. This is understandable since the apparent sky temperatures are higher at 94 GHz.

6. Bare Aluminum vs Grass vs Asphalt

Figures 48, 49, 10

These measurements were performed at the second location in Camp San Luis Obispo.

a. 16.5 GHz Data

As shown in Figure 48, the apparent sky temperature and aluminum plots are very similar to those appearing in Figure 32. In the case of H polarization, the asphalt curve is typical (in shape) and shows a contrast of 30°K from the apparent temperature of grass, at $\phi = 45^{\circ}$. As expected, the apparent temperature of grass is relatively constant from $\phi = 30^{\circ}$ to $\phi = 65^{\circ}$, although a 12°K drop is shown over this range of incidence angles indicating a slight polarization effect. Also, since a difference of 26°K exists between the apparent temperature and surface temperature of the grass, at $\phi = 45^{\circ}$, this material does not appear to be a perfect emitter.

At V polarization, the contrast between asphalt and grass disappears; the slightly higher apparent temperature of the asphalt, for part of the plot, is probably due to measurement errors.

b. 94 GHz Data

Figure 49 shows high apparent temperatures for both asphalt and grass with very little separation between these materials, at both polarizations. The grass appears to be a better emitter at this frequency than at 16.5 GHz. This seems logical since the wavelength is shorter by almost a factor of 6.

7. Painted Aluminum vs Bare Aluminum

Figures 50 and 51

As shown in both of the above plots, there is essentially no contrast between painted and bare aluminum at 16.5 and 94 GHz. This is particularly clear at the lower frequency. It will be noted that no polarization effect is evident at 16.5 GHz. In the case of 94 GHz, an excessively low apparent sky temperature has brought the absolute levels of the target curves, at V polarization, to a rather low level. This is probably the result of a calibration error. If one were to ignore the absolute level, the shapes of the target curves are somewhat similar to the vertically polarized bare aluminum curves shown in Figures 37 and 41.

8. Bare Aluminum - Weather Effects

Figures 52 and 53

Measurements were performed at the Piedras Blancas site to determine the effects of weather on the apparent temperatures of bare aluminum. There was no rain during these observations; however, considerable fog and heavy overcast prevailed during the measurements. To obtain as many runs as possible in the two days available for measurements, observations were limited to 9.5 and 94 GHz.

a. 9.5 GHz Data

Figure 52 shows three runs plotted for each polarization. No significant polarization effect is evident between the two groups of runs; however, within each group, the apparent temperatures of the bare aluminum are proportional to the values of apparent sky temperature observed in a given run. This is particularly clear in the H polarization plots. This result is as expected since bare aluminum is a very good reflector; its apparent temperatures should, therefore, vary closely with prevailing apparent sky temperatures.

b. 94 GHz Data

The results for this channel are shown in Figure 53. These are very similar to those for 9.5 GHz, with the exception that the absolute levels are somewhat higher for both apparent sky temperatures and apparent temperatures of the aluminum.

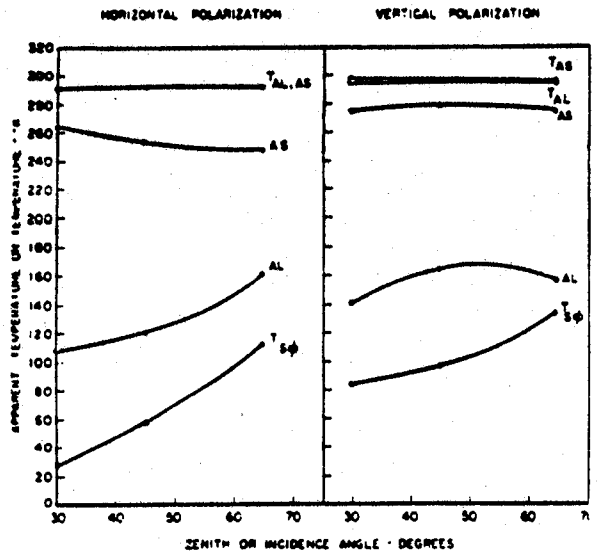

Figure 33. 94 GHz, aluminum-asphalt, dry

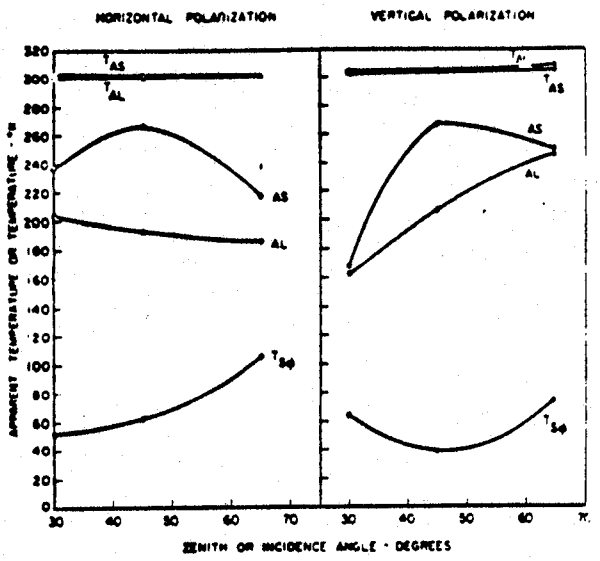

Figure 35. 94 GHz, aluminum-asphalt, wet

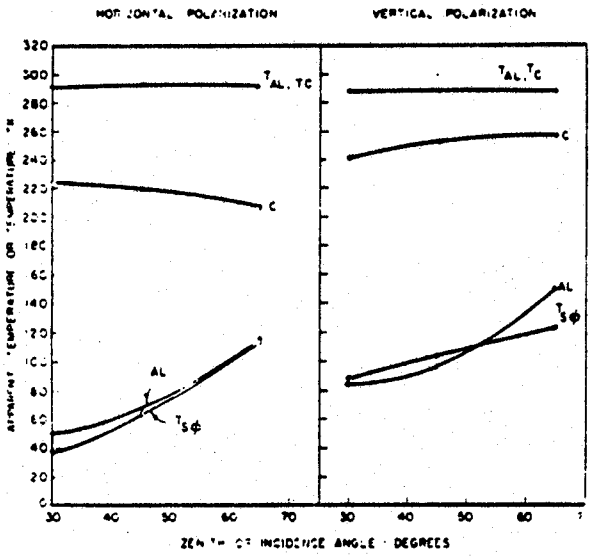

Figure 37. 94 GHz, aluminum-concrete, dry

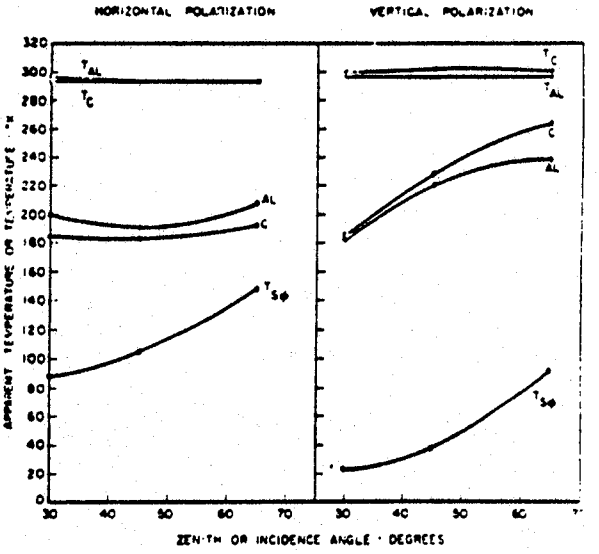

Figure 39. 94 GHz, aluminum-concrete, wet

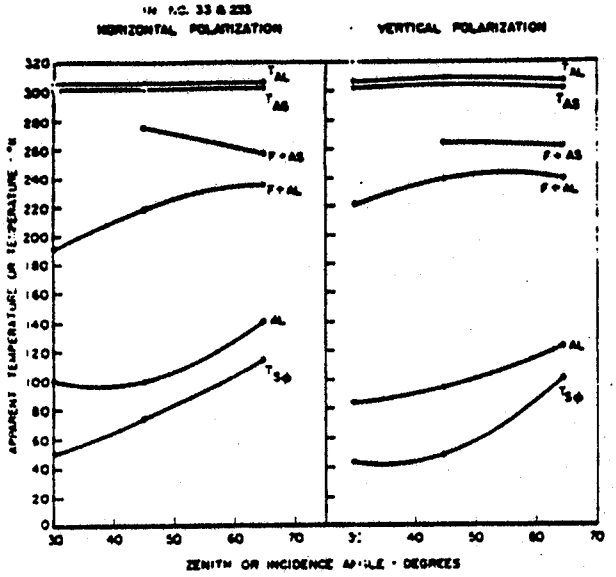

Figure 47. 94 GHz, aluminum-aluminum plus foliage-asphalt plus foliage, dry

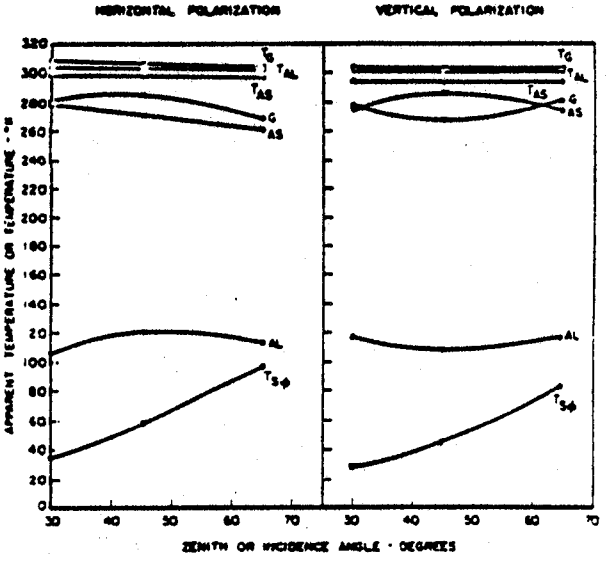

Figure 49. 94 GHz, aluminum-wood on aluminum, dry

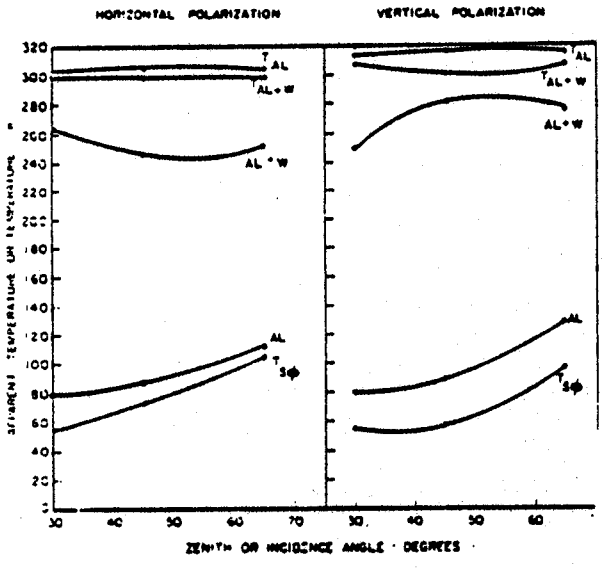

Figure 41. 94 GHz, aluminum-wood on aluminum, dry

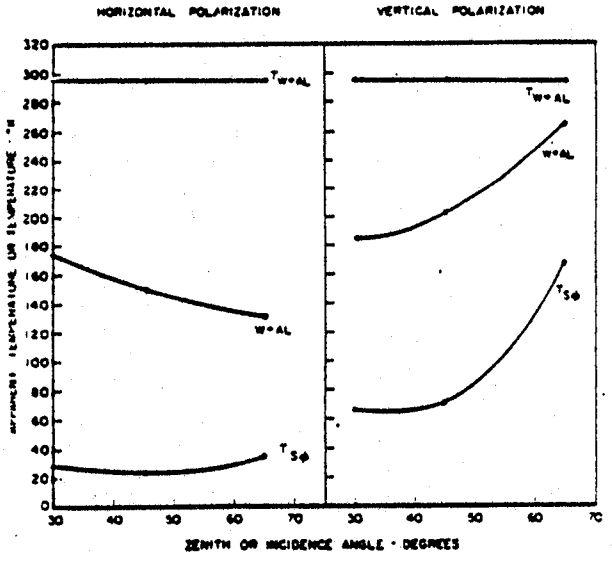

Figure 44. 94 GHz, wood on aluminum, wet

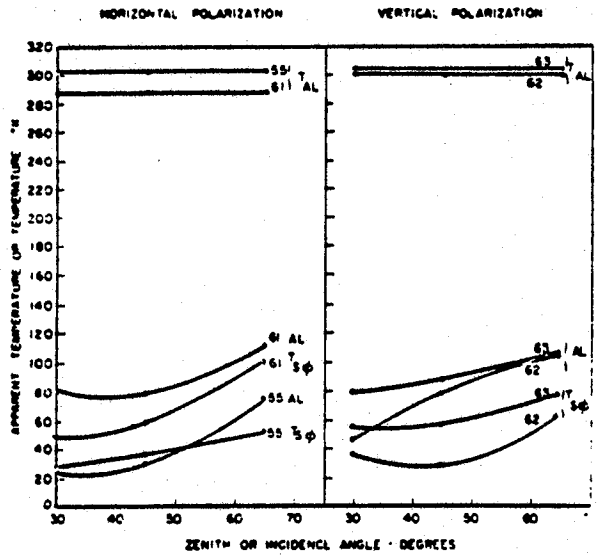

Figure 53. 94 GHz, bare aluminum, weather effects, dry

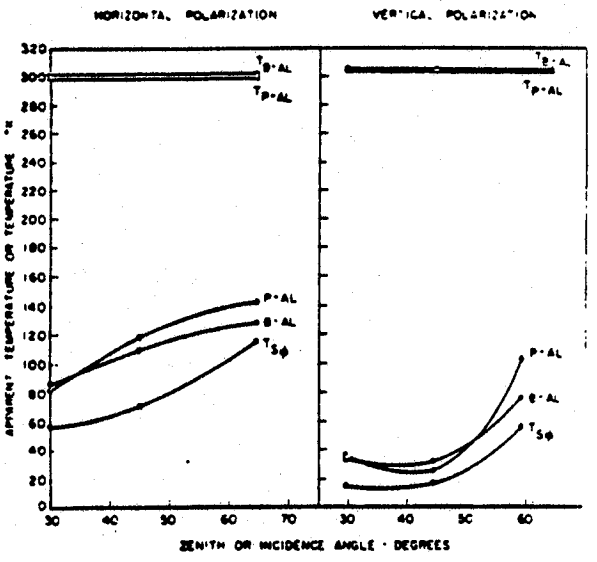

Figure 51. 94 GHz, painted aluminum, bare aluminum, dry

PREISSNER

THE INFLUENCE OF THE ATMOSPHERE ON PASSIVE RADIOMETRIC MEASUREMENTS

J. Preissner
Deutsche Forschungs- und Versuchsanstalt fuer Luft- und Raumfahrt e.V. (DFVLR)
8031 Wessling, West Germany

AGARD Conference Proceedings No. 245, February 1979
Millimeter and Submillimeter Wave Propagation and Circuits
Edited by E. Spitz and G. Cachier

This investigation is an attempt to describe completely the atmospheric influence on sensing of the earth's surface by microwave radiometers in the frequency range from 10 to 1000 GHz. The dominant influences (atmospheric gases, hydrometeors) are described. Primary attention is given to the so-called window frequencies in the range from 10 to 400 GHz.

A computer program was developed which determines, for any object on the ground, the brightness temperature as it is seen from an airborne sensor. The input required are the object parameters (physical temperature, reflectivity), parameters of the atmosphere (e.g., temperature, pressure, humidity) and parameters of hydrometeors, flight height, and sensor parameters (viewing angle, polarization, frequency). Statistical information about the atmospheric variables and the weather conditions valid for the area of West Germany is incorporated in the program in order to compute probabilities that at a given flight height and for certain regions and times of the year, objects (like woods, fields, roads, cars) can be detected. Some results of computation will be given and compared qualitatively with some actual airborne measurements at 11 GHz, 32 GHz and 90 GHz which were carried out at the DFVLR in the last few years. (Author)

EXTRACTS:

Fig. 13 shows the brightness temperatures of a lake at 90 GHz for five different flights. The fraction of cloud cover and the height of the clouds during the flights was described by the crew of the aircraft. The brightness temperature varies from about 225 to 260 K. In general the brightness temperature increases with an increase of cloud cover.

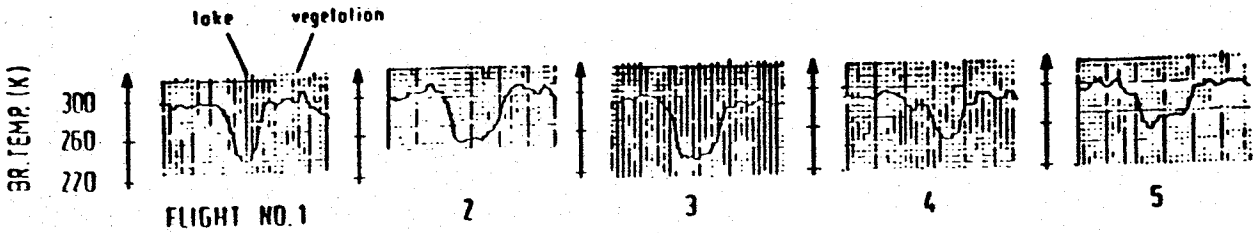

OUTPUT OF THE RADIOMETER AT A FREQUENCY OF 90 GHz

DATA ON THE WATER CONTENT OF THE CLOUDS ARE NOT AVAILABLE

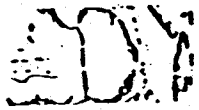

TOPOGRAPHIC MAP

FLIGHT HEIGHT :	400 M
SPATIAL RESOLUTION :	6 M
TEMPERATURE RESOLUTION :	10 K

FLIGHT NO.	CLOUD SITUATION
1	3/8 IN 1200 M
2	4/8 IN 1200 M
3	4/8 IN 600 M - 1500M
4	8/8 IN 400 M
5	8/8 IN 350 M

Figure 13 Example of a radiometric measurement at 90 GHz

RAINWATER, GALLAGHER, AND REINHART

SEASONAL ATMOSPHERIC EMISSION AT 94 GHz

J. H. Rainwater, J. J. Gallagher, and P. B. Reinhart
Georgia Institute of Technology
Engineering Experiment Station
Atlanta, GA 30332

Proceedings of the Workshop on Millimeter and Submillimeter Atmospheric Propagation Applicable to Radar and Missile Systems, Redstone Arsenal, AL 35809, O. M. Essenwanger and D. A. Stewart (editors)
Technical Report RR-80-3, 48-56, February 1980

A novel beam-waveguide millimeter radiometer feeding a 10 foot parabolic dish has been used to measure seasonal atmospheric emissions at 94 GHz. The radiometer incorporates a beam waveguide in the RF section which allows Dicke switching and calibration to be accomplished at the focal points between the beam waveguide lenses. A unique directional waveguide filter, designed and built at Georgia Tech, using a single circularly polarized cavity is used to inject the LO into a Schottky barrier mixer. The radiometric antenna half-power beamwidth is under 0.2°, thus these measurements represent atmospheric variations occuring within small spatial elements. Measurements to date have been made during high humidity, summertime conditions and during less humid, winter sky conditions; the data show seasonal emission variations due to clouds and other atmospheric conditions. Ground based measurements at the zenith and celestial equator with varying data integration times have been made. Antenna temperatures of the solar radiosphere have also been measured at a variety of azimuthal angles and atmospheric conditions. Theoretical calculations incorporating state-of-the-art H_2O, O_2, and O_3 absorption line shape expressions, water vapor distribution, temperature and pressure profiles, have been performed and exhibit a disparity with experimental measurements.

The empirical measurements have been reduced into a variety of formats including power spectral density plots which aid understanding of the nature of atmospheric "clutter". Theoretical calculations are compared with the experimental measurements and differences analyzed. (Authors)

EXTRACTS:

Using the model discussed in this article, a comparison between experimental and theoretical antenna temperatures was made.

	Antenna Temperatures (°K)			
	Experimental Min	Max	Theoretical	Figure Number
Zenith Emission Clear	144	173	142.2	2
Zenith Emission Clouds	139	266	147.56	3
Zenith Emission Short Integration	136	161	100.35	8
Solar Emission	2320	3182	3663.4	4

Some of the authors' figures are shown here.

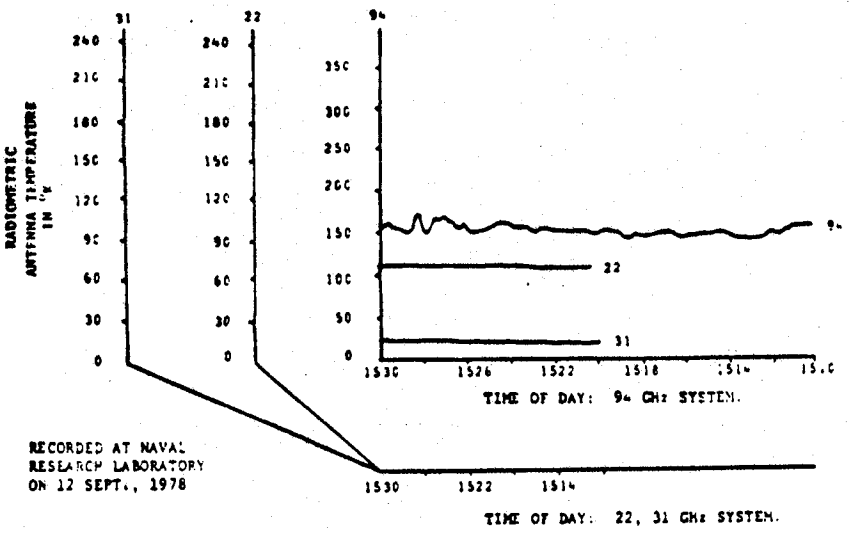

AVERAGE METEOROLOGICAL CONDITIONS AT ANTENNA SITE

AIR TEMP: 303.69°K WATER VAPOR: 20.53 g/m^3 PRESSURE: 1011.0 mb

Optically hazy with scattered cumulus clouds, no clouds over zenith during data run.

22, 31 GHz SYSTEM PARAMETERS

DSB HETERODYNE SYSTEM

LO FREQ. 22.23[illegible] GHz, 31.[illegible] GHz
IF FREQ. 10-300 MHz

POST DETECTION INTEGRATION CONSTANT 0.5 sec

ANTENNA TEMPERATURE NOISE . . . . . ΔT_{MIN} 0.098°K

ANTENNA BEAM HALF-WIDTH AT -20dB POWER POINTS 22 GHz, 10°
31 GHz, 9°

94 GHz SYSTEM PARAMETERS

DSB HETERODYNE SYSTEM

LO FREQ. 94.556 GHz
IF FREQ. 1.6 ± 0.7 GHz

POST DETECTION INTEGRATION CONSTANT 5.00 sec

ANTENNA TEMPERATURE NOISE . . . . . ΔT_{MIN} 1.13°K

Figure 2. Zenith Antenna Temperatures 22,31,94 Ghz On 12 Sept 78

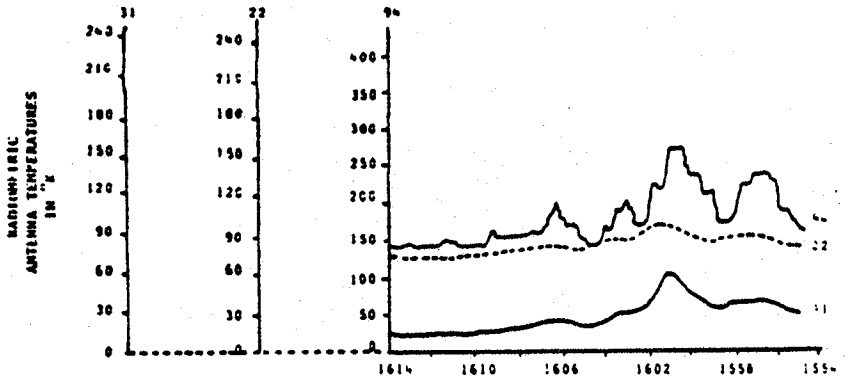

TIME OF DAY: 22, 31 and 94 GHz SYSTEMS

AVERAGE METEOROLOGICAL CONDITIONS AT ANTENNA SITE

AIR TEMP: 303.52°K WATER VAPOR: 21.75 g/m^3 PRESSURE: 1010.6 mb

Optically hazy with scattered cumulus clouds, clouds drifting over zenith during data run.

22, 31 GHz SYSTEM PARAMETERS

DSB HETERODYNE SYSTEM

LO FREQ. 22.234 GHz, 31.4 GHz
IF FREQ. 10-330 MHz

POST DETECTION INTEGRATION CONSTANT 0.5 sec

ANTENNA TEMPERATURE NOISE . . . . . ΔT_{MIN} 0.09°K

ANTENNA BEAM HALF-WIDTH AT -20dB POWER POINTS 22 GHz, 10°
31 GHz, 9°

94 GHz SYSTEM PARAMETERS

DSB HETERODYNE SYSTEM

LO FREQ. 94.554 GHz
IF FREQ. 1.6 ± 0.7 GHz

POST DETECTION INTEGRATION CONSTANT 5.00 sec

ANTENNA TEMPERATURE NOISE . . . . . ΔT_{MIN} 1.26°K

*22 and 31 GHz Antenna Temperatures plotted every 30 seconds such that time scales for 22, 31 and 94 GHz systems are coincident.

Figure 3. Zenith Antenna Temperatures : 22,31,94 GHz On 12 Sept 78

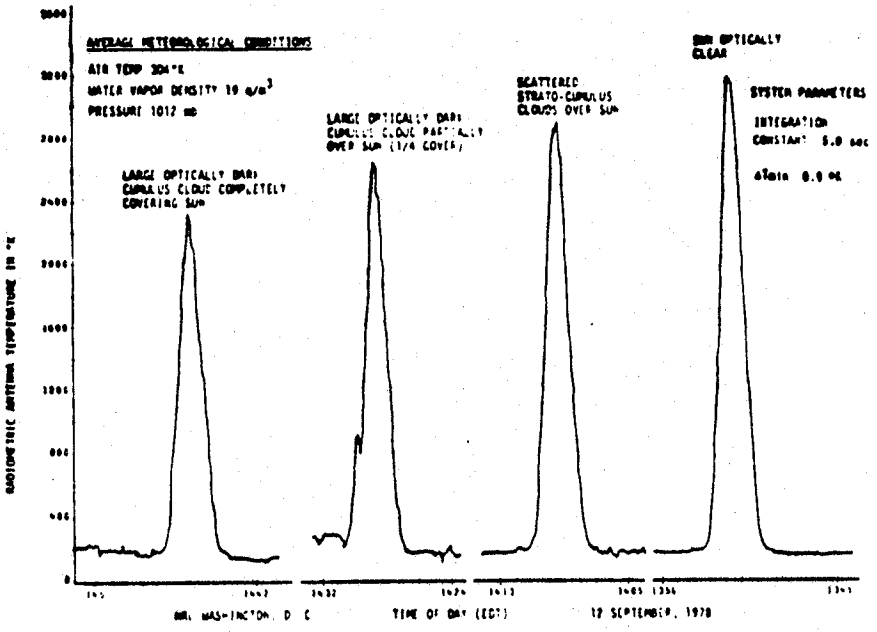

Figure 4. Attenuation Of Solar Radiation By Cumulus Cloud

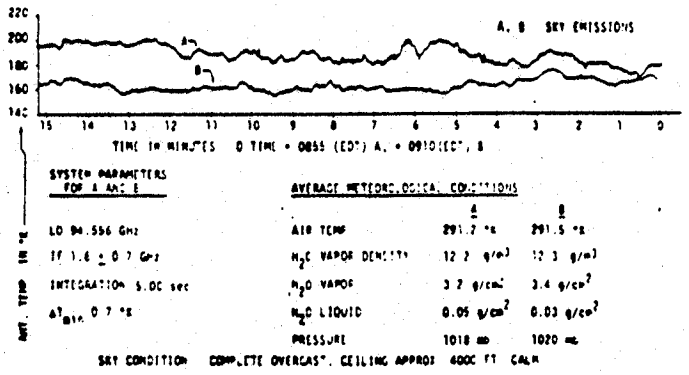

Figure 5. Emissions At Celestial Equator On 13 Sept 78

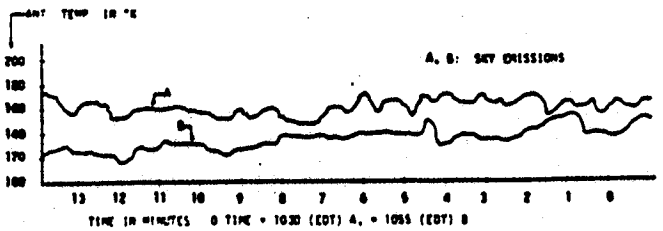

SYSTEM PARAMETERS FOR A AND B

LO 94 556 GHz
IF 1.6 ± 0 7 GHz
INTEGRATION 5 00 sec
ΔT_{min} 0.3 °K

AVERAGE METEOROLOGICAL CONDITIONS

	A	B
AIR TEMP	290 4 °K	290 9 °K
H_2O VAPOR DENSITY	12.0 g/m^3	12.0 g/m^3
H_2O VAPOR	3.5 g/cm^2	4.0 g/m^2
H_2O LIQUID	0.04 g/cm^2	0.02 g/cm^2
PRESSURE	1020 mb	1020 mb

SKY CONDITION: COMPLETE OVERCAST, CEILING APPROX 6000 FT
MODERATE BREEZE

Figure 6. Emissions At Zenith On 13 Sept 78

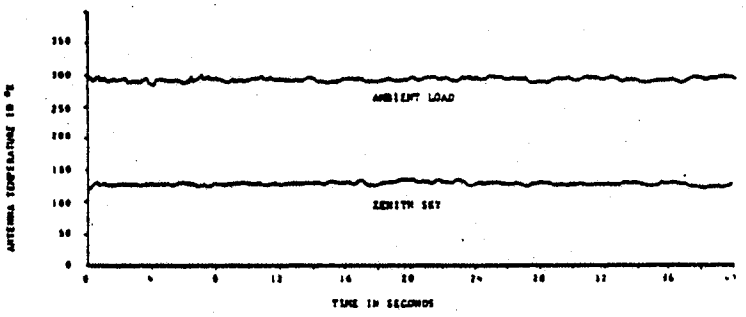

RECORDED AT NAVAL RESEARCH LABORATORY ON 13 SEPTEMBER 1978 AT 11.22 HOURS LOCAL

METEOROLOGICAL CONDITIONS AT ANTENNA SITE

AIR TEMPERATURE	291°K
WATER VAPOR	11.5 g/m^3
PRESSURE	1020.9 mb
SCATTERED STRATUS CLOUDS AT ZENITH	

94 GHz SYSTEM PARAMETERS

DBD HETERODYNE SYSTEM	
LO FREQ 94.556 GHz IF FREQ 1.6 ± 0 7 GHz	
POST DETECTION INTEGRATION CONSTANT	0.05 sec
ANTENNA TEMPERATURE NOISE ΔT_{min}	1.75°K

Figure 7. Emissions At Zenith On 13 Sept 78 -- Reduced Integration Constant

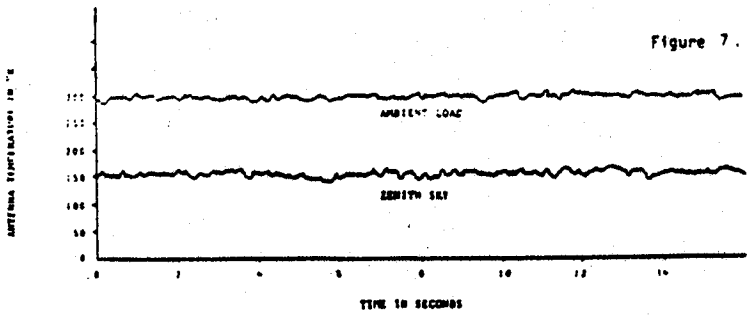

RECORDED AT NAVAL RESEARCH LABORATORY ON 13 SEPTEMBER 1978 AT 11:34 HOURS LOCAL

METEOROLOGICAL CONDITIONS AT ANTENNA SITE

AIR TEMPERATURE	291°K
WATER VAPOR	11.5 g/m^3
PRESSURE	1020 9 mb
SCATTERED STRATUS CLOUDS AT ZENITH	

94 GHz SYSTEM PARAMETERS

DBD HETERODYNE SYSTEM	
LO FREQ 94.556 GHz IF FREQ. 1.6 ± 0 7 GHz	
POST DETECTION INTEGRATION CONSTANT	0.016 sec
ANTENNA TEMPERATURE NOISE ΔT_{min}	1.0.1°K

Figure 8. Emissions At Zenith On 13 Sept 78 With 0.016 sec Integration Constant

ABSOLUTE MEASUREMENTS OF THE ATMOSPHERIC TRANSPARENCY AT SHORT MILLIMETER WAVELENGTHS

D. P. Rice
Division of Quantum Meteorology
National Physical Laboratory
Teddington, Middlesex

P. A. R. Ade
Department of Physics
Queen Mary College
Mile End Road
London E1 4NS

Preprint, 1979

Spectral measurements of the atmospheric opacity in the 0.77 - 3.3 mm region have been made using a phase-modulated Michelson interferometer. The data are calibrated using a black body source to give absolute measurements. An independent measurement of the total atmospheric water vapor concentration is obtained from a near-infrared hygrometer which is itself calibrated against simultaneous radiosonde data. A theoretical atmospheric transmission model is used to compare the two sets of data. We have found a large discrepancy between our theory and the experimental data amounting to more absorption than predicted. This anomalous absorption shows no spectral features and scales with water vapor concentration. There is no indication of any water vapor dimer lines or of any other minor features except those due to ozone. (Authors)

RICHARD*

MILLIMETER WAVE RADAR APPLICATIONS TO WEAPONS SYSTEMS

Victor W. Richard
U.S. Army Ballistic Research Laboratory
Aberdeen Proving Ground, MD 21005

BRL Report No. 2631, June 1976
ADB 012 103L (A79 06508)

Applications of millimeter wave radars in ground-to-air, ground-to-ground, and air-to-ground weapons systems are presented. The advantages and limitations of operating at millimeter wavelengths are defined.

The characteristics of millimeter wave propagation in adverse weather are described with emphasis on rain backscatter and attenuation theory, experimental data, and rain effects on radar system performance.

The theory of fluctuating clutter is discussed and a terrain clutter model is presented whose output is characterized by its power spectral density and probability density function. Several clutter discrimination techniques are described.

The status of millimeter-wave radars and components is reviewed and technology advances required are pointed out. (Author)

MILLIMETER WAVE RAIN BACKSCATTER MEASUREMENTS

Victor Richard and John Kammerer
U.S. Army Ballistic Research Laboratory
Aberdeen Proving Ground, MD 21005

1974 Millimeter Wave Techniques Conference, Volume I, Navy Electronics Laboratory Center, San Diego, CA 92152, p. B1-1 to B1-30, 26-28, March 1974
ADA 009 512 (A79 06241)

An experiment was conducted to measure rain backscatter at 10, 35, 70 and 95 GHz over a wide range of rain intensities. This experiment was prompted by our previous experience that there appeared to be an appreciable variance between the magnitude of observed and calculated rain backscatter at millimeter wavelengths. A search for references on rain backscatter above 10 GHz disclosed thirty-four technical articles[1-34] of which seven cite measurements.[11,12,13,20,21,22,28] It is significant to note that over three hundred references were found on rain attenuation above 10 GHz. Millimeter wave rain attenuation has been investigated in the past much more thoroughly than rain backscatter. No references were found on rain backscatter measurements made simultaneously at the different propagation window frequencies. In view of the wide spread of rain backscatter data typically observed during different rain storms of the same intensity, simultaneous measurements at different frequencies were considered essential to accurately determine the wavelength dependence of rain backscatter.

The experiment conducted was unique in that rain backscatter measurements were made simultaneously at 10, 35, 70 and 95 GHz while continuous measurements of raindrop size and rainfall rate were being made. Raindrop size distribution was measured with three drop-size spectrometers furnished by the Illinois State Water Survey, Urbana, Illinois. Rainfall rate was measured with three tipping bucket rain gauges.

The experiment was conducted at McCoy Air Force Base, Orlando, Florida, during August and September 1973. This site was selected because of the afternoon rains that occur almost daily in this area in the summer. It rained twenty-five times during the period of August 10 to September 7, ranging in intensity from drizzles up to a very heavy rainfall of 150 mm/hr. (Authors)

EXTRACTS:

We include here the author's list of references.

REFERENCES

1. Atlas, D. et al., "Weathors Effects on Radar, Air Force Surveys in Geophysics, No. 23, Cambridge, Air Force Cambridge Research Center, December 1952.

2. Boston, R. C., "Radar Attenuation and Reflectivity Due to Size-Distributed Hydrometeors," J. Appl. Meteor. 9:188-91, 1970.

3. Buige, A., and Levatich, J. L. "Measurement of Precipitation Scatter Effect on Propagation at 6, 12, and 18 GHz," AIAA Conference Proceedings, Los Angeles, California, April 1970.

4. Chu, C. W., "Scattering and Absorption of Water Droplets at Millimeter Wavelengths," Ph. D. Dissertation, University of Michigan, 1962.

5. Crane, R. K., "Microwave Scattering Parameters for New England Rain," Lincoln Laboratory, MIT, Tech Rpt 426, 3 October 1966.

6. Funakawa, K., "Measurement of Total Cross Sections of Water Drops at 5 mm Wave Length Utilizing the 'Shadow Theorem'," J. Inst. Elev. Common. Engrs. Japan, 48, pp 84-91, 1965.

7. Godard, S. L., "Propagation of Centimeter and Millimeter Wavelengths Through Precipitation," IEEE Trans. on Antennas and Propagation, Vol AP-18, No. 4, pp 530-534, July 1970.

8. Gunn, K. L. S., and East, T. W. R., "The Microwave Properties of Precipitation Particles," Quarterly Journal of the Royal Meteorological Society, Vol. 80, pp. 535-545, October 1954.

9. Hawkins, H. E., and La Plant, O., "Radar Performance Degradation in Fog and Rain," IRE Transactions on Aeronautical and Navigational Electronics, pp. 26-30, March 1959.

10. Hall, W. M. "Prediction of Pulse Radar Performance," Proc. of IRE, pp. 224-231, February 1956.

11. Hooper, J. E. N., and Kippax, A. A., "Radar Echos from Meteorological Precipitation," Proc. IEEE (London), Vol. 197, Part 1, pp. 89-97, May 1950.

12. Kiely, D. G., "Rain Clutter Measurements with CW Radar Systems Operating in the 8 mm Wavelength Band, Proc. IEEE (British), Vol. 101, Part 9, No. 70, pp. 101-108, March 1954.

13. Koester, K. L., Kosowsky, L., Chanzit, L., "Propagation of 70 GHz Energy Through Rain and Fog," Report No. 430280001, 16 March 1971, Norden Division of United Aircraft Corp., Norwalk, Connecticut.

14. Larmers, U., "Measurements of the Backscatter from Water Drops and the Effect of Their Shape on Millimetric Waves," Report from the Henrich Hertz Institute for Oscillation Research, Barliz Charlottenburg, NTZ-CJ, No. 4, pp. 167-169, 1967.

15. Mitchell, R. L., "Radar Meteorology at Millimeter Wavelengths," Aerospace Corp. Rpt. TR-669(6230-46)-9, June 1966, Air Force Report No. SSD-TR-66-11T, AD488085.

16. Mitchell, R. L., "Scattering and Absorption Cross Sections of Water Spheres at Millimeter Wavelengths," Aerospace Corp., El Segundo, California, Rpt. TR-669(6230-46)-11, 1966.

17. Mitchell, R. L., "Remote Sensing of Rain by Radar," Aerospace Corp., Rpt. No. TR-0158(3525-09)-1, Air Force Rpt., No. SAMSO-TR-68-115, Jan. 1968.

18. Mueller, E. A., and Sims, A. L., Relationships Between Reflectivity, Attenuation, and Rainfall Rate Derived from Drop Size Spectra," R&D Tech. Rpt. ECOH-02071-F, Final Report, May 1969, U.S. Army Electronics Command, Ft. Monmouth, N. J., Atmospheric Sciences Lab., Contract DA-28-043-AMC-02071(E), Illinois State Water Survey, Univ. of Illinois, Urbana, Ill.

19. Probert-Jones, J. R., "The Radar Equation in Meteorology," Quart. J. Roy. Meteor, Soc., 88:485-95, 1962.

20. Richard, V. W., "Millimeter Wave Radar Applications to Weapons Systems," Ballistic Research Laboratories, Aberdeen Proving Ground, Interim Memorandum Report No. 61, October 1972.

21. Robert, D. E., "Melting Bands and Precipitation Rates," Decca Radar, Radar Research Laboratories, RL 1902, 1959.

22. Robinson, N. P., "Measurements of the Effect of Rain, Snow, and Fogs on 8.6 mm Radar Echoes," IEEE London, Paper No. 1898R, Sep 1955.

23. Rogers, C. W. C., and Wexler, R., "Rainfall Determination from 0.86 and 1.82 cm Radar Measurements," Proc. Tenth Weather Radar Conference, Boston Amer. Meteor. Soc., pp. 260-270.

24. Rozenberg, V. I., "Radar Characteristics of Rain in Submillimeter Range," Radio Engineering and Electronic Physics, Vol. 15, No. 12, pp. 2157-2163, 1970.

25. Ryde, J. W., "The Attenuation and Radar Echoes Produced in Centimetre Wavelengths by Various Meteorological Phenomena," in "Meteorological Factors in Radio Wave Propagation," Physical Society Report, London, 1946.

26. Ryde, J. W., "The Attenuation of Centimetre Radio Waves and Echo Intensities Resulting from Atmospheric Phenomena," Jour. I.E.E., 93, Part IIIA, p. 101, 1946.

27. Straiton, A. W., Fannin, B. M., et al., "Atmospheric Limitations on the Use of Radio Waves with Frequencies of 15, 35, and 95 GHz," AFAL-TR-72 264, 22 Sep 72, AD 903 896.

28. Tolbert, C. W., Gerhardt, J. R., and C. O. Britt, "Backscattering Cross Sections of Water Droplets, Rain and Foliage at 4.3 Millimeter Radio Wavelengths," Electrical Eng. Research Lab., University of Texas, Report No. 91, 30 April 1957.

29. Usikov, A. Ya., German, V. L., Vakser, I. kh., "Investigation of the Absorption and Scatter of Millimeter Waves in Precipitations," Ukr. Fiz., Zh., Vol. 6, Mo. 5, pp. 618-640, 1961.

30. Vogel, W., "Rain Attenuation and Backscatter of Radio Waves in the Millimeter Region," Technical Report No. 69-3, AFAL, WPAFB, 30 April 1969, AD 852 713.

31. Vogel, W., "Scattering Intensity Plots and Transmission Coefficients for Millimeter-Wave Propagation Through Rain," Technical Report No. AFAL-TR-71-345, WPAFB, AFAL, 31 October 1971, AD 890 408.

32. Wexler, A., and Atlas, D., "Radar Reflectivity and Attenuation of Rain," J. Appl. Meteor, 2:276-80, 1963.

33. Wilcox, F. P., Ewen, K., Blair, L. R., et al., "Analysis and Definition of Millimeter-Wave Radars," TR AFAL-TR-73-232, July 1973, Goodyear Aerospace Corp., Litchfield Park, Arizona, WPAFB, AFAL, Contract F33615-72-C-1831.

34. "Precipitation Scattering Considerations at Frequencies Above 10 GHz," CCIR (International Radio Consultative Committee), Document V/117, June 16, 1969.

35. Probert-Jones, J. R., "The Radar Equation in Meteorology," Vol. 88, pp. 485-495, Quart. J. Roy. Meteorological Soc., 1962.

36. Grant, E. H., Buchanan, T. J., & Cook, H. F., "Dielectric Bch of Water at Microwave Frequencies," J. Chem. Phys. 26, No. 1, 1957.

RAIN BACKSCATTER MEASUREMENTS AND THEORY AT MILLIMETER WAVELENGTHS

Victor W. Richard and John E. Kammerer
Army Ballistic Research Laboratories
Aberdeen Proving Ground, MD 21005

BRL Report No. 1838, October 1975
ADB 008 173L (A79 06509)

An experiment was performed to measure the properties of rain backscatter between 10 and 100 GHz over a range of rain intensities from drizzles up to 100 mm/hr. Rain backscatter amplitude and fluctuation measurements were made simultaneously at 10, 35, 70, and 95 GHz with pulse radars for both linear and circular polarization along with rainfall rate and raindrop size measurements. The measured rain backscatter versus rainfall rate data are compared with data calculated by a number of authors based on a variety of raindrop-size distribution and scattering theory assumptions. The status of the theory of rain backscatter and attenuation at millimeter wavelengths is reviewed, supplemented by numerous references and a bibliography which contains a number of Soviet articles. A brief review of raindrop-size measuring technology is included.

Examples of the radar range reduction by rain backscatter and attenuation are given. The reduction in range by rain backscatter is shown to be severe in the region of 35 GHz compared with lower and higher frequencies for a constant antenna size. Particularly significant is the experimental verification of the expected decrease in the rain backscatter coefficient above 70 GHz. This experiment verifies the long-standing theoretically predicted capability of a radar to "see" a given size target above the rain clutter better at 95 GHz than at 70 or 35 GHz when the same antenna size is used. (Authors)

RICHARD, KAMMERER, AND REITZ

140-GHz ATTENUATION AND OPTICAL VISIBILITY MEASUREMENTS OF FOG, RAIN AND SNOW

V. W. Richard, J. E. Kammerer, and R. G. Reitz
U.S. Army Ballistic Research Laboratory
Aberdeen Proving Ground, MD 21005

BRL Memo Report No. 2800, December 1977
ADA 651 055 (A78 03741)

The attenuation of fog, rain and snow has been measured at 140 GHz for rainfall intensities varying from drizzles up to 20 mm/hr and over a wide range of fog and snowfall intensities. Measured attenuation data are compared with theoretically derived attenuation data. Optical visibility and 140-GHz attenuation measurements were made simultaneously, providing comparisons between optical and millimeter wave system capabilities under degraded weather conditons.

A brief review of the theoretical and experimental work of a number of authors on the computation and measurement of fog, rain and snow attenuation at 140 GHz is presented. An extensive reference and bibliography list is given which includes a number of articles from Soviet open literature. (Authors)

EXTRACTS:

Visibility was measured by continuously recording the level of light from a source at either 725 or 68 meters.

Measurements were taken 1.5 m above a field.

The transmitting antenna was 725 m away from the 140-GHz receiver.

Clear weather, rain, snow, and fog attenuations were measured and compared to calculated values. Visibility under these conditions was also measured.

We include here the authors' extensive bibliography and reference list.

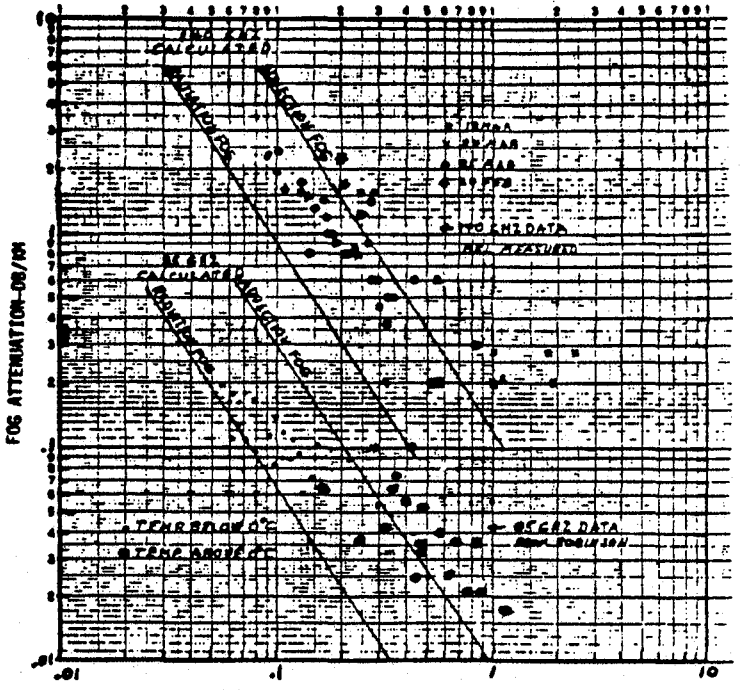

Figure 10. Measured and Calculated 35 and 140 GHz Fog Attenuation

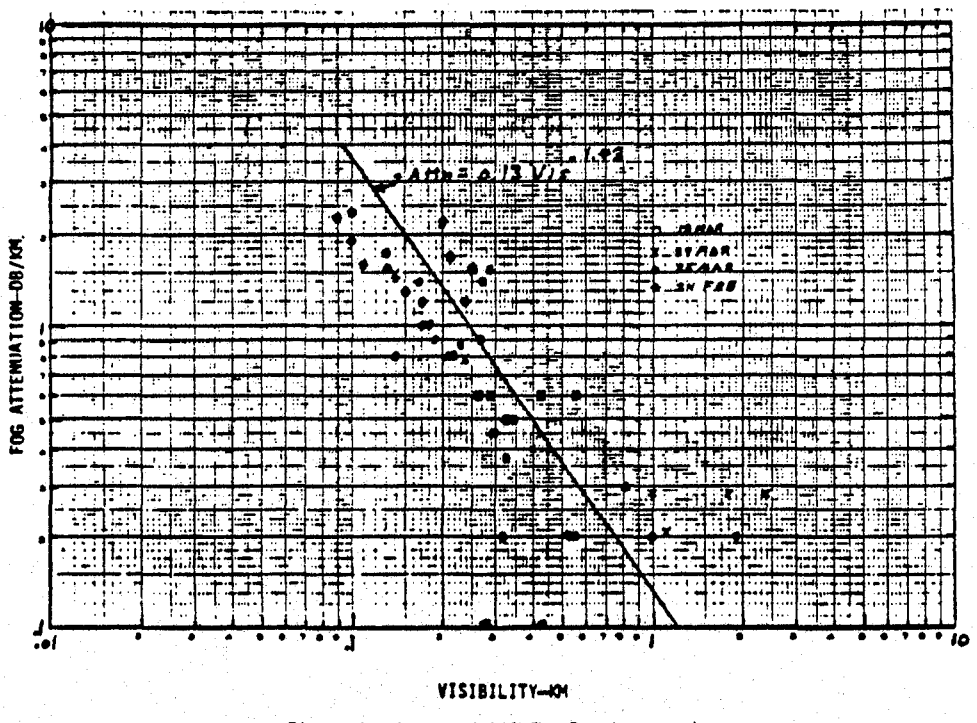

Figure 9. Measured 140 GHz Fog Attenuation

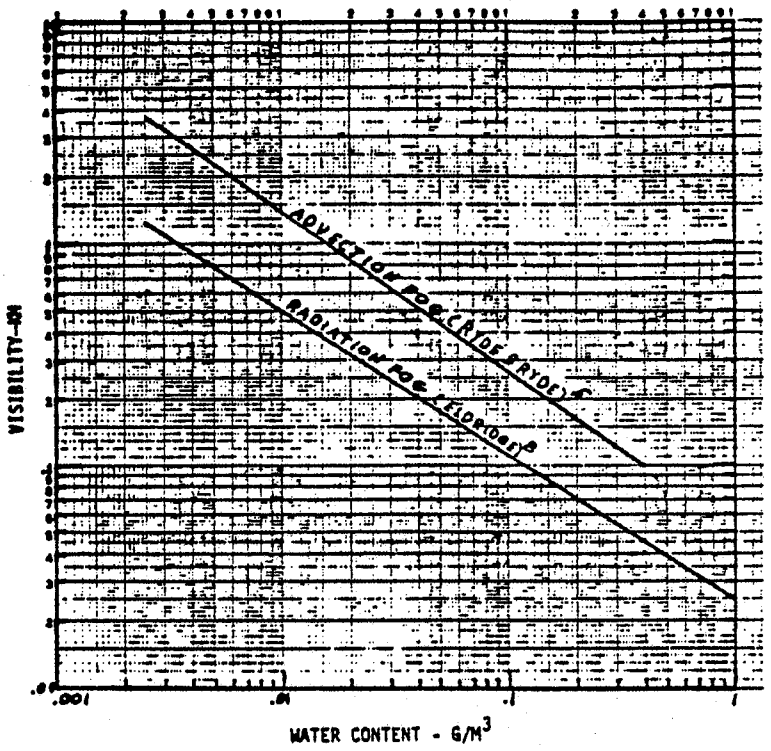

Figure 11. Fog Visibility Versus Liquid Water Content

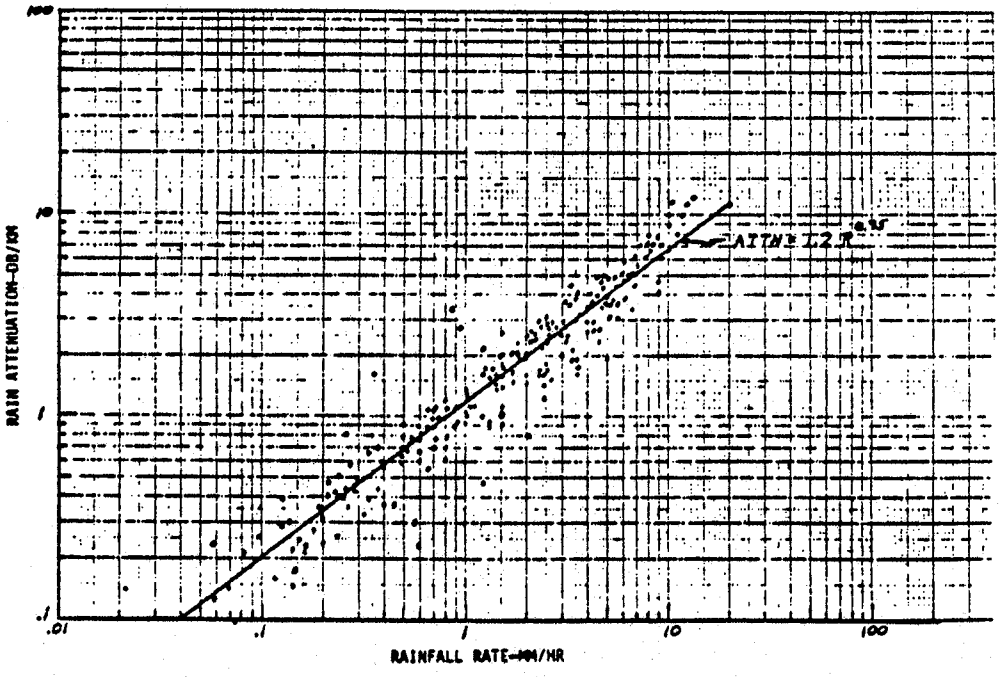

Figure 16. Measured One-Way Attenuation 140 GHz Versus Rainfall Rate

REFERENCES

1. Middleton, Visibility Through the Atmosphere, Univ. of Toronto Press, 1958.

2. Robinson, N.P., "Measurements of the Effect of Rain, Snow, and Fogs on 8.6 mm Radar Echoes," Proc. IEE, London, 102B, Paper No. 189R, 709-714, Sep 1955.

3. Lukes, G.D., "Penetrability of Haze, Fog, Clouds, and Precipitation on Radiant Energy Over the Spectral Range 0.1 Micron to 10 Centimeters," The Center for Naval Analyses, Univ. of Rochester, Study No. 61, May 1968. AD 847 658

4. Koester, K.L. and Kosowsky, L.H., "Attenuation of Millimeter Waves in Fog," 14th Radar Meteorology Conf., Tucson, AZ, 17-20 Nov 1970; also, Norden Div of United Aircraft Corp., Rpt X31051, 10 Aug 1970.

5. Koester, K.L. and Kosowsky, L.H., "Millimeter Wave Propagation in Fog," IEEE, Ant. and Prop. Symp., 20-24 Sep 1971, Los Angeles, CA; Norden Div United Aircraft Rpt X31059, 14 Jun 1971.

6. Ryde, J.W. and Ryde D., "Attenuation of Centimeter and Millimeter Waves by Rain, Fog, and Clouds," Tech Rpt 8670, British General Electric Co., Wambly, England, May 1945; also, earlier report, GEC No. 7831, Oct 1941, Ryde and Ryde. See also C.R. Burrows and S.S. Atwood, Radio Wave Propagation, Academic Press, NY, Vol II, Chap 5, 1949.

7. Kerr, D.E., Propagation of Short Radio Waves, McGraw-Hill, 11, NY, 1951.

8. Skolnik, M., Introduction to Radar Systems, McGraw-Hill, NY, 1962.

9. Eldridge, R.G., "Haze and Fog Aerosol Distributions," J. Atmospheric Sci., 23, 605-613, 1966.

10. Mason, E.J., The Physics of Clouds, Oxford, Clarendon Press, 1957.

11. Atlas, D. "Advances in Radar Meteorology," Advances in Geophysics, Vol 10, 317-478, Academic Press, NY, 1964.

12. Saxton, J.A. and Lane, J.A., "The Anomalous Dispersion of Water at Very High Radio-Frequencies," Meteorological Factors in Radiowave Propagation, Physical Society, London, Parts I, II and III, 1946.

13. Saxton, L.A., "Dielectric Dispersion in Pure Polar Liquids at Very High Radio-Frequencies, II. Relation of Experimental Results to Theory," Proc. Royal Soc., A, 213, p 473, 1952.

REFERENCES

14. Lane, J.A. and Saxton, J.A., "Dielectric Dispersion in Pure Polar Liquids at Very High Radio-Frequencies. I. Measurements of Water, Methyl, and Ethyl Alcohols," Proc. Royal Soc., 213, p 400, 1952; also, J. Opt. Soc. Proc. Royal Soc. Am., 56, No. 10, p 1398, 1966.

15. Chamberlain, J.E., et al, "Submillimetre Absorption and Dispersion of Liquid Water," Nature, 210, 790-791, May 21, 1966.

16. Deirmendjian, D., "Complete Microwave Scattering and Extinction Properties of Polydispersed Cloud and Rain Elements," The Rand Corp., R-422-PR, Dec 1963.

17 Deirmendjian, D., Electromagnetic Scattering and Spherical Polydispersions, American Elservier Pub. Co. Inc., NY, 1969.

18. Mitchell, R.A. "Radar Meteorology of Millimeter Wavelengths," Aerospace Corp., Rpt TR-699(6236-46)-9, Air Force Rpt SSD-TR-66-117, Jun 1966. AD 488 085.
NOTE: Fig. 4, rain attenuation at 1 mm wavelength, is in error according to Mitchell's later report, "Remote Sensing of Rain by Radar," TR-0158(3525-09)-1, AF No. SAMSO-TR-68-115, Jan 1968.

19. Stanevich, A.E., and Yaroslavskii, N.G., "Absorption of Liquid Water in the Lone-Wavelength Part of the Infrared Spectrum (42-2000 microns)," Optics and Spectroscopy, 10, 278-279, Apr 1961.

20. Malyshenko, Y.I. and Wachser, I.K., "Calculation of the Dielectric Constant of Water in the Submillimetre Range of Radio Waves," Ukrain. Phys., 15, No. 5, 1970.

21. Chu, T.S., and Hogg, D.C. "Effects of Precipitation at 0.63, 3.5, and 10.6 Microns," BSTJ, 47, No. 5, 723-759, May-Jun 1968.

22. Dudzinsky, S.J., "Atmospheric Effects on Terrestrial Millimeter-Wave Communications," Rand Corp., Rpt R-1335-ARPA, Mar 1974.

23. Wilcox, F., "Millimeter Wave Radar," Proj. No. 1709-74-D6, JERA-2048, Goodyear Aerospace Corp., Arizona Division, Litchfield Park, AZ, 85340, 10 Apr 75.

24. Rogers, T.F., "An Estimate of the Influence of the Atmosphere on Airborne Reconnaissance Radar Performance," Prop. Lab., Air Force Cambridge Reas. Ctr., 4 Jan 1953.

25. Tolbert, C.W. and Gerhardt, J.R. and Bahn, W.W., "Rainfall Attenuation of 2.15 MM Radio Wavelength," EERL Rpt 109, Univ. of Texas, Austin, TX, 12 Jun 1959.

REFERENCES

26. Sander, J., "Research on the Attenuation of Electromagnetic Waves by Rain with 52, 90.8, and 150 GHz," Doctoral Engineering Dissertation, Tech. Univ., Berlin, D83. Translation, US Army Foreign Science and Technology Center, FSTC-HT-23-299,75, DIA Task No. T741801, 27 Mar 75.

27. Sander, J., "Rain Attenuation of Millimeter Waves at λ = 5.77, 3.3, and 2 mm," IEEE Trans. Ant. & Prop., AP-23, 2, 213-220, Mar 75.

28. Zuffrey, C.H., "A Study of Rain Effects on Electromagnetic Waves in the 1-600 GHz Range," Master's Thesis, Dept Electrical Engineering, Univ. of Colorado, 1972.

29. Laws, O.J. and Parsons, D.A., "The Relation of Raindrop Size to Intensity," Trans. Am. Geophysical Union, Vol 24, 452-460, 1943.

30. Marshall, J.S. and Palmer, W. McK. "The Distribution of Raindrops With Size," Journ. of Meteorology, Vol. 5, 165-166, Aug 1948.

31. Lammers, U.H.W., "Electrostatic Analysis of Raindrop Distributions," J. Appl. Meteor., 8, 3, 330-334, 1969.

32. Setzer, D.E., "Computed Transmission Through Rain at Microwave and Visible Frequencies," BSTJ, 49, p1873-, 1970.

33. Sokolov, A.V. and Sukhonin, Ye. V., "Attenuation of Submillimetre Radio Waves in Rain," Radio Eng. and Elec. Phys, 15, 12, 2167-2171, Dec 1970.

34. Polakova, Ye. A., "Investigation of the Microstructure of Rains in Connection with the Question of Their Transparency," Trans. (Trudy GCO), Proc. of the Main Geophysical Observatory, Issue 220, Chap. 2, Sec 4, (Gidrometacizdat) 1967.

35. Rozenberg, V.I., "Radar Characteristics of Rain in Submillimetre Range," Radio Eng. and Elec. Phys., 15, 12, 2157-2163, Dec 1970.

36. Best, A.C., "The Size Distribution of Raindrops," Quart. J. Roy. Soc., 76, 16-36, 1950.

37. Naumov, A.D. and Stankevich, V.S., "On the Attenuation of Millimetre and Submillimetre Radio Waves in Rain," (Izv. Vuz), Radio Phys. & Quantum Elec., 145-147, Feb 1969.

38. Lammers, U. "Investigations on the Effects of Precipitation of MM-Wave Propagation," Doctoral-Engineering Dissertation, Tech. Univ., Berlin, D83, 1965. Translation by US Army Foreign Science and Technology Center, FSTC-HT-23-0298-75, DIA Task No. T741801, 1975.

REFERENCES

39. Lammers, U., "The Attenuation of MM-Waves by Meteorological Precipitation," Nachr. Tech. Z., 19, 1956 and NTZ-Commun. Jour., 16, No. 5-6, 1967.

40. Babkin, Yu. S., Ishakov, I.A., Sokolov, A.V., Stroganov, L.I., and Sukhonin, Ye. V., "Attenuation of Radiation at a Wavelength of 0.96 MM in Snow," Radio Eng. and Elec. Phys., 15, 12, 2171-2174, 1970.

41. Sokolov, A.V. "Attenuation of Visible and Infrared Radiation in Rain and Snow," Radio Eng. and Elec. Phys., 15, 12, 2175-2178, 1970.

42. Gunn, K.L.S., and East, T.W.R., "the Microwave Properties of Precipitation Particles," Quart. J. Roy. Meteor. Soc., 80, 533-545, Oct 1954.

43. Cumming, W.A., "The Dielectric Properties of Ice and Snow at 3.2 Cm," J. Appl. Phys., 23, p768, 1952.

44. Gunn, K.L.S. and Marshall, J.S., "The Distribution of Size of Aggregate Snowflakes," J. Meteor., 15, p452, 1958.

45. Langleben, M.P., "The Terminal Velocity of Snow Aggregates," Quart. J. Roy. Meteor. Soc., 80, p174, 1954.

46. Kislovskiy, L.D., Optics and Spectroscopy, No. 1, p672, 1956.

47. Steineman, A. and Granicher, H., Helv. Phys. Acta., 30, p553, 1957.

48. Smyth, C.P., and Hitchcock, C.S., J. Am. Chem. Soc., 54, p4631, 1932.

49. Asari, E., "Propagation in Snow," Electronics and Communications in Japan, 52-B, 11, 69-76, 1969.

50. Rozenblum, E.S., "Atmospheric Absorption of 10-400 KMCPS Radiation; Summary and Bibliography to 1960," MIT, Lincoln, Lab. Rpt. 826-0021, Aug 15, 1960, AD 242 598; also, Microwave Journal, Mar 1961.

51. Tolbert, C.W., Straiton, A.W. and Douglas, J.H., "Studies of 2.15 MM Propagation at an Elevation of 4 KM and the Millimeter Absorption Spectrum," EERL Rpt. No. 104, Univ. of Texas, Austin, TX, 1 Nov 1958.

52. Aganbekyan, K.A., Zrazhevskiy, A. Yu, and Malinkin, V., "Temperature Dependence of the Absorption of Radio Waves by Atmospheric Water Vapor at the 10 cm - 0.27 mm Wavelengths," Radio Eng. & Elect. Phys., 20, 1-6, Nov 1975.

BIBLIOGRAPHY

PROPAGATION AT AND ABOVE 140 GHZ

Survey and Literature Search Reports

1. DDC Report Bibliography, "MM Wave Propagation," DDC Search Control No. 023540, Nov 1974.

2. Hunt, W.T., "Survey of Attenuation by the Earth's Atmosphere at Millimeter Radio Wavelengths," Wright Air Dev. Div., USAF, Tech Note 60-232, Nov 1960. AD 252126.

3. Lurge, J., "Survey of the Literature on Millimeter and Submillimeter Waves," TRG-127-SR-2 for AFCRL, SR No. 2, June 30, 1960. AD 243342.

4. National Tech. Info. Service (NTIS), U. S. Dept. of Commerce, Springfield, VA 22151, "Millimeter Wave Rain Attenuation and Back-Scatter," March 11, 1975.

5. NASA Literature Search, "Attenuation and Backscattering of Millimeter Waves in the Atmosphere," NASA Science and Technical Information Division, P.O. Box 33, College Park, MD 20740, NASA Lit. Search No. 27541, 20 Nov 1974.

6. Straiton, A.W., Scarpero, D.C. & Vogel, W., "A Survey of Millimeter Wavelength Radio Propagation Through the Atmosphere," EERL, U. Texas, Austin, TR No. 68-1, 30 Nov 1968, AD 844946L.

7. Vogler, L. W. & Van Horn, S.F., "Bibliography on Propagation Effects from 10 to 1000 GHz," OT/TRER 30, OT, U.S. Dept. of Comm., March 1972.

Theoretical and Experimental Reports

8. Agabekyzn, K.A., Zrazhevskiy, A. Ju., Kolosov, M.A., Sokolov, A.V., "Study of the Absorption Dependence upon the Air Pressure at the Wave Length of 0.29, 0.36 and 0.45mm." Radio Eng. & Elect. Phys., 16, 8, P 1564, 1971.

9. Aganbekyna, K.A., Zrazhevskiy, A. Yu., Kolosov, M.A., and Sokolov, A.V., "Procedure and Results of Measurements of Absorption Coefficients of Submillimeter Radiation in Atmospheric Water Vapors," Proc. 9th All-Union Conference on Radiowave Propagation, Pt. II, p. 126, June, 1969.

BIBLIOGRAPHY (CONT.)

10. Babkin, Yu. S., Zimin, N.N., Izyumov, A.O., Sukhonin, Ye. V., & Shabalin, G. Ye., "Measurement of Attenuation in Rain Over 1 km Path at a Wavelength of 0.96mm," Radio Eng. & Elect. Phys., 15, 12, 2164-2166, Dec 1970.

11. Babkin, Yu.S., Izyumov, A.O. Smol'yaninova, L.I., Sokolov, A.V., Stroganov, L.I., & Sukhonin, Ye.V., "Investigation of Absorption of Submillimeter Waves in 850-960 μm range in the Atmosphere," Proc. 8-th All-Union Conference on Radiowave Propagation, 1967.

12. Basharinov, A. E. and Kutuza, B. G., "Study of the Radio Emission and Absorption of Waves of the Millimeter and Center Bands in a Cloudy Atmosphere," Trans. (Trudy) Main Geophys. Obs., No. 222, 1968.

13. Breeden, K. H., Rivers, W. K., and Sheppard, A. P., "Atmospheric Attenuation at Submilletre Wavelengths," Electronics Letters, 2, 3, p. 88, Mar 1966.

14. Burroughs, W. J., Pyatt, E. C., and Gebbie, H. A., "Transmission of Sub-millimetre Waves in Fog," Nature, 212, No. 5060, 387-388, Oct. 22, 1966.

15. Chang, S. Y. and Lester, J. D., "Atmospheric Attenuation Measurements at 600 GHz, "Memo Rpt M67-4-1, Frankford Arsenal, Philadelphia, PA August 1966. Also in IEEE, April 1966.

16. Chang, S. Y. and Lester, J. D., "Performance Characteristics of a 300 GHz Radiometer and Some Atmospheric Attenuation Measurements," IEE Trans. Ant. & Prop., AP-16(5), 588-591, 1968.

17. Coates, G. T., Bond, R. A., and Tolbert, C. W., "Propagation Measurements in the Vicinity of the 183 Gc/s Water Vapor Line," EERL, Univ. of Texas, Austin, Rpt No. 7-20, February 5, 1962.

18. Crane, R. K., "Propagation Phenomena Affecting Satellite Communications Systems Operating in the Centimeter and Millimeter Wave-Length Bands," Proc. IEEE, 59, 2, 173-188, Feb 1971.

19. Crawford, A. B., and Hogg, D. C., "Measurement of Atmospheric Attenuation at Millimeter Wavelengths," Bell Sys. Tech. J., 35, 907-915, July 1956.

20. Emery, R., "Atmospheric Absorption Measurements in the Region of 1mm Wavelength," Infrared Physics, 12, 65-79, 1972.

BIBLIOGRAPHY (CONT.)

21. Evans, A., Bachynski, M. P., and Wacher, A. G., "The Radio Spectrum from 10Gc to 300Gc in Aerospace Communications; Vol. IV - Absorption in Planetary Atmospheres and Sources of Noise," Tech. Rpt ASD-TR-61-589, Vol IV, RCA Victor Co., Ltd., Research Labs, Montreal, Canada, Aug. 1962. AD 294 452.

22. Gibbons, C. J., Gordon-Smith, A. C. & Gebbie, H.A., "Anomalous Absorption in the Atmosphere for 2.7mm Radiation," Nature, Vol. 243, 397-398, 15 June 1973.

23. Gurvich, A. S. and Naumov, A. P., "Theoretical Possibilities for Determining the Moisture Content of the Atmosphere through the Thermal Radio Emission in the Submillimeter Range," Atmos. and Oceanic Phys., 8, 307-309, May 1972.

24. Hoffman, L. A., "Millimeter-Wave Propagation and Systems Considerations," Aerospace Corp. Rpt. No. TR-0200 (4230-46)-1, SAMSO-TR-68-445, Oct 1968.

25. Hoffman, L. A., Hartwick, T. S., & H. J. Wintroub, "A Comparison of Millimeter and Laser Space-to-Space Communication Links," Aerospace Corp., SAMSO-TR-70-329, 31 Aug 1970.

26. Kammerer, J. E. & Richer, K. A., "140GHz Millimetric Bistatic Continuous Wave Measurements Radar," Ballistic Research Lab., APG, MD. Memo Rpt 1730, Jan 1966. AD484 693.

27. Kolosov, M. A., Sokolov, A. V. & Vvedenshii, B. A., "Investigations of the Propagation of Meter, Decimeter, Centimeter and Submillimeter Radio Waves," Radio Eng. & Elect. Phys., 12, 11, 1752-1771, Nov 1967.

28. Kolosov, M. A., & Sokolov, A. V., "Certain Problems of Propagation of Millimeter and Submillimeter Radiowaves," Radio Eng. and Elect. Phys., 15, 4, 563-570, Apr 1970.

29. Krasyuk, N. P., Rozenberg, V. I. & Chistyakov, D. A., "Effect of Different Distributions of Raindrop Sizes on Radar Performance," 13, 5, 679-681, Radio Eng. & Elect. Phys., May 1968.

30. Krasyuk, N. P. Rozenberg, V. I. & Chistyakov, D. A., "Attenuation and Scattering of Radio Waves by Raindrops of Various Origins," Atmos. & Ocean. Phys., 4, 11, 693-695, Nov. 1968.

BIBLIOGRAPHY (CONT.)

31. Krasyuk, N. P. Rozenberg, V.I., & Chistyakov, D. A., "Attenuation and Scattering of Radar Signals by Rains With Shifrin and Marshall-Palmer Drop Size Distributions," Radio Eng. & Elect. Phys., 13, 10, 1638-1440, Oct. 1968.

32. Krasyuk, N. P., Rozenberg, V. I., Chistyakov, D. A., "Attenuation and Dissipation of Electromagnetic Waves by Rain of Different Nature," Radio Phys. & Quant. Elec., 12, 10, 54-59, Oct. 1969. AD847658.

33. Krasyuk, N. P. Rozenberg, V.I., & Chistyakov, D. A., "Radar Characteristics of Precipitation of Different Nature, Spectra, Intensity and Temperatures in the Centimeter and Millimeter Ranges of Radio Waves," FTD-MT-24-246-69, Trans. Div. Foreign Tech. Div., WPAFB, 29 Oct 1969. AD 700401

34. Kukin, L. M., Lubyako, L.V., and Fedoseyev, L. I., "Measurement of Atmospheric Absorption in 1.8-0.87mm Range," Radio Phys. & Quant. Elect., 10, 6, 747, 1967.

35. Lane, J. A., Gordon-Smith, and Zavody, A. M., "Absorption and Scintillation Effects of 3mm Wavelength on a Short Line-of-Sight Radio Line," Electronic Letters, 3, 185-186, 1967.

36. Liebe, H. J. & Welch, W. M., "Molecular Attenuation and Phase Dispersion Between 40 and 140 GHz for Path Models from Different Altitudes," U. S. Dept of Commerce, Office of Telecommunications, OT Rpt. 73-10, May 1973.

37. Llewellyn-Jones, D. T., and Zavody, A.M., "Rainfall Attenuation at 110 and 890 GHz," Electronic Letters, 7, 12, June 17, 1971.

38. Malishko, Yu. I., "Absorption Factor Measurement of Water Vapour in the 1.3mm Transparency Window," Radio Eng. & Elect. Phys., 14, 3, 522-523, Mar 1969.

39. Malishenko, Yu. I., Vakser, I. Kh., "Measurement of the Attenuation Coefficient at 1.3 and 0.86mm in Showers," Radio Phys. & Quant. Elect., 14, 6, p.258, June 1971.

40. Mitchell, R. L., "Remote Sensing of Rain by Radar," Aerospace Corp., Report No. TR-0158 (3525-09)-1, Air Force Rpt No. SAMSO-TR-68-115, Jan 1968.

41. Mitchell, R. L., "Scattering and Absorption Cross Sections of Water Spheres at Millimeter Wavelengths," Aerospace Corp., El Segundo, CA Rpt TR-669 (6230-46)-11, 1966.

BIBLIOGRAPHY (CONT.)

42. Mondre, E., "Atmospheric Effects on Millimeter Wave Communication Channels," NASA, GSFC, X-733-70-250, Access. No. N70-34446, TMX-63985, Mar 1970.

43. Morgan, L. A., and Ekdahl, C. A., Jr., "Millimeter Wave Propagation," Tech. Rept. No. RADC-TR-66-342, Rome Air Development Center, Grifiss AFB, NY, 1966. AD 489 424.

44. Naumov, A. P. & Stankevich, V. S., "Attenuation of Millimeter and Submillimeter Radio Waves in Rains," Radio Phys. & Quant. Elect., 12, 2, 145-147, Feb 1969. NASA Rpt No. NASA-TT-F-12575, N69-36987.

45. Rogers, T. F., "An Estimate of Influence of the Atmosphere on Airborne Reconnaissance Radar Performance," Prop. Lab., AFCRC, 4 Jan 1953.

46. Rozenberg, V. I., "On Dielectric Penetrability of Water at 1.2 to 1.6 Millimeter Wavelength," Optics and Spectroscopy, 11, 2, 322-323, 1968.

47. Ryadov, V. Ya, Furashov, N. I., and Sharonov, G.W., "Measurement of Atmospheric Transparency to 0.87mm Waves," Radio Eng and Elect. Phys., 9, June 1964.

48. Ryadov, V. Ya. & Furashov, N. I., "Measurements of Atmospheric Absorption of Radiowaves in 0.76-1.15mm Range," Radio Phys. & Quant. Elect., 9, 5, p. 859, 1966.

49. Ryadov, V. Ya. & Sharonov, G. A., "Experimental Investigation of the Transparency of Earth's Atmosphere at Submillimeter Wavelengths," Radio Eng. & Elect. Phys., 11, p. 902, 1966.

50. Sander, J., "Computation of Attenuation of Electromagnetic Waves with λ = 5.77, 3.3 & 2mm With Special Attenuation to Raindrop Size Distribution," Tech. Rpt. 121, Heinrich Hertz Inst., Berlin-Charlottenberg, 1970.

51. Sander, J., "Investigations on the Attenuation of Electromagnetic Wavesby Rain at 52, 90.8 and 150 GHz," (Untersuchugen zur Daempfung Elektromagnetischer Wellen durch Regen bei 52, 190.8 and 150 GHz) Tech Rept 153, Heinrich Hertz Inst., Berlin-W, 17 April 1972, NASA N74-11978/5.

52. Sander, J.,"Rain Attenuation of Millimeter Waves at λ=5.77, 3.3 and 2mm," Heinrich-Hertz-Institut, Berlin-Charlottenburg, Germany, 1 Berlin 10, Einsteinufer 37. Final draft completed while a post-doctoral Fellow at RLE, MIT, 1973.

BIBLIOGRAPHY (CONT.)

76. Vakser, I.Kn., Malyshenko, Yu. I. & Kopilovich, L.E., "The Effect of Rain on the Millimeter and Submillimeter Radio Distribution," Atmos. & Oceanic Phys., 6, 9, 568-570, Sep 1970.

77. Vogel, W., "Scattering Intensity Plots and Transmission Coeffients for Millimeter Wave Propagation Through Rain," Univ. of Texas, Austin, TR-71-345, Dec 1971. AD 890-408L.

78. Vvedenskii, B.A., Kolosov, M.A., & Sokolov, A.V., "Investigations of the Propagation of Meter Decimeter and Submillimeter Radio Waves," Radio Eng. & Elect. Phys., 12, 11, 1752-1771, Nov 1967.

79. Whaley, T.W., "The Experimental Evaluation and Analysis of Free Space Propagation of Coherent Signals Between the Frequencies of 160 and 260 GHz," EERL, Univ of Texas, Austin, TR-3, Feb 1967, AD-808 516L.

80. Yaroslavsky, N.G. & Stanevich, A.E., "The Long Wavelength Infrared Spectrum of H_2O Vapor and the Absorption Spectrum of Atmospheric Air in the Region 20-2500μ (500-4cm^{-1})," Optics and Spectroscopy, 7, 380-382, 1959.

81. Zhevakin, S.A. & Naumov, A.P., "Absorption of Electromagnetic Radiation by Water Vapor on 10μ-2cm Waves in the Upper Layers of the Atmosphere," Geomagnetism and Aeronomy, Vol 3, 537-546, 1963.

82. Zhevakin, S.A. & Naumov, A.P.,"Coefficient of Absorption of Electromagnetic Waves by Water Vapor in Range 10μ to 2cm," Radio Phys. & Quant. Elect., 6, 4, p. 674, Apr 1963.

83. Zhevakin, S.A. & Naumov, A.P., "Absorption of Centimeter and Millimeter Radio Waves by Atmospheric Water Vapor," Radio Eng. & Elect. Phys., 9, 8, 1097-1104, Aug 1964.

84. Zhevakin, S.A. & Naumov, A.P. , "Calculation of Atmospheric-Oxygen Absorption Coefficients for Centimeter and Millimeter Radio Waves," Radio Eng. & Elect. Phys., 10, 6, June 1965.

85. Zhevakin, S.A. & Naumov, A.P., "The Propagation of Centimeter, Millimeter, and Submillimeter Radio Waves in the Earth's Atmosphere," Radiophysics & Quant. Elect., 10, 9 & 10, 678-694, Sep - Oct 1967, AD694 411.

86. Zoloterev, V.M., Mikhailov, B.A., Alperovich, L.I & Popov, S.I., "Dispersion and Absorption of Liquid Water in the Infrared and Radio Regions of the Spectrum," Optics and Spectroscopy, 27, 430-432, 1969.

NEAR-EARTH MILLIMETER WAVE RADIOMETER MEASUREMENTS

K. A. Richer and D. G. Bauerle
Ballistic Research Laboratories
Aberdeen Proving Ground, MD 21005

BRL Report #1267, December 1964
AD 460 300 (A65 6413)

Radiometric measurements of the atmosphere and natural emissive and reflective features of terrain at wavelengths of 8.58, 4.29, and 2.14 mm are discussed. Characteristics of experimental radiometers operating at 1.45, 1.33, and 0.5 mm wavelengths are also given. The quantitative effects of weather on radiometric performance at these wavelengths are considered. The performance characteristics of low noise millimeter wave radiometric antenna systems are investigated. The merits and shortcomings of various types of measurements with these radiometers are discussed. (Authors)

EXTRACTS:

The forest background brightness temperature at 70 GHz is 15 K less than that of ambient air (294 K), while at 140 GHz both brightness temperatures are equal to within 1 K.

Terrain Emissivity (35 GHz) Versus Grazing Angle

	Polarization					
	Horizontal			Vertical		
Grazing Angle	10°	30°	50°	10°	30°	50°
Earth	0.86	0.95	0.99	0.87	0.99	0.99
3" Grass	0.96	0.99	1.0	0.88	1.0	1.0
5' Marsh Weeds	0.93	0.99	1.0	---	---	---
Bay Water	0.38	0.36	0.45	---	---	---
Sheet Metal	0.40	0.27	0.25	0.36	0.25	0.25

For grazing angles higher than 30 degrees, there was essentially no difference in emissivity between vertically and horizontally polarized signals.

RICHER, BAUERLE, AND KNOX*

94-GHz RADAR CROSS SECTION OF VEHICLES

Kenneth A. Richer, Donald G. Bauerle and Joseph E. Knox
Ballistic Research Laboratories
Aberdeen Proving Ground, MD 21005

BRL MR 2491, June 1975
ADC 002 505 (A79 07859)

CONFIDENTIAL

Wide-band FM-CW measurements of radar cross section (σ°) at 94 GHz are shown for the M551 Sheridan tank, M48 tank, and M119 armored personnel carrier. These measurements were made at grazing angles of 0.8 and 5.0 degrees from a 15.2 meter-high tower against a dirt background with a σ° of -22.0 dB. (Authors)

MILLIMETER-WAVE SEMIACTIVE GUIDANCE SYSTEM CONCEPT INVESTIGATION

R. S. Roeder, W. B. Day, J. L. Connors, M. W. Milstead, and L. W. Hoffman
Sperry Microwave Electronics
P.O. Box 4648
Clearwater, FL 33518

SJ-242-8457-5, November 1976
DARPA Order-3146
AD-C011 448L (A79 08186)

CONFIDENTIAL

This report describes a study program leading to a preliminary design concept for a millimeter wave semiactive guidance system. Atmospheric and propagation effects, target and clutter characteristics, and millimeter wave component capabilities were studied and reported. Various system concepts were considered and subjected to analysis, including computer simulation of the guidance performance. A preliminary design concept is selected, and estimated performance characteristics presented.

The selected design is shown to have high terminal accuracy, will operate under adverse environmental conditions, and accepts the reflected signal from an illuminated target without locking on to the illuminator. (Authors)

EXTRACTS:

SOURCE	ONE-WAY LOSSES AT 94 GHz	COMMENTS
Rainfall 1 mm/hr	1.6 dB/km	
4 mm/hr	3.85 dB/km	
Fog 100 ft visibility	4.08 dB/km	LWC‡ = 1.2 g/m^3, T = 20°C
800 ft visibility	2.04 dB/km	LWC‡ = 0.6 g/m^3, T = 20°C
Clouds Cumulonimbus (rain)	35.04 dB/km	clouds typically only few
Cumulus (dry)	3.78 dB/km	hundred meters thick
Oxygen (O_2)	0.075 dB/km	STP
Uncondensed Water Vapor		
7.5 g/m^3	0.35 dB/km	20°C, 40% relative humidity
15.0 g/m^3	0.75 dB/km	25°C, 60% relative humidity
30.0 g/m^3	1.80 dB/km	30°C, 90% relative humidity
Water Layer on Radome		
Seeker	0.6 dB	Mach 1 speed 4 mm/hr rainfall
Illuminator	2.0 dB	Zero Velocity 4 mm/hr rainfall
Snow	0.028 dB/km	About 1 mm/hr water content

‡LWC - liquid water content
93-GHz contour maps of a truck are shown.

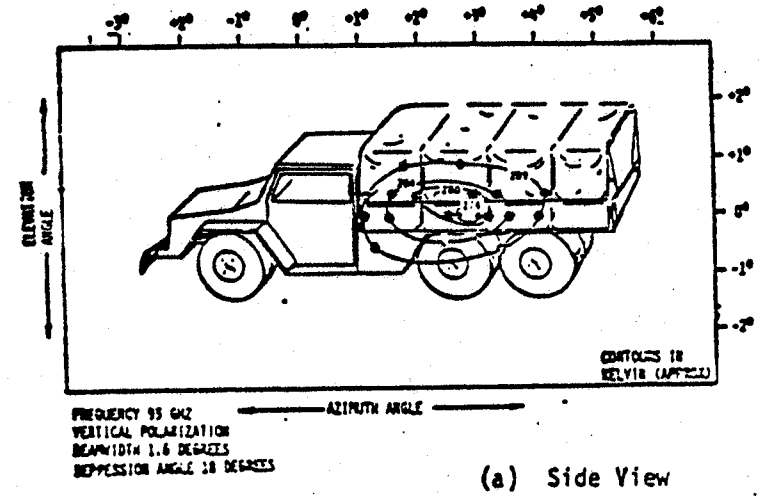

(a) Side View

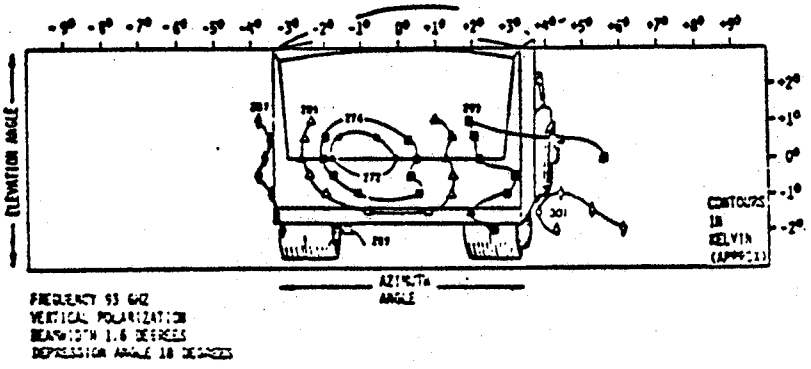

(b) Rear with Canvas Top Up

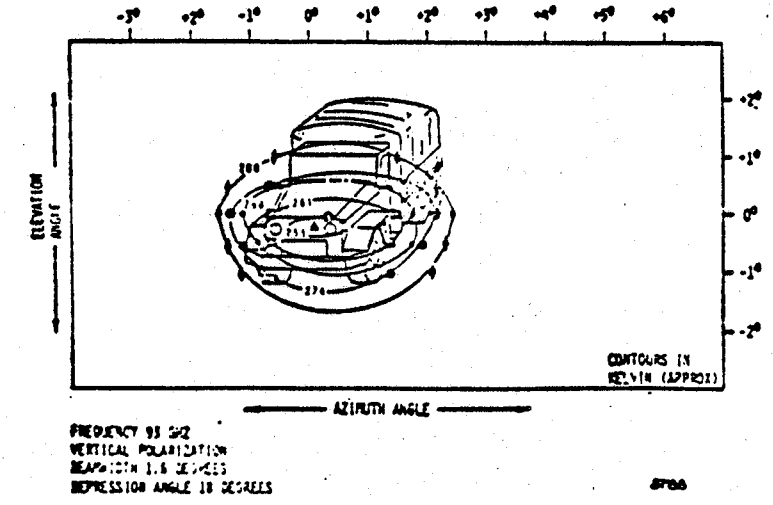

(c) Front View

(U) Figure 4-5. Passive Radiometer Profile - 2½ Ton Truck

TARGET DETECTION BY MILLIMETER WAVE RADIOMETRY

Robert S. Roeder, Robert E. Wilt, and Michael W. Milstead
Sperry Microwave Electronics
Sperry Rand Corporation
Clearwater, FL 33518

Proceedings of the Sixth DARPA/Tri-Service Millimeter Wave Conference
Tactical Technology Office (editor), Defense Advanced Research Projects Agency, 1400 Wilson Blvd., Arlington, VA 22209, p. 140-149, November 1977
(A78 01438)

SECRET

Air-to-ground detection range performance of 35, 94, and 140 GHz radiometers operating against small flat metal targets is addressed. Effects of weather and target antenna beamfill on predicted performance are given special attention. A detection range equation is derived which includes receiver parameters, search scan characteristics, target to background contrast, atmospheric attenuation, and a 3-dimensional model of the antenna beam which reflects the beamfill by the target for both low and high beamfill ratios. Parametric detection range curves are presented which allow systems engineers to obtain performance predictions for 35, 94 and 140 GHz radiometer sensors. Comparative performance is illustrated for a 5 inch diameter aperture and ac coupled total power radiometers using state-of-the-art components. The target is assumed to be a flat metal reflector with an area of 10 m^2 against a uniform, near ambient temperature background. Weather effects are incorporated in the range analysis using both measured and computed sky temperature data. Measured data was obtained at 35 and 94 GHz with calibrated measurement radiometers. (Authors)

EXTRACTS:

Sample data are shown.

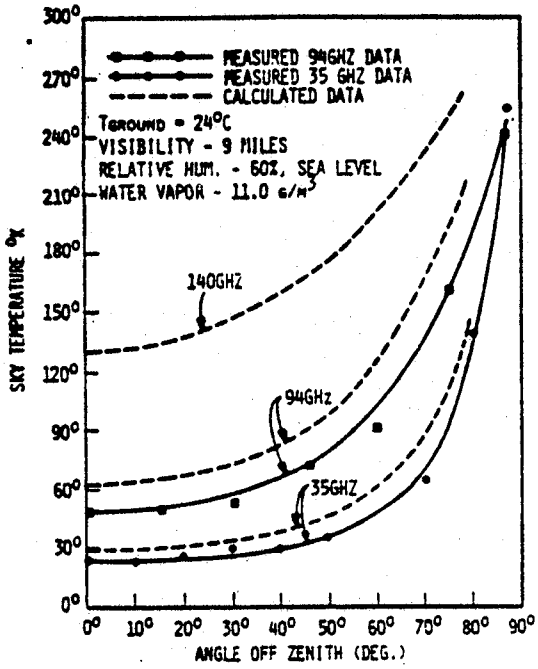

Figure 4. Passive Radiometric Sky Temperature (Clear)

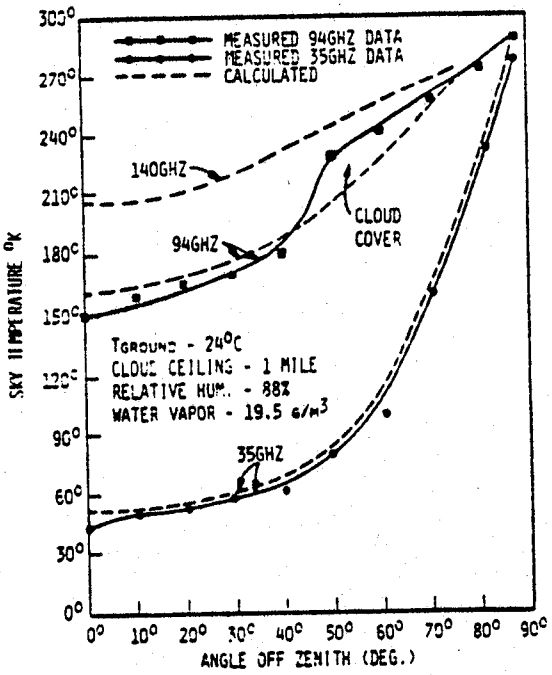

Figure 5. Passive Radiometric Sky Temperature (Partly Cloudy)

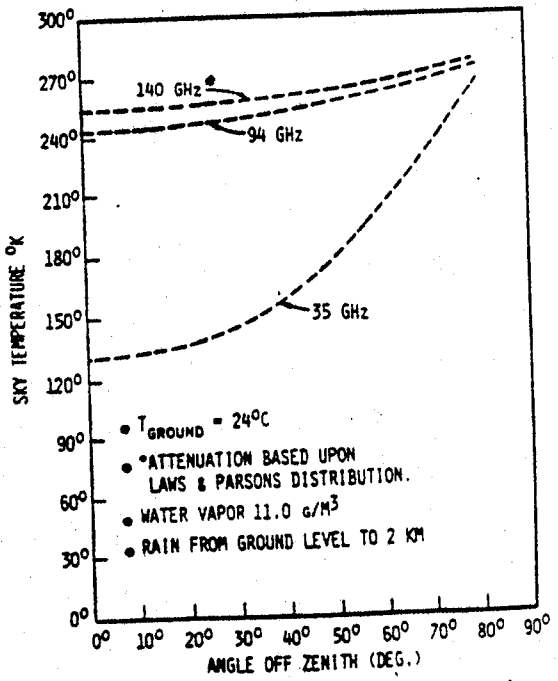

Figure 6. Passive Radiometric Sky Temperature (4MM/Hr Rain)

RAIN ATTENUATION OF MILLIMETER WAVES AT WAVELENGTHS OF 5.77, 3.3, AND 2 mm

Jeorg Sander
Heinrich-Hertz-Institut
Berlin-Charlottenburg
Federal Republic of Germany

IEEE AP-23, No. 2, 213-220, March 1975

Measurements of rainfall attenuation of millimeter waves at wavelengths of 5.77, 3.3, and 2 mm were conducted during the years 1969-1970. Simultaneously recorded meteorological quantities were the rainfall rate and part of the drop-size spectrum. Attenuation coefficients as a function of rainfall rate were thus determined. These attenuation coefficients were related to parameters that, under certain assumptions, describe the drop-size distribution in rain. (Author)

EXTRACTS:

Experimentally measured rain attenuation coefficients for 90 GHz vary from 0.20 to 15 dB for rainfall rates of 0.20 to 50 mm/hr. For 150 GHz, attenuation varies from 0.20 to 20 dB for rainfall rates of 0.20 to 40 mm/hr.

Attenuation coefficients at 2 and 3.3-mm versus rainfall rate are shown in the accompanying figures.

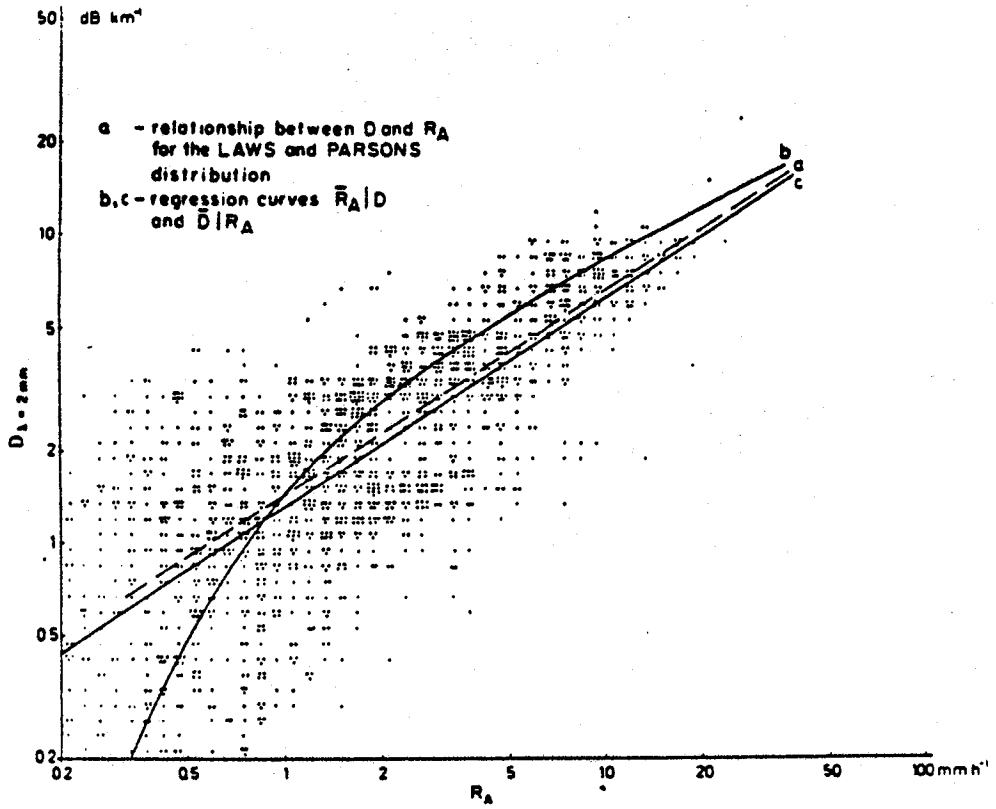

Fig. 6. Measured attenuation coefficients versus rainfall rate at λ = 2 mm.

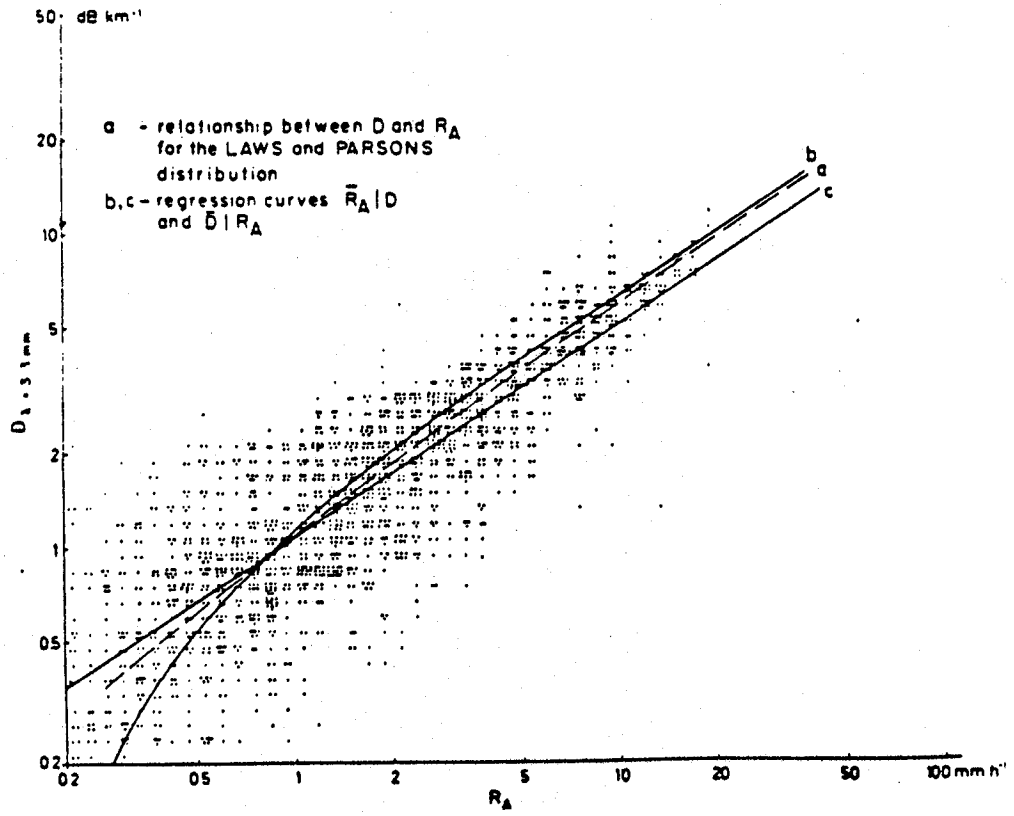

Fig. 5. Measured attenuation coefficients versus rainfall rate at λ = 3.3 mm.

A COMPARISON OF THERMAL IMAGING AT MICROWAVE AND INFRARED WAVELENGTHS

G. Schaerer
Institute for Applied Physics
Berne University
3000 Berne, Switzerland

Project No. 1.5/9-68, June 1974
N76 10553 (A76 02055)

In German.

EXTRACTS:

Physical explanations are given of thermal infrared and microwave pictures of trucks at 200 m, a Volkswagen auto at 120 m, partially snow-covered mountains at 7.5 km, and a mountain with a lake in the foreground.

At 3.3 mm, the image of the mountain with a lake in the foreground yielded brightness temperatures of 210 °K and 270 °K, for the sky and mountain respectively. The lake had a horizontal reflection coefficient of 0.64-0.67 and a vertically polarized one of 0.04.

Images are shown in the entry under Schaerer and Schanda.

SCHAERER

TERRESTRIAL RADIOMETRY AT 3-mm WAVELENGTH

G. Schaerer
Institut fuer Angewandte Physik
Berne University
3000 Berne, Switzerland

Berne University Project No. 01.05/009-68, June 1974
N76 10606 (A76 02058)

In German.

EXTRACTS:

Thermograms were taken of mountains with a lake in the foreground. At a water temperature of 15°C, the normal reflectivity at 92 GHz from the lake is 0.38. At elevation angles of 75° and 77°, the horizontally polarized reflectivity is 0.64 and 0.67, respectively. At the Brewster angle, 76°, the lake is barely discernible when viewed with vertical polarization (reflectivity is 0.04). A reflectivity of 0.95 was obtained from a thermogram taken on an aircraft 5 km above the lake surface (elevation angle of 89°).

The brightness temperature difference between the sky and a partially snow-covered mountain ridge 7.5-km high was ≈ 100 K. No details are discernible in the snow-covered regions though the snow/land boundaries are detectable in the thermogram. An approximately constant sky emission temperature is measured from 0° to 30° above the horizon. The authors believe this result is due to the high reflectivity of snow and the position of the snow-covered mountains.

During fogs, contrast reduction and blurring as well as lower quality absorption measurements were observed.

Ships may be detected at distances up to 3 km by sky emission reflected from their metal surfaces.

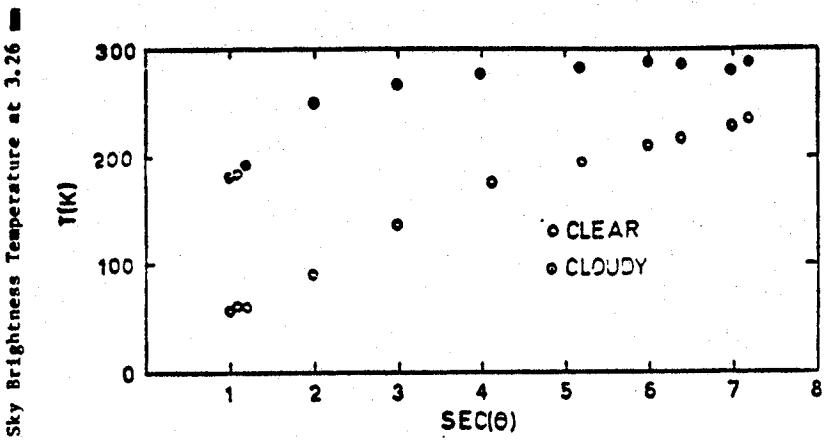

Brightness temperature (degrees K)	Weather condition	Air temperature (Centigrade)	Humidity (%)
40 - 80	clear sky	25 - 30	50 - 60
80 - 120	high clouds/cirrus	20 - 26	50 - 60
120 - 200	medium and low clouds/stratus/ strato cumulus/ altocumulus	16 - 20	50 - 60
200 - 240	dark thunderstorm clouds	10 - 15	60 - 70

Table 1 - 3.26-mm Zenith Sky brightness temperatures under different weather conditions at Thun, Switzerland (565 m above sea level).

Rain Intensity (mm/hr)	Attenuation (dB/km)
6	3 ± 1
10	8 ± 2
15	10 ± 2
25	15 ± 3

Table 2 - Attenuation at 3.26 mm due to rain, measured at Thun, Switzerland

SCHAERER AND SCHANDA

DETERIORATING EFFECTS ON 3-mm WAVE PASSIVE IMAGERY

G. Schaerer and E. Schanda
Institute of Applied Physics
University of Berne
3000 Berne, Switzerland

Proceedings of the 9th International Symposium on Remote Sensing of the Environment, 15-19 April 1974, 1593-1595, Environmental Research Institute, University of Michigan, Ann Arbor, MI 48104
ADA 008 469 (A77 00616)

A high resolution (10 arcminutes) microwave scanning radiometer with a real-time display on a TV screen, operating at 3.3-mm wavelength, has been used for thermal mapping. Radiometric images of characteristic soil signatures (snow and water) are presented and some special features are discussed. Deteriorated thermograms due to various atmospheric effects are presented. The presence of clouds along the line of sight can severely limit thermogram quality by reducing image contrasts. (Author)

EXTRACTS:

All of the authors' thermograms are shown here.

a)

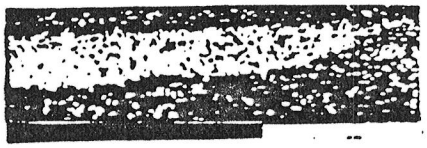

b)

Fig.1.a) Radiometric 3 mm-wave thermal image of a lake at a distance of 2-6kms. Integration time 1 sec. Image points 24 x 24 minutes of arc. 4 grey steps: 60-180 K/180-220 K/220-260 K/260-300 K.

b) Photographic identification of a)

a)

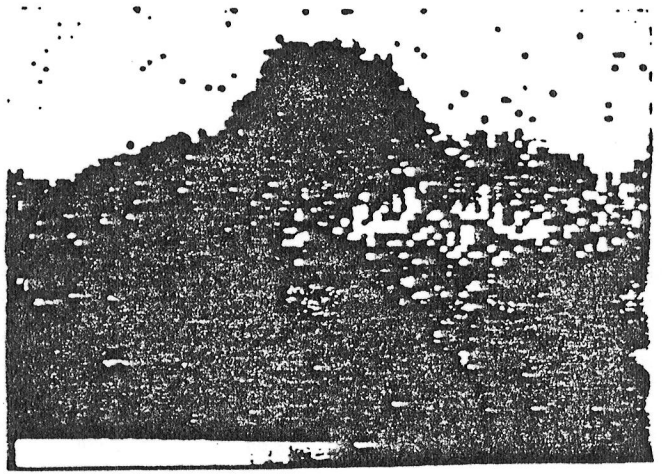

b)

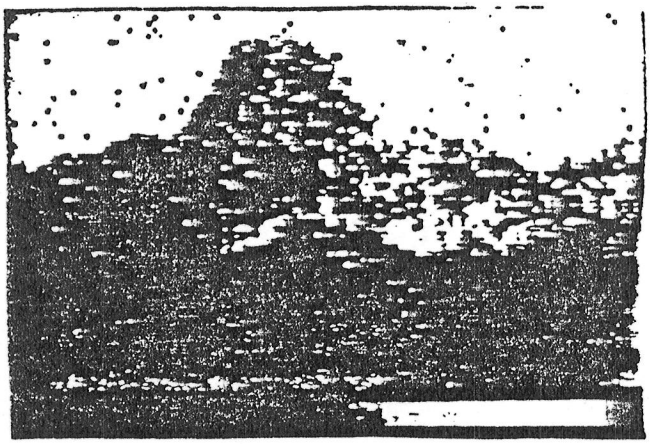

c)

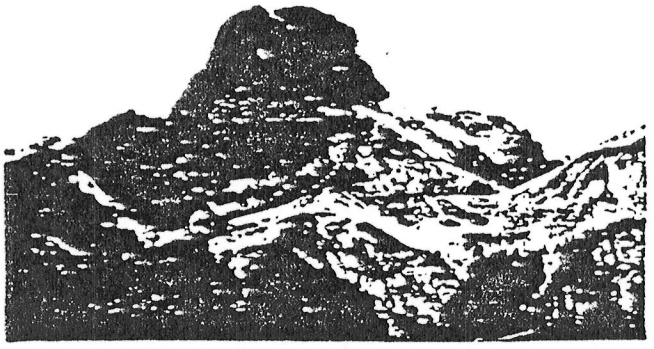

Fig.2.a) MM-wave thermal image of a partly snow-covered mountain.Distance to the mountain peak 7.5 kms.Integration time 1 sec.Image points 6 x 6 minutes of arc.11 grey steps:50-150 K/150-165 K/165-180 K/180-195 K/195-210 K/210-225 K/225-240 K/240-255 K/255-270 K/270-285 K/285-300 K.

b) The same scenery as a),one day later.

c) Photographic identification of a) and b)

a)

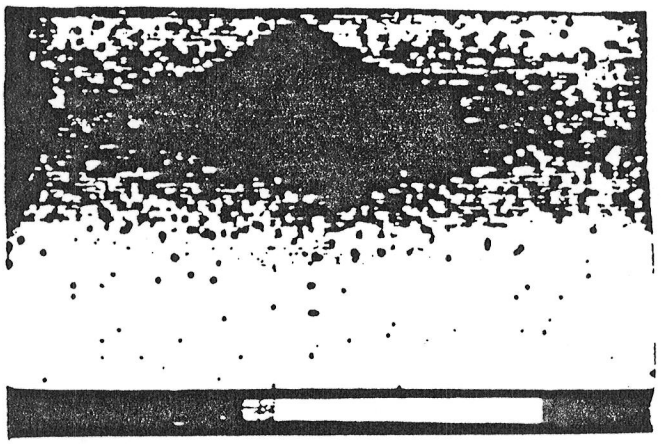

b)

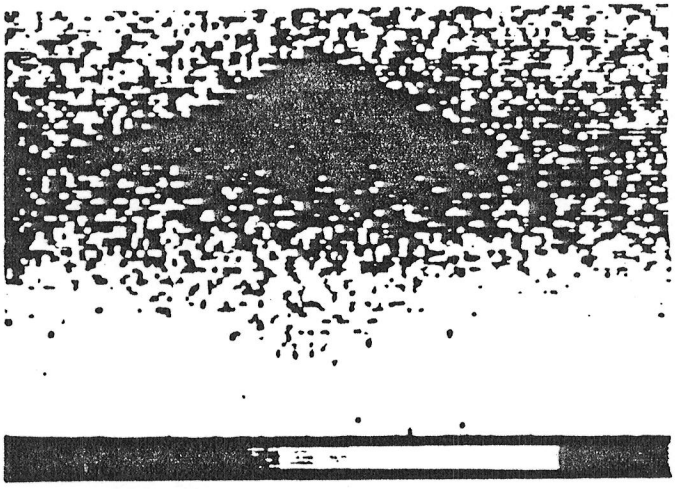

Fig. 3 MM-wave thermal image of a mountain with a lake in the foreground. Distance to the mountain peak 8.5 kms. Radiometer 6 m above the water surface. 10 grey steps: 50-120 K/120-140 K/140-160 K/160-180 K/180-200 K 200-220 K/220-240 K/240-260 K/260-280 K/280-300 K. Image points 24 x24 minutes of arc.

a) Integration time 1 sec.

b) Integration time 0.1 sec.

c)

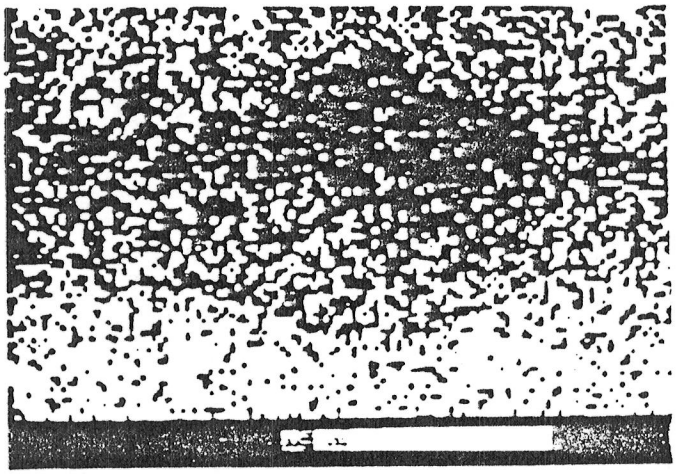

d)

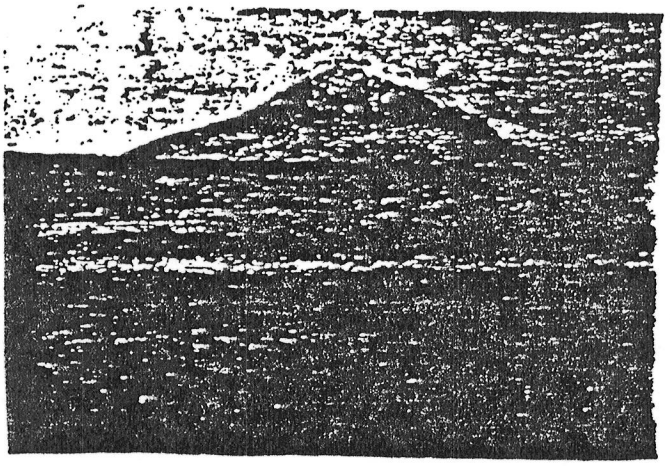

Fig. 3 MM-wave thermal image of a mountain with a lake in the foreground. Distance to the mountain peak 8.5 kms. Radiometer 6 m above the water surface. 10 grey steps: 50-120 K/120-140 K/140-160 K/160-180 K/180-200 K 200-220 K/220-240 K/240-260 K/260-280 K/280-300 K. Image points 24 x24 minutes of arc.

c) Integration time 0.01 sec.

d) Photographic identification of a),b) and c)

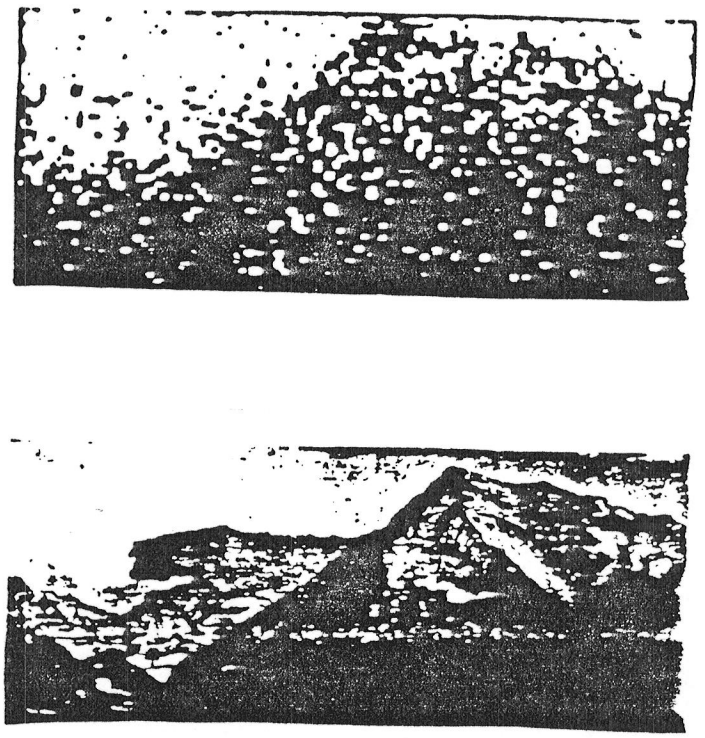

Fig. 4 a) Thermogram of a mountain, deteriorated due to the large atmospheric path (13 kms to the mountain peak) and due to the low elevation angle(8 degrees of arc). Integration time 1 sec. Image points 6 x 6 minutes of arc. 9 grey steps: 50-185 K/185-200 K/200-215 K/215-230 K/230-245 K/245-260 K/260-275 K 275-290 K/290-300 K.

b) Photographic identification of a).

a)

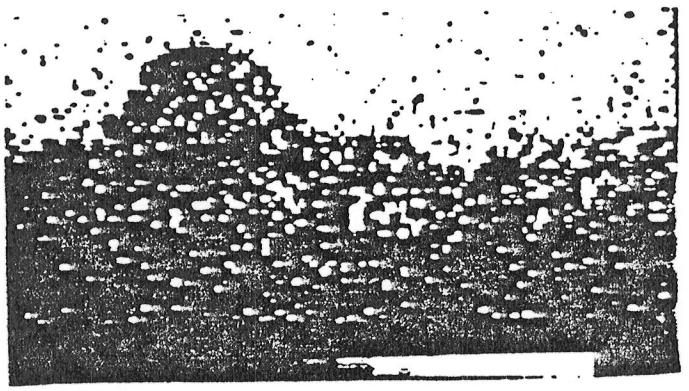

b)

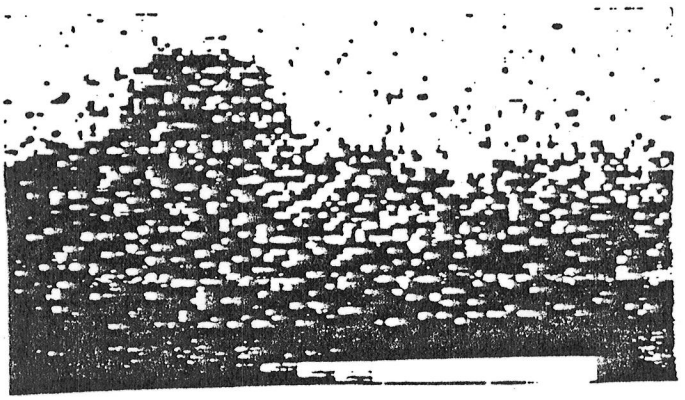

Fig.5. MM-wave thermal image of the same scenery as in Fig.2.at unfavourable atmospheric conditions.Integration time 1 sec.Image points 6 x 6 minutes of arc.11 grey steps as in Fig.2.

a) Medium cloud cover (zenith sky noise temperature 13o K).

b) Additional path absorption of 3 dB.

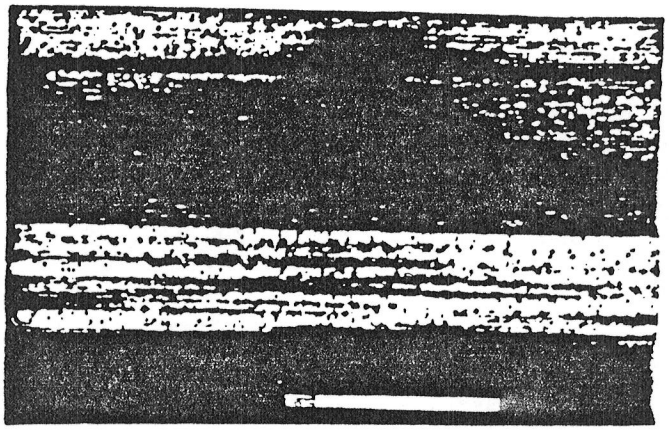

Fig.6 MM-wave thermal image that is displaying simultaneously the influence of clear,cloudy and rainy weather conditions.The photographic identification is given in Figure 3d) .Integration time 1 sec.Image points 12 x 12 minutes of arc.lo grey steps as in Figure 3.

SCHANDA*

MICROWAVE RADIOMETRY APPLICATIONS TO REMOTE SENSING

Erwin Schanda
Institute of Applied Physics
University of Berne
CH-3012 Berne, Switzerland

Surveillance of Environmental Pollution and Resources by Electromagnetic Waves, 253-273, NATO, T. Lund (editor), Reidel Pub. Co., Netherlands
(TD/77 L962 1978)

Physical fundamentals and constraints of passive microwave remote sensing are discussed. Applications areas are indicated, the rationale for multi-wavelength operation of passive microwave sensors is reviewed and the state of the art in radiometer systems is summarized. Examples of applications and of basic research in meteorology and hydrology are given and a future utilization in atmospheric science is indicated. (Author)

MICROWAVE LIMB SOUNDING OF STRATO- AND MESOSPHERE

Erwin Schanda, Joachim Fulde and Klaus Kunzi
Institute of Applied Physics
University of Berne
3000 Berne, Switzerland

Atmospheric Physics from Spacelab, 135-146, 1976, J. J. Burger, et al (editors), Reidel Pub. Co., Netherlands
(QC 801 B954 1976)

A considerable number of atmospheric constituents — O_2, H_2O, O_3, CO, N_2O, NO, CO, and others -- exhibit a series of spectral lines in the millimeter wave region due to transition between the rotational states of their electric or magnetic dipole moments. The maintenance of the thermodynamic equilibrium (collisional dominated) of this line spectrum up to mesopause altitudes is a specific advantage for the reliable determination of composition and temperature profiles throughout the strato- and mesosphere.

Space-borne experiments (e.g., Staelin et al., 1976 and Waters et al., 1975) have already demonstrated the feasibility of this method for global monitoring of the total water vapor and of the temperature profile in a downward-looking mode. The variable background radiation from the ground and the widths of the weighting functions are limiting the accuracy and the height resolution in the measuring situation. The weakness of the line radiations by the minor constituents would allow only very coarse determinations of the composition. The method of limb sounding as proposed by various groups (Waters et al., 1974; Schanda et al., 1974) allows for a height resolution of 3 km or better throughout the range between the tropopause and the lower thermosphere. The long ray path at the tangential height and the absence of the more dense layers within the ray enhance the detectability of the weak emission by the less abundant molecules. (Authors)

EMISSIVITIES AND FORWARD SCATTERING OF NATURAL AND MAN-MADE MATERIAL AT 3 mm WAVELENGTH

E. Schanda and R. Hofer
Institute of Applied Physics
University of Berne
3000 Berne, Switzerland

Proceedings of the 9th International Symposium on Remote Sensing of the Environment, 15-19 April 1974, 1585-1592, Environmental Research Institute, University of Michigan, Ann Arbor, Michigan
ADA 008 469 (QC 808.5 5981 1974)

An investigation of the emissivities of natural and man-made materials has been performed to interpret the thermal images produced by our high resolution 3-mm scanning radiometer. In order to exclude the atmospheric contributions to the measured radiation and to study the angular dispersion of a reflected wave due to surface structuring, mainly the forward scatter properties have been investigated. In general, the emissivities of all materials are closer to unity at 3 mm than at 3 cm wavelength. The emissivity of water varies from roughly 0.7 to 0.6 for temperatures of a few degrees centigrade up to about 40°C. An oilfilm of 0.15 mm increases the emissivity by 0.05. (Authors)

EXTRACTS:

This article is a summary of R. Hofer's thesis (published in German).

The authors' table and figures of 3.3-mm measurements follow.

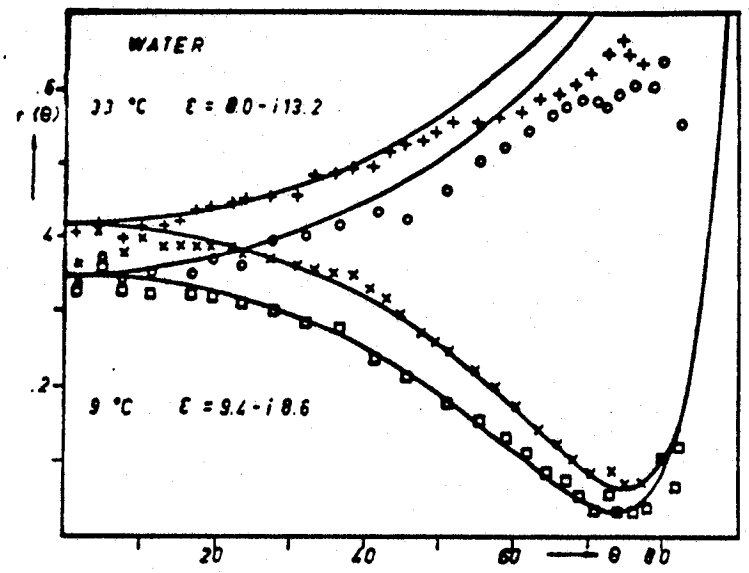

FIGURE 1. Reflection coefficients of water at 33° C and 9° C as a function of the incidence angle (0° = vertical) for horizontal and vertical polarization. Measuring points and best-fit Fresnel curves.

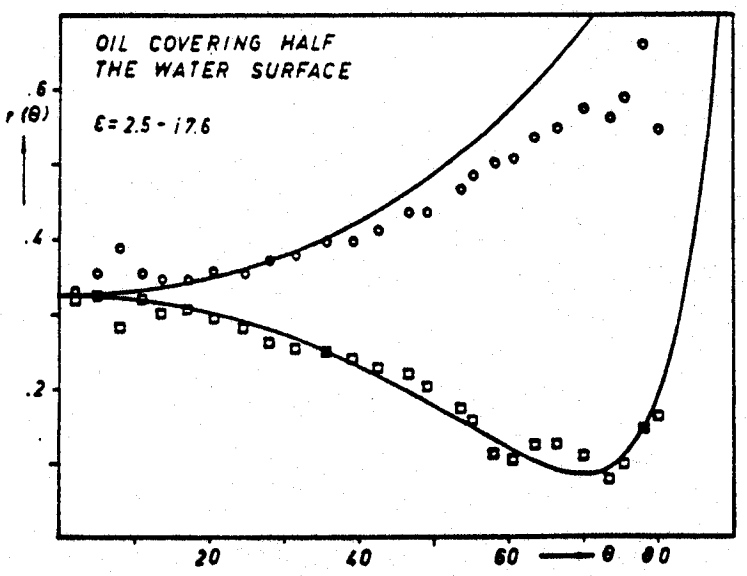

FIGURE 2. Reflection coefficients of water covered by oil blobs of approximately 0.15 mm thickness and 3 cm diameter, occupying half of the surface.

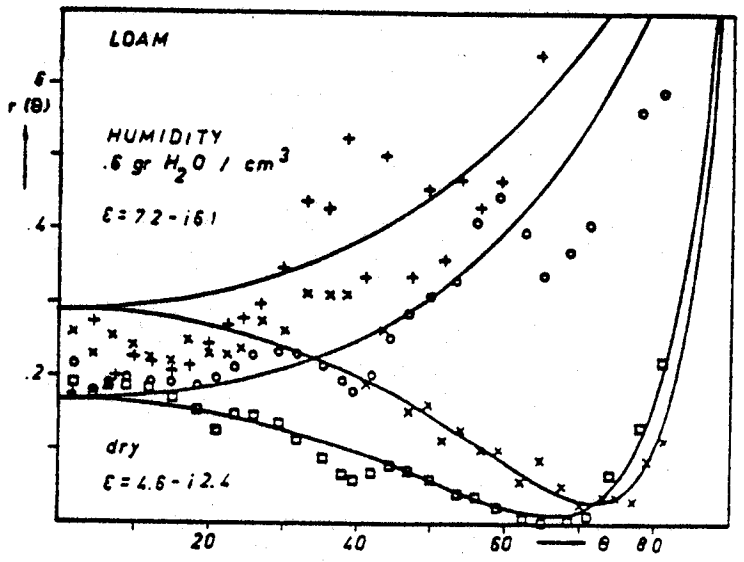

FIGURE 3. Reflection coefficients of dry and humid loam (smoothed). Only the results for the vertical polarization (curves going through the Brewster angle minimum) have been used for all the determinations of the dielectric constants.

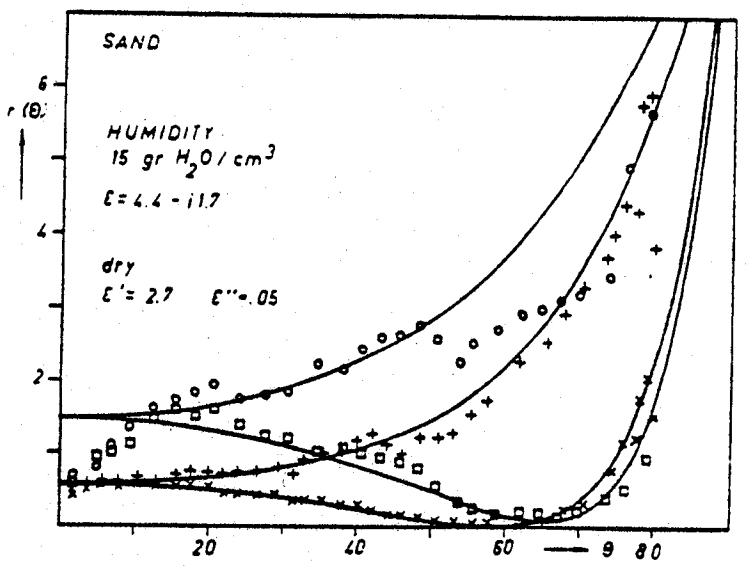

FIGURE 4. Reflection coefficients for dry and humid sand.

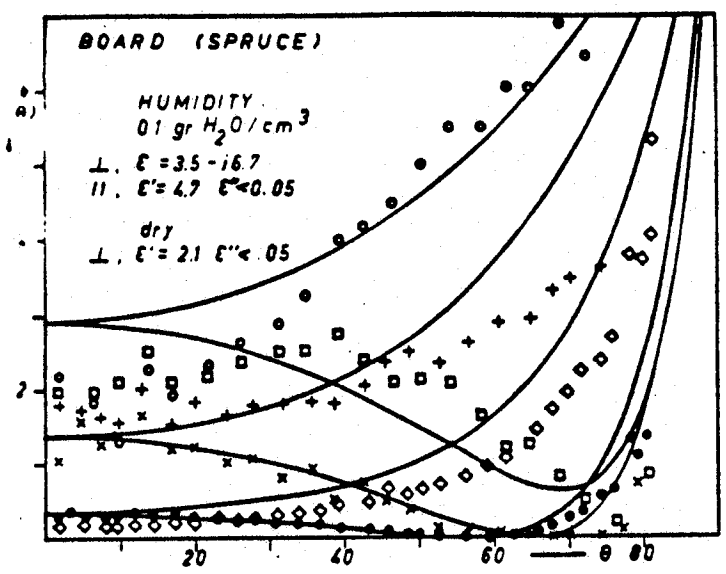

FIGURE 5. Reflection coefficients of boards cut out of spruce. The fibres perpendicular ⊥ and parallel ∥ to the plane of incidence.

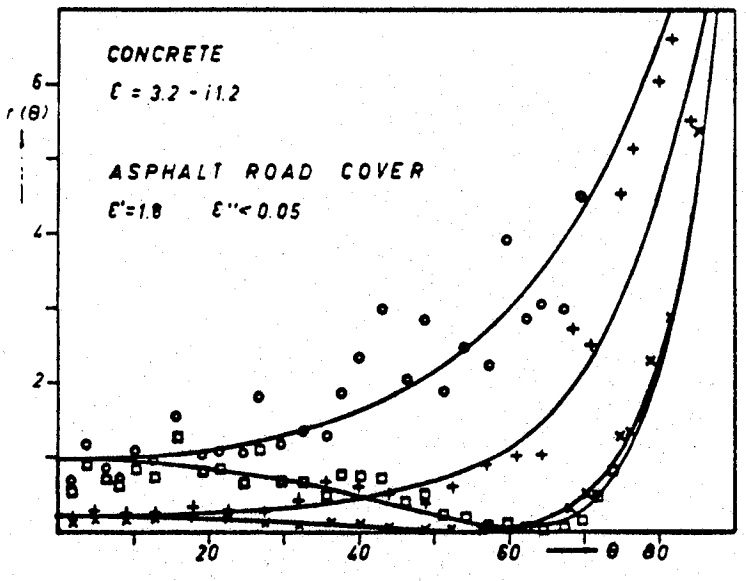

FIGURE 6 Reflection coefficients of conrete and asphalt road cover.

TABLE 1. COMPARISON OF REFLECTIVITIES AND DIELECTRIC CONSTANTS AT 94 GHZ AND 10 GHZ

	94 GHz		10 GHz	
	r(0)	ε' / ε"	r(0)	ε' / ε"
water at 33° Centigrade	0.40	8.0 / 13.2	0.62	51 / 39
20° "	0.38			56 / 36
15° "	0.37	7.3 / 10.6		60 / 33
9° "	0.34	9.4 / 8.6		64 / 26
Oil covering half the water surface (0.15 mm thick) 20°C	0.33	2.5 / 7.6		
asphalt road cover	0.02	1.8 / < 0.05	0.02	6.0 / 1.4
concrete	0.08	3.2 / 1.2	0.14	4.8 / 0.8
brick	0.02	1.1 / < 0.05	0.10	3.8 / 0.1
loam, dry			0.10	4.5 / 0.4
humidity, ≈ 0.2 gH_2O/cm^3	0.17	4.6 / 2.4	0.30	10 / 5
" , ≈ 0.6 gH_2O/cm^3	0.22	7.2 / 6.1	0.42	20 / 10
sand, dry	0.06	2.7 / < 0.05	0.07	3.0 / 1.0
humidity, ≈ 0.15 gH_2O/cm^3	0.14	4.4 / 1.7	0.10	4.2 / 0.6
board (spruce) ⊥ : dry	0.02	2.1 / < 0.05	0.03	1.7 / 0.7
≈ 0.15 gH_2O/cm^3	0.24	3.5 / 6.7	0.20	5.4 / 3.0
∥ : dry	0.03	1.9 / < 0.05	0.03	2.0 / 0.3
≈ 0.15 gH_2O/cm^3	0.14	4.7 / < 0.05		

SCATTERING, EMISSION AND PENETRATION OF 3-mm WAVES IN SOIL

Erwin Schanda and Roland Hofer
Institute of Physics
University of Berne
3000 Berne, Switzerland

Proceedings of the URSI Commission II, Specialist Meeting on Microwave Scattering and Emission from the Earth, 23-26 September 1974, 141-149
(QC 09 M6 I61 1974)

Controlled experiments on the emission behavior of various natural and man-made types of soil at 3.2-mm wavelength have been performed. Additional forward scatter measurements on the same materials allow the elimination of the atmospheric contributions and an approximate determination of the effective permittivities. By the use of a metal plate underneath soil layers of various thicknesses, the penetration depth of 3-mm waves in a few specific soils have been characterized. The effects of humidity and polarization have been studied and a comparison to earlier measured emissivities at 3-cm wavelength has been established. The investigated media are: humus, lawn, gravel, fine-grained sand, concrete, road asphalt cover, board, and eternit. (Authors)

The entire article appears in the Appendix.

RADIOMETRIC TERRAIN MAPPING AT 3-mm WAVELENGTH

E. Schanda, G. Schaerer and M. Wuthrich
Institute of Applied Physics
University of Berne
3000 Berne, Switzerland

Eighth Annual International Symposium on the Remote Sensing of the Environment J. J. Cook, et al. (editors) 1972, Environmental Research Institute of Michigan, Center for Remote Sensing, University of Michigan, Ann Arbor, MI 48104

A narrow beam (10 arcminutes) microwave scanning radiometer, operating at 92 GHz has been used for thermal mapping. Real time display of the sceneries is performed on a TV screen. Radiometric images of distant areas, urban sceneries, and single buildings are presented and some special features are discussed. The data acquisition system of the radiometer is equipped with a calculator which performs subtraction of information from different images, enabling display of the changes within a certain scene. (Authors)

REFLECTIVITY CHARACTERISTICS OF CLUTTER AT 35 AND 95 GHz

J. A. Scheer and D. L. Odom
Georgia Institute of Technology
Atlanta, GA 30332

R. C. Haraway
MIRADCOM
Redstone Arsenal, AL 35809

Proceedings of the Eighth DARPA/Tri-Service Millimeter Wave Conference
System Planning Corporation (editor), 1500 Wilson Blvd., Arlington, VA 22209,
p. 67-76, April 1979
(A80 00206)

SECRET

This paper describes the results of preliminary analysis of [radar] reflectivity from military vehicles and clutter at 35 and 95 GHz. The analysis includes correlation properties, spectral analyses, and amplitude and polarimetric phase statistics. (Authors)

EXTRACTS:

No data presented.

SCHMUGGE, WILHEIT, WEBSTER, JR.,
AND GLOERSEN*

REMOTE SENSING OF SOIL MOISTURE WITH MICROWAVE RADIOMETERS-II

T. Schmugge, T. Wilheit, W. Webster, Jr., and P. Gloersen
Goddard Space Flight Center
Greenbelt, MD 20771

NASA Technical Note No. D-8321, September 1976
N76-32625 (A79 00918)

The results presented here are derived from measurements made by microwave radiometers during the March 1972 and February 1973 flights of National Aeronautics and Space Administration (NASA) Convair-990 aircraft over agricultural test sites in the southwestern part of United States. The purpose of the missions was to study the use of microwave radiometers for the remote sensing of soil moisture. The microwave radiometers covered the 0.8- to 21-cm wavelength range. The results show a good linear correlation between the observed microwave brightness temperature and moisture content of the 0- to 1-cm layer of soil. The results at the largest wavelength (21 cm) show the greatest sensitivity to soil moisture variations and indicate the possibility of sensing these variations through a vegetative canopy. The effect of soil texture on the emission from the soil was also studied and it was found that this effect can be compensated for by expressing soil moistures as a percent of field capacity‡ for the soil. The results are compared with calculations based on a radiative transfer model for layered dielectrics, and the agreement is very good at the longer wavelengths. At the shorter wavelengths, surface roughness effects are larger and the agreement becomes poorer. (Authors)

EXTRACTS:

Water content of different soils:

	Wilt Point at -15 bar	Field Capacity‡ at -1/3 bar	Saturation at 0 bar
Navajo Clay	0.22 cm^3/cm^3	0.35 cm^3/cm^3	0.70 cm^3/cm^3
Cashion Silty Clay	0.22	0.33	0.50
Avondale Loam	0.11	0.25	0.44
Gran Sandy Loam	0.06	0.15	0.36

Available water capacity (Field Capacity - Wilt Point) is approximately the same for all these soil types.

‡Field capacity is the amount of water which remains after the soil has been saturated and free drainage has ceased.

mm-WAVE RADAR AND RADIOMETER SENSORS FOR GUIDANCE SYSTEMS

C. R. Seashore, J. E. Miley, and B. A. Kearns
Defense Systems Division
Honeywell, Inc.
Minneapolis, MN 55400

Microwave Journal 22, No. 8, 47-52, August 1979

Development is currently being carried out for millimeter-wave radar and radiometer sensor hardware to be used in a wide range of weapons, including air-to-ground and ground-to-ground missiles and free-fall bombs. The objective of this activity is to obtain precise fixes and improve guidance under adverse weather conditions, electronically—without manual assistance. It is all part of an effort to make weapons more autonomous, improve kill ratios and to take the man out of the loop. Even after conceptual feasibility of these systems has been demonstrated, the challenge of system weaponization remains, especially in terms of realizing the compact, low-cost, high-performance sensor hardware. It should be noted that in essentially all of the millimeter-wave guidance system demonstration programs presently underway, the millimeter-wave sensor assemblies are at least partially configured using costly, fragile conventional waveguide components. This points out the critical need for advanced engineering development of millimeter-wave components and subassemblies in order for these guidance sensors to have the reliability and low production costs necessary for high volume production. (Authors)

EXTRACTS:

The article does not indicate whether the following are calculated or measured quantities.

	94 GHz Attenuation (dB/km)	140 GHz Attenuation (dB/km)
Clear Weather	0.4	1.6
Rain: 0.25 mm/hr	0.17	0.2
1.0	0.6	0.7
4.0	3.0	3.2
16.0	8.0	9.0
Fog: light 0.01 g/mm	0.035	0.07
thick 0.1	0.35	0.7
dense 1.0	3.5	7.0

	94 GHz Apparent Sky Temperature (°K)	140 GHz Apparent Sky Temperature (°K)
Clear	50	81
Moderate Overcast	120	200
Rain	220	250

MEASURING THE DIELECTRIC CONSTANT OF MATERIALS IN THE MILLIMETER WAVE RANGE

V. A. Shcherbov, E. M. Kuleshov, and A. I. Goroshko

Radio Engineering, Republican Interdepartmental Scientific-Technical Collection, No. 9, 145-152, 1969
AD 727 941 (A79 06022)

A procedure is investigated for measuring the dielectric constant E of homogenous and inhomogeneous substances used in the millimeter and submillimeter wave range. The determination of E is based on measuring the optical thickness of the sample or the microwave phase shift caused by the step of the investigated sample. In the experiment E was measured with the help of a phase meter operating at Lambda equals 1.6 mm. Results are presented from measuring E of substances, and the measurement errors are analyzed. It is demonstrated that the measurement of accuracy as applied to substances with E equals 2-4 is within the limits of plus or minus (0.6-1.4) percent. (Authors)

EXTRACTS:

Dielectric constant measurements:

	Wavelength (mm)					
Material	1.6	1.79	2.14	2.3	2.51	2.98
Teflon	2.06 ± 0.02	—	2.05 ± 0.01	2.06 ± 0.02	—	2.13 ± 0.09
Polychlorovinyl	2.71 ± 0.03	—	—	—	—	—
Plexiglas	2.58 ± 0.04	2.56	—	2.57 ± 0.03	2.59	—
Micarta	3.53 ± 0.06	—	—	—	—	—
Ebonite	2.93 ± 0.05	—	—	2.76 ± 0.03	—	2.72 ± 0.02
Caprolon	2.99 ± 0.05	—	—	—	—	—
Ethyl Cellulose	3.94 ± 0.09	—	—	—	—	—
Carbolite	2.30 ± 0.08	—	—	—	—	—

ATTENUATION AND EMMISSION OF THE ATMOSPHERE AT 3.3 mm

F. I. Shimabukuro and E. E. Epstein
The Aerospace Corporation
P.O. Box 92957
Los Angeles, CA 90009

IEEE AP-18, No. 4, 485-489, July 1970

Four empirical relationships are presented between the 3.3-mm attenuation determined from observations of the sun and 1) radiosonde measurements of the total amount of precipitable water in the atmosphere, 2) surface measurements of absolute humidity, 3) IR spectral hygrometer observations of the sun, and 4) observations of differential atmospheric emission at 3.3 mm. Fluctuations in atmospheric emission at 3.3 mm during good weather do not put any limit on the sensitivity of a dual-beam observing system using a receiver whose rms noise fluctuations in an output bandwidth of 0.25 Hz are ≈ 0.5°K. (Authors)

EXTRACTS:

$A(dB) = 0.16 + 0.40\ W$ (std. dev. = 0.18 dB), where W is the precipitable water vapor in cm.

This result differs from Gibbins et al.: $A(dB) = 0.28(\pm 0.25) + 1.19(\pm 0.14)\ W$.

SIMONIS

OPTICAL MATERIAL LITERATURE INDEX FOR THE NEAR-MILLIMETER WAVE SPECTRAL REGION

G. J. Simonis
ERADCOM
Harry Diamond Laboratories
2800 Powder Mill Road
Adelphi, MD 20783

Fourth International Conference on Infrared and Millimeter Waves and Their Applications
IEEE Cat. No. 79 CH 1384-7 MTT, p. 18, December 10-15, 1979.

The primary frequency interval of interest here is the near-millimeter wave spectral region (NMMW--roughly 0.3 to 3 mm). This spectral region falls between the more actively researched far infrared and millimeter regions but has not itself received much attention until recently. Work has gone on at a relatively low level of effort, conducted by diverse microwave and infrared groups, using many different techniques, reporting in various wavelength and parameter notations in diverse journals. This paper reports on the preparation of a literature index to these references, and on observations based on that index. Particular thanks is due to Birch and Parker for their extensive bibliography on dispersive Fourier transform spectrometry, from which a number of material references were obtained. The emphasis in the index prepared thus far is on solid materials. Over 400 entries are included, taken from over 100 references. The format of the index is an alphabetical listing of materials, mostly by chemical name with cross referencing for more common names. (Author)

EXTRACTS:

This entry is only a description of the index.

MEASURED EFFECTS OF BATTLEFIELD DUST AND SMOKE ON VISIBLE, INFRARED, AND MILLIMETER WAVELENGTH PROPAGATION: A PRELIMINARY REPORT ON DUSTY INFRARED TEST-I (DIRT-I)

Donald Snider
Atmospheric Sciences Laboratory
White Sands Missile Range, NM 88002

R. W. McMillan and J. J. Gallagher
Georgia Institute of Technology
Atlanta, GA 30332

Compiled by James D. Lindberg, Test Director, Atmospheric Sciences Laboratory, White Sands Missile Range, NM 88002

This report describes the background, operation, and preliminary results of the Dusty Infrared Test-I (DIRT-I) conducted at White Sands Missile Range in October 1978. Examples of several visible and infrared transmissometer, lidar, and imaging measurements are discussed. Propagation conditions at various wavelengths, including 94 gigahertz, are compared. Particle size distributions obtained with an airborne payload sampling dust clouds generated by 155-millimeter artillery barrages, TNT explosions, and an oil/rubber fire are presented. The applicability of helicopter-borne payloads to further battlefield dust testing is discussed in detail. Preliminary results of the application of Fourier transform spectrometry to the battlefield dust problem along with new innovations in digitized visible and infrared imagery are presented for the first time. Relationships between explosive charge size, depth of burial and the resulting crater dimensions are also examined. (Author)

EXTRACTS:

Additional reports on the DIRT I measurements are:

1. "Millimeter Wave Propagation through Battlefield Dust," by R. W. McMillan, R. Rogers, R. Platt, D. Guillory, and J. J. Gallagher.

2. Measurements of Attenuation Due to Simulated Battlefield Dust at 94 and 140 GHz by J. J. Gallagher, R. W. McMillan, R. C. Rogers, and D. E. Snider.

Examples of attenuation measurements follow.

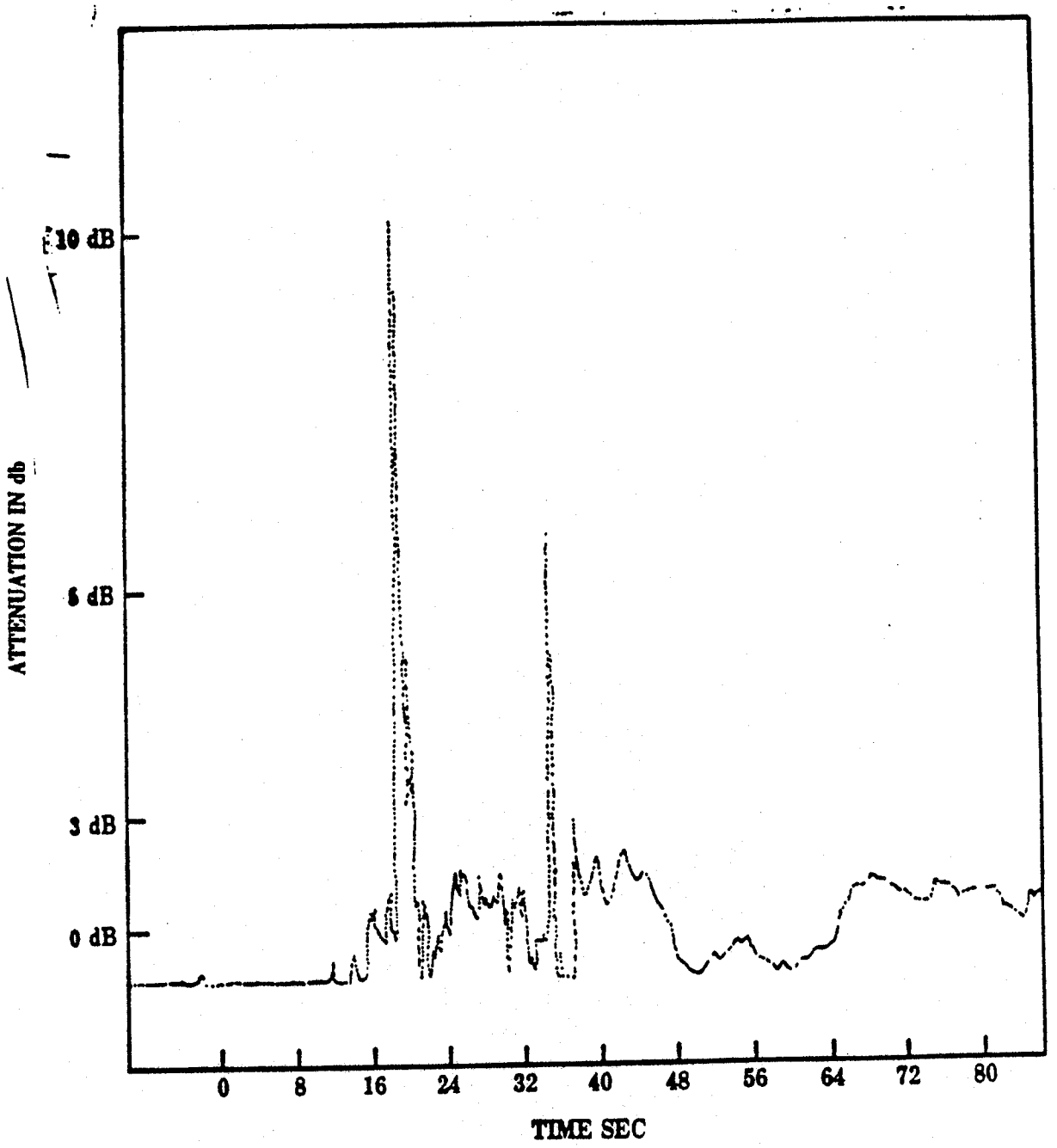

Figure 5-7. Attenuation measurement made at 94 GHz during event F-5 of 13 October 1978. Chart speed 15 cm/min, time constant 40 msec.

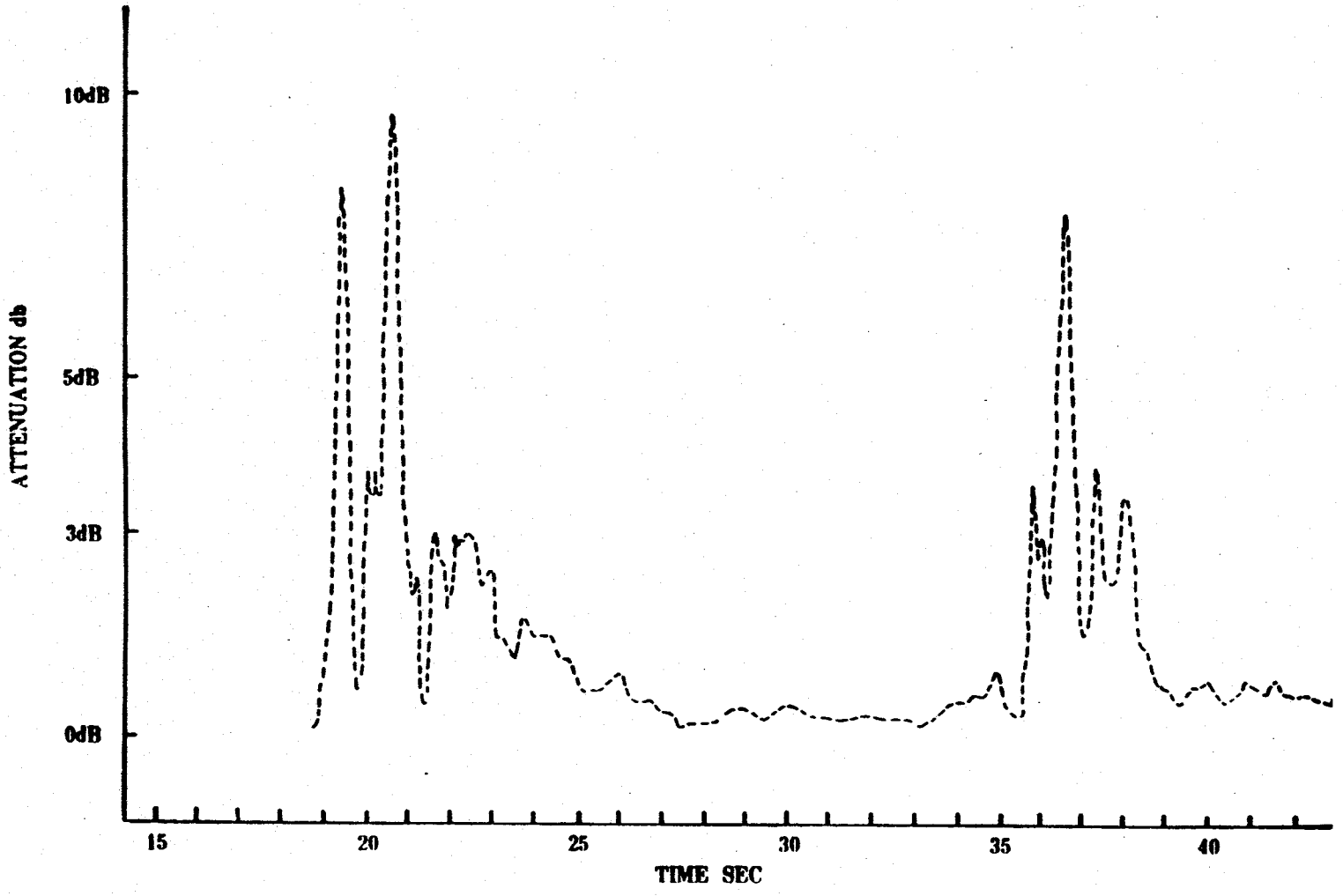

Figure 5-9. Attenuation measurements made at 94 GHz during event F-7 of 13 October 1978. Chart speed 1.25 cm/sec, time constant 40 msec.

SOKOLOV AND SUKHONIN

ATTENUATION OF SUBMILLIMETER RADIO WAVES IN RAIN

A. V. Sokolov and Ye. V. Sukhonin
Institute of Radio Engineering and Electronics
Academy of Sciences of the USSR
Moscow, USSR

Radio Engineering and Electronic Physics 15, No. 12, 2167-2171, 1970

The results of a theoretical computation of attenuation of radio waves in 0.1-2.0 mm range are presented; the computations are made taking account of new experimental data on the complex refractive index of liquid water with dropsize distribution given by Best and Polyakova. It is shown that the computation of attenuation in rain with intensity less than 10 - 12 mm/hr, based on rigorous Mie theory, are in satisfactory agreement with the experimental data at the wavelength of 0.96 mm. (Authors)

RADAT (Radiometric Detection and Tracking Flight Test Program)

Radiometry Department
Sperry Microwave Electronics
Clearwater, FL 33515

AFAL-TR-73-416, September 1973
AD 529 361L (A74 05612)

CONFIDENTIAL

The significance of this research and development to the Air Force is the investigation of the performance of a microwave radiometer sensor for terminal guidance applications. A standoff, adverse weather weapon guidance capability for use against tactical military targets is a continuing Air Force requirement. Existing techniques in microwave radiometry offer promising solutions to this need; consequently, the Air Force (AFAL/NVA-679A) purchased a Model K519 Dual-Mode 35-GHz Radiometric Tracker for flight test evaluation (Contract No. F33615-72-C-2066). Tracking performance tests against targets in typical backgrounds and quantitative measurement of target and background characteristics are the basis of evaluating the sensor technique. This report documents the flight test program -- preparation, measurements, data obtained, analysis and results. (Authors)

STEWART*

INFRARED AND SUBMILLIMETER EXTINCTION BY FOG

D. A. Stewart
Physical Sciences Directorate
Technology Laboratory
U.S. Army Missile Research and Development Command
Redstone Arsenal, AL 35809

Technical Report TR-77-9, 14 July 1977
ADA 045 181

A thorough literature survey of fog drop-size distributions throughout the world is discussed, and data from 36 references are summarized.

The review of an extensive list of over 100 references includes additional important information. Ranges of liquid water content and problems of relating this to visibility are examined. Changes in fog characteristics from place to place and from time to time are also considered, and the discussion includes small-scale spatial and temporal fluctuations.

A representative sample of data is used to compute extinction of electromagnetic energy with wavelengths of 0.55, 10.5, 870, and 1250 micrometers. Extinction of the 1250-micrometer wavelengths by fog droplets is always less than extinction of the 870-micrometer energy which is always less than the visible extinction and the 10.5-micrometer energy. The relationship between the visible and the infrared extinctions depends upon the drop-size distribution. The 10.5-micrometer wavelength is frequently attenuated about the same amount as the visible, and it is not uncommon for the infrared extinction to be greater than the visible extinction. (Author)

EXTRACTS:

This report is a survey of drop-size distribution, with a small quantity of 1.25-mm data correlated with data from other wavelengths.

THE ABSORPTION AND RERADIATION OF RADIO WAVES BY OXYGEN AND WATER VAPOR IN THE ATMOSPHERE

A. W. Straiton
College of Engineering
University of Texas
Austin, TX 78757

IEEE AP-23, 593-597, July 1975

This is a brief review paper on the interaction of radio waves with oxygen and water vapor in the atmosphere. It is the first of a series of mini-reviews sponsored by the Wave Propagation Standards Committee of IEEE and is intended primarily for those persons who have not had occasion to study extensively in the subject. (Author)

STRAITON

CLOUD ATTENUATION AT 35 AND 95 GHz AND ATTENUATION DIVERSITY MEASUREMENTS AT 30 GHz

A. W. Straiton
College of Engineering
University of Texas
Austin, TX 78757

Second DOD Workshop on Millimeter Wave Terminal Guidance Systems
(Adverse Weather Effects)
Report No. RADC-TM-76-9, May 1976
ADA 026 270 (A76 5072)

Attenuations for a variety of cloud conditions have been measured at frequencies of 35 and 95 GHz during 1972 and 1973. Clouds producing the highest attenuation were the rain-bearing cumulonimbus types. It was observed that the higher in altitude the thunderstorm, the higher the attenuation. Non-rain clouds such as the stratocumulus and cumulus produced very low attenuations. A thunderstorm's horizontal extent was usually less than 11 km and the joint probability of sites separated by that distance having high attenuations simultaneously was very low. (Author)

ATMOSPHERIC LIMITATIONS ON THE USE OF RADIO WAVES WITH FREQUENCIES OF 15, 35, AND 95 GHz

A. Straiton, B. M. Fannin, et al.
Electrical Engineering Research Laboratory
University of Texas
Austin, TX 78757

Final Report AFAL-TR-72-264, 22 September 1972

This report describes the results of theoretical and experimental studies of the atmospheric limitations on the use of radio waves at frequencies of 15, 35, and 95 GHz. Background information is presented on the absorption by atmospheric gases, the attenuation by rain and clouds, and the effects of inhomogeneities in the atmosphere.

Transmission measurements were made over a 9.5-mile path near Austin, Texas, and on several overwater paths in the vicinity of Galveston, Texas. The Austin clear air data showed only minor variations in signal level except during the passage of a cold front and during periods of strong refraction. The Galveston paths were examples of low level trapping and fading levels of 3 to 10 dB occurred consistently.

Rain effects were observed over the 9.5-mile path near Austin and over a 2000-foot path at Balcones Research Center of the University of Texas. Spatial variations of rainfall rates on the 9.5-mile path prevented close comparison of attenuation and rain rates. Such a comparison on the 2000-foot path was accomplished although rain rate differences were noted even over the short length of this path.

The attenuations of 35- and 95-GHz frequencies by clouds were studied by the use of radiometers at these frequencies. The radiometers were used both in the sun tracking and in the sky temperature modes. Possible uses of these techniques for the remote sensing of cloud parameters are examined. (Authors)

TARGETS AND BACKGROUNDS

G. H. Suits
Environmental Research Institute of Michigan
Ann Arbor, MI

B. D. Guenther
Missile Research Directorate
Technology Laboratory
U.S. Army Missile and Development Command
Redstone Arsenal, AL 35809

Technical Report T-78-71, 21 July 1978

The near millimeter wave radiative properties of military targets and of the backgrounds with which they may be associated are the fundamental data required to begin to assess the probable performance of a large number of military applications of millimeter wave systems. The incident and scattering angles are shown schematically. In general, the data base for discrete tactical targets is not extensive especially for millimeter wave frequencies. The millimeter wave data which have been found in the present literature search are all for the monostatic mode and primarily for frequencies of 94 GHz and below. This data is presented to allow estimation of near millimeter wave cross sections by extrapolation. (Authors)

EXTRACTS:

Classified material collected during this study may be found in the final report of the DARPA NMMW Technology Base Study (Volume IV) edited by Drs. S. M. Kulpa and E. A. Brown of the Harry Diamond Laboratories, report number HDL-SR-79-8, November 1979.

NEAR-GROUND ATMOSPHERIC ATTENUATION OF 0.89 mm RADIATION

G. A. Tanton, J. D. Stettler, R. L. Morgan, and J. F. Osmundsen
Research Directorate
U.S. Army Missile Command
Redstone Arsenal, AL 35809

S. S. Mitra
Department of Electrical Engineering
University of Rhode Island
Kingston, RI 02881

J. G. Castle, Jr.
Physics Department
University of Alabama in Huntsville
Huntsville, AL 35807

Fourth International Conference on Infrared and Millimeter Waves and Their Applications
IEEE Cat. No. 79 CH 1384-7 MTT, December 10-15, 1979, S. Perkowitz (editor)
Post-Deadline Digest Contributions, p. 27

EXTRACTS:

From data taken during clear and cloudy days in the summer:

$$\alpha \text{ (dB/km)} = 0.6 + 0.8\,\rho + 0.05\,\rho^2$$

where ρ is the absolute humidity.

TARGET SIGNATURE ANALYSIS CENTER*

TARGET SIGNATURE ANALYSIS CENTER: DATA COMPILATION

Tenth Supplement, July 1969
AD 489 968 (A67 7655)

EXTRACTS:

Microwave radar data for 0.1 to 35.19 GHz.

TARGET SIGNATURE ANALYSIS CENTER: DATA COMPILATION ELEVENTH SUPPLEMENT

Target Signature Analysis Center
Infrared and Optics Division
Willow Run Laboratories
The University of Michigan
Ann Arbor, MI 48104

Volume II, Bidirectional Reflectance: Graphic Data, October 1972
(A67 07655) AFAL-TR-72-226

This report is the eleventh supplement to the Target Signature Analysis Center: Data Compilation and contains 2200 curves of bidirectional reflectance versus angle. The significance of this report to the Air Force is that these data provide the Air Force with essential optical properties-of-materials data to analyze the angular dependence of the reflected radiance from various targets. Volume I contains a definition of the parameters pertinent to the bidirectional reflectance, a discussion of the data, some equations for application of the data, and an index and cross reference of the data contained in Volume II. Bidirectional reflectance data are presented graphically in Volume II.

This supplement to the Target Signature Analysis Center: Data Compilation augments an ordered, indexed compilation of reflectance, radar cross sections, and apparent temperatures of target and background materials. The Data Compilation includes spectral reflectances and transmittances in the optical region from 0.3 to 15 micrometers, normalized radar cross-sections, and apparent temperatures at mm wavelengths. When available, the experimental parameters associated with each curve are listed to provide the user with a description of the important experimental conditions. (Authors)

EXTRACTS:

Reflectance data compilation of paint, cloth and canvas, wood, soil, vegetation, asphalt and concrete, reflectance standards material, metal and other materials.

THOMPSON*

DUST CLOUDS--MODELS AND PROPAGATION EFFECTS

J. H. Thompson
General Electric-TEMPO
Santa Barbara, CA 91302

Proceedings of the Workshop on Millimeter and Submillimeter Atmospheric Propagation Applicable to Radar and Missile Systems, Redstone Arsenal, AL 38509, O. M. Essenwanger and D. A. Stewart (editors)
Technical Report RR-80-3, 114-117, February 1980

In a nuclear battlefield environment, large extensive dust clouds are generated by low altitude and surface nuclear bursts. In a tactical battlefield environment, a great number of small dust clouds are produced by munitions impacting the ground. Millimeter and submillimeter waves propagating through these dust clouds can suffer various degrading effects including absorption, scattering, decorrelation and scintillations.

Under contracts from the U.S. Army Atmospheric Sciences Laboratory and the Defense Nuclear Agency, General Electric-TEMPO has developed models describing the tactical and nuclear dust clouds and the absorption and scattering propagation effects. A new efficient exact Mie cross section code has been developed. This code calculates the Mie absorption and scattering cross sections and scattering pattern for both individual particles and for distributions of particles. Utilizing the Mie parameters, analytic algorithms have been developed to calculate the absorption, single and multiple scattering effects. Sample calculations of dust cloud models and propagation effects are presented and compared with the exact theoretical or experimental data. (Author)

A REVIEW OF RADIOMETRIC MEASUREMENTS OF ATMOSPHERIC ATTENUATION AT WAVELENGTHS FROM 75 CENTIMETERS TO 2 MILLIMETERS

W. I. Thompson III and G. G. Haroules
NASA Electronics Research Center
Cambridge, MA 02167

NASA TN D-5087, April 1969
N69 22949 (A69 03969)

Published values of vertical attenuation resulting from radiometric measurements of absorption and emission of the Earth's atmosphere in the wavelength range from 75 cm to 2 mm are presented. The literature search included a review of several hundred publications. These data emphasize the need for further theoretical and experimental work in the calculation and measurement of attenuation in this portion of the spectrum. (Authors)

EXTRACTS:

Clear-sky attenuation at 91 GHz varies from 0.31 to 0.80 dB (Shimabukuro; "Propagation Through the Atmosphere at a Wavelength of 3.3 mm," Aerospace Corp., SSD-TR-65-69, 1965) and at 140 GHz it is 4.0 dB (Tolbert, Krause and Straiton, J. Geophys. Res. 69, 1349-1357, 1964). Note that this 1965 reference is superseded by the Shimabukuro and Epstein reference cited in this document.

The "classic" graph of zenith attenuation between 10 and 170 GHz is shown here.

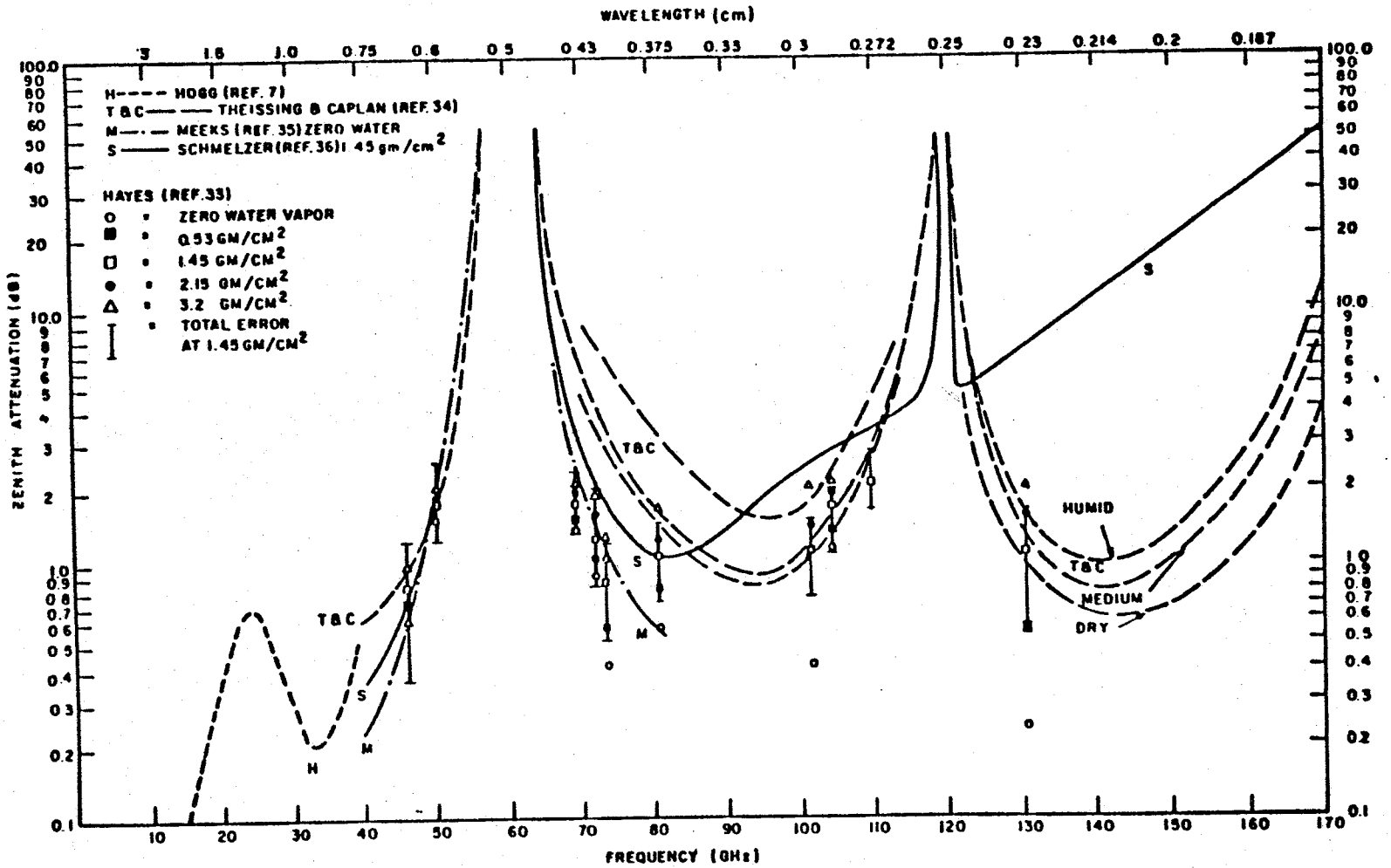

-- Theoretical and measured values of zenith atmospheric attenuation in the frequency range 10 to 170 GHz

REMOTE SENSING OF THE EARTH BY MICROWAVES

Kiyo Tomiyasu
General Electric Company
Valley Forge Space Center
Philadelphia, PA 19101

Proc. IEEE 62, No. 1, 86-92, January 1974

Extant techniques for remotely sensing the earth with instruments operating at microwave frequencies are surveyed. Microwave sensors can provide day-night operations and almost an all-weather capability due to higher transmission through clouds at microwave than at visible or infrared wavelengths. Passive (radiometers), active (radars, altimeters, and scatterometers), and composite (passive-active) microwave sensors are in use or planned for such diverse applications as measuring ocean surface dynamics, ocean salinity, soil moisture content, atmospheric temperature and atmospheric constitutents; detecting sea ice, oil slicks, and storm cells; and identifying agricultural crops. These measurements have been taken with sensors located in towers, aircraft, and, most recently, satellites. (Author)

EXTRACTS:

A general summary report.

TREBITS, CURRIE, DYER, AND TETI*

MULTIFREQUENCY MILLIMETER RADAR SEA CLUTTER MEASUREMENTS

R. N. Trebits, N. C. Currie, and F. B. Dyer
Engineering Experiment Station
Georgia Institute of Technology
Atlanta, GA 30332

J. J. Teti
Naval Surface Weapons Center
Dahlgren Laboratory, VA 22313

Proceedings of the Eighth DARPA/Tri-Service Millimeter Wave Conference
System Planning Corporation (editor), 1500 Wilson Blvd., Arlington,
VA 22209, p. 109-118, April 1979
(A80 00206)

SECRET

A recent radar sea clutter backscatter measurement program at 9.5, 16, 35, and 95 GHz is described; parallel- and cross-polarized data were recorded for a variety of wave height, wind speed, wind direction, and geometric conditons. Preliminary analyses of selected data are presented for horizontal and vertical transmitted polarizations. (Authors)

mm-WAVE REFLECTIVITY OF LAND AND SEA

R. N. Trebits, R. D. Hayes and L. C. Bomar
Georgia Institute of Technology
Atlanta, GA 30332

Microwave Journal 21, 49, August 1978

Presents a synopsis of the currently available amplitude and power spectral characteristics of land clutter, sea clutter, and rain backscatter above K_u-band. Emphasis in the data presented is placed on those environmental and radar parameters that can affect the statistical properties of the radar backscatter. In addition, clutter characteristics in the millimeter-wave region are compared with those for the lower radar frequencies.

EXTRACTS:

Gives some of the more pertinent radar characteristics of terrain, sea, and rain at 9.4, 15, 35, and 95 GHz.

TRERISE

94-GHz RADIOMETRIC SENSOR

B. L. Trerise
Ground Systems Group
Hughes Aircraft Company
P.O. Box 3310
Fullerton, CA 92634

Hughes Fullerton #FR-78-11-1407, 15 November 1978
ADB 036 553L (A79 06226)

The development of a passive, solid-state, 94-GHz radiometer was addressed using image guide techniques in a balanced mixer configuration. A digital signal processor based on a CMOS microprocessor was developed for solution detection and detonate algorithms. Tests of the radiometer were conducted from a rotating airborne platform at altitudes and spin rates that simulate the operating conditions of a new class of munitions. It was found that the performance of the image guide radiometer was not acceptable when fabricated with presently available beam lead silicon mixer diodes (750 GHz). Acceptable performance should be obtained from gallium arsenide beam lead diodes now nearing availability. These diodes should exhibit frequencies on the order of 2000 GHz. Definitive signature data for targets of interest were obtained that indicate high potential for warhead fuzing applications. (Author)

EXTRACTS:

This report contains 94-GHz experimental radiometric sensing of a truck on a road, a tank, an aluminum reflector, and water. A large amount of target response data (in the form of voltages) taken at different polarizations and aspect angles are presented graphically as a function of target range.

ABSORPTION IN THE 220-GHz ATMOSPHERIC WINDOW

Fawwaz T. Ulaby
University of Kansas Center for Research, Inc.
Lawrence, KN 66044

IEEE A & P Communications-21, 266-269, March 1973

The atmospheric absorption spectrum in the 220-GHz window region is controlled primarily by the water vapor lines centered at 183.3 and 323.8 GHz. There are however, numerous other lines in the submillimeter part of the spectrum which contribute significantly to the losses. At the longer millimeter wavelengths, it has been the practice to lump the contributions of the submillimeter lines using the Van Vleck low frequency approximations. This procedure is not permissible for the 220-GHz window region because of the proximity of some of the submillimeter lines. Experimental measurements substantiate this observation. The present study introduces an alternative approximation for calculating the residual effect of submillimeter lines. The results, larger by a factor of 2, are in closer agreement with experimental observations. (Author)

ULABY AND STRAITON*

ATMOSPHERIC ABSORPTION OF RADIO WAVES BETWEEN 150 AND 350 GHz

F. Ulaby
University of Kansas Center for Research, Inc.
Lawrence, KN 66044

A. W. Straiton
Electrical Engineering Research Laboratory
University of Texas
Austin, TX 78705

IEEE AP-18, 479-485, No. 4, July 1970

This paper compares several forms for the absorption line shapes for atmospheric gases as applied to frequencies between 150 and 350 GHz. The contributions of various lines to the absorption in this frequency range are examined. Equations are presented for direct calculation of attenuation as a function of pressure, temperature, and water vapor density. (Authors)

THE EFFECT OF RAIN ON THE MILLIMETER AND SUBMILLIMETER RADIOWAVE DISTRIBUTION

I. Kh. Vakser, Yu. I. Malyshenko and L. E. Kopilovich
Institute of Radio Physics and Electronics
Academy of Sciences, USSR

Izv. Atmospheric and Oceanic Physics 6, 956-959, No. 9, 1970
(Translated by J. Findlay)

In this paper we consider the effect of rain on the attenuation of radio waves in the millimeter and submillimeter ranges and give the results of calculating the attenuation and backscattering coefficients. (Authors)

MEASUREMENTS OF THE 980-1600 MICROMETER ATMOSPHERIC ABSORPTION BY RADIOASTRONOMICAL MEANS

A. S. Vardanyan, I. A. Iskhakov, A. V. Sokolov, and Ye. V. Sukhonin
Institute of Radio Engineering and Electronics
Academy of the Sciences of the USSR
Karl Marx Avenue 18
Moscow, USSR

Radio Eng. and Electron. Phys. 18, No. 2, 163-165, February 1973

The article describes measurement of the absorption of water vapor between 980 and 1600 micrometers at sea level in various latitudes. The absorption is minimum (0.6 dB/gm^{-3}) in the transmission window at 1260 micrometers. The results were compared with theories and data presented by other researchers, as well as with results of radiosonde measurements. (Authors)

EXTRACTS:

Total vertical absorption at 1.26 mm (daily averages):

14 Dec 1971	0.6 dB	humidity = 1.04
20 Dec 1971	1.18 dB	= 2.03
25 Dec 1971	0.91 dB	= 1.5

Average total "specific" absorption measured with the radioastronomical technique at 1.26 mm is 0.6 dB/gm^{-3}.

SCATTERING INTENSITY PLOTS AND TRANSMISSION COEFFICIENTS FOR MILLIMETER-WAVE PROPAGATION THROUGH RAIN

Wolfhard Vogel
Millimeter Wave Group
Electrical Engineering Research Laboratory
The University of Texas at Austin
Austin, TX 78705

Report No. AFAL-TR-71-345, December 1971
AD 890 408L

This report presents the results of computer calculations of the scattering of millimeter radio waves by rain and hail. Polar plots of the intensity of scattering are shown for frequencies of 30, 100, 150, and 300 GHz impinging on single drops ranging in size from 0.5 mm to 7.0 mm, ice spheres from 1.0 mm to 7.0 mm, and on distributions of raindrop sizes associated with rainfall rates from 0.25 mm/hr to 150 mm/hr.

In addition, tables are presented for these frequencies and these rainfall rates of the attenuation from absorption from scattering and from their combination. The fractions of energy backscattered and forward scattered per unit solid angle are also tabulated for the rain rates studied. (Author)

VOTE*

TACTICAL TARGET/CLUTTER SIGNATURE STUDIES AT K_u/K_a BAND

F. W. Vote
MIT Lincoln Laboratory
Lexington, MA 02173

Proceedings of the Eighth DARPA/Tri-Service Millimeter Wave Conference
System Planning Corporation (editor), 1500 Wilson Blvd., Arlington,
VA 22209, p. 77-90, April 1979
(A80 00206)

SECRET

This paper presents results of a K_u/K_a band signature of tactical targets and field clutter measured in the Concord-Fort Devens area of Massachusetts. Signature comparisons are made at the two frequencies, and the implications as far as CFAR performance for millimeter acquisition studies are shown. (Author)

35-GHz RADIOMETRIC SIGNATURES OF ARTILLERY PIECES AND THEIR APPLICATIONS TO HOWLS‡

H. B. Wallace
Ballistic Research Laboratory
Aberdeen Proving Ground, MD 21005

BRL Memorandum Report No. 2727 (Supersedes IMR No. 445)
February 1977
AD C009 321 (A78 05338)

CONFIDENTIAL

This report is in response to a request by Lincoln Laboratory of MIT for radiometric signature data of artillery pieces at 35 GHz. Temperature profiles and cross sections were measured using a 35-GHz radiometer with a 6-inch antenna. A survey was also made of other sources of radiometer artillery signatures. Analysis of an RPV based scanning system was made and it was concluded that a scanning radiometer would not be suitable for the location of the artillery pieces with the possible exception of the M109, 155 mm S/P Howitzer. (Author)

‡HOWLS and HWLA are acronyms for Hostile Weapons Locating Systems.

WEST AND ASHWELL*

PASSIVE RADIOMETER PERFORMANCE IN FOUL WEATHER

M. West, Jr. and J. R. Ashwell
Martin Marietta Aerospace
Orlando, FL 32802

Proceedings of the Sixth DARPA/Tri-Service Millimeter Wave Conference
Tactical Technology Office Defense Advanced Research Projects Agency,
1400 Wilson Blvd., Arlington, VA 22209, p. 190-198, November 1977
(A78 01438)

SECRET

A model is described which predicts the attenuation and backscatter properties of falling snow at millimeter wavelengths. Attenuation and backscatter coefficients are calculated for wavelengths of 8.6 and 3.2 mm for varying snowfall intensities. Attenuation coefficients of weather constituents along with standard weather models are used to calculate the range reduction of passive radiometers operating in weather. (Authors)

94-GHz RADIOMETER

Robert L. Wilt
Sperry Microwave Electronics
Sperry Rand Corporation
P.O. Box 4648
Clearwater, FL 33518

AFAL-TR-77-19, June 1977
ADB 020 739L (A79 06628)

A 94-GHz microwave radiometer was designed, fabricated, and tested. A temperature measurement sensitivity of 3.5 K was achieved with a 150-Hz output bandwidth. Radiometer noise figure and IF bandwidth were 12.5 dB and 230 MHz, respectively. Government-furnished IMPATT local oscillator and mixer assemblies were evaluated and incorporated into the radiometer. The IMPATT oscillator was seen to limit radiometer performance due to its noise content. The radiometer is an AC coupled total power radiometer with periodic calibration and automatic gain stabilization (AGS). An IMPATT diode operating strictly as a noise generator was successfully employed as AGC reference source with compensation for its environmental temperature sensitivity. (Author)

WISLER AND HOLLINGER*

ESTIMATION OF MARINE ENVIRONMENTAL PARAMETERS USING MICROWAVE RADIOMETRIC REMOTE SENSING SYSTEMS

Macmillan M. Wisler and James P. Hollinger
Advanced Space Sensing Applications Branch
Space Sciences Division
Naval Research Laboratory
Washington, DC 20375

NRL Memorandum Report 3661, November 1977

This is an interim report on an ongoing program to develop a passive microwave system for the remote all-weather measurement of sea surface temperature from a satellite platform. It presents a general method for obtaining optimal linear algorithms for the reduction of multi-frequency radiometer data to determine marine environmental variables. The mean square errors in determining the environmental variables are also determined, thereby enabling the evaluation of different passive microwave radiometric systems. The method, called the "Environmental Transfer Function", includes in its analysis the error contributions from three sources: errors in measuring microwave brightness temperature, the statistical variances of the environmental parameters, and uncertainties in the equations used to relate the brightness temperature to the environmental parameters. The mathematical formulation is first developed and then an example application is given to evaluate the remote sensing capability of selected radiometric systems. (Authors)

MEASUREMENTS OF ATMOSPHERIC ATTENUATION ON AN EARTH-SPACE PATH AT 90 GHz USING A SUN TRACKER

Gerard T. Wrixon
Department of Electrical Engineering
University College, Cork, Ireland

Bell System Technical Journal 50, 103-114, January 1971

Measurements of 90 GHz attenuation through the total atmosphere due to absorption by clouds, fog and rain are presented and compared with simultaneous measurements at 16 GHz. It is seen that rain is the most important contributor to atmospheric extinction at 90 GHz, light rain causing greater than 25 dB attenuation on a number of occasions during the measurement period. (Author)

EXTRACTS:

Reproduced here are summaries of cloud, rain, fog and heavy overcast measurements.

Signal fluctuation is less rapid in heavy overcast conditions.

Average attenuation due to heavy fog (ambient temperature = 11°C) is 3.2 dB at 90 GHz.

TABLE II—SUMMARY OF RAIN ATTENUATION MEASUREMENTS

Date Type of Rain	90-GHz Attenuation	Corresponding 16-GHz Attenuation	Ratio $\frac{\text{90-GHz Atten.}}{\text{16-GHz}}$	Comments
12/10: Light rain observed from 1:30 P.M. to 2:30 P.M. Between 1:30 P.M. and 3 P.M., a rainfall of 0.5 mm was measured by the Crawford Hill Rain Gauge.	Min. 5.22 dB Max. >25 dB	0.2 dB 0.9 dB	dB Ratio varied randomly between 25 ~ 29	Attenuation increased monotonically both at 16 and 90 GHz during this period.
12/14: Rain mixed with snow, turning to rain observed from 12:00 P.M. to 2 P.M. No rain gauge reading obtained as gauge was full of snow. Ground temperature, 35° to 37°F.	Min. 7.00 dB (end of rain) Max. 13.6 dB	0.3 dB 0.54 dB	Ratio decreased from 28 to about 17 and increased again to 23	The maximum 90-GHz attenuation was measured before the minimum ratio of 90/16 GHz attenuation was attained.
12/8: (a) Steady rain observed from 9 to 9:30 A.M. Rain gauge measurement ~0.8 mm/hr.	16.5 dB	0.6 dB	~27	Attenuation remained reasonably constant at both frequencies during this rain (see Fig. 2).
(b) Between 10:15 A.M. and noon, showers were observed. Total amount of rain that fell during this period (from rain gauge) was ~0.5 mm.	15 dB 20 dB 24 dB >25 dB	0.65 dB 0.75 dB 0.9 dB 1 dB	23 27 27 >25	These are the values of attenuation measured at the peak of various showers (see Fig. 2).

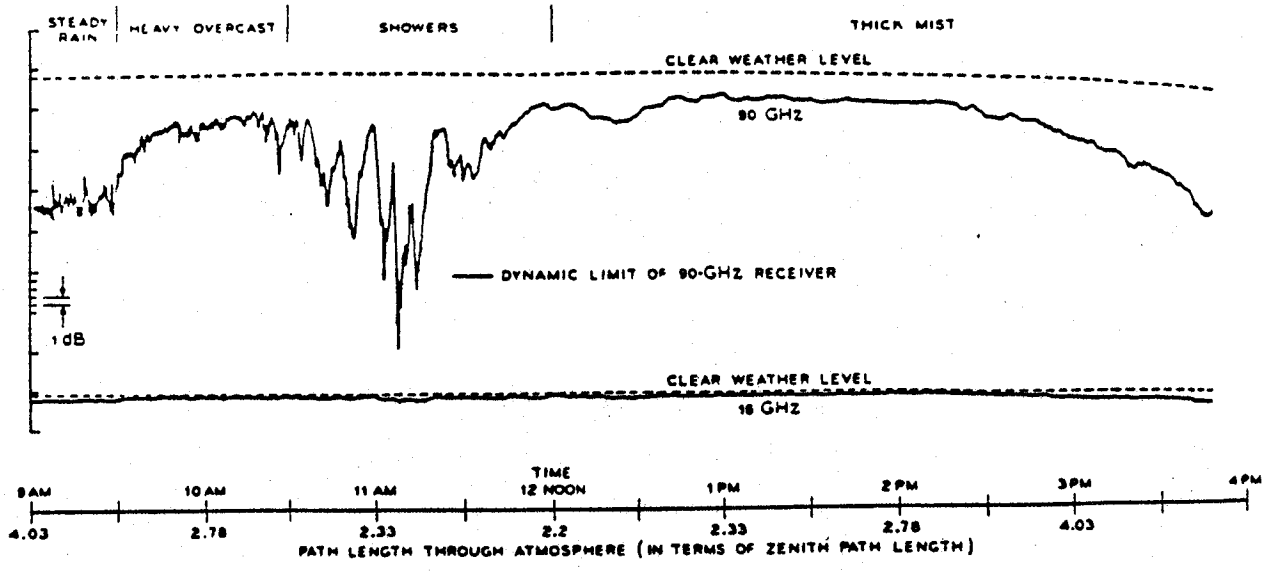

Fig 2—Logarithmic record of 90-GHz and 16-GHz attenuation for December 8, 1969.

TABLE I—SUMMARY OF CLOUD ATTENUATION MEASUREMENTS

Case Number and Type of Cloud Cover	Ground Temperature	Relative Humidity	90-GHz Atten.	Corresponding 16-GHz Atten.	Ratio 90-GHz Atten. / 16-GHz	Comments
1. Individual Cumulous Clouds in an otherwise clear sky	9°C	45%	Maximum: 3.7 dB Typical: 2.1 dB	0.16 dB 0.1 dB	~22	See text for note on maximum attenuation.
2. Overcast sky (no rain)	8°C	55%	Maximum: 1.6 dB	0.07 dB	~23	Signal continuously fluctuates as cloud cover moves across sky. Typical fluctuation ~1 dB at 90 GHz. No fluctuation at 16 GHz.
3. Heavily overcast sky between periods of rain (see Fig. 2)	10°C	100%	Maximum: 7.2 dB Typical: 5.2 dB	0.3 dB 0.21 dB	~24	
4. Overcast sky on cold day (no rain)	1°C	65%	Maximum: 1.64 dB	0.12 dB	~14	Most of the time there was little attenuation (<0.5 dB at 90 GHz) due to this cloud cover and no continuous fluctuations were present as in No. 2 above.

MEASUREMENTS OF EARTH-SPACE ATTENUATION AT 30 GHz

G. T. Wrixon
Department of Electrical Engineering
University College, Cork, Ireland

R. W. McMillan
Engineering Experiment Station
Georgia Institute of Technology
Atlanta, GA 30332

IEEE MTT-26, 434-439, No. 6, June 1978

Measurements of attenuation at 230 GHz through the total atmosphere due to the presence of oxygen and water vapor molecules, clouds, and rain are presented and discussed. The measurements were carried out using a specially designed superheterodyne receiver mounted on a sun tracker. Simultaneous measurements were also carried out at 13 GHz. For a measuring site close to sea level at Holmdel, NJ, the "clear sky" zenith attenuation was found to be given by A (dB) = 0.35 ρ, where ρ was the measured ground water vapor density in g/m^3. When the ground temperature was below about 7°C, most cloud and overcast gave less than 0.5 dB attenuation, whereas with a ground temperature greater than 13°C, cloud attenuation was 8 - 10 times greater. Calculations of zenith attenuation in the 230-GHz atmospheric window were also made using the Gross analytic line shape, Schulze-Tolbert empirical line shape, and an empirically modified Gross line shape. These calculations were based on determinations of water vapor density and temperature made at the measurement site, and on radiosonde measurements made at a distance of 80 km away. Measured and calculated results are graphically compared. It is concluded that either the modified Gross line shape or the Schulze-Tolbert line shape gives conservative estimates of zenith attenuation at 230 GHz for clear days, while the Gross line shape gives fair agreement with measured results. (Authors)

EXTRACTS:

Cloud attenuation at 230 GHz (5 days of measurements; first 4 days: T = 3 - 7 °C; 5th day: T = 13 - 15 °C; same type of clouds on all 5 days):

	230-GHz Excess‡ Attenuation (dB)	
Cloud Type	Cold Days	Warm Day
dark cumulus	0.3 - 0.5	1 - 2 (occasionally 5 dB)
light overcast	~0	1.5
heavy overcast	0.5 (=twice an hour: 2-2.5 dB)	

The excess attenuation was much greater on warmer days.

‡Excess over attenuation of clear sky.

MILLIMETER WAVE MEASUREMENTS OF TARGETS AND CLUTTER

B. S. Yaplee, J. P. Hollinger, and B. E. Troy
Naval Research Laboratory
Washington, D.C. 20390

Proceedings of the Eighth DARPA/Tri-Service Millimeter Wave Conference
System Planning Corporation (editor), 1500 Wilson Blvd., Arlington,
VA 22209, p. 189-196, April 1979
(A80 00206)

SECRET

Optimum passive detection of an object in a clutter background requires a knowledge of the transfer characteristics of the object and of the background. The millimeter wavelength characteristics of selected targets and backgrounds measured at 90 GHz are described and target detection enhancement is discussed. (Authors)

ATTENUATION OF RADIATION AT WAVELENGTHS OF 1.25 AND 2.0 mm

V. F. Zabolotniy
State Sternberg Astronomical Institute
University Avenue 13, Moscow, USSR

I. A. Iskhakov, A. V. Sokolov and E. V. Sukhonin
Institute of Radioengineering and Electronics
Academy of Sciences
Marx Avenue 18, Moscow 103907, USSR

Infrared Physics 18, 815-817, 1978

The results of measurements of radiation attenuation at wavelengths of 1.25 and 2.0 mm in clouds, carried out in the Crimea, using the RT-22 radio telescope are presented. This telescope has an antenna diameter of 22 m and is coupled to a Fabry-Perot interferometer and a liquid-helium cooled n-type InSb detector. (Authors)

EXTRACTS:

Average Zenith Attenuation (dB)

Wavelength (mm):	0.45	0.73	1.2	2.0
Cloud Type:				
Altocumulus	1.5	0.6	0.36	0.16
Cumulus	17.5	10	1.6	----
Cumulus Congested	51	20	19	9.0

The authors indicate that these are rough values only; unfortunately, they do not indicate dispersion in the data.

METHOD OF CALCULATING THE ATMOSPHERIC WATER VAPOR ABSORPTION OF MILLIMETER AND SUBMILLIMETER WAVES

A. Yu. Zrazhevskiy
[Institutional affiliation not given]

Radio Engineering and Electronic Physics 21, 31-36, No. 5, May 1976

An engineering method has been developed for calculating the molecular absorption in water vapour. This method is obtained from the following conditions: its results must agree with the experimental data for normal conditions in the atmosphere and the form of the dependences of attenuation on the humidity, pressure, and temperature must agree with the relationships from quantum mechanical formulas. The absorption coefficient is found as the sum of two terms. One of these terms takes account of the attenuation contribution of spectral lines (transition frequencies < 36.6 cm^{-1}); the other is determined from the semi-empirical relationship that satisfies the above stated conditions. The engineering calculation method can be used to estimate the absorption values in the earth's atmosphere at wavelengths greater than 0.28 mm. (Author)

APPENDIX

Simultaneous Radiometric Measurements at 32 GHz and 90 GHz

K. Grüner

Deutsche Forschungs- und Versuchsanstalt für Luft- und Raumfahrt

D 8031 Oberpfaffenhofen, Federal Republic of Germany

ABSTRACT

The paper gives an insight upon a part of the present experimental activities at DFVLR in the area of microwave radiometry. A preliminary selection of measurements which were made from a stationary platform 21 metres above ground is discussed.

1. INTRODUCTION

This paper and the paper "Airborne Microwave Radiometric Measurements at DFVLR, Oberpfaffenhofen", are devised to give an insight upon the present experimental activities at DFVLR in the area of microwave radiometry.

Since late last year, we have had a set of three operational radiometers in the atmospheric window ranges at 11,32 and 90 GHz. This equipment is being used the next years for intensive, simultaneous measurements. The measurements are running under two different programs depending upon the platform used:

1. Fixed platform on top of a tower or vehicle
2. Airborne measurements.

The measurements were started from a 21 m tower that is part of one of the DFVLR out door antenna test ranges, this spring.

The following goals have been and are being aimed at, with the towermeasurements:

1. Reliability tests,
   in fact, the 11 GHz radiometer was defect after a short period of time, although it had been working without fault since 1968. Unfortunately the damage to the equipment was such that it had to be taken down for the then running series of measurements.
2. Gathering of experiences concerning the preparation and execution of multispectral measurements.
3. Initiation and test of evaluation methods

and last but not least

4. Collection of further experiences in the area of thermal microwave radiation of our environment.

Up till now, we have gained the opinion from our activities that we are in this case confronted with a lengthy process of learning, a process of learning to see in a spectral range that yields in part totally different impressions of our environment than we are used to in the optical window. This philosophy is the basis of our work.

Measurements from a fixed platform are advantageous in various respect:

1. Simple reproducibility.
2. Improved temperatur resolution due to longer integration times.
3. Improved angular resolution due to larger antenna apertures.
4. More individual tests per time span.
5. Less costs.

2. EQUIPMENT

Before the nature of measurements is told that have been conducted until now, it is necessary to go into a little more detail concerning the present equipment (Fig. 1.). The 11 GHz radiometer will be included in the following data. The receivers operate either by using the common Dicke principle or else by using a technique that uses a second reference source and thus allows a continous autocalibration.

For the 11, 32 and 90 GHz radiometers, the temperature resolution at 1s integration time comes out to be 0.1, 0.5, 1.5 K respectively. The microwave bandwidth is 1 GHz, two-times 300 MHz - both sidebands are used - and 2 GHz. The 3 dB-bandwidths of the antennas are 1.8, 2.1 and 0.4 degrees (a primary focused paraboloid for 11 GHz, an excentric section of paraboloid at 32 GHz and a cassegrain antenna at 90 GHz are used).

For the first series of measurements that are reported in this paper, we wanted to have one antenna with high angular resolution whereas the other two antennas were designed to have approximately identical resolution. In the upright position of the combination the 90 GHz radiometer received the vertically polarized, the rest received the horizontally polarized portion of the thermal microwave radiation. In this way, we can expect the optimum signal differentiation for inclined looking angles. Further we expect a maximum of qualitativ information on the scattering properties of the object under observation.

The three radiometers are mounted together on a three axis platform. An automatic control unit that was developed for the radiometric measurements allows line scanning of given angular ranges. Objects on the ground can be observed under angles from zero to forty degrees below the horizon.

3. NATURE OF MEASUREMENTS AND RESULTS

The following measurements have up to now been conducted:

1. Registration of brightness temperatures of man made and natural objects on earth (buildings, concrete roads, cars behind and in front of trees, different soils) in dependence of weather and vegetation and supplemented by registration of radiometric sky temperature, air temperature, air moisture, soil temperature and optical brightness of the objects.
2. Registration of traffic in various environment.
3. Mapping of the environment around the tower (parking area with and without cars, buildings with and without trees in the foreground, airfield with hangars and so on).

These measuring programs yielded a great amount of data. The complete evaluation will take some more time. The following figures represent a first preliminary selection.

By brightness temperatures antenna temperatures are meant. A correction to obtain the actual brightness temperatures requires the knowledge of the spurious radiation from the closer and more distant surroundings around the object, depending on the desired degree of accuracy, which is under realistic environmental conditions very often impossible.

The conditions of radiation especially for objects on the land area are at times extremely complex and subject to so many influences that in our mind only a statistical evaluation could lead to more dependable results in these cases.

For instance let us consider the brightness temperature of the sky, which to a lesser or greater degree is part of the brightness temperature of an object under observation. As shown in Fig. 2. fluctuations of 40 K at 90 GHz and 20 K at 32 GHz were accounted during the measuring period, although the measurements did not take place under extreme weather conditions like rain showers.

With datas in the pertaining literature, we felt in past sometimes uneasy about the fact that very often no additional information was given, concerning the weather parameters. For this reason, the above mentioned physical quantities were and will be recorded in order to find out, to what degree they are correlated with the brightness temperatures of the objects under observation, and to get a feeling for brightness temperature of objects under realistic conditions.

To give an idea of the kind of registration in Fig. 3. two examples for large area objects are shown. Six measurements each for both polarizations, that were made in the period between march and may were evaluated. These values must be understood as the beginning of a statistic, which needs measurements over a long period. The seven pairs of plots below the brightness temperature plots of the objects observed are identical for both objects, since

the measurements took place within short time periods, so that the environmental conditions can be regarded identical. For the skytemperatures at 32 and 90 GHz a sort of average over elevation is plotted, since all the surface structures regarded must be called rough. Surprisingly enough, the curves at 32 and 90 GHz are very similar with the only difference that at 90 GHz we observe a larger fluctuation. As a matter of fact one would expect a greater correlation of the skytemperatures with the general weather conditions. This does however not apply, at least when purely optically differentiating properties are chosen. The general weather conditions are on the other hand correlated with the relative air moisture, thus one could do, without optically observing the weather. Air temperature which is plotted as a full line, seems to be correlated with the sky temperatures on the right hand side of the graphs. If the sky temperatures could be estimated coarse in this simple way, our work would be made easier. The plots on the left hand side don't however show this correspondence. The measuring points 2 and 3 would have to be different.

A correlation of air pressure with any of the other curves cannot be found. Changes in air pressure of this order are to little to result in a visible influence on the brightness-temperatures of the sky.

Let us now take a look at the brightness temperatures of the objects observed. In the first instance (Fig. 3(a)) we are dealing with a grassy surface, seen under an angle of approximately 10 degrees. The curves obtained from the 32 and 90 GHz radiometers show a very similar tendency, although cross polarized radiations are compared. Since we have a great correlation with the ground temperature we can conclude a strongly absorbing effect of grass at 32 and 90 GHz. This absorption is not one hundred percent, because the brightness temperatures are in the range of 260 K, instead of about 280 K at 100 percent absorption. Since a measuring error in this order of quantity can easily be excluded at the given conditions, scattering properties must be conceded to a grassy surface, which are at 90 GHz more strongly visible.

In the second instance (Fig. 3(b)) we have a concrete plane. At first view, we see some lower brightness temperatures for 32 as well as 90 GHz at horizontal polarization. This leads to the conclusion that a distinct Brewster-angle exists for this material. The effect is more pronounced at 32 GHz than at 90 GHz. The temperatures corresponding with the vertically polarized radiations follow the tendency of air and ground temperatures. The same measurements at horizontal polarization do not show, on the other hand, a correlation either with the sky or air temperatures. We are in this case, undoubtedly confronted with a complicated behaviour in reflection and scattering. Taking a closer look at our concrete plane, we found a regular surface structure in the form of surface corrugations running across the concrete surface normal to our viewing direction. The depth of corrugation was in the order of the 90 GHz wavelength.

In all cases the optical brightness of the objects under observation was recorded. The angular resolution of the light sensor was 0.9 degree. We expected to find a correlation with the degree of cloud cover of the sky. After evaluating the measurements we found however, that skytemperatures cannot be correlated with the optical brightness of the objects.

Microwave images are an ideal means of speeding up the process of learning to see in the microwaveregion. Two disadvantages have to be put up with unfortunately:

1. A relatively poor angular resolution.
2. A long recording time, if a receiver of common quality and a temperatur resolution of 1 to 2 Kelvin is used.

That is why short term weather changes do not show in the images.

Point number two will no doubt lose in importance as advanced technology becomes available. Enhanced resolutions can, however, only be obtained by using larger antenna apertures. The disadvantage of relatively poor angular resolution, may partly be compensated for, if we are able to display the many additional informations that a multifrequency and polarization radiometersystem can yield at the same time. In this respect, of course, we have yet a long way to go.

The rest of the pictures show photographs and the corresponding microwave images of the following two sceneries:

1. Forest, group of trees, dirt-road, gravelly soil, and two cars (Fig. 4.-6.).
2. Parking area with and without cars (Fig. 7.-9.).

Because of the lesser resolution at 32 GHz the corresponding images at 32 and 90 GHz cannot immidiately be compared. The microwave pictures were produced by means of an ordinary line printer of a computer. A quick look equipment satisfying modern requirements is presently being developed in our laboratory. The text underneath the microwave pictures gives the frequency (GHz), the polarization and the temperature range (K) where the full gray scale is spread.

In the case of scenery 1 at 32 GHz the group of trees, the dirt-road, the gravelly soil and the forest are clearly discernable. The lorry contrasts clearly with it environment. At 90 GHz additional the passenger car, the roof and the hood of the lorry stick out clearly. Even individual structures may be seen in the area of the forest.

Our measurements yielded surprising results for scenery 2. In the cases (a) the parking area was full of cars. In the cases (b) it was nearly empty. At first the results at 90 GHz. Fig. 8(a) was taken during sun shine. The cars can be clearly discerned against the surroundings. Fig. 8(b) was taken at 6.30 in the next morning. Very low sky temperatures were recorded at the time, so the asphalt surface of the parking area appeared colder than the cars on the day before.

The same tendency can be observed at 32 GHz and horizontal polarization. If we compare 9(a) with 9(b) it is not possible to decide whether the parking area is full or empty. In order to come to a clear statement, the recorded temperature values would have to be corrected for the difference in sky temperatures.

Other scenes were taken also, like for instance buildings behind leafless trees. We were left with such poor contrast however, that improved data handling will be necessary to achieve satisfactory results.

4. CONCLUSION

In future measurements, the 11 GHz radiometer will also be used again. Further we are going for a standard antenna beamwidth for all frequencies for certain types of measurements. In addition, a continous recording of sky temperatures appears mandatory, in order to be able to use it any time for a reference, further the registration of soil moisture seems to be necessary. The measuring program will of course, be continuously be adapted to the experiences gained and the particular problems encountered.

5. FIGURES

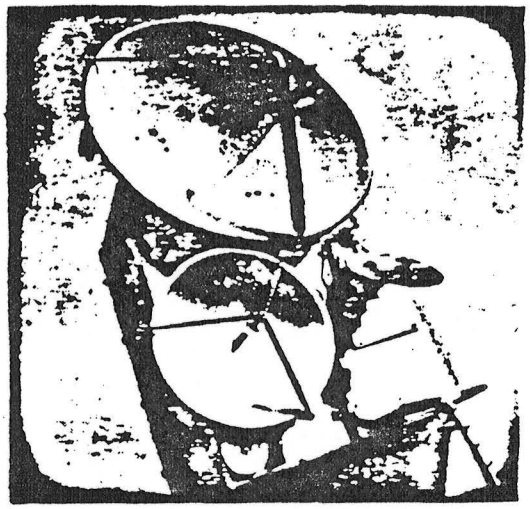

FIGURE 1. EQUIPMENT FOR SIMULTANEOUS RADIOMETRIC MEASUREMENTS AT 11, 32 AND 90 GHZ.

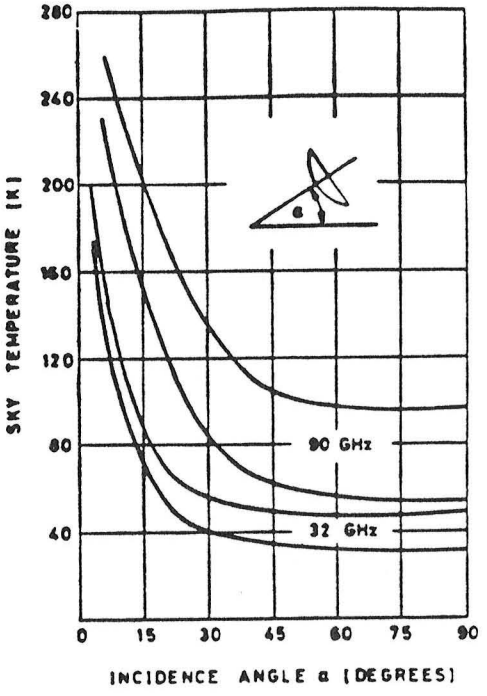

FIGURE 2. MAXIMUM AND MINIMUM OF SKY TEMPERATURES VS INCIDANCE ANGLE DURING THE PERIOD OF MEASUREMENTS.

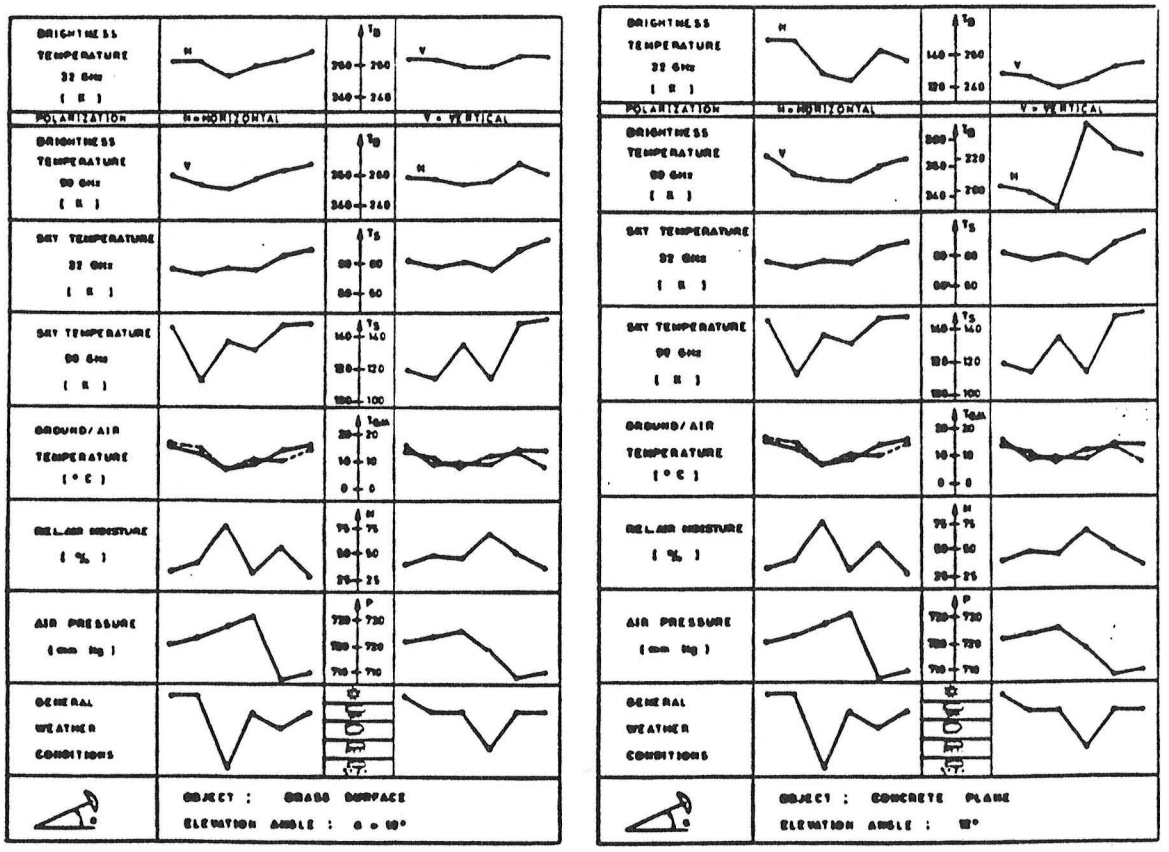

FIGURE 3. BRIGHTNESS TEMPERATURES OF TERRAIN ELEMENTS AT 32/90 GHZ AND DIFFERENT ENVIRONMENTAL INFLUENCES.

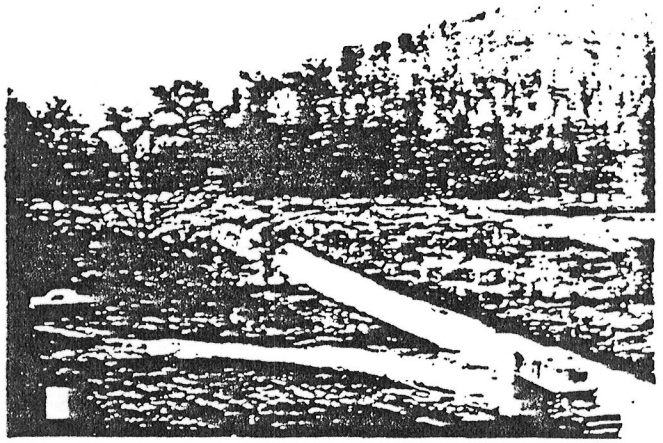

FIGURE 4. PHOTOGRAPH OF SCENERY 1.

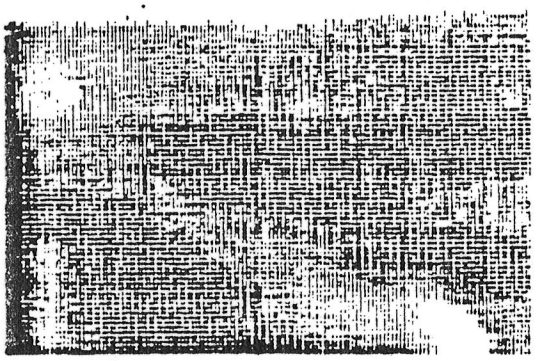

FIGURE 5. 32-GHZ-IMAGE OF SCENERY 1.

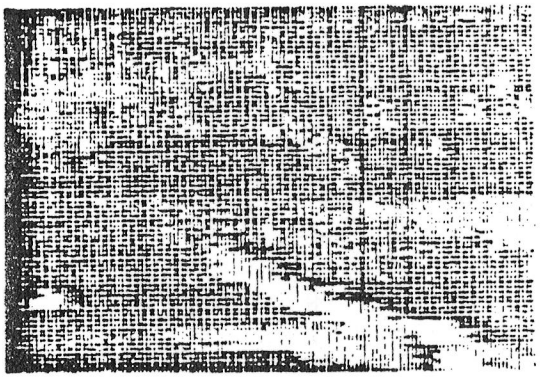

FIGURE 6. 90-GHZ-IMAGE OF SCENERY 1.

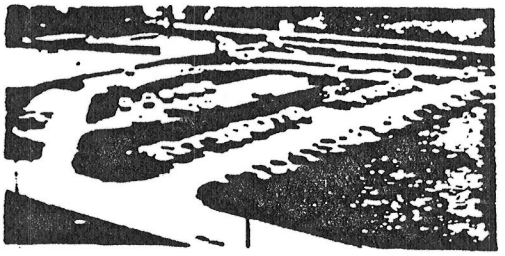

FIGURE 7. PHOTOGRAPH OF SCENERY 2.

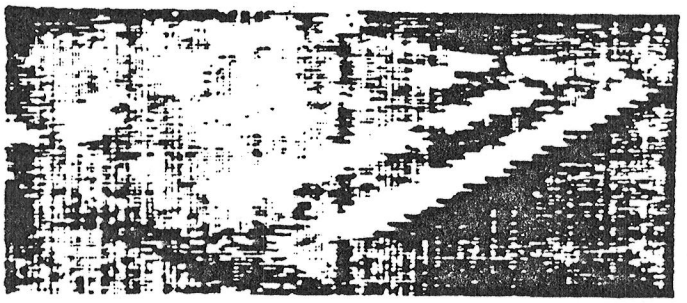

(a)

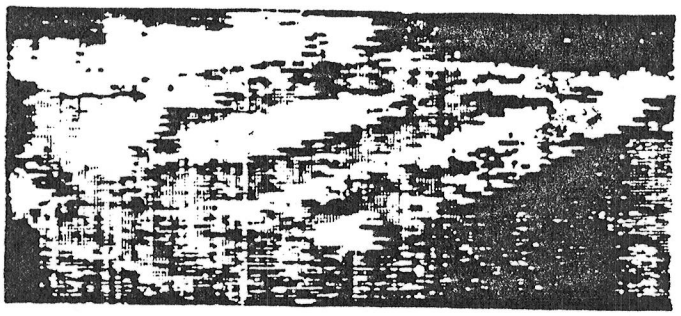

(b)

FIGURE 8. 90-GHz-IMAGE OF SCENERY 2.

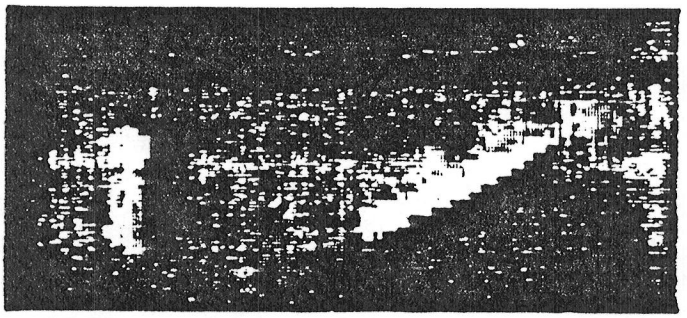

(a)

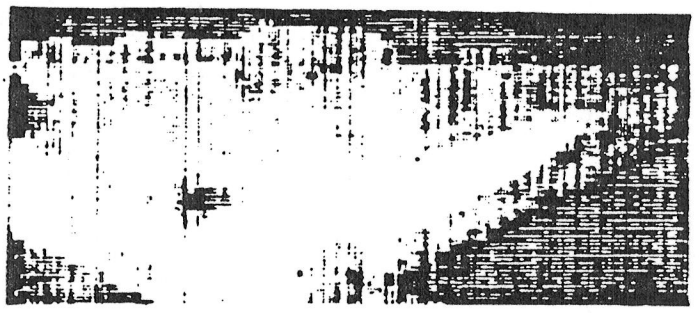

(b)

FIGURE 9. 32-GHz-IMAGE OF SCENERY 2.

EMISSION PROPERTIES OF WATER SURFACES AT 3 MM WAVELENGTH

R. Hofer, E. Schanda

Institute of Applied Physics
University of Berne
Switzerland

ABSTRACT

Antenna temperature- and forwardscattering measurements at 94 GHz on watersurfaces in a temperature range between 7 and 43° C are compared and discussed. The angular dependence of the considerable contribution of the atmosphere in this frequency region according to the secans-law is verified and taken into account for all measurements. An oil-polluted watersurface and surfacewaves are studied.

1. INTRODUCTION

For a reliable interpretation of remotely sensed features it is necessary to know their emissive properties. With our small scale measuring method we are able to collect the "ground truth" and the data of two remote sensing techniques of the same sample at exactly the same time. In our controlled reproducible laboratory experiments the mainlobe of the antenna lies at least for non-grazing angles within the well-specified sample.

After Kirchhoff's law and the principle of energy-conservation it is possible to determine the emission-coefficient e of a sample from its albedo a, i.e. the total power reflected into the upper hemisphere:

$$e_i(\theta_o, \phi_o) = 1 - a_i(\theta_o, \phi_o) \qquad (1)$$

where i : polarisation of the incident wave, i.e. horizontal or vertical

θ_o, ϕ_o : direction of the incident wave

For homogeneous materials (compared to the penetration depth) and smooth surfaces (compared to the wavelength), which is very well fulfilled for quiet water, the albedo reduces to the Fresnel-reflectioncoefficient, because scattering becomes specular reflection. Therefore the total of the reflected power is easily measured with a forward scattering method. In our set-up the looking angles θ of the transmitter and the receiver can be varied independently in one plane between 2°, i.e. nearly vertical incidence, and 85°.

2. COMPARISON OF FORWARDSCATTERING- AND EMISSIONMEASUREMENTS

Although reflection- and emissionmeasurements are in principle equivalent (formula (1)), in practice there are great differences. The advantages of our active forwardscattering-method are:

1) Atmospheric effects are completely eliminated by the short distances (about 1.2 m) of transmitter and receiver from the sample.
2) In our case the detectable power is about 10^6 times greater than that of direct emission measurements.

3) With modulation techniques it is possible to eliminate disturbing signals from external sources as radar stations etc.

4) If the relative permeability of the sample equals unity it is possible to calculate the complex dielectric constant of the material with the aid of the Fresnel-Formulae.

5) For inhomogeneous materials or not completely smooth surfaces the measurement of the beam-dispersion and -depolarisation gives information on the irregularities of the sample.[1]

On the other hand our radiometer-measurements are a more realistic simulation of a real remote sensing situation than the bistatic scattering method. But even in the special geometry of our experiment the emissioncoefficient is at least masked by the atmospherical brightnesstemperature T_S, which changes drastically with zenithangle θ and weathersituation due to the total watervapor-content of the air:

$$T_i(\theta) = e_i(\theta)T_L + \{1 - e_i(\theta)\}T_S(\theta) \qquad (2)$$

where:
T_i : measured antenna temperature for polarisation i
$e_i(\theta)$: emissioncoefficient } of the sample
T_L : physical temperature
T_S : brightnesstemperature of the atmosphere

For a horizontally assumed and homogeneous atmosphere it is possible to calculate its brightnesstemperature from its physical temperature on the earth T_A and its zenithopacity O_Z after the secans-law [2]:

$$T_S(\theta) = T_A(1 - e^{-O_Z \sec\theta}) \qquad (3)$$

Fulde (personal communication) calculated the watervapor-content at earth's surface from the zenithopacity due to various atmospheric models.

3. RESULTS AND DISCUSSION

Figure 1 and 2 show measuring points for the reflection-coefficients as a function of the incident nadirangle for horizontal and vertical polarisation. The plotted curves are best-fit Fresnel curves determined by a Gaussian regression for the measuring points with vertical polarisation (lower points) only [3]. The given complex permittivity is the result of this regression and the parameter used in the calculation for both Fresnel curves, i.e. for the curves representing horizontal and vertical polarisation respectively.

The reflectioncoefficient of fresh water (figure 1) increases with increasing water temperature over the whole angular range. The Brewster angle on the other hand does not change significantly with water temperature. When the water surface is covered by oil-blobs of approximately 0.15 mm thickness and 3 cm diameter which occupied roughly half of the water surface, the reflectivity (i.e. the reflectioncoefficient for vertical incidence) of the surface is reduced by 10 % compared to the unpolluted water at the same temperature of 15° C (figure 2). The undulations in the measuring points especially recognizable close to the Brewster minimum are caused by the inhomogeneities of the surface and interference between the waves reflected at the water- and the oil-surfaces respectively.

Table I shows a comparison between our results and results at 10 GHz earlier obtained by Mätzler [4]. For 94 GHz also the permittivity after Debye's theory [5] is given. At 10 GHz the emissivity (i.e. the emissioncoefficient for $\theta = 0°$) reaches only about 60 % of the value at 94 GHz and is independent of watertemperature, but at 94 GHz the emissivity increases with decreasing watertemperature. The related curve in the ε'-ε''-plane crosses the lines of constant emissivities almost perpendicular ([1], figure 1), i.e. the alteration of the complex permittivity with temperature causes a maximum variation of the emissivity. The dielectric constant of the oilfilm is a mean value for the inhomogeneous oil-water-system as described before.

TABLE I : Emissivities e and permittivities (ε'/ε'') of fresh water at 94 GHz and 10 GHz.

Water-temperature °C	94 GHz e	94 GHz (ε'/ε'') measurement	94 GHz (ε'/ε'') Debye	10 GHz e	10 GHz (ε'/ε'')
9	0.66	9.4 / 8.6	6.8 / 9.6		51 / 39
15	0.63	7.3 / 10.6	7.5 / 11.9	} 0.38	56 / 36
20	0.62		8.0 / 13.0		60 / 33
23	0.60	8.0 / 13.2	9.6 / 16.5		64 / 26
Oilfilm	0.67	(2.5 / 7.6)			

Figures 3 to 8 show the results of the passive radiometer measurements. Antennatemperatures T are plotted versus nadirangle for horizontal and vertical polarisation. The instrument used has an overall noisefigure less than 17 dB i.e. the temperatureresolution is better than 0.3 °K at an integrationtime of 1 second. The antennatemperatures for the first ten degrees of zenithangle decrease steeply due to the decreasing reflections of the instrumental setup into the mainlobe of the antenna. Therefore these parts of the curves have no significance for the interpretation. The whole radiometersystem is calibrated before every measurement. Two referencetemperatures are determined: RT_1 which is identical with the physical temperature T_A of the air and RT_2 the temperature of liquid nitrogen (77°K). Afterwards the signal of the measured temperaturedifference was magnified by a factor one, two or three (depending on the sample) relative to the third calibration mark (zero-level of the system) at the T-axis of the diagrams, thus shifting the "77°K" mark RT_2 to higher values. The zenith brightnesstemperature T_Z is measured for every diagram too. The values T_A and T_Z are used to compute the zenithopacity O_Z after the secans-law (formula (37)). ε_R and ε_D are the permittivities calculated from the reflectionmeasurements and due to Debye's theory respectively. After formulas (2) and (3) the expected antennatemperature is computed with the dielectric constants, zenithopacity and the physical temperatures of the sample and the air as parameters and is plotted into figures 4, 5, 7 and 8. The shape of the mainlobe of the antenna was taken into account for the computation.

The accuracy of the secans-law is demonstrated in figure 3. For clear blue sky we measured zenithbrightness-temperatures between 40 and 80 °K corresponding to a watervapor content of the air on the earth's surface of between 8 and 27 gr H_2O/m^2 for the model of the "Annual Tropic Atmosphere".

Curves after the secans-law are plotted according to the two extreme zenithbrightness-temperatures. A third curve is calculated for the highest measured zenithbrightness-temperature: 210 °K for dark thunderstorm clouds. Because our radiometer is viewing only downwards, the atmosphere is measured over a reflecting metal plate. There are two reasons why this technique is allowed:

1) There is no difference to the single curve measured with the instrument turned upwards.

2) No influence of polarisation-direction could be measured over the reflecting plate.

The different measured curves vary due to changes of watervapor content within one day. From the two enveloppes we conclude that when we start the calculation with the real zenithbrightnesstemperature the computed and measured brightnesstemperatures agree very well. Each measurement of the samples was carried out under a clear blue sky. Therefore the secans-law is a good approximation of the real atmospheric brightnesstemperature.

Figures 4 and 5 show results for water of two different temperatures. The calculated curves fit the measured very well, i.e. forwardscattering- and antennatemperature-measurements completely agree. The differences between the calculations with the two permittivities ε_R and ε_D and the measured curves are comparable to the absolute accuracy of $\pm$ 5 ^oK of our system. For showing the influence of the atmospheric brightnesstemperature in figure 4 a third curve is computed with a zenithbrightness-temperature of 80 ^oK instead of the real value. Especially for the horizontal polarisation (lower curves) the shape changes drastically. At the Brewster angle the maximum of the antennatemperature is always less than the physical watertemperature because of the relatively high reflection-coefficient (compared to other materials [3]) and the angle of the antennalobe, which is comparable to the width of the Brewster-minimum.

Figure 6 represents the results of the two extreme watertemperatures measured at the same weathersituation copied into a single diagram. For the antennatemperature measurements the high reflectioncoefficients of the horizontal polarisation mask the physical temperatures of the samples. On the other hand the difference of these temperatures is detectable at the minimum of the reflection at the Brewster angle. There, in addition the width of the maximum of the antennatemperature decreases with increasing watertemperature, because the reflectivities at the Brewster angle are always less than 0.1.

In figure 7 the results of four oilfilm-thicknesses and the corresponding covering by the oilblobs in percent of the total surface-area are presented. For horizontal polarisation the antennatemperature increases nearly linearly with the quantitiy of the oil. For vertical polarisation the angular dependence is reduced with increasing oil-quantity. The Brewster-effect vanishes completely for an oilfilm thicker than 0.2 mm. At an incident angle of about 53° it is impossible to distinguish any oilfilm from unpolluted water at least up to a thickness of half a millimeter. The curves for fresh water and for a somewhat different oil-covering situation during the forwardscattering-measurements are plotted. The surface-inhomogeneities cause the discrepancy (especially for the vertical polarisation) between the two measuring-methods.

Figure 8 shows results for standing waterwaves. The length of the waterwaves ($\sim$ 10 cm) is smaller than the footprint of the antenna-mainlobe ($\sim$ 20cm diameter for the - 3 dB - points at vertical incidence) and their frequency ($\sim$ 2 Hz) is higher than the integration time of 1 sec. Therefore the angular dependence of the antennatemperature is reduced compared to the smooth surface, because a few wavelengths are within the beam and a mean-value of several "incident angles" is measured. For waves perpendicular to the plane of incidence ($\perp$) the wooden frame of the instrument-mounting is reflected into the antenna-beam over a wider region of incident angles than for waves parallel ($\parallel$) to this plane. Therefore their antennatemperature is increased. On the other hand forwardscattering-measurements of an undulating surface as described before are completely impossible without integrating of the output signal.

4. CONCLUSIONS

For homogeneous materials and smooth surfaces forwardscattering- and antennatemperature-measurements are absolutely equivalent. Both methods have their advantages for determing the emissive properties of well specified samples in laboratory experiments. For rough or inhomogeneous materials the determination of the emissioncoefficients can only be achieved by radiometer-techniques, but scattering measurements may give additional information on the irregularities of the sample.

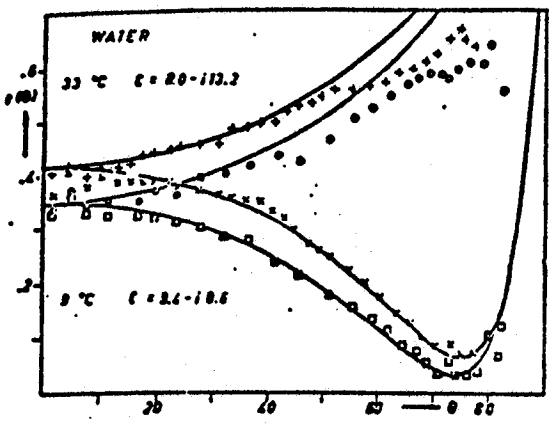

FIGURE 1

Reflectioncoefficients and best-fit Fresnel curves for water of 33° and 9°C.

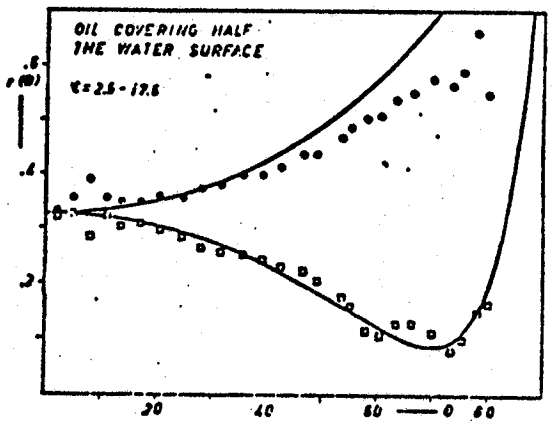

FIGURE 2

Reflectioncoefficients versus nadirangle for oil-blobs of approximately 0.15 mm thickness and 3 cm diameter covering half of a watersurface of 15°C.

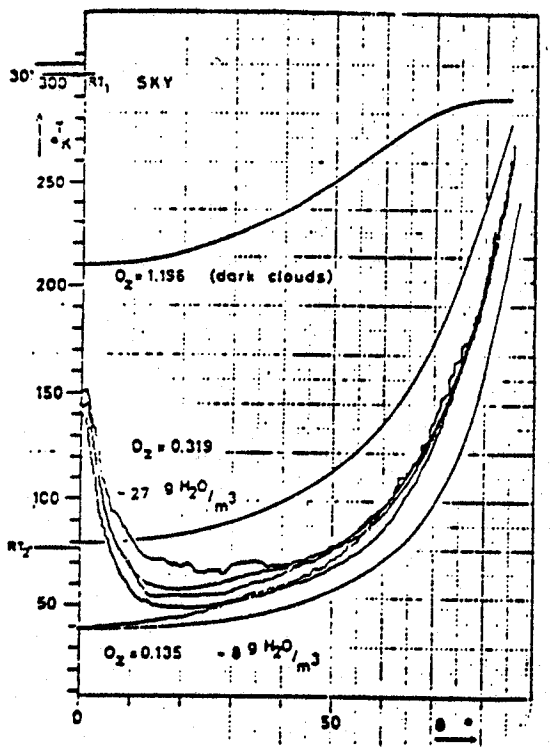

FIGURE 3

Secans-law and measured atmospheric brightnesstemperatures versus zenithangle for different watercontents of the air during clear blue sky.

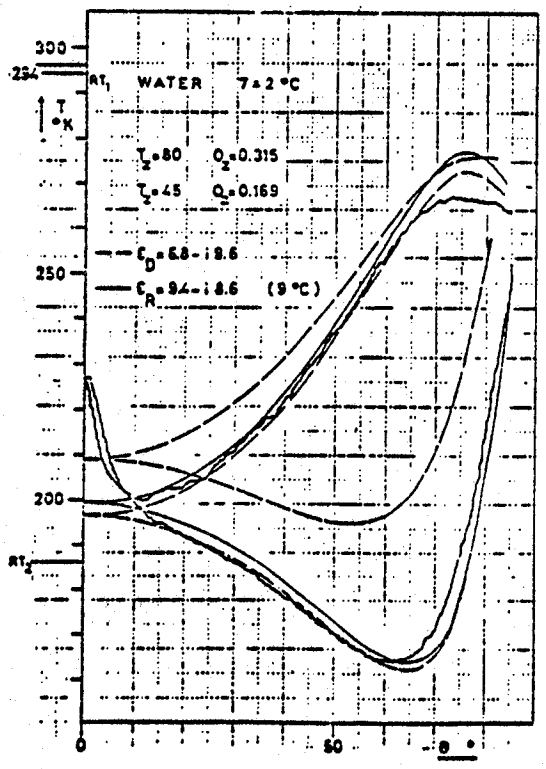

FIGURE 4

Computed and measured antennatemperatures versus nadirangle for water of 7°C.

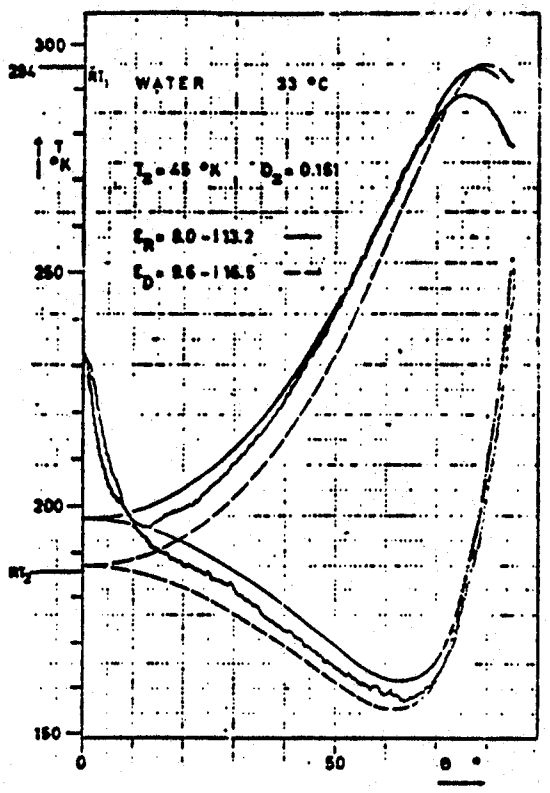

FIGURE 5

Computed and measured antenna-temperatures versus nadirangle for water of 33°C.

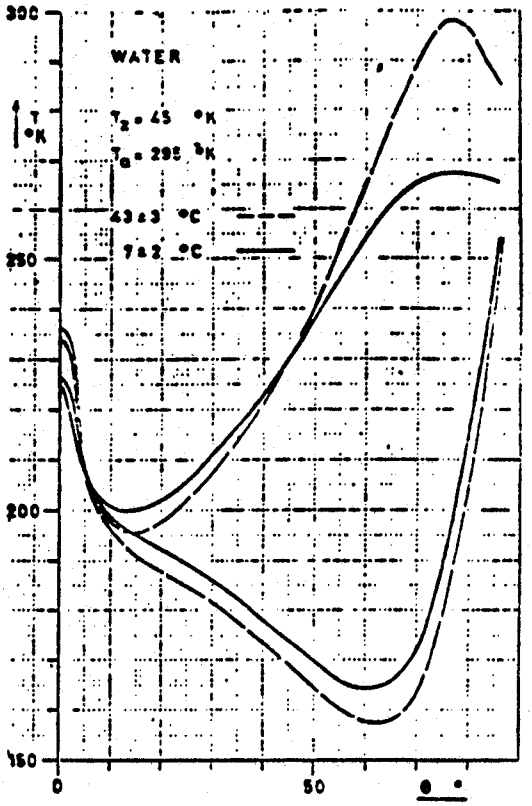

FIGURE 6

Copy of measured antennatemperatures versus nadirangle for water of 43 and 7°C into one diagram.

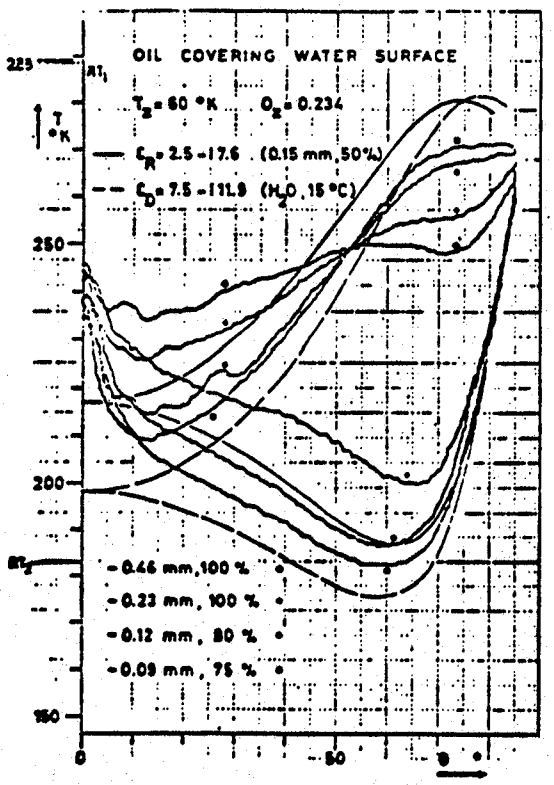

FIGURE 7

Four different oilfilm-thicknesses covering the watersurface of 15°C.

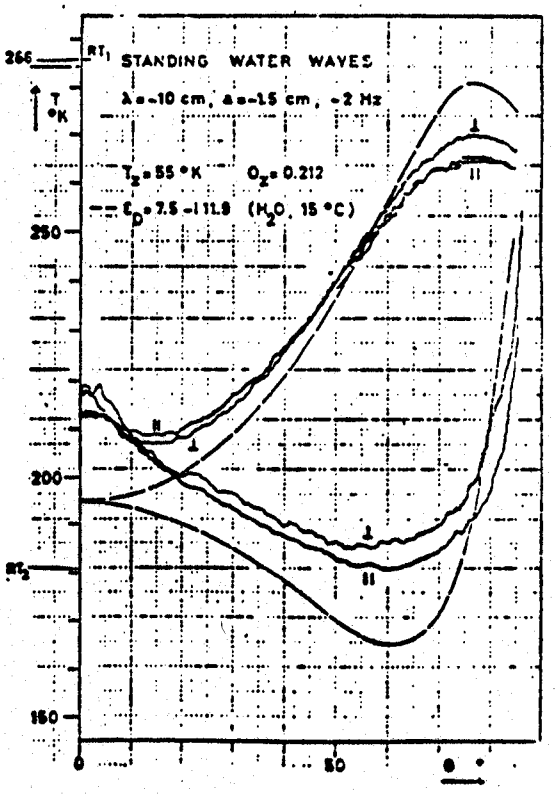

FIGURE 8

Standing water waves parallel (∥) and perpendicular (⊥) to the plane of incidence.

5. REFERENCES

[1] E. Schanda, R. Hofer, Scattering, emission and penetration of 3 mm waves in soil, Proc. URSI-meeting on Microwave Scattering and Emission from the Earth,141-149,Univ. of Berne, Switzerland, (1974).

[2] G. Schaerer, Passive sensing experiments and mapping at 3.3 mm wavelength, Remote Sensing of Environment, vol. 3, no. 2, (1974).

[3] R. Hofer, Streuung und Emissionseigenschaften natürlicher Materialien bei 3 mm Wellenlänge, Diploma Thesis, Institute of Applied Physics, University of Berne, (1974).

[4] C. Mätzler, Messung der Wärmestrahlung der Erdoberfläche im Mikrowellengebiet, Diploma Thesis, Institute of Applied Physics, University of Berne, (1970).

[5] J.B. Birks (ed.) Progress in Dielectrics, vol. 3, p. 78, Jliffe Books, (1961).

ABSORPTION OF NEAR-MILLIMETER RADIATION BY LIQUID FOGS

S. M. Kulpa and E. A. Brown
US Army Electronics Research and Development Command
Harry Diamond Laboratories
2800 Powder Mill Road
Adelphi, MD 20783

Interest in the near-millimeter wave (NMMW) portion of the spectrum stems principally from the fact that in limited visibility situations such radiation offers a compromise between the high-resolution capabilities of infrared and low-loss propagation characteristics of microwaves. Since fog penetration is a central concern, numerous estimates have been made [1] in attempts to quantify NMMW attenuation effects in such environments. In this paper we compare various calculations of absorption effects based on limited theoretical and experimental data for the temperature and frequency dependence of the NMMW dielectric constants of water.

Rozenberg [2] and Hollinger [3] have reported extensive theoretical calculations of water dielectric constants using the Debye [4] model. Their predicted values of ε' and ε'' at 0 and 20 C are shown in figure 1. Since Hollinger's analysis is based on the Saxton and Lane [5] values for the relaxation time, static dielectric constant, and optical dielectric constant, his curves are labeled "Saxton and Lane."

Recently, Afsar et al [6], Blue [7], and Simpson et al [8] have reported measured values of ε' and ε'' throughout the NMMW region. Figure 1 includes the Blue and Afsar results. Blue's measurements were made at 20 C, whereas Afsar's measurements were made at 4, 30, and 57 C. Extrapolation of these latter results was used to obtain values of ε' and ε'' at 0 and 20 C. Simpson's measurements at 25 C, though not shown in the figure, agree well with Afsar's results.

In typical fogs, since the particle size is small compared to the wavelength of concern, the Rayleigh approximation [1] is valid. Attenuation by scattering may be neglected and the absorption, α, due to the fog may be written as

$$\alpha = \frac{0.82\varepsilon''}{(\varepsilon' + 2)^2 + (\varepsilon'')^2} \rho_g \nu \quad (\text{dB/km}),$$

where ρ_g is the fog's liquid water content (g/m^3) and ν is the frequency (GHz).

In figures 2 and 3 we show calculated absorptions for 0 and 20 C respectively based on the dielectric constant data discussed above.

Several factors are worthy of note. First, above approximately 200 GHz, the absorptions calculated from measured values of the dielectric constants exceed those based upon Rozenberg's and Hollinger's theoretical values for ε' and ε''. The difference increases with frequency, being more than a factor of two (dB/km) at the upper end of the NMMW region. Below 200 GHz, little difference exists between the various calculations. Effects at 0 and 20 C are comparable.

Second, understanding the practical significance of figures 2 and 3 requires some comment on the types of fogs that might be of interest. Note that both figures are normalized absorption, i.e., $\rho_g = 1\ g/m^3$. Typically, depending on the type of fog, ρ_g may range [1] between 0.1 and 0.5 g/m^3 with respective visibilities of approximately 300 to 50 m.

Third, it should be noted that in providing total path attenuation, one must also account for the effects of water vapor. Under saturation conditions, such as fogs, the interaction of vapor and liquid components is not well understood. Usually the assumption is made that vapor and liquid effects are simply additive. There is evidence, however, that under saturation conditions, this assumption may be in error. So-called "anomalous" effects may be significant [1].

References

[1] S. M. Kulpa and E. A. Brown, "Near-Millimeter Wave Technology Base Study — Vol I," Harry Diamond Laboratories, HDL-SR-79-8, November 1979.

[2] V. I. Rozenberg, "Scattering and Attenuation of Electromagnetic Radiation by Atmospheric Particles," Hydrometeorological Press, Leningrad, USSR, 1972.

[3] J. P. Hollinger, "Microwave Properties of a Calm Sea," Naval Research Laboratory Report No. 7110-2, 15 August 1973.

[4] P. Debye, "Polar Molecules," The Chemical Catalog Co., Inc., New York, 1929.

[5] J. A. Saxton and J. A. Lane, "Electrical Properties of Sea Water," Wireless Engineer, pp. 269-275, October 1952.

[6] M. N. Afsar and J. B. Hasted, "Submillimeter Wave Measurements of Optical Constants of Water at Various Temperatures," Infrared Physics, vol. 18, pp. 835-841, December 1978.

[7] M. D. Blue, "Permittivity of Sea Water at Millimeter Wavelengths," Georgia Institute of Technology EES, Final Report, NASA Grant No. NSG-5082, 15 May 1978.

[8] D. A. Simpson, B. L. Bean, and S. Perkowitz, "Far Infrared Optical Constants of Liquid Water Measured with an Optically Pumped Laser," to be published.

KULPA AND BROWN

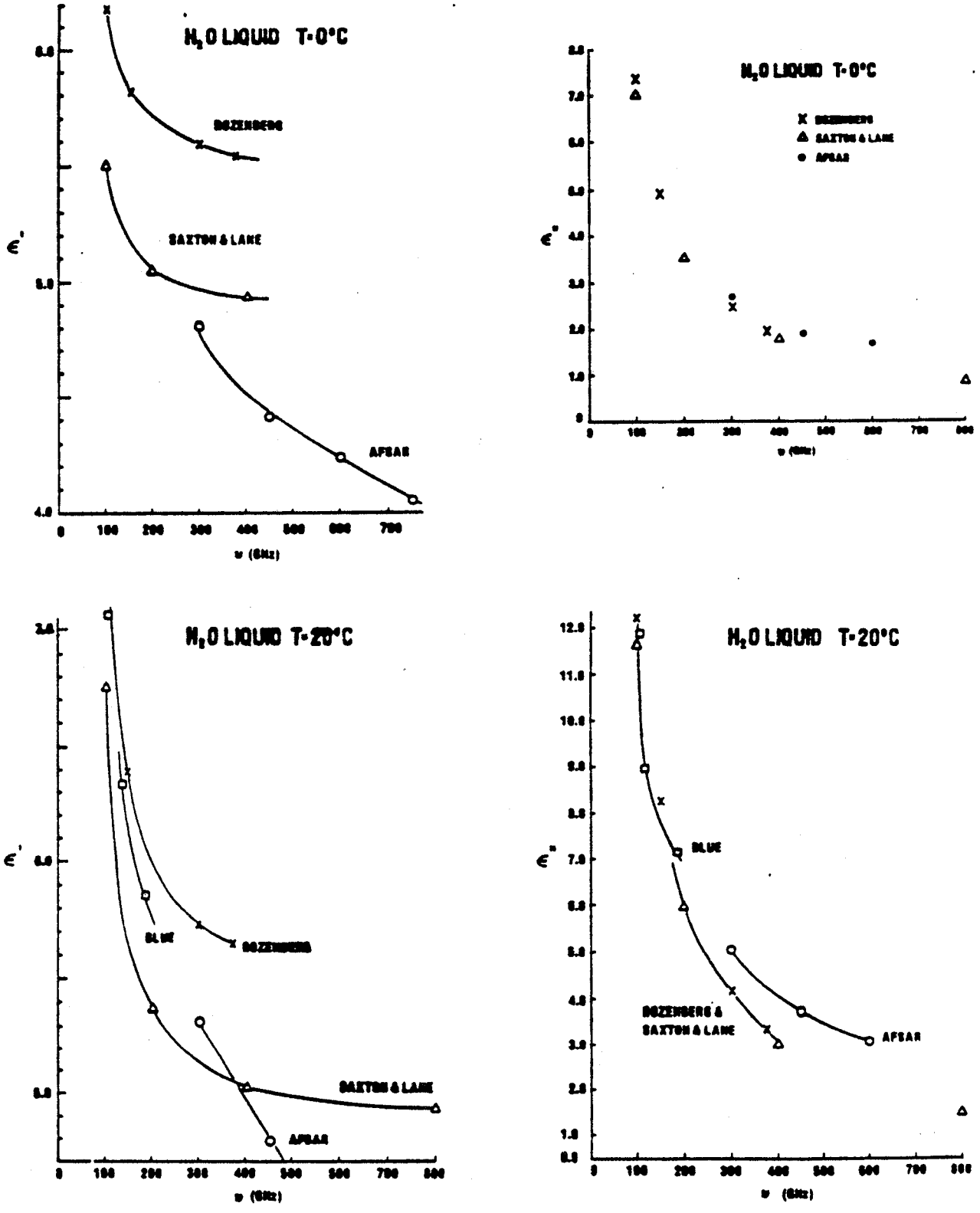

Figure 1. Water dielectric constants at 0 and 20 C.

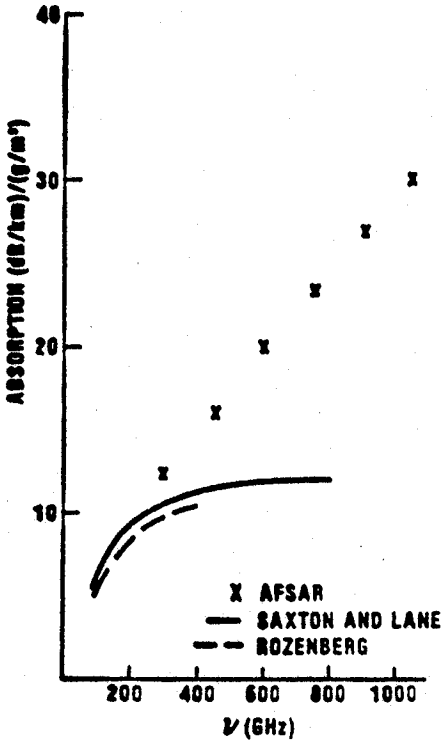

Figure 2. Calculated liquid fog absorption at 0 C.

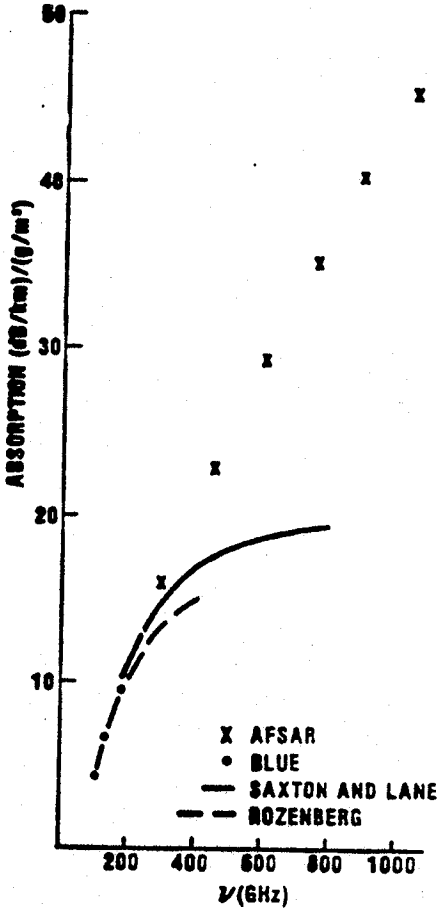

Figure 3. Calculated liquid fog absorption at 20 C.

SCATTERING, EMISSION AND PENETRATION OF THREE MILLIMETER WAVES IN SOIL

Erwin Schanda
Roland Hofer

Institute of Applied Physics
University of Berne
Berne, Switzerland

ABSTRACT

Controlled experiments on the emission behaviour of various natural and man-made types of soil at 3.2 mm wavelength have been performed. Additional forward scatter measurements on the same materials allow the elimination of the atmospheric contributions and an approximate determination of the effective permittivities. By the use of a metal plate underneath soil-layers of various thickness the penetration depth of 3 mm waves in a few specific soils has been determined. The effects of humidity and polarization have been studied and a comparison to earlier measured emissivities at 3 cm wavelength has been established. The investigated media are: humus, lawn, gravel, fine grain sand, concrete, road asphalt cover, board, eternit.

1. THE UTILITY OF THE FORWARD-SCATTER MEASUREMENTS

The atmosphere has a considerable effect on the performance of passive sensing at millimeter waves. As outlined in an earlier publication [1], the measurement of the forward scatter properties of a natural surface can eliminate the atmospheric effect if the distance between receiver and transmitter is sufficiently small. Besides other advantages of the forward scatter method (see [2]), it allows the approximate determination of an effective complex permittivity by the use of the Fresnel-formula for specular reflection [3]. This permittivity is only a representative value for a planely and homogeneously assumed surface layer causing exactly the same dependence of the reflections on polarization and on incident angle as the real surface layer does. With this assumption and the condition of a layer thickness which is opaque for the wavelengths used, the measured reflection coefficient can be used for calculating the emission coefficient.

The complex wavenumber $k = \alpha + i\beta = i\omega\sqrt{\mu_o\varepsilon}$ with the attenuation and phase coefficients α and β respectively is determined by the permittivity $\varepsilon = \varepsilon_o(\varepsilon' - i\varepsilon'')$ with the real (ε') and imaginary part (ε'') of the relative permittivity. For vertical incidence the normalized penetration depth (in numbers of wavelengths in air) can therefore be taken as $\delta = \gamma\alpha\lambda$.

Figure 1 is a diagram of the emissivity (vertical incidence) and the penetration depth as a function of the real and imaginary parts of the permittivity. The respective values of a number of materials are marked, which have been determined by standard laboratory measurements of the permittivity at 3 cm wavelength [4] and by forward scatter measurements at 3 mm [3]. The procedure to determine the permittivity by the forward scatter data is described earlier in [1] and in more detail in [3].

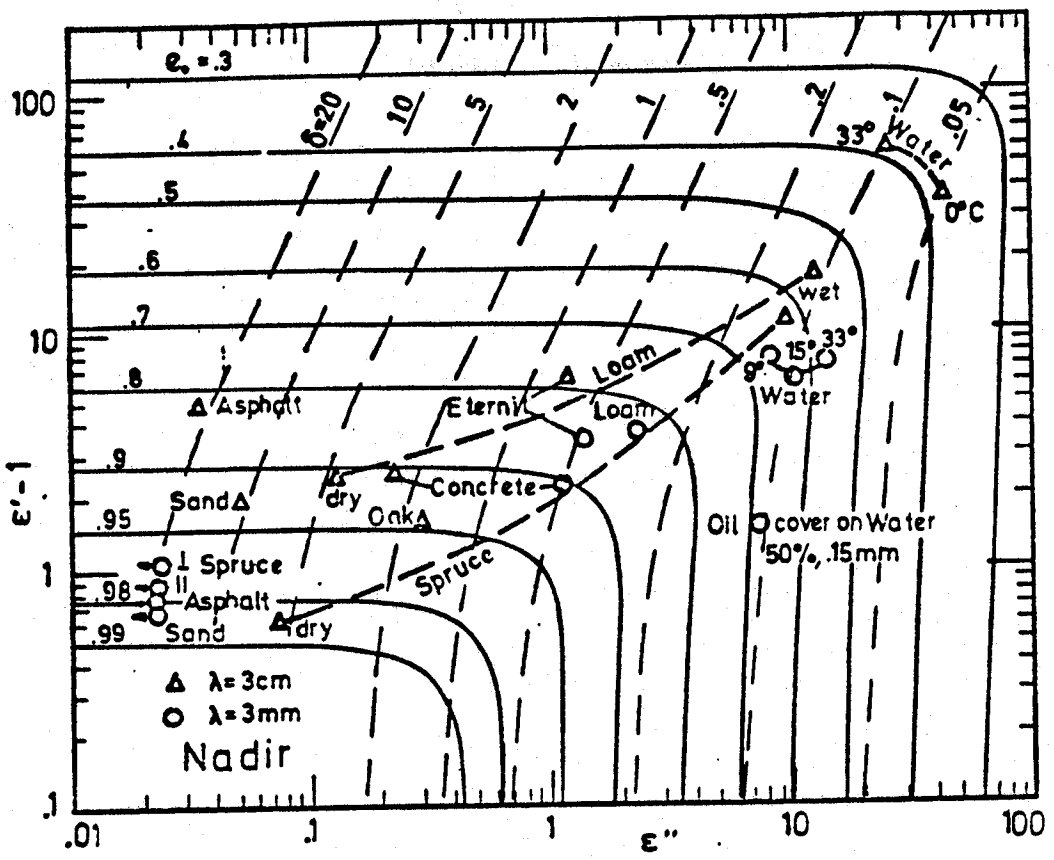

FIGURE 1

Emissivity (Nadir viewing) and penetration depth as functions of the complex permittivity. Some materials measured at 3 cm and 3 mm wavelength are marked. Loam and spruce for varying humidity (λ = 3 cm) and fresh water for varying temperature at both wavelengths.

2. THE MEASUREMENT OF THE EMISSION COEFFICIENTS

The instrumental set-up for the emission measurements on soil is the same as the one utilized for liquid media and is described in another contribution to this meeting giving an account of that investigation [2]. The surface of the samples is 1.4 x .94 m^2 in area and the thickness can be varied up to several times the penetration depth of most of the investigated materials. The distance of the receiver horn from the soil surface is approximately 1.2 m and the footprint of the beam (3 db width) is about 20 cm in diameter at nadir position. The criterion $d \geq 2a^2/\lambda$ for the minimum distance d required for the far-field approximation (cross-sectional dimension of the horn a = 28mm, wavelength λ = 3.2 mm) yields $d \geq 0.5$ meter which is fulfilled for the 3 db beamwidth even at the oblique incidence of 85° from nadir. The effect of the atmosphere is presented in [2] for all zenith opacities encountered during this investigation and the equivalence of the reflexion of the sky brightness on a metallic plate with the directly measured sky temperature has been demonstrated for the largest part of the range of incidence angles.

Figures 2 to 5, 7 to 10 and 12 to 15 represent the measured brightness temperatures as a function of the viewing angle (from nadir) and for two polarisations of samples of almost all kinds of roughness, of a wide range of permittivities and of a variety of heterogeneities.

In the case of a board of spruce (Fig. 2) the anisotropy of the emission is clearly recognizeable. The meaning of the marks $\parallel$ and $\perp$ is: fibres of the wood parallel and perpendicular to the plane of incidence; i.e. for the upper two curves (vertical polarization) of a set of four, $\perp$ means: the electric field is perpendicular to the fibres, $\parallel$: there is a component of the electric field parallel to the fibres; for the lower curves (horizontal polarization)

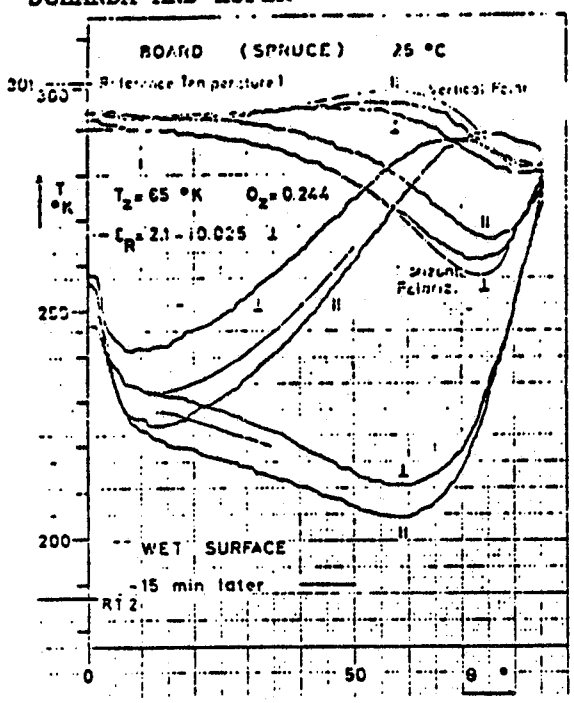

FIGURE 2
Emission coefficient of a board cut of spruce as a function of the viewing angle (measured from nadir). Permittivity of dry board from forward scatter measurement.

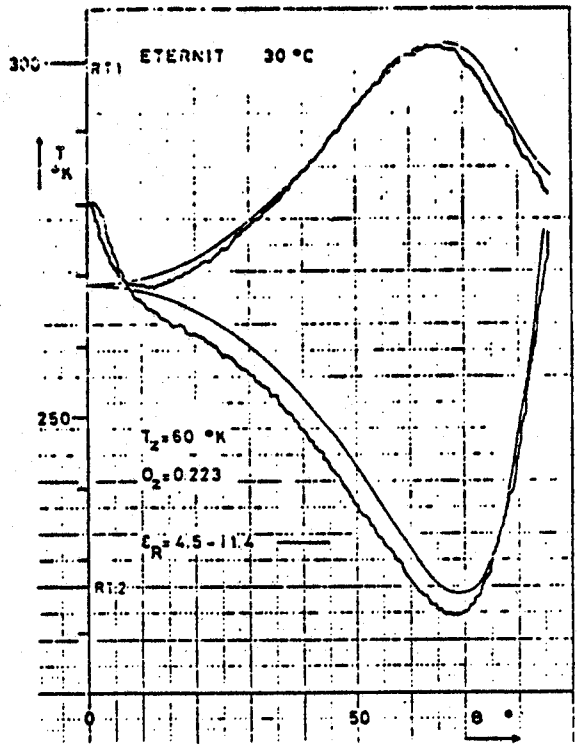

FIGURE 3
Emission coefficient of eternit, calculated curve (Fresnel formula) for comparison.

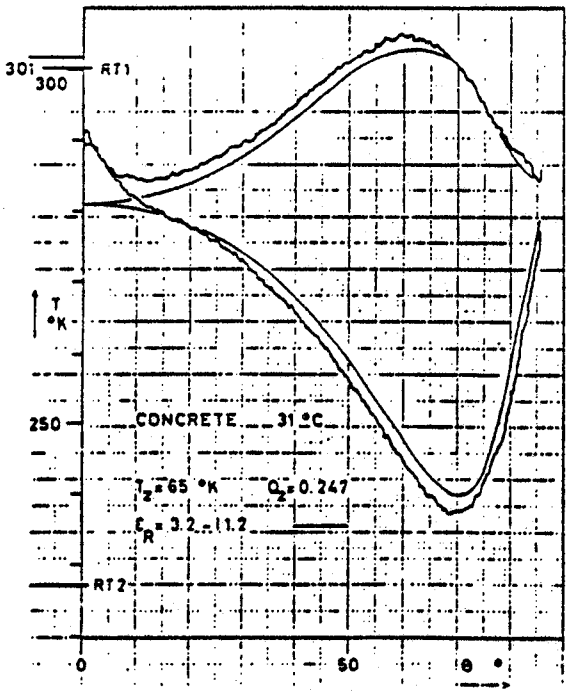

FIGURE 4
Emission coefficient of concrete; zenith brightness temperature T_z and related opacity O_z.

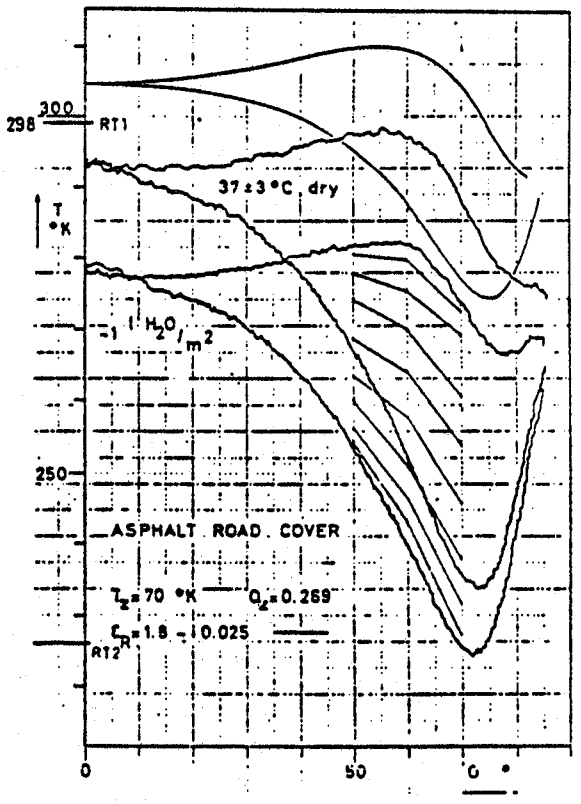

FIGURE 5
Emission of Asphalt road cover. Effect of polarization changes (in steps of 10 degrees) for viewing angles 5° to 70° on the wet surface.

however $\perp$ means: the electric field is parallel to the fibres, $\parallel$: the electric field is perpendicular to the fibres. The effective permittivity deduced from the forward scatter measurement (ε_p) with the electric field perpendicular to the fibres is given. The result of the wet board is to be taken with some caution because of the rapid change due to drying. The radiation temperatures at nearly nadir viewing (up to 10^0) have no significance due to the reflection of the measuring set-up on the sample. Eternit (Fig. 3) is an asbestos cement construction material with a very slight roughness (undulations) of a small fraction of the wavelength. The thin smooth line along the measured curve gives the emission coefficient calculated by the Fresnel formula using the permittivity (4.5 - i 1.4) determined by the forward scatter procedure and taking into account the atmospheric contribution. The zenith sky temperatures T_z and the related zenith opacities O_z are given for each measurement and their significance on the result can be estimated according to [2].

The roughness of the surface of concrete (Fig. 4) has a scale of up to about half the wavelength but the measured curve is still approximated satisfactory by a plane-surface Fresnel curve with a single-valued permittivity.

The asphalt road cover of a quality and construction as used typically on Swiss roads (Fig. 5) yields a large discrepancy between the measured emissivity and the calculated one by using the permittivity obtained from the scatter experiment. But the considerable difference between vertical and horizontal polarization leads to the conclusion that the surface can still be represented by an effective plane. Also the effect of changing the polarization in steps of 10 degrees within an important range of viewing angles in the case of a wet surface (1 liter water per square meter) yields a smooth transition between horizontal and vertical polarization.

3. THE PENETRATION DEPTH AND THE EFFECTS OF ROUGHNESS AND HETEROGENEITY

As soon as the scale of the surface roughness equals the wavelength the question arises whether the scattering and emission of waves are dominated by the surface structure and one of the roughness models has to be applied or whether they are dominated by the heterogeneous texture of a thick (many wavelengths) layer representable by an effective dielectric of the mixture (e.g. air/grains of sand).

The estimation of the penetration depth from the knowledge of the complex permittivity of the medium becomes less accurate for an increasing degree of roughness. A direct determination by the use of a perfectly reflecting plate underneath layers of various thickness will certainly give more realistic results.

Figure 6 is a schematic representation of the measuring situation with a soil layer of thickness t on a metallic plate. Due to the loss-less reflection the integrated equation of radiative transfer yields for the received

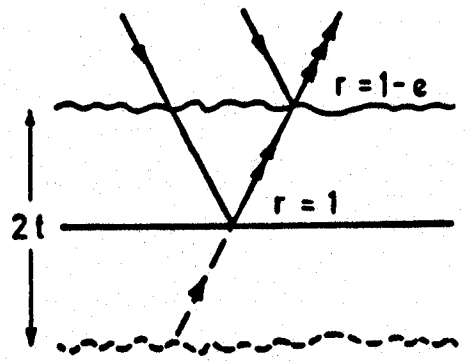

FIGURE 6

Schematic representation of the determination of the penetration depth by the use of a metallic reflector.

radiation temperature

$$T = T_S(1 - e) + e\,T_S \exp(-4t\alpha) + eT_L\,[1 - \exp(-4t\alpha)] \qquad (1)$$

where the emissivity of an assumed infinitely thick layer is e, the (amplitude) attenuation coefficient is α and T_s and T_L are the total sky radiation temperature in the considered direction and the physical layer temperature respectively.

Figure 7 represents the measured radiation temperatures for layers of various thickness of a fine grain sand (mean grain size approximately 0.5 mm, maximum about 1 mm) on a reflecting plate. Applying (1) to the emissivities (extrapolated to $\theta = 0$) of the most reliable curves (t = 10 mm and t = 20 mm) and taking a zenith air brightness temperature of 60 K (related water vapor content near to the ground : ~ 17 gramms per cubicmeter) the attenuation coefficient can be determined as $\alpha = 0.285 \pm 0.015$ /cm and from this the penetration depth follows as 3.5 ± 0.2 cm which is approximately eleven times the wavelength in air. Figure 8 shows the radiation temperatures of a 5 cm thick layer on a metal and on a strongly absorbing (see Figure 3)eternit plate respectively. The deviations are negligible. The effect of changing polarization (by steps of 10 degrees) has been recorded in the same range of viewing angles as for asphalt road cover and again a smooth change of the resulting brightness temperature has been found.

The effect of humidity of sand is demonstrated in Figure 9. The Fresnel curves for dry sand and a humidity of .15 grams water per cubiccentimeter are added. The permittivities used for this computation have been obtained from the forward scatter experiments on the same sample of sand. The modest reliability of the emissivity curves of wet sand is demonstrated by the bar crossing the curve of the 0.4 g/cm^3 horizontally polarized values. The radiation temperature at a nadir angle 50° starts at the lower end of the bar for 0.4 g/cm^3; during the time of 10 minutes the effects of seeping and drying cause an increase of the radiation temperature up to the top end of the bar.

A regular wavy structure of the sand surface (wavelength of the structure 3 cm and peak-amplitude 1 cm) causes a measurable anisotropy (Figure 10). The symbols $\parallel$ and $\perp$ mean: plane of incidence parallel and perpendicular to the structure. The plain surface measurement is repeated for comparison. The physical temperature of the sample on the surface (0 cm) and at approximate depths of 1 cm and 3 cm respectively are given.

The geometrical scale of the surface roughness of the sand samples is approximately one third of the wavelength in air but there is still a significant separation of the curves for vertical and horizontal polarization (some 30 K around the nadir angle of 60° for dry sand) and there is still a remarkable correspondence of the measured curves with the calculated ones using a single valued permittivity in the Fresnel formula. It is well-known that the effect of roughness on the scattering and emission behaviour of a surface increases with increasing conductivity i.e. with decreasing penetration depth.

Figure 11a is a schematic cross-section of a heterogeneous structure, resulting in a rough surface; for the following consideration it can be represented by some substituting homogeneous medium with the same emissive properties as the real material. The equation of radiative transfer allows to divide the vertically emanating brightness temperature into two parts originating from below and above a certain depth x respectively

$$T = T_b \exp(-2\alpha x) + T_a\,[1 - \exp(-2\alpha x)] \qquad (2)$$

Figure 11b gives the respective shares of both parts of the total apparent temperature assuming the physical temperatures of both parts equal $T_a = T_b$. Remembering the definition of the penetration depth as $\alpha\delta\lambda = 1$ resulting in exp(- 2) in the curves of Fig. 11b. From this we may conclude that for a penetration depth equal or smaller than the scale of the roughness ($\delta\lambda \lesssim R$) the radiation and scattering behaviour of that surface is dominated by the surface roughness, while for $\delta\lambda \gtrsim 10\,R$ the behavior is dominated by the subsurface material i.e. eventually by the heterogeneous texture with only a minor effect due to surface roughness. Within the transition range in between these two limiting cases $R \lesssim \lambda\delta \lesssim 10\,R$ the emission and scattering behavior is affected by both the surface roughness and the heterogeneity,

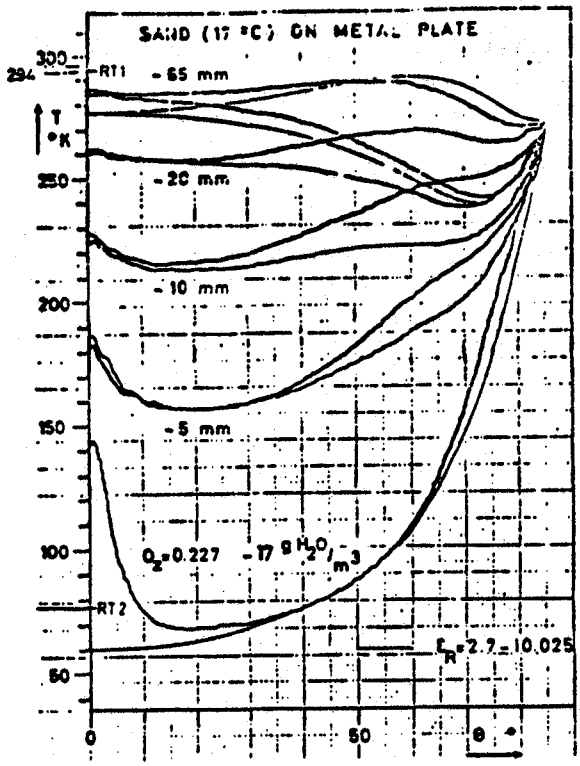

FIGURE 7

Various layers of fine grain sand on a metallic reflector plate. Lowest curve: contribution by the atmosphere via metal plate. Zenith opacity O_z and related water vapor content.

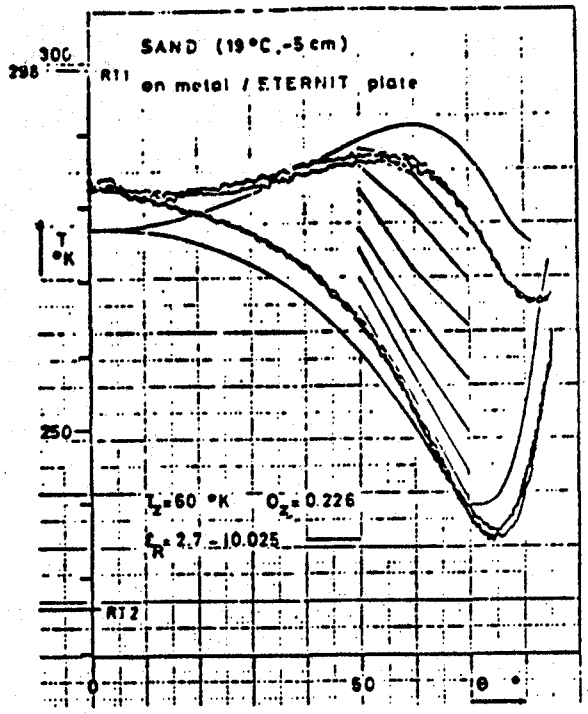

FIGURE 8

Effect of various substrates (metal/eternit) underneath a 5 cm layer of sand. Polarization changes in steps of 10° within the range of viewing angles of 50° to 70°.

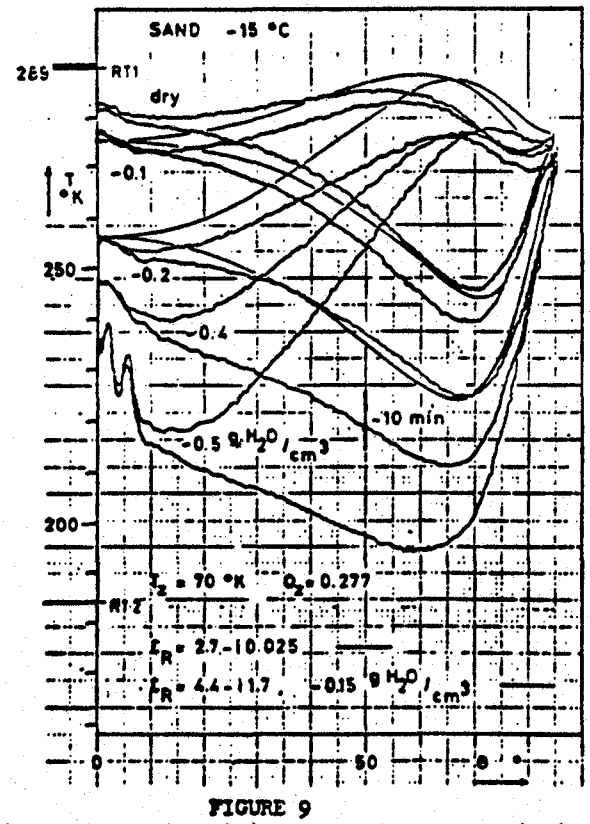

FIGURE 9

The effect of humidity of sand on the emission coefficient. The permittivity has been determined by the reflection (forward scatter) method (ε_R) for dry sand and .15 g/cm^3 water content.

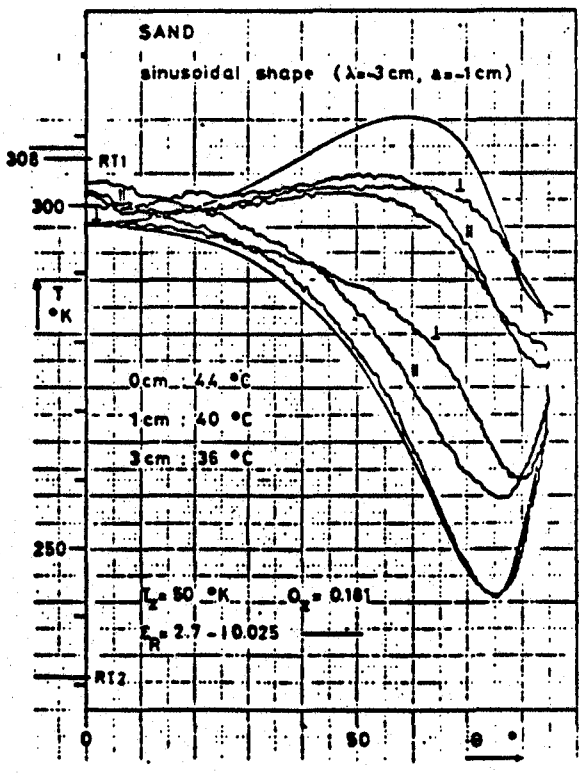

FIGURE 10

Sinusoidally shaped surface of the sand. The temperature on the surface and at two depths is marked. Flat surface for comparison.

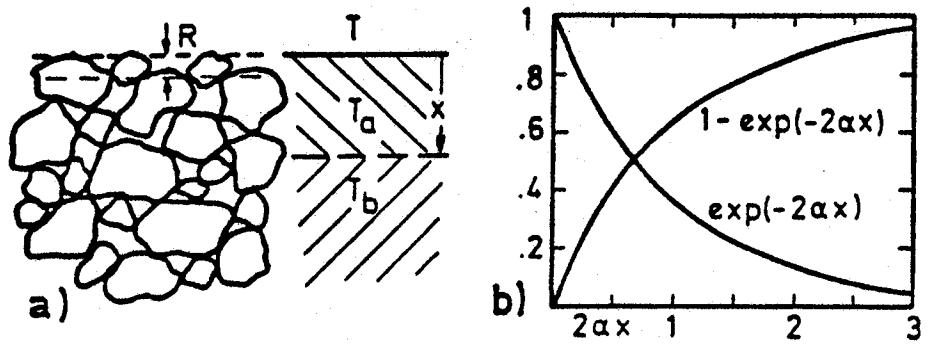

FIGURE 11

Rough surface of a heterogeneous structure; a) schematic cross-section, b) contributions of a layer above a depth x and of the medium below x respectively.

resulting in a situation where the emission coefficients for vertical and horizontal polarization show still a measurable separation but a satisfying description by the Fresnel formula does no longer exist.

Figure 12 represents the determination of the penetration depth in humus. Utilizing (1) as in the case of sand the penetration depth of that specific type of humus is approximately 7 to 8 millimeters at 3.2 mm wavelength i.e. $\epsilon = 2.2$ to 2.5. Regarding the surface roughness of about 3 to 4 millimeter in our experiment we may state that this surface may be classified as belonging to the transition range, somewhat closer to the roughness dominated limit (see the curves for 10 ± 2 mm thickness of the layer). By adding some water not the increase of conductivity of the highest protruding peaks of the surface causes the most important change but the formation of an effective, smoothing layer of increased water content is dominating the emission behavior.

Figure 13 shows the emission coefficient of lawn, a roughness dominated surface. Just in the range of viewing angles, where the Fresnel curves (permittivity determined by the forward scatter experiment) are suggesting some separation of horizontal and vertical polarization, there is absolutely no difference for both polarizations.

A surface of coarse-grained stones of the mineral Serpentine (mean size about 2 to 3 cm) seems to exhibit a significant separation of the emission coefficients for the orthogonal polarizations (Figure 14). But the stone fragments have preferential fracture planes and are unavoidably ordered to some extent when poured down on a plane, thus simulating a Fresnel type character of the emission.

Finally an artificial rough surface (Figure 15) with a roughness scale several orders of magnitude higher than the penetration depth has been measured and compared with the plane metal plate. Up to about 70° from nadir there is a very efficient reflection of the integral sky temperature (including some objects around the measuring set-up) into the antenna. At about 80° the brightness temperature due to the metal turnings is lower than that of the plane reflector because of the contributions from sky regions close to the zenith.

3 1176 00500 3109

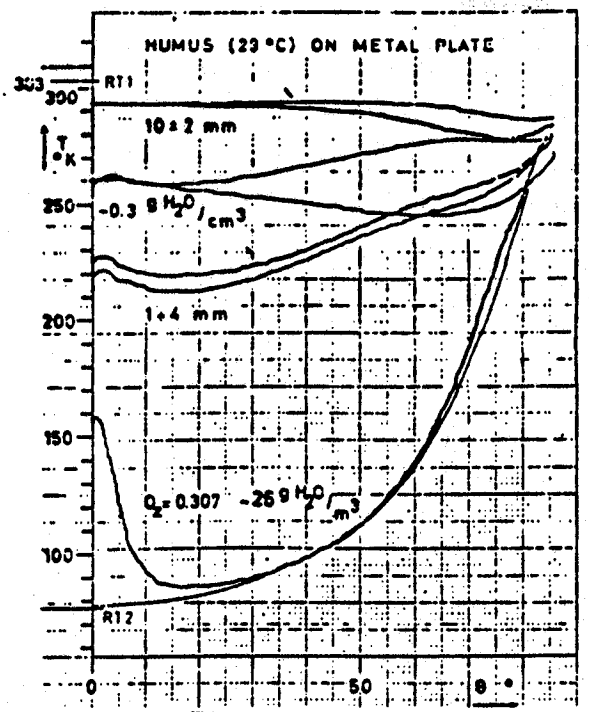

FIGURE 12

Various layers of humus on a metallic reflector. Lowest curve: contribution by the atmosphere via metal plate. The effect of humidity on the 10 mm layer.

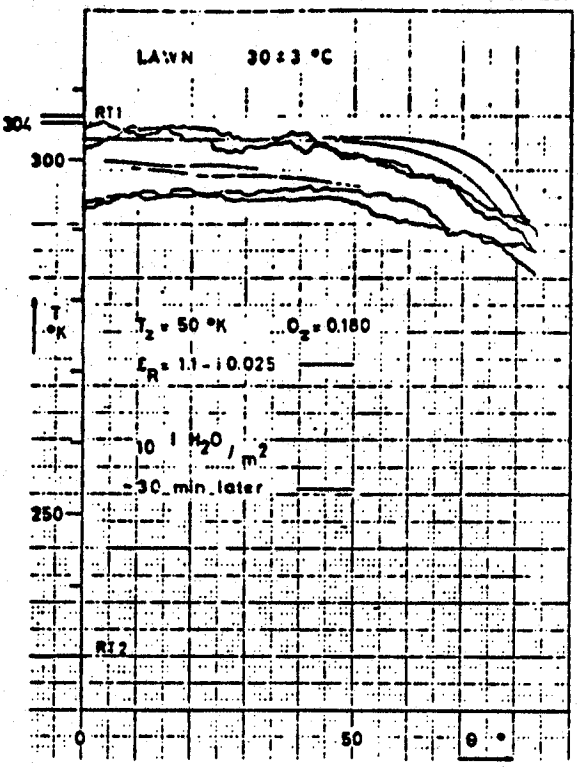

FIGURE 13

Emission coefficients of dry and wet lawn.

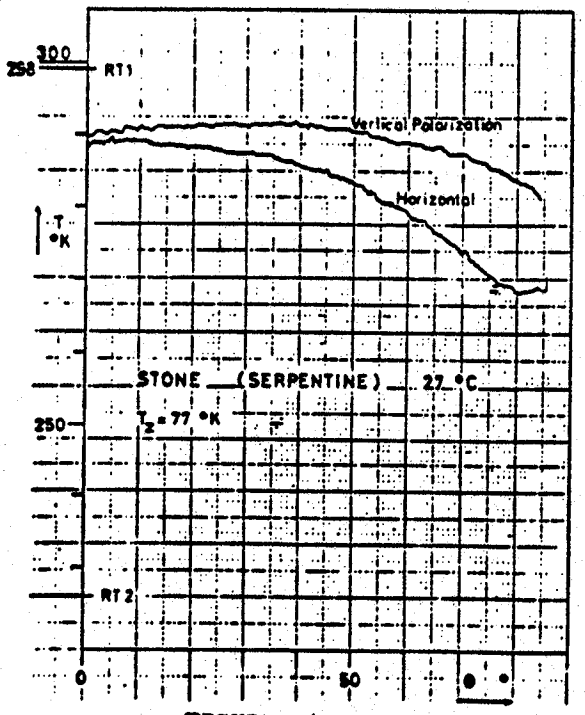

FIGURE 14

A stratum of coarse fragments of Serpentine.

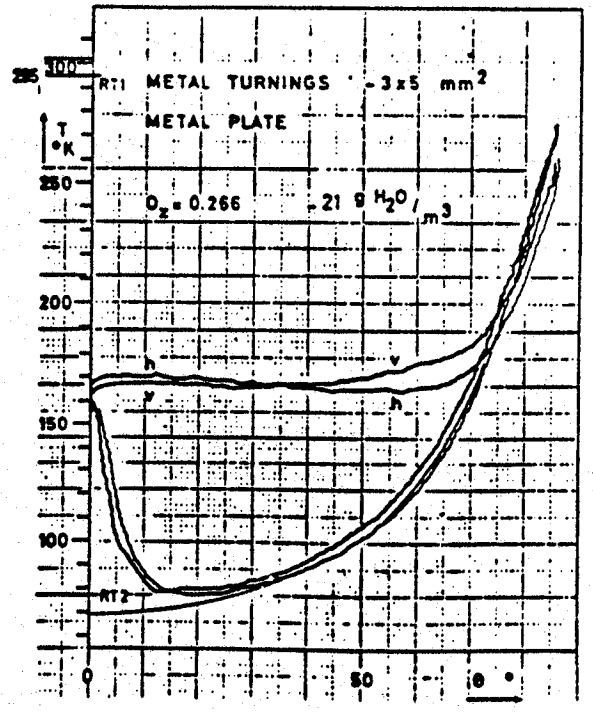

FIGURE 15

A stratum of metal turnings. The plane metal plate for comparison.

4. REFERENCES

[1] E. Schanda, R. Hofer, Emissivities and forward scattering of natural and man-made material at three millimeter wavelength, Proc. 9th Symp. Rem. Sens. Environment, Univ. of Michigan, Ann Arbor, (1974).

[2] R. Hofer, E. Schanda, Emission properties of water surface at three millimeter wavelength, Proc. URSI meeting on Microwave Scattering and Emission from the Earth, 17 - 23, Univ. of Berne, Switzerland, (1974).

[3] R. Hofer, Streu- und Emissionseigenschaften natürlicher Materialien bei 3 mm Wellenlänge, Diploma Thesis, Institute of Applied Physics, University of Berne, (1974).

[4] C. Mätzler, Messung der Wärmestrahlung der Erdoberfläche im Mikrowellengebiet, Diploma Thesis, Institute of Applied Physics, University of Berne, (1970).